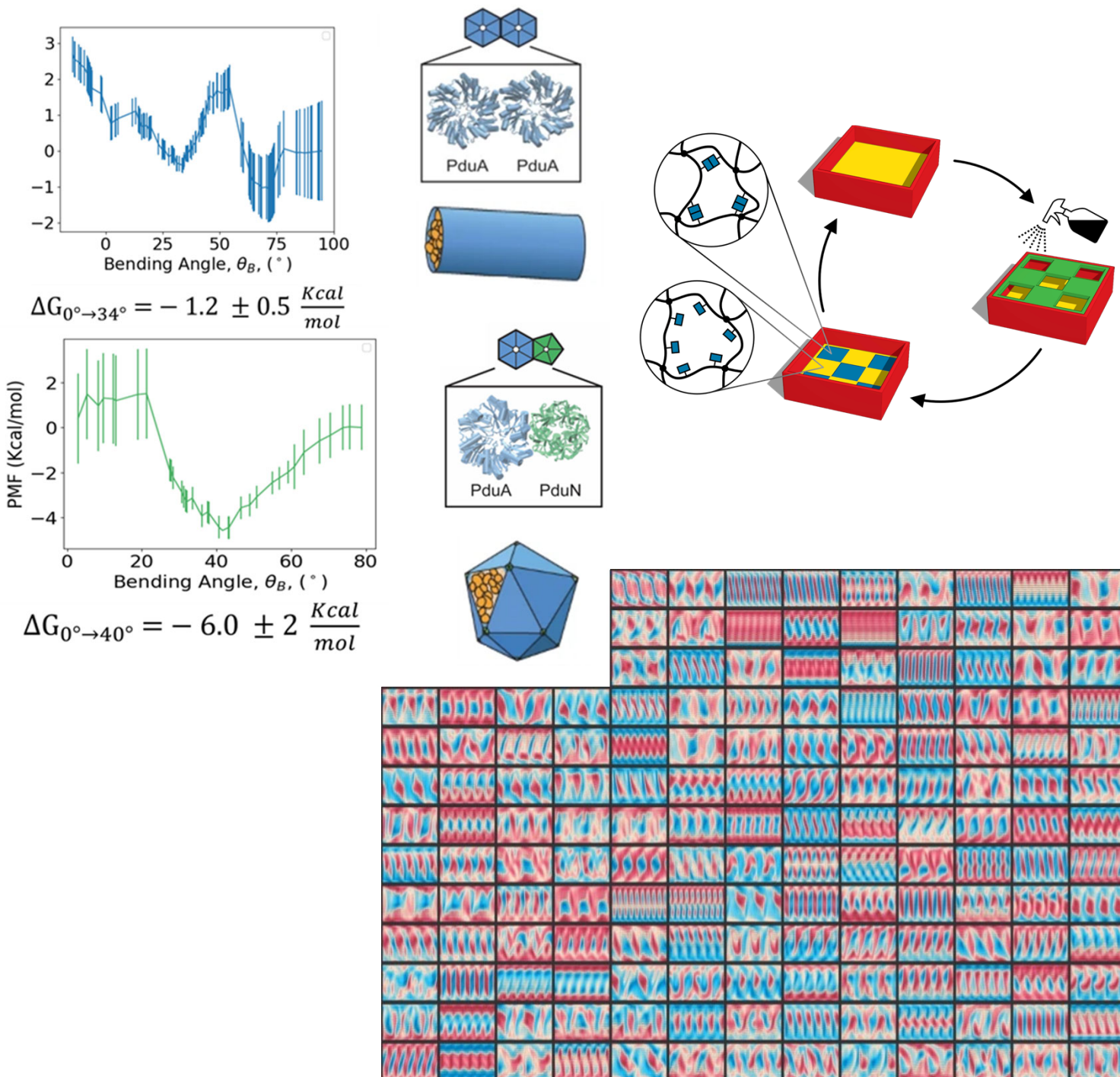


# Biomolecular Materials

## Principal Investigators' Meeting

Virtual Meeting, August 1-3, 2023

### *Program and Abstracts*



## On the Cover

Cover photo credits:

**Top Left:** Dictating Nanoreactor Shape and Performance. Molecular dynamics simulations are used to quantify the preferred interaction angles between hexameric shell proteins and the pentameric vertex protein PduN. Experiments show that deleting the vertex protein leads to the formation of tubes. Simulations show how the unique interactions of vertex protein PduN control the interaction angle, leading tubes to form in its absence. M. Olvera de la Cruz, Northwestern University

**Top Right:** Chemically Fueled Reinforcement of Polymer Materials. Carboxylic-acid-containing polymer networks undergo temporary crosslinking, increasing mechanical properties, on treatment with carbodiimides. Unlike related nonequilibrium systems, these materials remain solids throughout the experiments. This enables new behavior, like temporary adhesion and surface patterning. Spraying a hydrogel film with a solution of carbodiimide gives a pattern of mechanically reinforced areas that eventually relax back to the starting state. C.S. Hartley and D. Konkolewicz, Miami University

**Bottom Right:** Various Flow States of Active Nematic Co-existing in Active Turbulence. A mosaic of snapshots of a subset of Exact Coherent Structures (ECS) computed in the turbulent regime at single value of activity, all unstable. The color is vorticity (red + /blue -). P. Grover, University of Nebraska-Lincoln

## Foreword

This volume comprises the scientific content of the presentations made at the 2023 Biomolecular Materials Principal Investigators' Meeting, sponsored by the Materials Sciences and Engineering (MSE) division in the Office of Basic Energy Sciences (BES) of the U.S. Department of Energy (DOE). The meeting's focus is on the fundamental science supported by the Biomolecular Material Core Research Area (CRA) to create materials and multiscale systems that exhibit well-coordinated resiliency, functionality and information content approaching that of biological materials but capable of functioning under harsher, non-biological environments. The meeting took place August 1-3, 2023 as a virtual event conducted entirely over the internet.

This is one of a series of Principal Investigators' Meetings organized regularly by BES. The purpose of the meeting is to bring together all the Principal Investigators with currently active projects in the Biomolecular Materials program for the multiple purposes of raising awareness among PIs of the overall program content and of each other's research, encouraging exchange of ideas, promoting collaboration, and stimulating innovation. The meeting also provides an opportunity for the Program Managers and MSE/BES management to get a comprehensive overview of the program on a periodic basis, which provides opportunities to identify program needs and potential new research directions.

Biomolecular Materials (BMM) program supports fundamental materials science research for discovery, design and synthesis of functional materials and complex structures based on principles and concepts of biology. Biology provides a blueprint for translating atomic and nanoscale phenomena into mesoscale materials that display complex yet well-coordinated collective behavior. New synthetic approaches, unconventional assembly pathways, and development of predictive models and AI/ML for data-driven science are sought to accelerate discovery/design of materials with transformative potential on carbon dioxide removal, advanced manufacturing, and energy transfer and storage technologies.

I would like to thank the meeting attendees for their active participation and for sharing their ideas and new research results, which will bring fresh insights for the continued development of this field and its value to DOE as has been the case at past BES Principal Investigators' Meetings. Sincere thanks also go to Teresa Crockett of BES/MSE and Tia Moua and her colleagues at the Oak Ridge Institute of Science and Education (ORISE) for their excellent work providing all the logistical support for the meeting.

J. Aura Gimm  
Program Manager, Biomolecular Materials  
Materials Sciences and Engineering Division  
Office of Basic Energy Sciences  
U.S. Department of Energy

## Table of Contents

<b>Agenda</b> .....	<b>vi</b>
<b>Poster Session</b> .....	<b>x</b>
<b><u>Abstracts</u></b>	
<b>Laboratory Abstracts</b>	
<b>Computationally Driven Design and Synthesis for Electron Transfer Materials based on Nonnatural Polymers</b>	
<i>Marcel D. Baer</i> .....	2
<b>Bio-inspired Durable Storage of CO<sub>2</sub></b>	
<i>Chun-Long Chen, Jim De Yoreo, Chris Mundy, Kevin Rosso, Wendy Shaw, Jinhui Tao, Praveen Thallapally, Marvin Bayro</i> .....	6
<b>Bioinspired Metamaterials</b>	
<i>Surya Mallapragada, Andrew Hillier, Marit Nilsen-Hamilton, Tanya Prozorov, Alex Travasset, David Vaknin, Wenjie Wang</i> .....	10
<b>Precision synthesis and assembly of ionic and liquid crystalline polymers</b>	
<i>Paul F. Nealey, Matthew V. Tirrell, Juan J. de Pablo</i> .....	14
<b>Design, Synthesis, and Assembly of Biomimetic Materials with Novel Functionality</b>	
<i>Aleksandr Noy, Anthony van Burren, David Baker, James De Yoreo, Chun-Long Chen, Marcel Baer</i> .....	19
<b>Adaptive Interfacial Assemblies Towards Structuring Liquids (KCTR16)</b>	
<i>Ahmad Omar, Paul Ashby, Brett Helms, Alex Zettl, Thomas P. Russell</i> .....	24
<b>Dynamics of Active Self-Assembled Materials</b>	
<i>Alexey Snezhko, Andrey Sokolov, Andreas Glatz</i> .....	29
<b>University Abstracts</b>	
<b>Bioinspired Active Transport and Energy Transduction using Liquid Crystals Beyond Equilibrium</b>	
<i>Nicholas L. Abbott, Juan J. de Pablo</i> .....	35
<b>Self-assembled adaptive materials via 3D printed active programmable building blocks</b>	
<i>Igor Aronson, Ayusman Sen</i> .....	40

<b>Protein Design Using Deep Learning</b> <i>David Baker</i> .....	44
<b>Controlling Physical and Chemical Dynamics of Heterogeneous Networks Constructed from Soft Macromolecular Building Blocks</b> <i>Anna C. Balaz, Krzysztof Matyjaszewski, Tomasz Kowalewski</i> .....	46
<b>DNA Origami Templated Inorganic Nanostructures</b> <i>Carlos E. Castro, Michael G. Poirier, Ralf Bundschuh, Jessica O. Winter</i> .....	51
<b>Self-Assembly and Self-Replication of Novel Materials from Particles with Specific Recognition DE-SC0007991</b> <i>Paul M. Chaikin, David Pine, Ruoji Sha, Marcus Weck</i> .....	56
<b>Energy-Efficient Self-Organization and Swarm Behavior in Active Matter</b> <i>Paul Chaikin, Jerome Delhommelle, Stefano Sacanna</i> .....	62
<b>Design Principles of Biomolecular Metamaterials</b> <i>Jong Hyun Choi</i> .....	67
<b>Porin-Inspired Ionomers with sub-nm Gated Ion Channels for High Ion Conductivity and Selectivity</b> <i>Shudipto Konika Dishari</i> .....	71
<b>Active interfaces driven by microtubule-based active matter</b> <i>Zyonimir Dogic, Christina Marchetti</i> .....	76
<b>Reactive, Functional Droplets in Bio-inspired Materials and Smart Interfaces</b> <i>Todd Emrick</i> .....	80
<b>Early Formation Stages and Pathway Complexity in Functional Bio-Hybrid Nanomaterials</b> <i>Lara A. Estroff, Ulrich Wiesner</i> .....	85
<b>Programmable Dynamic Self-Assembly of DNA Nanostructures</b> <i>Elisa Franco, Rebecca Shulman</i> .....	90
<b>Controlling Lattice Organization, Assembly Pathways and Defects in Self- Assembled DNA-Based Nanomaterials</b> <i>Oleg Gang, Sanat K. Kumar</i> .....	95
<b>A reduced-order dynamical systems approach to modeling, sensing and control of active fluids</b> <i>Piyush Grover, Jae Sung Park, Michael M. Norton</i> .....	99

<b>Bioinspired Design of Electrically Fueled Dissipative Self-assembly of Supramolecular Materials</b>	
<i>Zhibin Guan</i> .....	104
<b>Machine learning approaches to understanding and controlling 3D active matter</b>	
<i>Michael F. Hagan, Seth Fraden, Pengyu Hong, Zvonimir Dogic</i> .....	108
<b>Propulsion of synthetic protocells and coacervates driven by biochemical catalysis</b>	
<i>Daniel A. Hammer, Daeyeon Lee, Matthew C. Good</i> .....	112
<b>Chemically fueled dissipative assembly of complex molecular architectures</b>	
<i>C. Scott Hartley, Dominik Konkolewicz</i> .....	117
<b>Activity-Enhanced Self-Assembly of Colloidal-Based Materials</b>	
<i>Daphne Klotsa, David Pine, John Brady</i> .....	121
<b>Transport and Molecular Discrimination in Biomimetic Artificial Water Channels for Lanthanide Separations</b>	
<i>Manish Kumar</i> .....	124
<b>Understanding functional dynamics on the nanoscale through an integrated experimental–computational framework</b>	
<i>Erik Luijten, Qian Chen</i> .....	128
<b>Memories and training in matter using inspiration from biology</b>	
<i>Sidney R. Nagel</i> .....	133
<b>Electrostatic Driven Self-Assembly Design of Functional Nanostructures</b>	
<i>Monica Olvera de la Cruz, Michael J. Bedzyk</i> .....	138
<b>Biomolecules for non-biological things: Peptide ‘Bundlemers’ design for model colloidal particle creation and hierarchical solution assembly</b>	
<i>Darrin J. Pochan, Christopher J. Kloxin, Jeffrey G. Saven</i> .....	143
<b>Self-organization of biomolecular motors and configurable substrates</b>	
<i>Tyler D. Ross, Paul W. K. Rothemund</i> .....	147
<b>Dissipation and control in nonequilibrium self-assembly</b>	
<i>Grant M. Rotskoff</i> .....	151
<b>Tension- and Curvature- Controlled Fluid-Solid Domain Patterning in Single Lamellae</b>	
<i>Maria M. Santore, Gregory M. Grason</i> .....	155

<b>Synthesizing functionality in excitonic systems using DNA origami</b> <i>Gabriela S. Schlau-Cohen, Mark Bathe, Adam P. Willard</i> .....	159
<b>Bio-inspired Polymer Membranes for Resilience of Electrochemical Energy Devices</b> <i>Meredith N. Silberstein</i> .....	164
<b>Biomimetic Strategies for Defect Annealing in Colloidal Crystallization</b> <i>Michael J. Solomon, Sharon C. Glotzer</i> .....	168
<b>Far-from-equilibrium topological defects on active colloids in nematic liquid crystals for bio-inspired materials assembly</b> <i>Kathleen J. Stebe</i> .....	173
<b>Materials Exhibiting Biomimetic Carbon Fixation and Self Repair: Theory and Experiment</b> <i>Michael S. Strano</i> .....	177
<b>Supramolecular Dynamics in Self-Assembling Materials</b> <i>Samuel I. Stupp</i> .....	181
<b>Protein Self-Assembly by Rational Chemical Design</b> <i>Akif Tezcan</i> .....	186
<b>Towards principles for bio-inspired and far-from-equilibrium adaptive, information storing materials.</b> <i>Suriyanarayanan Vaikuntanathan</i> .....	191
<b>Steering the Pathways of Hierarchical Self-assembly at Solid Surfaces</b> <i>Tao Ye, Yonggang Ke, Gaurav Arya</i> .....	194
<b>Author Index</b> .....	199
<b>Participant List</b> .....	202

## Agenda

### 2023 Biomolecular Materials Virtual Principal Investigators' Meeting August 1-3, 2023

All times are Eastern Time

#### Tuesday, August 1

10:45 AM Zoom Log in

#### Opening Remarks

11:00 AM Welcome and Introductory Remarks  
**J. Aura Gimm**, BMM Program Manager

11:15 AM Materials Sciences and Engineering Division Update  
**Andrew Schwartz**, Division Director, *MSED, DOE-BES*

#### Session 1 *20-minute presentation, 10-minute Q&A*

11:30 AM *Biomimetic strategies for defect annealing in colloidal crystallization*  
**Michael Solomon**, University of Michigan

12:00 PM *Designed peptide building blocks for polymerization and hierarchical self-assembly*  
**Darrin Pochan**, University of Delaware; **Jeffrey Saven**, University of Pennsylvania

12:30 PM *Investigation of design principles for synthetic light harvesting and conductive protein assemblies*  
**David Baker**, University of Washington

1:00 PM *Bioinspired Materials*  
**Surya Mallapragada**, Ames Laboratory

1:30 PM *BREAK, 20 minutes*

#### New Projects *10-minute presentation, 5-minute Q&A*

1:50 PM *(ECRP FY22) Characterizing the limits of nonequilibrium control for dissipative self-assembly*  
**Grant Rotskoff**, Stanford University

2:05 PM *(ECRP FY21) Computationally Driven Design and Synthesis for Electron Transfer Materials based on Non-natural Polymers*  
**Marcel Baer**, Pacific Northwest National Laboratory

- 2:20 PM *Activity-enhanced self-assembly of colloidal-based materials*  
**Daphne Klotsa**, UNC – Chapel Hill; **David Pine**, NYU; **John Brady**, Caltech
- 2:35 PM *Far-from-equilibrium topological defects on active colloids in nematic liquid crystals for bio-inspired materials assembly*  
**Kathleen Stebe**, University of Pennsylvania
- 2:50 PM *(CEM FY22) Transport and Molecular Discrimination in Biomimetic Artificial Water Channels for Lanthanide Separations*  
**Manish Kumar**, University of Texas - Austin
- 3:05 PM *(CEM FY22) Bio-inspired Durable Storage of CO<sub>2</sub>*  
**Chunlong Chen**, Pacific Northwest National Laboratory
- 3:20 PM *BREAK, 10 minutes*

### Poster Session I

- 3:30 PM *See Poster Session Directory*
- 6:00 PM *ADJOURN*

## Wednesday, August 2

- 10:45 AM Zoom Log in
- Session 3** *20-minute presentation, 10-minute Q&A*
- 11:00 AM *Bio-inspired shape-morphing and self-propelled active sheets*  
**Anna Balazs**, University of Pittsburgh
- 11:30 AM *Design, Synthesis, and Assembly of Biomimetic Materials with Novel Functionality*  
**Aleksandr Noy**, Lawrence Livermore National Laboratory; **James De Yoreo**, Pacific Northwest National
- 12:00 PM *Porin Inspired Ionomers with sub-nm Gated Ion Channels for High Ion Conductivity and Selectivity*  
**Shudipto Dishari**, University of Nebraska-Lincoln
- 12:30 PM *Propulsion of synthetic protocells and coacervates driven by biochemical catalysis*  
**Daniel Hammer**, University of Pennsylvania
- 1:00 PM *BREAK, 20 minutes*

- Session 4**     *20-minute presentation, 10-minute Q&A*
- 1:20 PM     *Self-Assembly and Self-Replication of Novel Materials from Particles with Specific Recognition*  
**Paul Chaikin**, New York University
- 1:50 PM     *Conformationally-Steered Hierarchical Self-Assembly at Solid Surfaces*  
**Tao Ye**, University of California-Merced; **Yonggang Ke**, Emory University; **Gaurav Arya**, Duke University
- 2:20 PM     *Reactive, Functional Droplets in Bio-inspired Materials and Smart Interfaces*  
**Todd Emrick**, University of Massachusetts-Amherst
- 2:50 PM     *Chemically-fueled Dissipative Assembly of Complex Molecular Architectures*  
**C. Scott Hartley**, Miami University
- 3:20 PM     *BREAK, 10 minutes*
- Poster Session II**
- 3:30 PM     *See Poster Session Directory*
- 6:00 PM     *ADJOURN*

## Thursday, August 3

- 10:45 AM     Zoom Log in
- Session 5**     *20-minute presentation, 10-minute Q&A*
- 11:00 AM     *Materials Exhibiting Biomimetic Carbon Fixation and Self-Repair: Theory and Experiment*  
**Michael Strano**, Massachusetts Institute of Technology
- 11:30 AM     *Energy-Efficient Self-Organization and Swarm Behavior in Active Matter*  
**Jerome Delhommelle**, UMass-Lowell; **Stefano Sacanna**, NYU
- 12:00 PM     *Tension- and Curvature- Controlled Fluid Solid Domain Patterning in Single Lamellae*  
**Maria Santore**, University of Massachusetts-Amherst
- 12:30 PM     *Bioinspired Design of Dissipative Self-assembly of Active Materials*  
**Zhibin Guan**, University of California-Irvine
- 1:00 PM     *BREAK, 20 minutes*

- Session 6**     *20-minute presentation, 10-minute Q&A*
- 1:20 PM     *Dynamics and Control of Active Nematics using Nonlinear Reduced-Order Models*  
**Piyush Grover**, University of Nebraska - Lincoln
- 1:50 PM     *Machine learning approaches to understanding and controlling 3D active matter*  
**Michael Hagan**, Brandeis University
- 2:20 PM     *Bio-inspired Polymer Membranes for Resilience of Electrochemical Energy Devices*  
**Meredith Silberstein**, Cornell University
- 2:50 PM     Closing Remarks
- 3:00 PM     *PI MEETING ADJOURN*
- 3:15 PM - 5:00 PM     PM Virtual Office Hour (separate link and sign-up)

## Poster Session

Posters will be up for both days, but will be manned for one day as listed.

### Tuesday, August 1 – Poster Session I

*Bioinspired Active Transport and Energy Transduction using Liquid Crystals Beyond Equilibrium*

**Nicholas Abbott**, Cornell University

*Reversibly growing crosslinked polymers with programmable sizes and properties*

**Joanna Aizenberg**, Harvard University

*Self-assembled adaptive materials via 3D printed active programmable building blocks*

**Igor Aronson**, Pennsylvania State University

*Design Principles of Biomolecular Metamaterials*

**Jong Hyun Choi**, Purdue University

1. *What Can A Particle Tell Us About Its Local Environment? Triblock Terpolymer Thin Film*

*Nanocomposites Enabling Two-Color Optical Super-Resolution Microscopy*

2. *What Does a Particle See? Visualizing The Local Nanoscale Chemistry and Topography of Water-Block Copolymer Interfacial Regions with 3D - AFM*

**Lara Estroff**, Cornell University

1. *Memory formation matter*

2. *Allosteric training at finite temperature*

**Andrea Liu**, University of Pennsylvania; **Sidney Nagel**, University of Chicago

1. *Nanoscale engineering principles from particle kinetics*

2. *Understanding functional dynamics on the nanoscale*

**Erik Luijten**, Northwestern University; **Qian Chen**, UIUC

*Electrostatic Driven Self-Assembly Design of Functional Nanostructures*

**Monica Olvera de la Cruz**, Northwestern University

**Paul Rothemund**, California Institute of Technology

1. *Controlling exciton dynamics with complex-valued coupling: A theoretical model study*

2. *Using DNA origami to probe coupled chromophore dynamics*

3. *Synthesizing functionality in excitonic systems using DNA origami*

**Gabrielle Schlau-Cohen**, Massachusetts Institute of Technology

1. *Dynamics of Active Self-Assembled Materials: Active Colloids*

2. *Dynamics of Active Self-Assembled Materials: Active Liquid Crystals*

**Alexey Snezhko**, Argonne National Laboratory

*Supramolecular Dynamics in Self-Assembling Materials*

**Samuel Stupp**, Northwestern University

*DNA Origami Templated Inorganic Nanostructures*

**Jessica Winter**, Ohio State University

## Wednesday, August 2 – Poster Session II

1. *Quasi-2D active liquid-liquid interfaces*

2. *3D Active Liquid-liquid Phase Separation: Experiment and Theory*

**Zvonimir Dogic**, University of California - Santa Barbara

1. *Timing nanotube populations through cascaded artificial gene networks*

2. *Programmable dynamic self-assembled DNA nanostructures as linear actuators*

**Elisa Franco**, UCLA; **Rebecca Schulman**, JHU

1. *Self-Assembly of hierarchical 3D architectures through inverse design of programmable DNA bonds*

2. *Controlling the self-assembly of DNA origami octahedra via manipulation of inter-vertex interactions and characterizing DNA nanocrystals orientations using Machine Learning*

**Oleg Gang**, Columbia University

1. *Precision Synthesis and Assembly of Ionic and Liquid Crystalline Polymers: Sequence-Controlled Polyampholyte Coacervates as Models of Membraneless Organelles*

2. *Precision Synthesis and Assembly of Ionic and Liquid Crystalline Polymers: Scattering Evidence of Charge Correlations in Polyelectrolyte Complex Coacervates*

**Paul Nealey**, Argonne National Laboratory

*Adaptive Interfacial Assemblies Towards Structuring Liquids (KCTR16)*

**Thomas Russell**, Lawrence Berkeley National Laboratory

1. *Polymer-Integrated Protein Crystals as Dynamic, Multifunctional Materials*

2. *Rational Design of Protein Weaves*

**F. Akif Tezcan**, University of California, San Diego

1. *Sloppy but near optimal control from thermodynamic inspired learning and feedback rules*

2. *Enhanced information storage and retrieval in materials and synthetic networks through non-equilibrium activity*

**Suriyanarayanan Vaikuntanathan**, University of Chicago

## Optional

*The dynamical systems approach to active nematics: Exact Coherent Structures and symmetry*

**Piyush Grover**, University of Nebraska-Lincoln

1. *Data-Driven Methods for Understanding Active Matters*

2. *Spatiotemporal Control of Active Materials*

**Michael Hagan**, Brandeis University

1. *Data-Driven Methods for Understanding Active Matters*

2. *Activity-Enhanced Colloidal Assembly*

3. *Active-assisted Assembly of Colloidal Crystal in 3D*

**Daphne Klotsa**, UNC - Chapel Hill; **David Pine**, NYU; **John Brady**, Caltech

*Emergent Micro-robotic Oscillator via Asymmetry-induced Ordering*

**Michael Strano**, MIT

*Laboratory  
Abstracts*

# Computationally Driven Design and Synthesis for Electron Transfer Materials based on Nonnatural Polymers

Marcel D. Baer, Pacific Northwest National Laboratory

**Keywords:** nonnatural polymer, reduction potential, computational design

## Research Scope

This project centers around the computational design of biomimetic polymer units containing tunable redox centers and structural features to facilitate assembly into robust materials.

The precise control of electron transfer processes in materials is crucial for addressing energy production and storage challenges. Nature's utilization of small protein modules containing redox centers, which enable coupled oxidation and reduction reactions, serves as a model for achieving this control. However, adapting nature's intricate modular design for energy technologies requires overcoming the limitations of harsh non-biological conditions.

This project aims to computationally design macromolecular units with tunable redox potentials by incorporating iron-sulfur (FeS) clusters and optimizing their local environment. The objectives include predicting the minimal sequence for binding redox clusters, elucidating the conformational stability of non-natural polymers, and developing biomimetic units for higher length-scale organization. These designed units can enable materials that mimic nature's spatial control of electron transfer, offering complex functionality in non-biological conditions.

## Recent Progress

We have made progress in developing atomistic interaction potentials, with the capability to incorporate new chemical functionalities efficiently. Additionally, we established a computational framework to predict reduction potentials for iron-containing materials. These advancements address the challenge posed by the need for directly applicable computational methods for biomimetic materials.

**Development of a systematic and extensible force field for peptoids (STEPS).** Peptoids (N-substituted glycines) are a class of biomimetic polymers that have attracted significant attention due to their accessible synthesis and enzymatic and thermal stability relative to their naturally occurring counterparts (polypeptides). While these polymers provide the promise of more robust functional materials via hierarchical approaches, they present a new challenge for the computational prediction of structure for materials design. The developed force field is a reparameterization of GAFF2 based on a bottom-up approach utilizing thousands of density functional theory energies (B3LYP) for each new chemical functionality. The charge scheme is designed to be systematically extensible to different solvents to account for solvent-specific polarization. An automated workflow starting from simple SMILE string allows for systematic

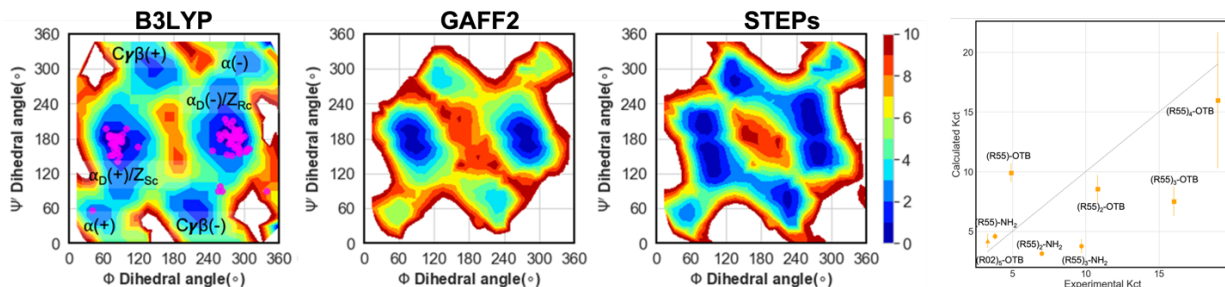


**Figure 1.** Potential energy surfaces for sarcosine for B3LYP, GAFF2 and the new force field STEPs. Scalebars are normalized potential energies in kcal/mol between 0-10, while white corresponds to values greater than 10 kcal/mol. Magenta dots for B3LYP correspond to known experimental structures. Calculated Kct values plotted against experimental literature values. Dashed line corresponds to perfect correlation.

and fast addition of new chemical functionality. The developed force field contains 100 different side chains, which is a significant advance to previous efforts, which are spread out resulting in a replication of efforts and a fragmented collection of a few parameterized sidechains. We validated STEPs based on the ability to replicate core peptoid backbone features in potential energy and free energy surfaces as well as replicated experimental equilibrium distributions of cis and trans amide bonds for common helix forming structures, see **Figure 1**. To enable community-based expansion all structures and energies are shared as an open access databank.

**Development of structural models of peptoid sequences experimentally shown to form a Zn-binding moiety using two helical segments, as well as compact multi-helical structures.** Designed helical bundles, engineered through rational design or computational methods, hold tremendous promise for creating customized biomaterials, synthetic enzymes, and molecular machines. Their precise control over sequence and interactions enables tailored properties, offering applications in biotechnology, drug delivery, and nanotechnology. Only a few sequences are reported thus far for peptoids that are assumed to form helical bundles,<sup>2</sup> one including a Zn-binding motif,<sup>1</sup> but no atomistic structure is solved. Using the newly developed STEPs force field in conjunction with extensive replica exchange molecular dynamics we developed models for the Zn-binding motif, see **Figure 2**, as well as dimer-, trimer- and tetrameric helical bundles. These peptoid structures will be a foundation for designing scaffolds capable of binding inorganic clusters.

**We developed a predictive qualitative model for understanding shifts in reduction potential.** In synthetic iron containing clusters, control over structure and reduction potential is accomplished through the high diversity of accessible ligands and reaction conditions compared

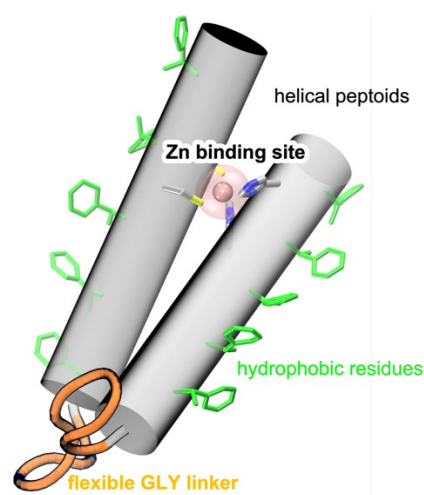


**Figure 2.** Predicted Structure using the STEPs force field and replica exchange molecular dynamics for experimentally known peptoid sequences with zinc binding motif.

to nature, where most of the observed control over the reduction potential is due to second-sphere effects,<sup>4</sup> see **Figure 3.A**. The ability to compute and design the reduction potential of small clusters is significant as it allows for fine-tuning and control of electron transfer processes in various applications, such as energy conversion, catalysis, and electronic devices. Screening large amounts of potential ligands requires efficient and reliable computational methods. After extensive testing of about 50 DFT functionals, B3LYP was chosen as the most reliable for the prediction of reduction potentials for iron-sulfur complexes. We then tested the semi-empirical XTB<sup>3</sup> tight binding method for the ab initio prediction of reduction potentials against the higher level DFT B3LYP predictions for an extensive set of single iron containing clusters, see **Figure 3.B**. Scaling of XTB predicted relative reduction potentials allows for quantitative agreement with the higher level DFT method. The reduction in computational cost allows to test the hypothesis that a combination of multiple ligands, which cannot be achieved in classical synthetic methods, will allow for a fine tuning of the reduction potential for FeS clusters by only focusing on thiol containing ligands.

**We developed and tested a Pyrosetta/XTB workflow for estimating ensemble averaged ionization potentials for Rubredoxin analogues.** The simplest, single iron containing redox protein is Rubredoxin, for which multiple short peptide analogues have been studied.<sup>5</sup> As a benchmark we focused on analogues forming clusters with two ligating short peptides to develop a workflow, see **Figure 4**. We employ Pyrosetta for fast and efficient generation of structures and XTB to predict ensemble averaged reduction potentials. This workflow correctly predicts the qualitative relative shifts observed for the MAP-6 peptide mutants. We have extended the original functionality of peptoids in Pyrosetta<sup>5</sup> to include all sidechains parameterized with the STEPs force field enabling this workflow to be applied for the prediction of inorganic clusters ligated by peptoids. We are now able to test the hypothesis that redox cofactors stabilized and tuned locally by the residues of synthetic nonnatural, sequence-defined polymers without relying on secondary structure elements will have the same range of redox properties as natural redox cofactors stabilized by proteins or within short peptides.

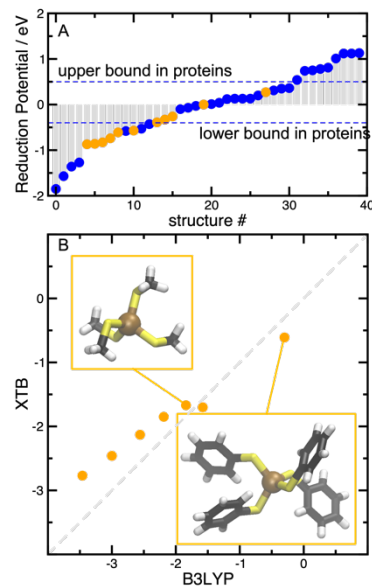


**Figure 3.** A) Calculated reduction potentials for a large set of Fe containing complexes, highlighting thiol containing ligands in orange. The blue dashed lines indicate the range for reduction potentials for single iron containing proteins. B) Correlation between B3LYP and XTB calculated ionization potentials in [eV] for thiol containing ligands.

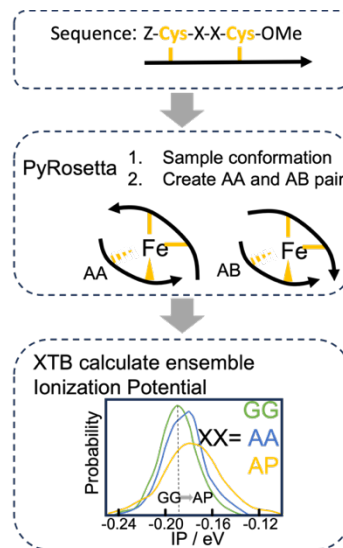


**Figure 4.** Workflow from sequence to ensemble average ionization potential

## Future Plans

To explore the conformational space, we will utilize advancements in Pyrosetta to predict sequences capable of coordinating FeS clusters for stable assemblies. By screening reduction potentials using XTB theory and testing promising candidates with higher-level methods, critical factors controlling the polymer's conformational space, including sequence, side chain identity, FeS cluster binding, and reduction potential, will be determined. Furthermore, we will test ligand combinations to precisely position ligands around the cluster, achieving defined redox potential. This approach allows testing the hypothesis that synthetic sequence-defined polymers can stabilize and tune FeS clusters locally, without relying on secondary structure elements with the same redox properties as natural redox cofactors.

We will examine the qualitative effects on the electronic properties of these secondary structure elements using quantum mechanical methods. We will utilize the already-developed force field by systematically modifying side chain chemistry (charged, hydrophobic, steric). This approach will allow us to test the hypothesis that secondary structure elements' stability and electronic properties can be tuned through side chain chemistry and linker choice, enabling the design of features that either block or enhance electron transfer.

Building upon the peptoid bundle structures, we will assess the stability of the assemblies against mutations using newly added rotamer libraries and atomistic simulations. Identifying stable mutations will facilitate the development of structural models with designed scaffolds for FeS cluster binding and examine the factors governing the assembly process. This approach tests the hypothesis that secondary structure elements of peptoids and other sequence-defined polymers can be tuned for assembly into biomimetic units, enabling higher length-scale organization towards multi-unit ET chains.

## References

1. Lee, B. C.; Chu, T. K.; Dill, K. A.; Zuckermann, R. N., Biomimetic nanostructures: creating a high-affinity zinc-binding site in a folded nonbiological polymer. *J Am Chem Soc*, 130 (27), 8847-55 (2008).
2. Lee, B. C.; Zuckermann, R. N.; Dill, K. A., Folding a nonbiological polymer into a compact multihelical structure. *J Am Chem Soc*, 127 (31), 10999-1009, (2005).
3. Bannwarth, C.; Ehlert, S.; Grimme, S., GFN2-xTB—An Accurate and Broadly Parametrized Self-Consistent Tight-Binding Quantum Chemical Method with Multipole Electrostatics and Density-Dependent Dispersion Contributions. *J. Chem. Theo. Comp.* 15 (3), 1652-1671 (2019).
4. Liu, J.; Chakraborty, S.; Hosseinzadeh, P.; Yu, Y.; Tian, S. Petrik, I.; Bhagi, A.; Lu, Y., Metalloproteins Containing Cytochrome, Iron–Sulfur, or Copper Redox Centers. *Chem. Rev.* 114 (8), 4366-4469 (2014).
5. A. E. Boncella, E. T. Sabo, R. M. Santore, J. Carter, J. Whalen, J. D. Hudspeth, et al. The expanding utility of iron-sulfur clusters: Their functional roles in biology, synthetic small molecules, maquettes and artificial proteins, biomimetic materials, and therapeutic strategies. *Coord. Chem. Rev.*, 453, 214229 (2022).

## Publications

1. B. S. Harris, K. K. Bejagam, and M. D. Baer, Development of a Systematic and Extensible Force Field for Peptoids (STEPs), *J. Phys. Chem. B* (Special Issue entitled: Early-Career and Emerging Researchers in Physical Chemistry Volume 2), accepted.

## Bio-inspired Durable Storage of CO<sub>2</sub>

**Principal Investigator:** Chun-Long Chen, Pacific Northwest National Laboratory (PNNL) and University of Washington (UW)

**Co-Principal Investigators:** James De Yoreo (PNNL/UW), Chris Mundy (PNNL/UW), Kevin Rosso (PNNL), Wendy Shaw (PNNL), Jinhui Tao (PNNL), Praveen Thallapally (PNNL), Marvin Bayro (University of Puerto Rico)

**Keywords:** Peptoids, CO<sub>2</sub> mineralization, crystal nucleation and growth, phase transformation

### Research Scope:

The purpose of this project is to develop bio-inspired peptoid-based materials that enable removal and durable storage of atmospheric CO<sub>2</sub>. Our proposed work exploits and extends nature's model by using programmable peptoid materials.<sup>1</sup> These materials mimic the efficient CO<sub>2</sub> capture and storage seen in natural systems by both promoting CO<sub>2</sub> hydration and accelerating metal carbonate precipitation. Motivated by the urgency of reducing CO<sub>2</sub> levels in the atmosphere, our vision is to (1) discover and exploit the physical and chemical principles underlying accelerated CO<sub>2</sub> mineralization by peptoids and (2) use those principles to develop rules for designing robust and scalable organic additives that convert CO<sub>2</sub> into useful metal carbonate materials.

### Recent Progress

#### Peptoid-promoted calcium carbonate (CaCO<sub>3</sub>) phase transformation.

Inspired by the bio-controlled crystal morphological controls and phase transformation during biomineralization, herein, we designed and used three sequence-defined peptoids with different hydrophilicity to regulate CaCO<sub>3</sub> crystallization pathway. By introducing hydrophilic side chains with different numbers of -COOH groups, we successfully tailored the resulting shapes from perfect rhombohedrons to elongated rhombohedrons, and even spindle-like calcite structures with different aspect ratios.

These results confirm the capability of peptoids to modulate the kinetics of calcite crystal growth. Further characterizations, including time-dependent ex-situ transmission electron microscopy (TEM) and energy dispersive spectroscopy (EDS), in situ optical microscopy, as well as liquid-phase TEM, show that these peptoids could stabilize the amorphous CaCO<sub>3</sub> (ACC) (Figure 1). More importantly, they can effectively promote the formation of calcite - the most stable

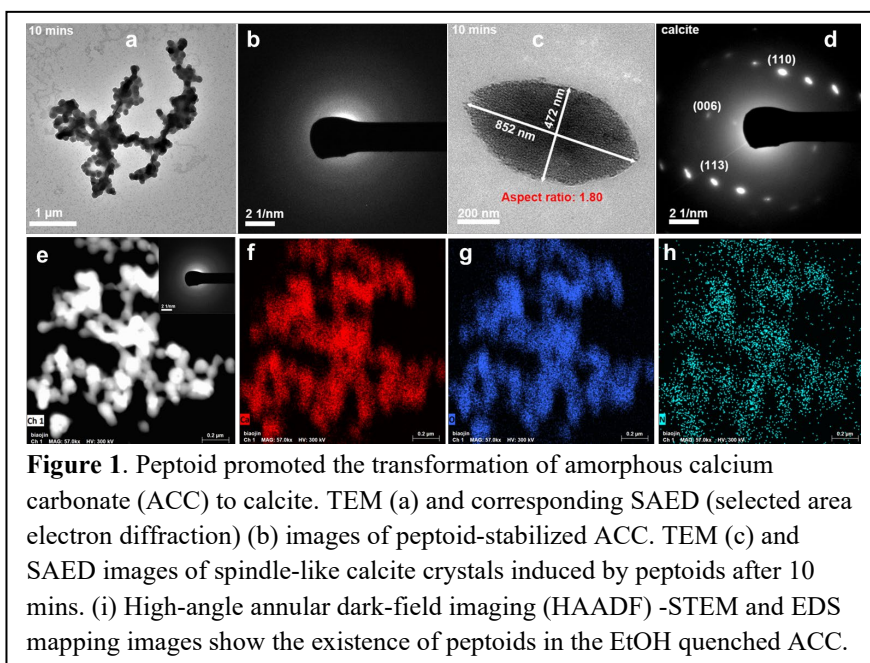


**Figure 1.** Peptoid promoted the transformation of amorphous calcium carbonate (ACC) to calcite. TEM (a) and corresponding SAED (selected area electron diffraction) (b) images of peptoid-stabilized ACC. TEM (c) and SAED images of spindle-like calcite crystals induced by peptoids after 10 mins. (i) High-angle annular dark-field imaging (HAADF)-STEM and EDS mapping images show the existence of peptoids in the EtOH quenched ACC.

polymorph of  $\text{CaCO}_3$ , while inhibiting the phase transformation of ACC-to-vaterite. We are currently working on the mechanistic understanding of the peptoid-promoted ACC-to-calcite phase transformation and the role of peptoids in this promotion process, using state-of-art imaging techniques combined with computational simulations.

**Role of peptoid design in regulating the kinetics of calcite crystal growth.** To unravel the role of peptoids in regulating the kinetics of calcite crystal growth,<sup>2</sup> we conducted in-situ atomic force microscopy (AFM) experiments to directly observe calcite growth processes in the presence of peptoids. AFM allows us to quantify the step migration rates for the layered growth of calcite crystals in supersaturated solutions. It can also reveal phenomena such as step-specific growth rates and step-pinning, to provide new insights into the mechanistic understanding of carbonate crystal growth rate acceleration. We have successfully developed a reliable approach to measure the step migration rates on a growth hillock on seeded calcite crystals, both with and without the addition of peptoids. Our investigation has yielded several findings. Firstly, we observed that peptoids exhibit a more pronounced acceleration effect in solutions that are only slightly supersaturated. Secondly, we discovered an inverse relationship between the acceleration effect and the degree of solution supersaturation. Thirdly, we conducted experiments using a range of peptoids with varied numbers of carboxylic acid groups and phenyl groups. These investigations revealed that peptoids with a higher number of carboxylic acid groups exhibited stronger binding to the steps, resulting in acceleration at lower peptoid concentrations. Conversely, the number of hydrophobic groups had a comparatively lesser impact on the growth kinetics. Notably, we observed distinct behavior between two types of steps, with peptoids displaying a stronger affinity to negative steps compared to positive steps.

The implications of these findings are twofold. 1) they provide valuable guidelines for the development of sequence-specific, non-natural polymers that can serve as effective promoters for carbonate crystallization. 2) our research sheds light on the microscopic interactions between biomaterials and mineral surfaces, offering insights into the specific interactions at play.

**Computational understanding of peptoid-promoted  $\text{CaCO}_3$  nucleation.** We aim to probe the initial stages of  $\text{CaCO}_3$  nucleation in the presence of designed peptoids using the tools of theory and molecular simulation. We have previously developed tools for modeling the initial stages of nucleation under bulk homogenous conditions,<sup>3</sup> which necessitated the development of a reduced model for ion—ion interactions via the potential of mean force (PMF) between all ion pairs. This reduced description of ion—ion representation treats water—ion interactions at the mean field level and resembles an implicit water model. This model was shown to be both efficient and accurate in modeling the initial stages of nucleation based on agreement with both titration experiments (speciation) and X-ray Absorption Near Edge

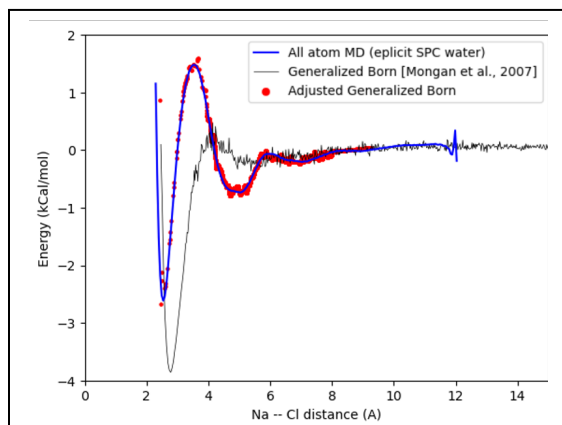


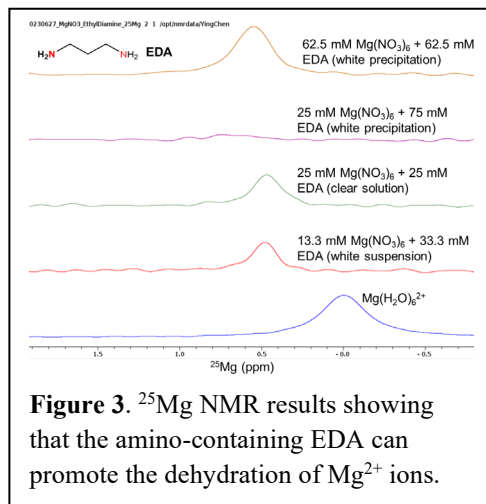
**Figure 2.** Energy as a function of distance between ions in simulation with  $\text{Na}^+$  and  $\text{Cl}^-$  in a box of water. PMF from all atom simulation with explicit water (blue). PMF using forces from Generalized Born Model (black). Effective potential energy of  $\text{Na}^+$  and  $\text{Cl}^-$  system as a function of distance between the ions (red).

Spectroscopy (XANES) measurements (local structure). Extending these concepts to nucleation in the presence of peptoids requires a reduced model of the peptoid and its conformational flexibility under dilute electrolyte conditions. This will require development of an accurate implicit water for both peptoid and ions under aqueous conditions. Herein, we aim to develop a simulation protocol for accurately and efficiently simulating both ions and peptoids to ascertain how the clustering statistics of ions is influenced by peptoid design. To treat both ions and the peptoids on equal footing we utilize a Generalized Born implicit solvent model to describe the important long-range Coulomb interactions (dielectric theory) that is augmented by describing the short-range interactions through a molecular description via the PMF. We demonstrate this approach by simulating the interaction of Na—Cl in water. The benchmark interaction between ions the PMF in a fully atomistic treatment (Figure 2). This is then compared to the PMF using the Generalized Born to describe the effective ion—water interactions. Clear differences between the all-atom and the Generalized Born protocols are seen (Figure 2). We correct for this difference by adding an external potential that represents the difference between the Generalized Born and the all-atom PMF. Once this correction is implemented, we achieve perfect agreement with the all-atom PMF (Figure 2). Future work will be to incorporate this protocol to describe both the conformational flexibility of the peptoid and the ion-peptoid interactions. The resulting model will be 100x more efficient and reproduce salient interactions at the all-atom level to perform ensemble level simulations of CaCO<sub>3</sub> nucleation in the presence of designed peptoids.

**Peptoid-promoted the formation of MgCO<sub>3</sub> crystals.** Due to the slow rates of magnesite and dolomite formation in natural environments, precipitation of CO<sub>2</sub> to form these minerals as permeant carbon storage is currently very limited. Herein, we focused our effort on developing small molecules as peptoid side chains to accelerate dehydration of Mg<sup>2+</sup> ions. Our findings reveal that small molecules containing primary amines, like benzylamine, could accelerate the formation of MgCO<sub>3</sub> crystals. Our recent <sup>25</sup>Mg NMR results further confirmed this finding (Figure 3). Our future research will focus on design of peptoids that containing amino groups as side chains to test the influence of those designed peptoids in the dehydration of Mg<sup>2+</sup> ions to achieve the accelerated formation of MgCO<sub>3</sub> crystals and the formation of MgCO<sub>3</sub> crystals on the self-assembled peptoid material surfaces.

### Bio-inspired design of self-assembling peptoids to mimic carbonic anhydrases (CAs) for enhanced CO<sub>2</sub>

**hydration.** Inspired by the crystal structure and coordination environment of Zn<sup>2+</sup> active site of CAs, herein, we designed and synthesized a variety of ligand-containing self-assembling peptoids to coordinate with metal cations, including Zn<sup>2+</sup>, to form crystalline self-assembled nanomaterials with precise arrangement of ligand-metal active sites that mimic CAs (Figure 4). Our recent results show that self-assembling peptoids with imidazole as ligands can coordinate with Zn<sup>2+</sup> to form highly crystalline nanosheet materials (Figure 4). These self-assembled peptoid-Zn<sup>2+</sup> nanosheets show an excellent CA-mimicking activity by testing their capability of converting 4-nitrophenyl acetate (4-NPA) - an assay often used to evaluate the CA-mimicking activity. Hydrolysis activity was measured in UV-vis by monitoring the concentration change of 4-NPA ( $\lambda_{\text{max}} = 270 \text{ nm}$ ) to 4-nitrophenol alcohol ( $\lambda_{\text{max}} = 400 \text{ nm}$ ) at different time points (Figure 4). Future work will focus on



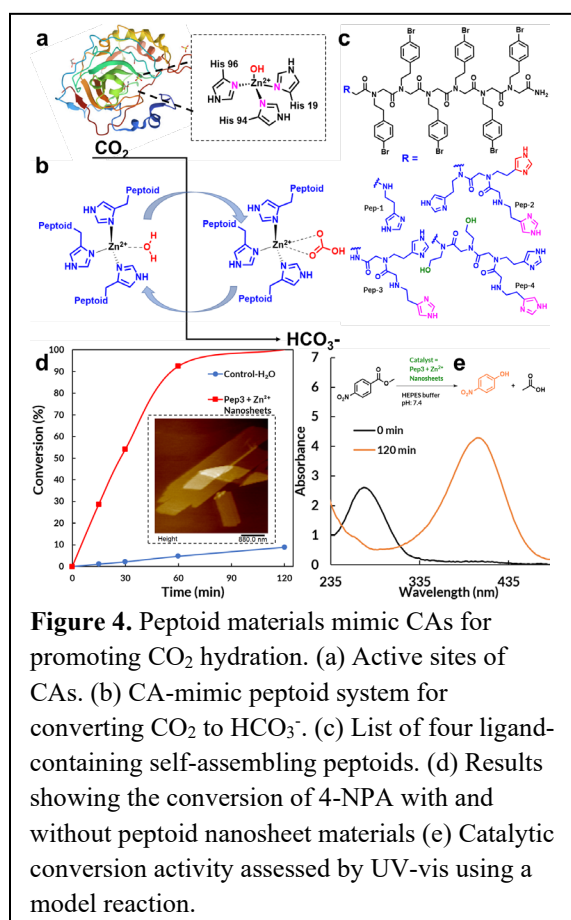
studying the influence of side chains, cofactors – such as  $Zn^{2+}$  vs  $Cu^{2+}$ , and nanostructures of self-assembled crystalline materials for enhanced  $CO_2$  hydration and mineralization.

## Future Plans

Our future plans center on continuing to design and synthesize additional peptoid sequences with tunable side chain chemistries for promoting the nucleation and crystal growth of calcite crystals, and the promotion of  $MgCO_3$  crystallization. We will begin solid-state NMR experiments studying how peptoids interact with calcite crystals for accelerated crystal growth, and use AFM-based 3D Fast Force Mapping to investigate the water structure at the solid-solution interaction and how peptoids impact the interfacial solution structure. Our next step will also include the usage of self-assembled peptoid nanosheets with different functional side groups, such as  $-NH_2$ ,  $-OH$  and  $-COOH$ , as well as nanosheets with different density of such groups, to investigate their influences on the nucleation and phase transformation during the formation of  $CaCO_3$  and  $MgCO_3$  crystals.

## References

1. B. Cai, Z. Li, C.-L. Chen, Programming Amphiphilic Peptoid Oligomers for Hierarchical Assembly and Inorganic Crystallization. *Acc. Chem. Res.* 54, 81-91 (2021).
2. C. L. Chen, J. H. Qi, J. H. Tao, R. N. Zuckermann, J. J. DeYoreo, Tuning calcite morphology and growth acceleration by a rational design of highly stable protein-mimetics. *Sci. Rep.* 4, 6266 (2014).
3. 3K. Henzler et al., Supersaturated calcium carbonate solutions are classical. *Science Advances* 4, eaao6283 (2018).



## **Bioinspired Metamaterials**

**PIs:** Surya Mallapragada, Andrew Hillier, Marit Nilsen-Hamilton, Tanya Prozorov, Alex Traveset, David Vaknin, and Wenjie Wang, Ames Laboratory

**Affiliation:** Division of Materials Science and Engineering, Ames Laboratory, Ames, IA 50011

**Keywords:** metamaterials, DNA origami, metallization, self-assembly

### **Research Scope**

The Bioinspired Metamaterials FWP at the Ames National Laboratory focuses on developing fundamental bioinspired approaches for creating self-assembled mesoscale two- and three-dimensional (2D and 3D) structures that can serve as functional optical metamaterials. We are developing bioinspired, bottom-up synthesis approaches using DNA origami templates for further metallization to create nanoresonators that are functionalized to enable their assembly into 2D and 3D mesoscale organization and alignment. Our interdisciplinary collaborative approach integrates experiment and theory and aligns with DOE's priorities laid out in the Synthesis Science workshop report for the synthesis of complex nanostructures and multi-scale assemblies. It also addresses the *DOE's Grand Challenge*, to orchestrate atomic and electronic constituents to control material properties.

### **Recent Progress**

Our efforts have focused on: (i) creating individual metallic nanoresonators such as split-ring resonators, and other meta-atoms using bottom-up approaches. We have used DNA origami templating to create gold nanostructures, to serve as nanoresonators and meta-atom building blocks. We have characterized optical scattering from these metallic nanostructures; and (ii) developing 2D and 3D assembly methods for gold nanostructures based on polymer functionalization with assembly driven by various stimuli, as predicted by theory, and characterizing these assemblies using scattering and electron microscopy. Synthesis and fabrication approaches are complemented by development and use of synchrotron X-ray scattering, and scanning transmission electron microscopy (STEM) techniques to characterize meta-atoms and their assemblies. The experimental approaches have been closely coupled with theoretical efforts for optical properties, as well as for predicting self-assemblies of functionalized nanostructures.

**Creation and Characterization of Individual Meta-atoms:** We have used DNA origami to create desired uniform metallic nanoresonator structures serving as split-ring resonators, measured optical properties of individual metallized nanostructures, and compared the experimental results with the theoretical predictions. We have developed methods for chemical annealing of metallized DNA origami using gold etching/redeposition to convert particle-like morphology to smooth, continuous structures for enhanced optical and electronic response [1].

We have also developed methods for nanoparticle binding to DNA origami using pairing between complementary oligonucleotides. Optical response of individual DNA origami-based metallized meta-atoms using polarized optical scattering [2]

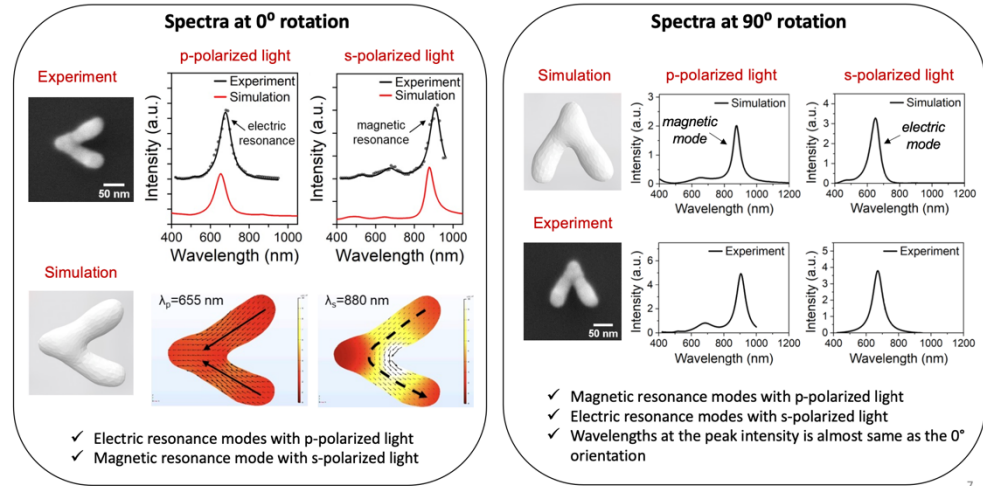


**Fig. 1** Scattering spectra of DNA-templated V-shaped nanoresonators

demonstrated the presence of both magnetic and electric resonance modes in asymmetric meta-atoms versus the presence of only electric modes in symmetric structures. (**Fig. 1**) We have developed disorder models for DNA-templated metallized meta atoms to predict the degree of disorder that the self-assembled structures can tolerate to still exhibit the desired optical properties. We have created magnetic nanoparticles using Mms6 mineralization proteins from magnetotactic bacteria, which can be tethered to the DNA origami through Mms6 to create dynamic and tunable metastructures [3]. We used High Angle Annular Dark Field Scanning Transmission Electron Microscopy (HAADF-S/TEM) imaging to follow metallization of DNA origami triangles utilizing a two-step approach: (1) formation of Pd clusters (seeds) at the surface of DNA origami triangles, and (2) forming Au particles at the surface of seeded DNA triangles, with Pd clusters acting as nucleation points. The evolution of metallic particle growth at the surface of seeded DNA origami triangles was visualized by monitoring direct reduction of HAuCl<sub>4</sub> by the electron beam taking place at the surface of the seeded triangles. We have introduced a “Pd seeding density” parameter as a factor determining the overall quality of two-step DNA origami triangle metallization.

**2D and 3D assembly of Nanostructures into Mesoscale Superstructures:** We created patterned hydrophilic domains with enhanced binding of DNA origami on silicon oxide surfaces to create an array of meta-atoms (**Fig. 2**). We have used gold nanoparticles as model nanostructures to develop methods for 2D and 3D self-assembly by functionalizing with polymers such as poly(ethylene glycol) (PEG) and poly(N-isopropyl acrylamide) (PNIPAM) and employing stimuli such as salts to drive the assembly. We showed that the polymer chain length can be used to tune the spacing between the metallic nanostructures in the superlattice [4]. We have used interpolymer complexation to create robust nanoparticle superlattices that can be tuned by

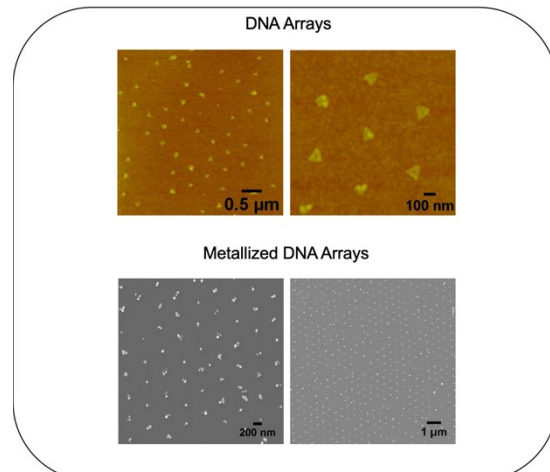


**Fig. 2** Fabrication of metallized DNA-origami metasurfaces nanoresonators

changing temperature and/or pH. The experimental results have been complemented by computational studies to investigate effects induced by a substrate. We have shown that we can create nanoparticle superlattices with negative thermal expansion (NTE) coefficients using this approach, with NTE coefficients of two to four orders in magnitude larger than previously reported NTE materials. A detailed theoretical model was developed to provide insights into the mechanism involved and lead to prediction of the lattice constants, and to tunable crystal sizes [5].

We have employed the low grafting density of ligand PEG to silver nanoparticles (AgNPs) to achieve bidirectional interparticle binding and to form lamellar structures at aqueous surfaces and in suspensions [6]. We have derived theoretical approaches to pack cubic nanocrystals as well as mixtures of cubic and spherical nanocrystals [7]. The model allows for prediction of packing density without any fitting parameters. We demonstrated the assembly of a new type of chiral superlattice in a collaborative study, where the chirality is induced by the substrate [8]. The simplicity and versatility of substrate-supported chiral superlattices facilitate the manufacture of metastructured coatings with unusual optical, mechanical and electronic characteristics. We also showed that two distinct complex two-dimensional binary superlattices were self-assembled by co-crystallizing gold nanoparticles (AuNPs) of two distinct sizes, allowing for greater control over the packing density [9]. Switching from the charge-neutral PEG ligand terminal [10], methyl, to negatively and positively charged terminals, allows us to assemble ordered assemblies via regulating the strength of the Coulombic interactions. Based on synchrotron small-angle x-ray scattering data, we show that oppositely charged AuNPs with carboxyl and amine terminals can act as super-ions and form various 3D binary ionic superlattices in suspensions. We have shown that we can create pH-controlled superstructures with different lattice arrangements.

## Future Plans

Our future work will build on our work described above, to create hierarchically self-assembled 2D and 3D mesoscale structures from individual meta-atoms that demonstrate the existence of the desired resonances characteristic of functional metamaterials. We will create 3D meta-atom morphologies and dynamic metastructures for enhanced optical responses, including enhancing optical and electronic quality of meta-atoms using enhanced metallization strategies, using the seeding density as an additional handle for achieving desired metallization quality of final structures. Ongoing experiments also involve imaging optimization, liquid phase imaging, and assessment of the electron dose on the metallization process. We will extend our simulations of

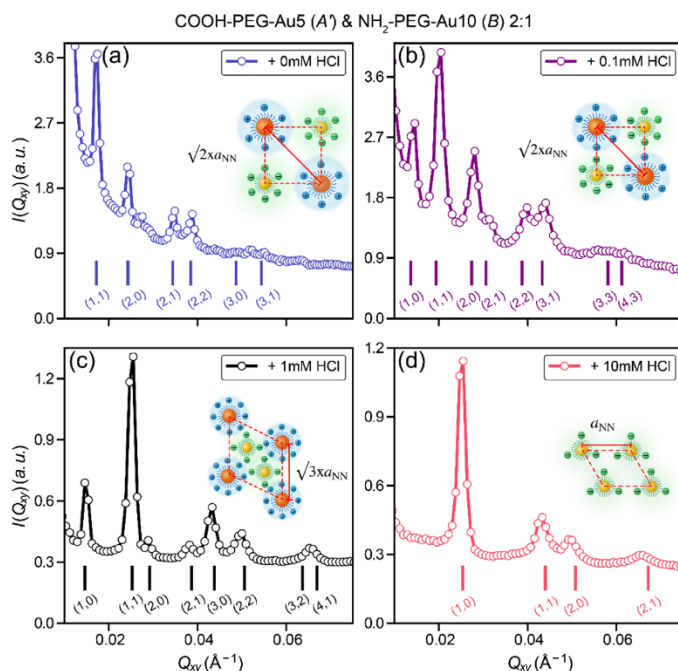


**Fig. 3** pH-controlled self-assembled superstructures

metallized-DNA meta-atoms to assess sensitivity to orientational and positional disorder. We will create metallized split-ring nanoresonators functionalized by synthetic polymers whose 2D and 3D assemblies will be mediated by interpolymer complexation, salt, pH, and/or temperature, using approaches similar to those developed for gold nanoparticles and anisotropic gold nanostructures described above. We will focus on measurement of optical properties of assemblies of metallized nanostructures and compare the experimental results with the theoretical predictions.

### **Publications** (10 most relevant, out of a total of 17)

1. Alam, S., Palo, P., Bendickson, L., Islam, M., Hillier, A., Nilsen-Hamilton, M., & Prozorov, T. *In-situ STEM Metallization of DNA Origami*, *Microscopy and Microanalysis*, **27**(S2), 35-36 (2021). doi:10.1017/S1431927621013179.
2. M.M. Islam, M.M. Hossen, T. Koschny, A.C. Hillier, *Shape and Orientation Mapping of Isolated Gold Nanostructures using Polarized Dark-Field Microscopy*, *J. Phys. Chem. C*, **125**(21), 11478 (2021). (DOI: [10.1021/acs.jpcc.1c03671](https://doi.org/10.1021/acs.jpcc.1c03671))
3. D. Singappuli-Arachchige, S. Feng, L. Wang, P.E. Palo, S.O. Shobade, M. Thomas, M. Nilsen-Hamilton, The Magnetosome Protein, Mms6 from *Magnetospirillum magneticum* Strain AMB-1, is a Lipid-Activated Ferric Reductase, *Int. J. Mol. Sci.* **23**(18), 10305 (2022). <https://doi.org/10.3390/ijms231810305>
4. H.J. Kim, W. Wang, H. Zhang, G. Freychet, B.M. Ocko, A. Travesset, S.K. Mallapragada, and D. Vaknin, *Effect of Polymer Chain Length on the Superlattice Assembly of Functionalized Gold Nanoparticles*, *Langmuir*, **37**(33), 10143-49 (2021). <https://doi.org/10.1021/acs.langmuir.1c01547>
5. H.J. Kim, W. Wang, S.K. Mallapragada, D. Vaknin, D., and A. Travesset, *Nanoparticle Superlattices with Negative Thermal Expansion Coefficients*, *J. Phys. Chem. C*, **125** (18), 10090-95 (2021). <https://doi.org/10.1021/acs.jpcc.1c01354>
6. Kim, H.J., Wang, W., Bu, W., Mallapragada, S. K. and Vaknin, D., *Lamellar and Hexagonal Assemblies of PEG-Grafted Silver Nanoparticles: Implications for Plasmonics and Photonics*, *ACS Appl. Nanomaterials*, **5**, 17556-64 (2022). <https://doi.org/10.1021/acsanm.2c03042>
7. Hallstrom, J., Cherniukh, I., Zha, X., Kovalenko, M.V. and Travesset, A., *Ligand Effects in Assembly of Cubic and Spherical Nanocrystals: Applications to Packing of Perovskite Nanocubes*, *ACS Nano*, **17**, 7219-7228 (2023).
8. Zhou, S., Li, J., Lu, J., Liu, H., Kim, J. Y., Kim, A., Yao, L., Liu, C., Qian, C., Hood, Z., D., Lin, X., Chen, W., Gage, T. E., Arslan, I., Travesset, A., Sun, K., Kotov, N.A. and Chen, Q., *Chiral Assemblies of Pinwheel Superlattices on Substrates*, *Nature*, **612**, 259–265 (2022).
9. H.J. Kim, W. Wang, H. Zhang, G. Freychet, B.M. Ocko, A. Travesset, S.K. Mallapragada, D. Vaknin, *Binary Superlattices of Gold Nanoparticles in Two Dimensions*, *J. Phys. Chem. Lett.*, **13** (15), 3424-3430 (2022). <https://doi.org/10.1021/acs.jpcclett.2c00625>
10. Macias, E., and Travesset, A., *Hydrogen Bond Network Disruption by Hydration Layers in Water Solutions with Salt and Hydrogen Bonding Polymers (PEO)*, *J. Chem. Phys. B* (2023).

## **Precision synthesis and assembly of ionic and liquid crystalline polymers**

**Paul F. Nealey, Matthew V. Tirrell, and Juan J. de Pablo**

**Materials Science Division, Argonne National Laboratory, Lemont, Illinois 60439, USA**

**Keywords:** precision synthesis, self-assembly, molecular simulation, nanostructured polyelectrolytes, liquid crystals

### **Research Scope**

Molecular self-assembly is a promising strategy for imparting structure and function to materials at the molecular, meso-, and macro-scale and for developing high-performance soft and biomolecular materials for energy related applications. Encoding information into the building blocks of materials systems through precision synthesis introduces specific and controllable intra- and intermolecular interactions to drive assembly with hierarchical structure. Our FWP has played a leading role in broadening the available toolset to achieve precision organization of soft matter by advancing the fundamental understanding and manipulation of: 1) ionic and mesogenic interactions in polymers and liquid crystal systems, 2) multi-valent interactions, and 3) the use of external fields in processes of directed self-assembly to impart function in materials or better assess structure function relationships. Our activities are organized into three interrelated thrusts of increasing complexity, from the self-assembly of sequence-specific homopolymers in solution in Thrust 1: “Physics and materials science of hetero-charged polymers from A to Z (Polyampholytes to Polyzwitterions),” to the directed self-assembly and intrinsic ion-conducting properties of nanostructured ethylene oxide based polymers in Thrust 2: “Fundamental investigation of physical and electrochemical properties of block copolymer electrolytes,” to the most complex materials incorporating liquid crystallinity and charge in fully three-dimensional assemblies in Thrust 3: “Directed self-assembly of blue phase liquid crystals- fundamentals and functionality.” Because the assembly, structure, and dynamics of functional polymer and soft matter systems are complicated, a unifying concept and defining strength of our overall project is the combination of experiment, computation, and data driven approaches to accelerate materials discovery and design.

### **Recent Progress**

For this DOE-BES Biomolecular Materials Principal Investigators’ Meeting, we will focus on our research related to Thrust 1. Complexation of charged macromolecules is vital in biological contexts and in pharmaceutical, food, and cosmetic industries. Despite extensive research on flexible polyelectrolytes, our understanding of charged macromolecules and their complexation remain limited. These macromolecules, such as proteins, nucleic acids, and polysaccharides, are characterized by their distinct chain stiffness, charge sequence, and molecular shape, making it challenging to unravel their impact on complexation. We built a theoretical framework to describe the effect of chain stiffness and charge sequence on the phase behavior of oppositely charged

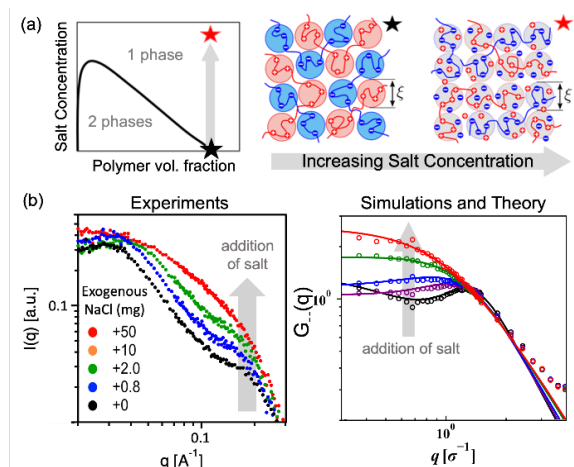


**Figure 1.** Scattering evidence of positional charge correlation in liquid polyelectrolyte complexes. (a) Evolution of blob structure upon addition of salt. (b) Polyanion structure factor obtained from SANS experiments (left), simulations (right, data points) and theory (right, solid lines), with addition of salt.

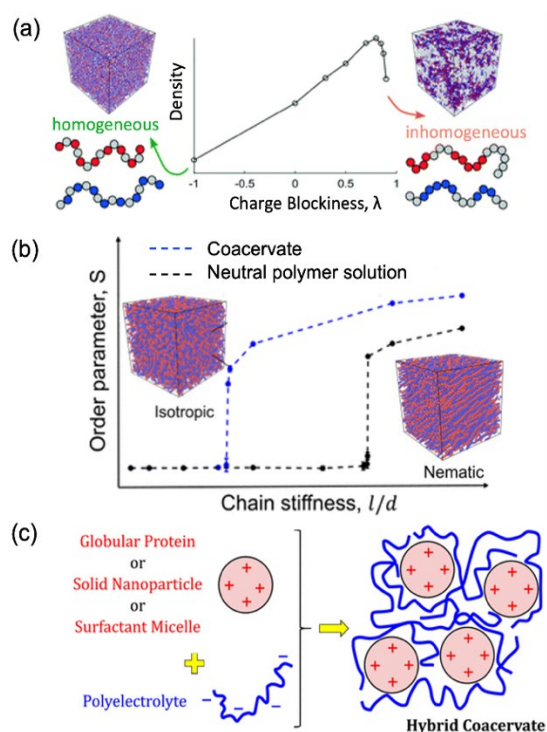


**Figure 2.** (a) Effect of charged monomer sequence on the density of polyelectrolyte complexes. (b) Effect of chain stiffness on the order parameter of semiflexible polyelectrolyte complexes. (c) Schematic illustration of hybrid coacervates between charged colloids and polyelectrolytes.

macromolecules. This framework is based on a hypothetical physical picture where electrostatic interactions originate from the positional correlation of oppositely charged electrostatic blobs (Figure 1a). However, this hypothesis requires testing, and the theories need verification.

By combining experimental and computational methods, we provided the first evidence of positional charge correlation in liquid polyelectrolyte complexes<sup>1</sup>. We synthesized a polycation/polyanion pair with/without deuterium labeling and charge fraction  $f = 0.3$ , by post-polymerization functionalization of a nearly ideally random copolymer of allyl glycidyl ether (AGE) and ethylene oxide (EO) or deuterated ethylene-d4 oxide (EO-d4). By contrast matching the solvent and deuterated polycation, the polyanion structure factor was obtained from the deuterated polyelectrolyte complex and showed a shoulder peak at  $q^* \approx 0.2 \text{ \AA}^{-1}$ . This peak was attributed to the electrostatic repulsion between polyanion fragments and their attractions to polycations, and it was the first experimental evidence of positional charge correlation. The addition of salt to the coacervates phase at a constant polymer concentration reduced the correlation peak, which further corroborated its electrostatic origin (Figure 1b). Theoretical predictions and molecular dynamics simulations further validated these findings, demonstrating the correspondence between the correlation peak in Fourier space and positional charge correlation in real space.

To investigate the molecular level control of polyelectrolyte complexation, we developed a comprehensive framework using a combination of simulation and theoretical method. Our coarse-grained models enabled us to study the phase behavior, structure, dynamics, and rheological properties of polyelectrolyte complexes with and without salt. Based on these models, we studied the effect of charge sequence and chain stiffness on phase behavior of polyelectrolytes complexation. In sequence-controlled complexes, we showed that higher charge sequence blockiness of constituting polyelectrolytes leads to higher complex concentration and salt resistance (Figure 2a)<sup>2</sup>. In

semiflexible polyelectrolyte complexes, we demonstrated that the electrostatic interactions facilitate the orientational ordering of polyelectrolyte chains and isotropic-to-nematic transition within the liquid complex (Figure 2b)<sup>3</sup>. Our simulation results were in good agreement with our previous theoretical predictions. We also developed a scaling theory for hybrid coacervates between charged colloids and polyelectrolytes (Figure 2c)<sup>4</sup>. This model system finds important applications in biological condensates involving globular proteins. This theory is being investigated by coarse-grained molecular dynamics simulations and is integrated with experimental efforts to design polyelectrolyte systems capable of delivering protein drugs.

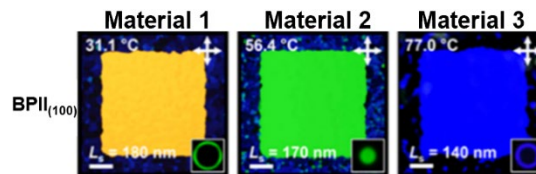


**Figure 3.** BP II single crystals grown for three different materials on chemical patterns. The three materials vary vastly in chemistry and complexity however the same design rules can be applied to all three of them.

Besides research activities mentioned above, we also **established generalizability of blue phase directed self-assembly**. Blue phases are stimuli-responsive photonic crystals with attractive properties for next generation displays and sensors. Owing to their superior material properties, single crystalline blue phases are preferred over their polycrystalline counterparts for applications. Combining experiments and simulations, we proposed successful design rules for assembling blue phase single crystals on chemically patterned surfaces. Our earlier experiments, however, utilized a single model blue phase-forming mixture. The general applicability of our approach across the broad chemical space of blue phase-formers was therefore untested. Recently, we demonstrated that our chemo-epitaxial approach is applicable across materials of different chemical composition and complexity<sup>5</sup>. Shown in Figure 3 are blue-phase single crystals from compositions varying in chemistry and composition. By combining directed self-assembly and photopolymerization, we created ideal, monodomain polymeric photonic crystals. Our work also tested the limits of continuum level descriptions of liquid crystals. The surfaces that guide assembly of different blue phase single crystals in our experiments were designed based on predictions of free energy functional based calculations.

## Future Plans

Our FWP excels in elucidating the fundamental chemistry, physics, and materials science of nanostructured and functional polymer and soft matter systems, with an emphasis on the role of charge on structure and dynamics both at equilibrium and well beyond equilibrium. Molecular self-assembly, with basic tenets derived from biology, is arguably the most promising strategy for imparting structure and function to functional soft and biomolecular materials at multiple length scales. Because the assembly, structure, and dynamics of functional polymer and soft matter systems are complicated, a unifying concept and defining strength of our project is the combination of experiment, theory, computation, and data-driven approaches to accelerate materials discovery and design. We will focus our future efforts on the following three interrelated thrusts:

**Thrust 1: Fundamental Investigation of Water Absorption and Ion Transport Mechanisms in Homopolymer and Block Copolymer Electrolytes.** Creating polyelectrolytes that selectively conduct anions is a bottleneck in the development and deployment of key energy technologies such as fuel cells, water electrolyzers, CO<sub>2</sub> electrolyzers, redox flow batteries, and seawater

desalination. We will address this knowledge gap through the precision synthesis, characterization, and simulation of the complex interplay between water absorption, ion transport, and mechanical properties of a new and highly flexible functional platform of homopolymer and block copolymers based on chemically stable polynorbornenes.

**Thrust 2: High-Throughput Robotic Experimentation and Computation for Designing Mixed Conducting Polymers.** Room-temperature ion transport in mixed conductors has almost exclusively been achieved using liquid electrolytes, ionic liquids, or by operating in high-moisture environments, posing limitations for existing fabrication processes and applications such as neuromorphic computing. We will develop ML-guided high-throughput experimental techniques, coupled to computational approaches, to identify correlations between the material composition, nanoconfinement effects (size and interface), and structural and transport properties to unravel new design principles and develop new solid-state mixed conducting polymers.

**Thrust 3: Hybrid Coacervation, Surface Interactions and Their Modification with Polyampholytes.** We will develop a systematic understanding of hybrid complex coacervation between polyelectrolytes and charged colloids or proteins. This work is particularly relevant in the context of biology and biomaterials, where membrane-less organelle formation is thought to be driven by complexation between proteins and polyelectrolytes, as well as other charged aggregates. That understanding will in turn provide a foundation for development of new classes of biomaterials and new separation processes that, in addition to charge, will also rely on charge distribution along a polymer backbone or the surface of a protein or colloid as design variables.

## References

1. Y. Fang, A. M. Romyantsev, A. E. Neitzel, H. Liang, W. T. Heller, P. F. Nealey, M. V. Tirrell, J. J. de Pablo, *Scattering Evidence of Positional Charge Correlations in Polyelectrolyte Complexes*. Proceedings of the National Academy of Sciences (2023), Accepted.
2. B. Yu, A. M. Romyantsev, N. E. Jackson, H. Liang, J. M. Ting, S. Meng, M. V. Tirrell, J. J. de Pablo, *Complex coacervation of statistical polyelectrolytes: role of monomer sequences and formation of inhomogeneous coacervates*. Molecular Systems Design & Engineering **6**, 790–804 (2021).
3. B. Yu, H. Liang, A. M. Romyantsev, J. J. de Pablo, *Isotropic-to-Nematic Transition in Salt-Free Polyelectrolyte Coacervates from Coarse-Grained Simulations*. Macromolecules **55**, 9627–9639 (2022).
4. A. M. Romyantsev, O. V. Borisov, J. J. de Pablo, *Structure and Dynamics of Hybrid Colloid–Polyelectrolyte Coacervates*. Macromolecules **56**, 1713–1730 (2023).
5. T. Emeršič; K. Bagchi, J. A. Martínez-González, X. Li, J. J. de Pablo, P. F. Nealey, *A Generalizable Approach to Direct the Self-Assembly of Functional Blue-Phase Liquid Crystals*. Advanced Functional Materials **32**, 2202721 (2022).

## Publications

### 10 most relevant out of total 41 publications are listed.

1. A. M. Romyantsev, O. V. Borisov, J. J. de Pablo, *Structure and Dynamics of Hybrid Colloid–Polyelectrolyte Coacervates*. *Macromolecules* **56**, 1713–1730 (2023).
2. H. Liang, J. J. de Pablo, *A Coarse-Grained Molecular Dynamics Study of Strongly Charged Polyelectrolyte Coacervates: Interfacial, Structural, and Dynamical Properties*. *Macromolecules* **55**, 4146–4158 (2022).
3. A. M. Romyantsev, A. Johner, M. V. Tirrell, J. J. de Pablo, *Unifying Weak and Strong Charge Correlations within the Random Phase Approximation: Polyampholytes of Various Sequences*. *Macromolecules* **55**, 6260–6274 (2022).
4. B. Yu, H. Liang, A. M. Romyantsev, J. J. de Pablo, *Isotropic-to-Nematic Transition in Salt-Free Polyelectrolyte Coacervates from Coarse-Grained Simulations*. *Macromolecules* **55**, 9627–9639 (2022).
5. J. Dinic, M. R. Schnorenberg, M. V. Tirrell, *Sequence-Controlled Secondary Structures and Stimuli Responsiveness of Bioinspired Polyampholytes*. *Biomacromolecules* **23**, 3798–3809 (2022).
6. T. Emeršič; K. Bagchi, J. A. Martínez-González, X. Li, J. J. de Pablo, P. F. Nealey, *A Generalizable Approach to Direct the Self-Assembly of Functional Blue-Phase Liquid Crystals*. *Advanced Functional Materials* **32**, 2202721 (2022).
7. B. Yu, A. M. Romyantsev, N. E. Jackson, H. Liang, J. M. Ting, S. Meng, M. V. Tirrell, J. J. de Pablo, *Complex Coacervation of Statistical Polyelectrolytes: Role of Monomer Sequences and Formation of Inhomogeneous Coacervates*. *Molecular Systems Design & Engineering* **6**, 790-804 (2021).
8. A. M. Romyantsev, A. Johner, J. J. de Pablo, *Sequence Blockiness Controls the Structure of Polyampholyte Necklaces*. *ACS Macro Letter* **10**, 1048–1054 (2021).
9. A. M. Romyantsev, N. E. Jackson, A. Johner, J. J. de Pablo, *Scaling Theory of Neutral Sequence-Specific Polyampholytes*. *Macromolecules* **54**, 3232–3246 (2021).
10. J. Dinic, A. B. Marciel, M. V. Tirrell, *Polyampholyte Physics: Liquid-Liquid Phase Separation and Biological Condensates*. *Current Opinion in Colloid & Interface Science* **54**, 101457 (2021).

## Design, Synthesis, and Assembly of Biomimetic Materials with Novel Functionality

**Aleksandr Noy, Anthony van Burren (LLNL), David Baker (U. of Washington), James J. De Yoreo, Chun-Long Chen, Marcel Baer (PNNL)**

**Keywords:** artificial membrane assemblies, biomimetic membrane channels, *de novo* designed proteins, designed sequence polymers, membrane transport

### Research Scope

The long-term vision of this project is to develop synthetic self-assembling systems that emulate the hierarchical nature of biology and carry out complex functions based on a predictive understanding of assembly and function. Specifically, we seek to create fully synthetic self-assembling biomimetic structures that mimic the environment, versatility, and functionality of cell membranes based on physico-chemical principles underlying (1) co-assembly of biomimetic membrane matrices, artificial membrane channels, and *de novo* designed protein nanopores into artificial membrane assemblies, (2) the structuring of water and ions near membrane surfaces and pores, and (3) fast and selective transport through the pores. Our proposed research seeks to achieve rational design of fully synthetic multicomponent membranes based on an understanding of (1) controls on co-assembly and ordering, (2) transport mechanisms through the synthetic protein nanopores and (3) the relationship between protein pore design and ion-selectivity. Our approach integrates synthesis of novel biomimetic materials, *in situ* characterization of interfacial structure, interactions, and assembly, molecular simulations of structure, assembly and transport, and measurements of ion and water transport through nanopores. These advances will build a foundation for designing biomimetic functional materials where the transport and selectivity can be tuned for applications in energy systems.

### Recent Progress

**Co-assembly of carbon nanotube porins into biomimetic peptoid membranes (*Small* 2023).** Our molecular dynamics (MD) simulations of the free energy associated with incorporation of CNTP pores into 2D peptoid membranes showed that CNTP pore is stabilized by ca. 35 kcal mol<sup>-1</sup> in the peptoid membrane, indicating that CNTPs should spontaneously incorporate into this matrix. To test this assumption, we integrated artificial CNTP channels into peptoid (Nbrpe<sub>6</sub>Nce<sub>6</sub>) nanosheets using a co-assembly protocol (Fig. 1). A combination of MD simulations, Raman, XRD, and AFM measurements verified the co-assembly of CNTP and peptoids and showed that it did not disrupt peptoid monomer packing within the membrane. These synthetic membranes combine the high stability of peptoid nanosheets<sup>1</sup> and selectivity and permeability of CNTP,<sup>2</sup> opening up a way to produce robust highly programmable synthetic membranes.

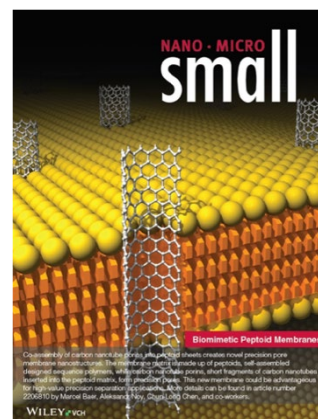


**Figure 1.** Co-assembly of CNTP channels into peptoid matrix.

**Atomic level characterization and simulation: Structure of peptoid membrane matrix** (*J. Phys. Chem. Lett.* 2021). We recently used time resolved x-ray scattering and MD simulations to understand assembly of halogen functionalized (Cl, Br and I) peptoid amphiphiles. SAXS measurements revealed that in all cases the peptoids first assemble into a nascent amorphous phase prior to crystallization. The crystallization kinetics were sequence dependent, with I-functionalized peptoids crystallizing in 5 minutes, while the Cl- and Br functionalized versions did so only after 2 and 6 hrs. Diffraction peaks associated with aromatic interactions were observed in the early stages and develop the fastest, with the aromatic domains arranging in a herringbone pattern (Fig. 2). These results demonstrate our ability to track the kinetics, structural development, and distribution during co-assembly of disparate building blocks.

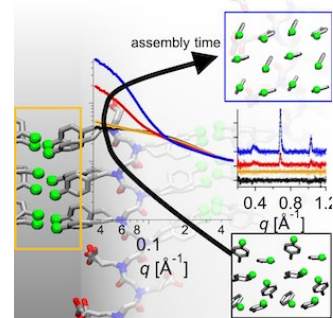


**Figure 2.** SAXS and MD simulation reveal atomic level structure of self-assembled peptoid membrane matrices.

**Peptoid assembly for antibacterial activity.** We have recently designed a new family of low molecular weight peptoid antibiotics that form membrane-disrupting assemblies that exhibit excellent broad-spectrum activity and high selectivity toward a panel of Gram-positive and Gram-

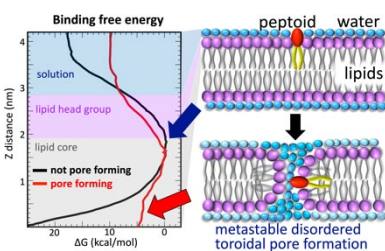


**Figure 3.** Computational simulations predict the penetration of amphiphilic peptoids into a POPC model lipid bilayer.

negative bacterial strains, including vancomycin-resistant *E. faecalis* (VREF), methicillin-resistant *S. aureus* (MRSA), methicillin-resistant *S. epidermidis* (MRSE), *E. coli*, *P. aeruginosa*, and *K. pneumoniae*. Mechanistic studies using *in situ* AFM, TEM, bacterial membrane depolarization and lysis, and time-kill kinetics assays along with MD simulations reveal that these peptoids kill bacteria through the formation of artificial channels in the cell membranes (Fig. 3). Tuning peptoid sidechain chemistry and structure enabled us to increase the efficacy of antimicrobial activity.

**Dynamics of peptoid self-assembly into 2D membranes.** We used *in situ* AFM to reveal the mechanism and dynamics of nucleation and growth by the three distinct membrane-forming peptoid sequences. The initial step involves deposition of liposome-like peptoid particles on to the surface forming isolated islands. Those islands then spread (Fig. 4a,b) through lateral diffusion of peptoids across the islands and attachment at their edges (Fig. 4c). Growth kinetics was consistent with step-edge propagation, limited by attachment and detachment reaction kinetics at the step edge. We observed that the addition of a short hydrophobic region to the sequence increases the kinetics of self-assembly, while switching of hydrophobic domain position influences particle size distribution and the island edge roughness. Furthermore, the sequence with the lowest kinetic coefficient also has the lowest equilibrium concentration i.e., once a growth unit attaches to the island no detachment of the unit occurs. These results have implications for predictive synthesis of self-assembled peptoid membrane matrices.

**Synthesis and transport characteristics of biomimetic carbon nanotube membrane channels.** (*JACS 2023, in review*). Our previous work showed we can cut longer CNTs into small (sub-10-nm) segments stabilized by lipid coating—carbon nanotube porins (CNTPs)—that self-insert into lipid matrices and form functional ion channels. We

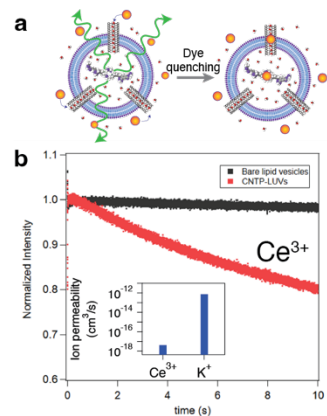


**Fig. 5.** Cation transport in carbon nanotube porins. **a.** Experiment schematics. **b.** Single channel permeability of 0.8 nm CNTPs for  $\text{Ce}^{3+}$  and  $\text{K}^+$  cations.

separations.

**Molecular transport in *de novo* designed protein pores.** *De novo* designed protein pores, developed by the Baker group, provide us with the possibility to use parametric design to achieve exquisite control over the size and precise functionality of the pore channels for incorporation into both lipid and peptoid membranes (Fig. 6). We have synthesized, and characterized a series of 8, 10, 12 and 14- stranded transmembrane  $\beta$ -barrel protein channels (Fig 7a), which exhibit an asymmetric structure with a barrel-like shape, that enhances the possibilities for controlling transport of water ions, and small molecules in these channels. Single channel conductance measurements in a planar lipid bilayer setup, which measure the conductance increase following a pore incorporation into the lipid bilayer patch, quantified the ion conductance of these pores with the data showing a clear increase of the conductance value with the pore size (Fig. 7b).

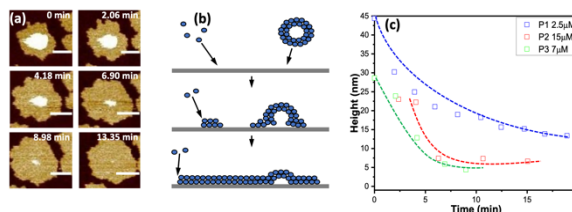


**Figure 4:** (a) AFM images showing deposition and spreading of a ca. 25 nm-high peptoid micelles on mica surface. Scale bar: 150nm. (b) Deposition and spreading mechanism. (c) Spreading kinetics determined from the AFM images.

that produces a variety of surfactant-stabilized CNTPs and demonstrated that they retain the membrane insertion activity and transport properties indistinguishable from the original lipid-stabilized CNTPs. Our previous studies also explored monovalent ion transport in CNTPs and established strong cation selectivity of these channels<sup>2</sup>. To probe how cation charge influences transport in membrane nanopores we have explored the permeability of 0.8 nm wide CNTPs for highly charged rare earth (REE)  $\text{Ce}^{3+}$  ions and compared them with the monovalent ions of similar size. Our data show that large dehydration energy penalty associated with the  $\text{Ce}^{3+}$  ion slows down its translocation through the CNTP channel by over 5 orders of magnitude, compared to a similarly sized monovalent  $\text{K}^+$  ion (Fig. 5). Ongoing work is exploring differential selectivity of CNTP pores for transport of other rare earth ions, which could be potentially used to build robust artificial membranes suitable for critical materials



**Fig. 6.** *De novo* designed protein pores.

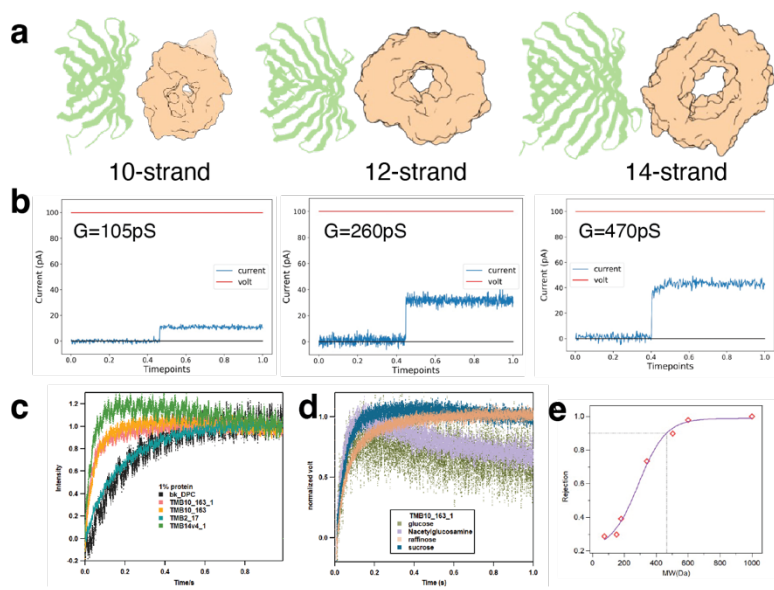


**Figure 7.** Transport in *de novo* designed protein pores. **a.** Structures of the  $\beta$ -barrel protein channels. **b.** Ion conductance of protein pores. **c.** Water transport in protein pores. Faster rise in light scattering intensity corresponds to faster water transport. **d.** Solute transport in protein pores. **e.** Size rejection curve determined for a 12-strand protein channel.

Stop-flow measurements of water transport through the protein pores incorporated in the walls of lipid vesicles (Fig. 7c) reveal that 10, 12, and 14-stranded designs have high water permeability comparable to those of aquaporins, whereas the narrower pore of the 8-stranded protein was unable to conduct water (Fig. 7c). Larger nm-scale pores of the 12 and 14 stranded designs also allow them to pass molecules larger than water; therefore, we have investigated the transport of neutral solutes with a stop flow assay. After water-filled vesicles with protein pores embedded in their walls were exposed to a solute solution, osmotic pressure caused rapid water efflux out of the vesicle and the corresponding light scattering increase. A slower light scattering signal decrease that followed this

rapid initial rise corresponded to the backflow of solute into the vesicles (Fig. 7d), with the faster kinetics indicating higher solute permeability of the pores. These measurements repeated over a range of neutral solutes with different size allowed us to determine the molecular weight cut-off of the protein pores (Fig. 7e), with the 12-stranded pore showing MWCO of 465Da, which was consistent with its structure.

## Future Plans

Our future research will be focused on assembling synthetic pores and *de novo* designed proteins into peptoid and block copolymer membrane matrices and determining the efficiency of water, ion, and proton transport in these assemblies. These measurements will focus on establishing the structure-function relationships in these assemblies, as well as refining the pore designs to target applications in energy-related systems.

## References

1. Li, Z.; Cai, B.; Yang, W.; Chen, C.-L. Hierarchical Nanomaterials Assembled from Peptoids and Other Sequence-Defined Synthetic Polymers. *Chem. Rev.* 121, 14031-14087 (2021).
2. Tunuguntla, R. H.; Henley, R. Y.; Yao, Y.-C.; Pham, T. A.; Wanunu, M.; Noy, A. Enhanced water permeability and tunable ion selectivity in subnanometer carbon nanotube porins. *Science* 357, 792-796, 2017.

## Publications

1. S. Zhang, J.J. Hettige, Y. Li, T. Jian, W. Yang, Y.-C. Yao, R. Zheng, Z. Lin, J. Tao, J.J. De Yoreo, M. Baer, A. Noy, C.-L. Chen, Co-Assembly of Carbon Nanotube Porins into Biomimetic Peptoid Membranes, *Small* 19, 2206810 (2023). Frontispiece Cover.
2. J.A. Hammons, M.D. Baer, T. Jian, J.R.I. Lee, T.M. Weiss, J.J. De Yoreo, A. Noy, C.-L. Chen, A. Van Buuren, Early-Stage Aggregation and Crystalline Interactions of Peptoid Nanomembranes, *J. Phys. Chem. Lett.* 12, 6126-6133 (2021).
3. W. Yang, Y. Zhou, B. Jin, X. Qi, B. Cai, Q. Yin, J. Pfaendtner, J.J. De Yoreo, C.-L. Chen, Designing sequence-defined peptoids for fibrillar self-assembly and silicification, *J. Coll. Interf. Sci.* 634, 450-459 (2023).
4. S. Akkineni, G.S. Doerk, C. Shi, B. Jin, S. Zhang, S. Habelitz, J.J. De Yoreo, Biomimetic Mineral Synthesis by Nanopatterned Supramolecular-Block Copolymer Templates, *Nano Lett.* 23, 4290-4297 (2023).
5. S. Zhao, A. J. Gillen, Y. Li, A. Noy, Sonochemical synthesis and ion transport properties of surfactant-stabilized carbon nanotube porins, *J. Am. Chem. Soc.*, in review (2023).
6. S. Akkineni, C. Zhu, J. Chen, M. Song, S.E. Hoff, J.S. Bonde, J. Tao, H. Heinz, S. Habelitz, J.J. De Yoreo, Amyloid-like amelogenin nanoribbons template mineralization via a low energy interface of ion binding sites, *Proc. Nat'l Acad. Sci. USA*, 119, e2106965119 (2022).
7. N.T. Ho, M. Siggel, K.V. Camacho, R.M. Bhaskara, J.M. Hicks, Y-C. Yao, Y. Zhang, J. Köfinger, G. Hummer, A. Noy, Drug delivery with carbon nanotube porin fusogens, *Proc. Natl. Acad. Sci. USA*, 118, e2016974118 (2021).
8. Z. Li, B. Cai, W. Yang, C.-L. Chen, Hierarchical Nanomaterials Assembled from Peptoids and Other Sequence-Defined Synthetic Polymers, *Chem. Rev.* 121, 14031-14087 (2021).
9. M. Wang, Y. Song, S. Zhang, X. Zhang, X. Cai, Y. Lin, J.J. De Yoreo, C.-L. Chen, Programmable two-dimensional nanocrystals assembled from POSS-containing peptoids as efficient artificial light-harvesting systems. *Science Advances*, 7, eabg1448 (2021).
10. X. Chen, A. Noy Antifouling strategies for protecting bioelectronic devices, *APL Materials*, 9, 020701 (2021).

## Adaptive Interfacial Assemblies Towards Structuring Liquids (KCTR16)

**Ahmad Omar**, Materials Science Department, University of California Berkeley

**Paul Ashby**, Molecular Foundry, Lawrence Berkeley National Laboratory

**Brett Helms**, Molecular Foundry, Lawrence Berkeley National Laboratory

**Alex Zettl**, Physics Department, University of California Berkeley

**Thomas P. Russell**, Materials Sciences Division, Lawrence Berkeley National Laboratory and  
Polymer Science and Engineering Department, University of Massachusetts-Amherst

**Keywords:** Structured liquids, spontaneous emulsification, dissipative interfacial assemblies, conductive interfacial assemblies, active matter

### Research Scope

This FWP advances a new concept in materials based on the interfacial formation, assembly and jamming of nanoparticle surfactants (NPSs). By learning how to manipulate the interfacial packing of the NPSs using external triggers, a new class of materials will emerge that synergistically combines the desirable characteristics of fluids with the structural stability of a solid, i.e., structured liquid. We are developing theoretical models to understand the interfacial packing of the NPSs, the limits in the packing to cause spontaneous emulsification, and the use of external fields to oversaturate the interface, to store a potential energy. Experimentally, we are understanding how to control and oversaturate the interfaces with NPSs and have demonstrated control over the release of the stored energy in the form of a ballistic ejection of a plume of microdroplet from the droplet surface. We have also shown directional control of the explosive event, using this as a new propulsion mechanism in all-liquid environments. We are pursuing the interfacial assembly of mixed NPSs systems to generate heterogenous assemblies and probe 2D phase separation behavior. With conductive NPSs we are investigating all-liquid electronic circuits that can be integrated with existing hard-wire technologies. By encapsulating active matter within the structured liquids, the shapes of structured liquid domains evolve with time, providing an ideal platform to mimic living systems. In each of these areas fundamental challenges are faced in tailoring NPS chemistry, assembly, and dynamics to affect controlled macroscopic in the system.

### Recent Progress

**Electric field-induced explosive emulsification (Omar, Ashby, Helms, Russell);** By applying an external electric field, packing of the nanoparticle surfactants (NPSs) at the interface between immiscible liquid phases can be over saturated. Application of a negative bias to the aqueous droplet yields significant improvements in the adsorption of

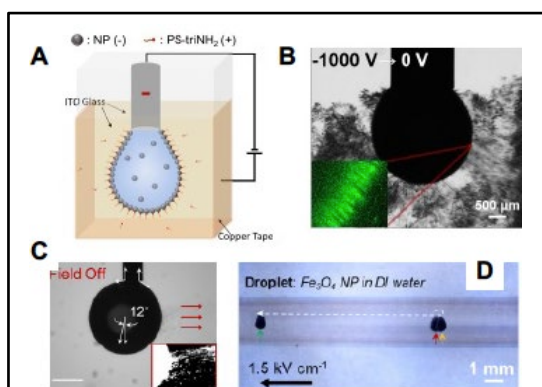


**Fig. 1** (A) Schematic of the experimental setup. (B) Optical images of the aqueous droplet ( $C_{\text{Fe}_3\text{O}_4} = 1 \text{ mg mL}^{-1}$ ) immersed in a PS-triNH<sub>2</sub> solution ( $1 \text{ mg mL}^{-1}$ ) in toluene after the negative bias is switched off, and the inset is the confocal image of the interface; (C) Aqueous droplet immersed in the toluene phase after turning a parallel electric field off. Inset shows binary contrast processed with ImageJ to highlight the droplet and microdroplets; (D) Trajectory of an aqueous droplet after a parallel electric field ( $1.5 \text{ kV cm}^{-1}$ ) is turned off.

NPs at the liquid-liquid interface (Figure 1a). Upon the rapid removal of the field, the accumulated energy is released, leading to the ballistic ejection of a plume charged microdroplets from the droplet surface, where the amount and the velocity of the ejected microdroplets increase with the applied electric field strength (Figure 1b). When applying a parallel electric field, only one side of the droplet becomes oversaturated with NPs, resulting in a directional explosive emulsification. (Figs. 1c). This ejection is directional, with the combined interaction force of the microdroplet plume propelling the millimeter-sized parent droplet distances tens of times its own size (Fig. 1d). Developing robust strategies to autonomously and repeatedly perform a programmed action in liquids is a major challenge confronting several disciplines. This propulsion is repeatable, autonomous and agnostic to nanoparticle composition.

**Electric response of a jammed interface:** Oversaturating the NPs within the jammed interfacial layer also holds great potential for active matter systems. In our research, we have investigated the influence of field strength and direction on the behavior of the jammed interface that is composed by the cationic polymer surfactant, PS-NH<sub>2</sub>, and negatively charged SiO<sub>2</sub> NP. When a negative bias is applied, the negatively charged NPs are attracted to the interface, resulting in their accumulation at the liquid-liquid interface. This accumulation leads to the inflation of the droplet due to the increased stiffness of the interfacial film caused by the presence of the NPs. Conversely, under the positive bias, the packing density of NPs at the interface is lower, and as a result, the droplet exhibits a more elongated shape.

### Thermodynamic origins of structured liquids

**(Omar, Russell, Ashby):** NPs assemble at the interface of two immiscible liquids in order to reduce the system's interfacial energy. The measured interfacial tension  $\gamma_{eff}$  is a monotonically decreasing function of the particle density. At some critical particle density, the system's interfacial tension is vanishingly small, so that thermodynamic fluctuations can spontaneously produce surface area. This is realized in the form of a microemulsion of droplets of one of the liquid components. This process is known as spontaneous emulsification and has been studied for a variety of surfactant

systems. Recently, we developed a thermodynamic theory that constructs a total free energy that describes the spontaneous emulsification process for nanoparticle surfactants and can predict the expected emulsion droplet size as a functional of the bulk particle density.

We developed a more general and accurate model for the NPs in the form of anisotropic attractive patchy particles (Figure 2A), coarse-graining the expected ligand-ligand interactions into attractive patches on the particle surface. Including these attractions changes our predictions for the micro-emulsion critical particle density, as well as the expected droplet size. To realize these predictions, we must develop accurate equations of state for these patchy colloids. We are using molecular dynamics (MD) simulations of large assemblies of these patchy particles to sample equilibrium thermodynamic properties such as the planar pressure  $P_{2D}$  and the bulk pressure  $P_{3D}$  (Figure 2). The addition of attraction also allows us to consider additional surface physics that are

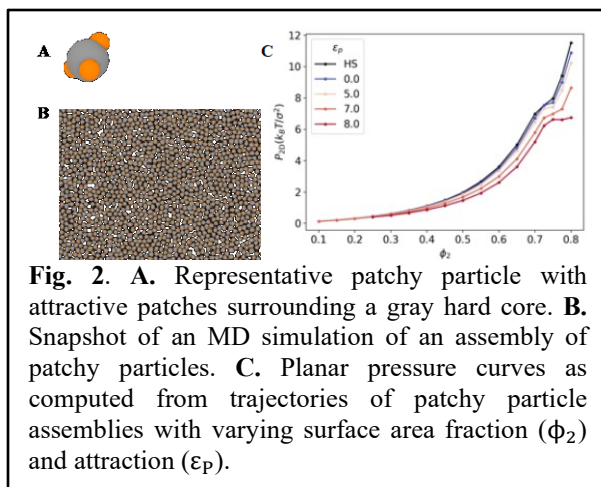


**Fig. 2.** **A.** Representative patchy particle with attractive patches surrounding a gray hard core. **B.** Snapshot of an MD simulation of an assembly of patchy particles. **C.** Planar pressure curves as computed from trajectories of patchy particle assemblies with varying surface area fraction ( $\phi_2$ ) and attraction ( $\epsilon_p$ ).

relevant to the droplet stability. The out-of-plane, elastic bending modulus is expected to be on the order of several orders of the thermal energy. The inclusion of this physically relevant property is expected to provide profound insights into the thermodynamics of droplet stability, in particular the stabilization of a “structured liquid” phase.

### In-Situ UV-VIS Reflection Spectroscopy of mixed NP assemblies (Ashby, Helms, Russell):

The in-plane packing of gold (Au), polystyrene (PS), and silica (SiO<sub>2</sub>) spherical nanoparticle (NP) mixtures at a water–oil interface were investigated *in situ* by UV-Vis reflection spectroscopy (Figure 3a). Noble metal NP assemblies, such as gold, exhibit coupled surface plasmon resonance characteristics of in-plane NP packing as the scattering, absorption, and reflection of light interacts differently with individual Au NPs and larger Au NP clusters. The plasmon excitation energy depends on the properties of Au NPs and the number of NPs in the ensemble, their relative locations, and interparticle distances. Since SiO<sub>2</sub> and PS do not have plasmon resonances, any change in the reflection spectrum can be attributed to changes in Au NP packing.

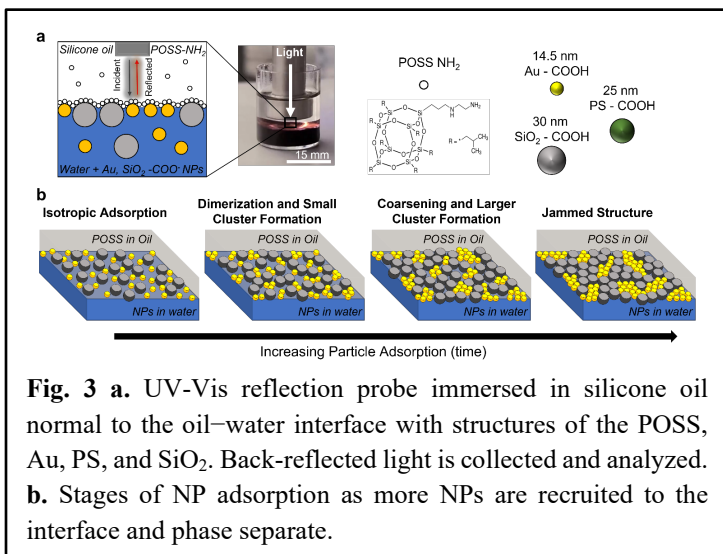


**Fig. 3 a.** UV-Vis reflection probe immersed in silicone oil normal to the oil–water interface with structures of the POSS, Au, PS, and SiO<sub>2</sub>. Back-reflected light is collected and analyzed. **b.** Stages of NP adsorption as more NPs are recruited to the interface and phase separate.

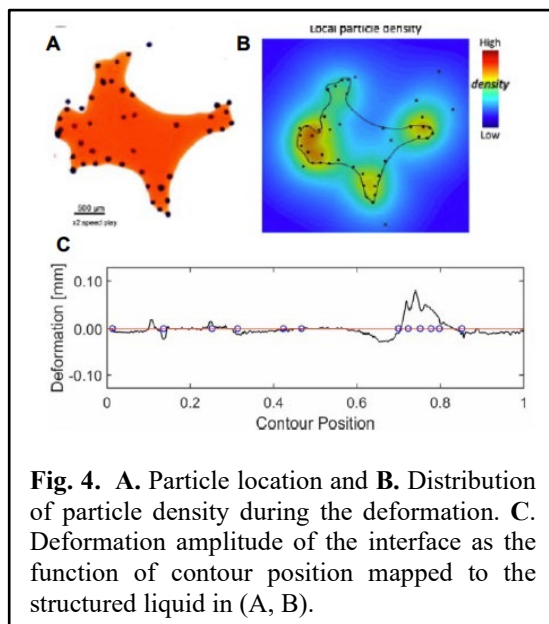
We found the number ratio of non-plasmonic NPs significantly affects the adsorption process and ultimately changes the equilibrium Au NP packing and domain size. As the interface saturates with NPs, Au NPs are brought into close contact, leading to an increase in the local surface plasmon resonance, and a redshift indicated the Au NPs were packed closer together by using well know plasmon ruler equations. A spectral narrowing at longer times for low and moderate non-plasmonic packing fraction suggested a slight increase in order and domain size (confirmed by GISAXS and ex-situ SEM). The results indicate that small clusters of 2-3 Au NP form after adsorption, while NP rearrangement opens space to accommodate additional Au NPs to the interface, which are later embedded into existing Au NP domains. By controlling the in-plane morphology of mixed nanoparticle (NP) assemblies, unique optical, electronic, and mechanical properties emerge where functional, large-scale interfacial structures can be tuned for advanced materials applications. The project will be transformative by encoding NPs with functionality to enable multi-length scale assembly and the generation of functional, hierarchical 3D structures.

**Conductive Liquid-Liquid Interfaces (Zettl, Ashby, Helms, Russell):** The rapid progression of modern electronics are primarily based on solid-state components, and grapple with inherent limitations in terms of reconfigurability and recyclability. To address these constraints, we used purely organic conductive components. We integrated the advantageous properties of phytic acid (PA) and sulfonated polyaniline (PANI) with the flexibility of 3D printing technology to generate conductive liquid wires. Here, the PA functions as a crosslinker between PANI moieties to create a more conductive jammed interface as the PANI is brought to the interface through the complementary interaction of the sulfonate and POSS amine. With an applied current of ~60  $\mu$ A, increasing the concentrations of the PANI and PA components (no POSS) separately in the system,

led to reductions in bulk resistance from the increase in the number charge carriers. With POSS ligand is introduced, there is two orders of magnitude decrease in the resistance, due to electrical conductivity from one PANI particle to another. Translating these results into a usable electrical device is straightforward as we have been able to turn on an LED though the connection of the LED legs to opposite ends of the liquid wire.

### Shape-Evolving Structured Liquids via Ferromagnetic Active Particles (Omar, Ashby, Russell):

The motion of active matter is the basic form of locomotion in biology, a vital ingredient in many functions of cells, and an essential design challenge in nanorobotics. Here, we integrated active matter into structured liquids to harness its motions to perform work on liquid interfaces. The structured liquids, produced by interfacial jamming of NPSs are reconfigurable and therefore provide an ideal platform for generating active energy-consuming systems. The liquid shape will evolve and respond to external stimuli when the interfacial tension is sufficiently low, i.e., 0.1 mN/m in this study. We used ferromagnetic active swimmers with relatively large momentum. Nickel particles with average diameters ranging from ~10 to ~60 microns were subjected to an external AC magnetic field to energize rolling motions on a solid substrate. When they are encapsulated in a droplet of structured liquids, the collisions of particles resulted in directional shape changes and translational motions of the droplet. Instead of bouncing off the interface, active particles trend to continuously push against and deform the interface (Figure 4A-B). As a result, “arms” of structured liquid grows as active particles accumulate on the deformed corner). We are currently quantifying the deformation of the interface (Figure 4C) to fully understand the origins of the shape changes. This strategy would provide a route to a new class of biomimetic, reconfigurable, and responsive materials, delivering mechanical responses unlike those of conventional materials.



### Future Plans

- To gain a more profound understanding of explosive spontaneous emulsification we plan to use *in-situ* small-angle X-ray scattering (SAXS at ALS) and x-ray photon correlation spectroscopy (XPCS at APS) as a function of particle concentration and pH where the areal density of the NPSs and the saturation conditions of the NPSs are varied. We will investigate the effect of NP shape on the interfacial assembly, beginning with cubic NPs.
- We are developing a theoretical model to predict and control the autonomous shape evolution of structured liquids by statistically investigating the dependence of the initial particle distribution and initial biased shapes. We will study how shape evolves from initial non-equilibrium 3D printed shapes.

- Experimental efforts on the shape evolution of the structured liquids with the incorporation of active particles will continue to quantify the parameters controlling the evolution.
- We have developed a liquid TEM cell to probe the assembly of the NPSs at liquid/liquid interfaces where the areal density of the NPSs can be varied, to obtain time dependent images of the NPSs to characterize, in real space, the dynamics of the assembled NPSs.
- We will continue efforts on the use of dissipative interfacial processes to generate chemically responsive interfacial assemblies.

## Publications (10 of 20)

1. Forth, J.; Mariano, A.; Chai, Y.; Toor, A.; Hasnain, J.; Jiang, Y. F.; Feng, W. Q.; Liu, X. B.; Geissler, P. L.; Menon, N.; Helms, B. A.; Ashby, P. D.; Russell, T. P. The Buckling Spectra of Nanoparticle Surfactant Assemblies, *Nano Lett.* **2021**, 21 (17), 7116-7122. DOI: 10.1021/acs.nanolett.1c01454.
2. Gu, P. Y.; Kim, P. Y.; Chai, Y.; Ashby, P. D.; Xu, Q. F.; Liu, F.; Chen, Q.; Lu, J. M.; Russell, T. P. Visualizing Assembly Dynamics of All-Liquid 3D Architectures, *Small* **2022**, 18 (6), 2105017. DOI: 10.1002/sml.202105017.
3. Kim, P. Y.; Fink, Z.; Zhang, Q.; Dufresne, E. M.; Narayanan, S.; Russell, T. P. Relaxation and aging of nanosphere assemblies at a water-oil interface, *ACS Nano* **2022**, 16 (6), 8967-8973. DOI: 10.1021/acsnano.2c00020.
4. Kim, P. Y.; Gao, Y. G.; Fink, Z.; Ribbe, A. E.; Hoagland, D. A.; Russell, T. P. Dynamic Reconfiguration of Compressed 2D Nanoparticle Monolayers, *ACS Nano* **2022**, 16 (4), 5496-5506. DOI: 10.1021/acsnano.1c09853.
5. Xie, G. H.; Li, P.; Kim, P. Y.; Gu, P. Y.; Helms, B. A.; Ashby, P. D.; Jiang, L.; Russell, T. P. Continuous, autonomous subsurface cargo shuttling by nature-inspired meniscus-climbing systems, *Nat. Chem* **2022**, 14 (2), 208-215. DOI: 10.1038/s41557-021-00837-5.
6. Yan, J.; Baird, M. A.; Popple, D. C.; Zettl, A.; Russell, T. P.; Helms, B. A. Structured-Liquid Batteries, *J. Am. Chem. Soc.* **2022**, 144 (9), 3979-3988. DOI: 10.1021/jacs.1c12417.
7. Zhao, S.; Zhang, J. Y.; Fu, Y. C.; Zhu, S. P.; Shum, H. C.; Liu, X. B.; Wang, Z. Y.; Ye, R. Q.; Tang, B. Z.; Russell, T. P.; Chai, Y. Shape-Reconfigurable Ferrofluids, *Nano Lett.* **2022**, 22 (13), 5538-5543. DOI: 10.1021/acs.nanolett.2c01721.
8. Popple, D.; Shekhirev, M.; Dai, C.; Kim, P.; Wang, K. X.; Ashby, P.; Helms, B. A.; Gogotsi, Y.; Russell, T. P.; Zettl, A. All-Liquid Reconfigurable Electronics Using Jammed MXene Interfaces, *Adv. Mater.* **2023**, 35 (13), e2208148. DOI: 10.1002/adma.202208148.
9. Wu, X.; Bordia, G.; Streubel, R.; Hasnain, J.; Pedroso, C. C. S.; Cohen, B. E.; Rad, B.; Ashby, P.; Omar, A. K.; Geissler, P. L.; Wang, D.; Xue, H.; Wang, J.; Russell, T. P. Ballistic Ejection of Microdroplets from Overpacked Interfacial Assemblies, *Adv. Funct. Mater.* **2023**, 33 (20), 2213844. DOI: 10.1002/adfm.202213844.
10. Yang, Y.; Sun, H.; Wang, M.; Li, M.; Zhang, Z.; Russell, T. P.; Shi, S. pH- and Redox-Responsive Pickering Emulsions Based on Cellulose Nanocrystal Surfactants, *Angew. Chem., Int. Ed.* **2023**, 62, e202218440. DOI: 10.1002/anie.202218440.

## Dynamics of Active Self-Assembled Materials

**PI: Alexey Snezhko. Co-Investigators: Andrey Sokolov, Andreas Glatz**

**Keywords:** active matter, out-of-equilibrium self-assembly

### Research Scope

Self-assembly, a natural tendency of simple building blocks to organize into complex architectures, is a unique opportunity for materials science. Materials that can spontaneously organize into hierarchical structures with unique and complex properties are currently exhibited only by living systems. An in-depth understanding of out-of-equilibrium self-assembly paves the way for the design of tailored smart materials and structures for emerging energy technologies, such as materials that can adapt, self-heal, regulate porosity, strength, or transport properties. Developing understanding and control of self-assembled out-of-equilibrium (also termed *active*) materials pose a significant challenge as they are intrinsically complex, with often hierarchical organization occurring on many nested length and time scales.

The program tackles the fundamental aspects of out-of-equilibrium dynamics and self-organization of bio-inspired materials. The program synergistically integrates experiment and simulations, and focuses on the fundamental issues at the forefront of contemporary materials science. The main research directions focus on the design of novel active materials that can arise from a fundamental understanding of dynamic self-assembly and organization in colloids far from equilibrium. We explore highly complementary model systems: self-propelled colloids driven by external fields, and active liquid crystals. The difference between the two is in the way the injected energy is utilized: driven colloids transform it into a mechanical particle motion, while in active liquid crystals it is used for reorientations of a local nematic order. The major challenges are: understanding fundamental principles that lead to a collective behavior and dynamic self-organization from the interactions between unitary building blocks outside of equilibrium, and designing new active materials with tunable structural and transport properties at the microscale.

### Recent Progress

In the past two years our program yielded discoveries of a hidden order and polar state reversal in active roller fluids [1], discovered novel arrested-motility states in populations of shape-anisotropic active Janus particles [2], demonstrated guided self-assembly of active colloids with temporal modulation of the activity [3], demonstrated hyperuniform active chiral fluids with tunable internal structure [4], investigated the emergence of globally correlated vortex lattices in active magnetic liquids [5]. For all these systems we have developed theoretical understanding leading to a better control of the self-assembled structures and dynamics.

Polar state reversal and hidden order in active fluids. Spontaneous emergence of correlated states such as flocks and vortices is a prime example of collective dynamics and self-organization observed in active matter. In geometrically confined systems, the formation of globally correlated polar states proceeds through the formation of a macroscopic steadily rotating vortex, which

spontaneously selects a clockwise or counterclockwise global chiral state. Once the global state is formed, it is often robust and stable. However, subsequent control of such polar states remains elusive. We discovered [1] that a global vortex formed by colloidal spherical Quincke rollers exhibits dynamic state memory, and that subsequent formation of the collective states upon temporal modulation of the activity is not random giving rise to a controllable polar state reversal of the globally correlated state. The robustness of the chiral state reversal long after the termination of the activity suggests the development of certain particle positional arrangements (hidden order) in the ensemble “imprinting” the dynamic state of the system and preserving it long after the activity is removed! We demonstrated that the information is preserved in structural asymmetries of the local particle positions. By introducing two local positional order parameters we revealed the hidden asymmetries that govern the collective behavior of the system upon activity modulations. Remarkably, a relatively weak level of local arrangement asymmetry is enough to prescribe the direction of the global vortex motion with high fidelity, see Figure 1. We combined experiments and simulations to elucidate how a combination of hydrodynamic and electrostatic interactions can lead to hidden asymmetries in the local particle positional order, reflecting the chiral state of the system. We revealed that hydrodynamic long-range interactions between the active particles are responsible for the emergence of locally asymmetric particle distributions. Electrostatic interactions, on the other hand, facilitate a mechanism by which the particle distributions become relevant in the process of a vortex formation. Our findings suggest that seemingly disordered dynamic patterns tend to develop local structural asymmetries in response to competing repulsive and aligning interactions between active particles, and within diffusion timescale, these asymmetries could be exploited to systematically control self-organized dynamic states with the aid of temporal modulation of activity. The results yield strategies for the control of active polar states, and microscale transport in active fluids.

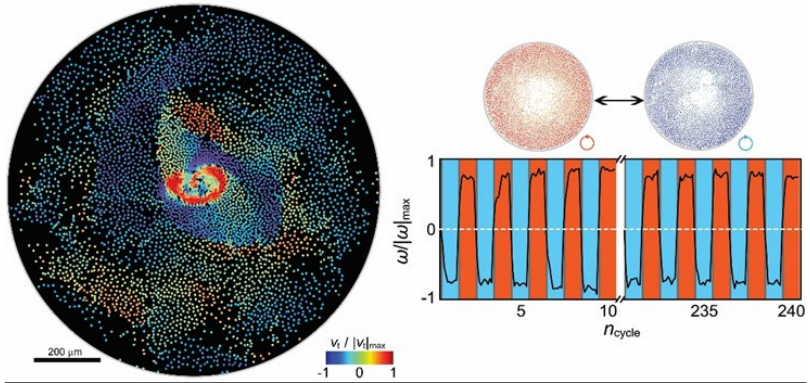


**Figure 1.** Polar state reversal in active systems. Left panel: experimental snapshot of a Quincke roller suspension during a vortex reversal induced by a temporal modulation of the activity. Groups of particles with identical color represent flocks moving in the same direction. Right panel: cycling of the vortex chiral states by a temporal termination and restoration of the activity controlled by the electric field. The system switches between clockwise (blue) and counter-clockwise (red) motion of a self-organized vortex.

Novel arrested-motility states in populations of shape-anisotropic active Janus particles. The emergence of large-scale collective phenomena from simple interactions between individual units is a hallmark of active matter systems. Active colloids with alignment-dominated interparticle

interactions tend to develop orientational order and form motile coherent states, such as flocks and swarms. Alternatively, a combination of self-propulsion and excluded-volume interactions results in self-trapping and active phase separation into dense clusters. We reveal unconventional arrested-motility states in ensembles of active discoidal particles powered by induced-charge electrophoresis [2]. Combining experiments and computational modeling, we have demonstrated that the shape asymmetry of the particles promotes the hydrodynamically assisted formation of active particles' bound states in a certain range of excitation parameters, ultimately leading to a spontaneous collective state with arrested motility that spontaneously form aggregates of reduced motility, an arrested-motility phase, driven by the particles' response to hydrodynamic fields created by their neighbors. The novel phase occurs spontaneously as a result of a positive feedback loop between slowing down of particles through hydrodynamics induced pair formation and subsequent hydrodynamic trapping of single particles by the pairs, which seeds further pair formation. Unlike the jammed clusters obtained through self-trapping, the arrested-motility phase remains sparse, dynamic, and reconfigurable. The arrested-motility phase is dynamic and reversible through the parameters of the driving field. The demonstrated mechanism of phase separation seeded by bound state formation in ensembles of oblate active particles is generic and should be applicable to other active colloidal systems to orchestrate their collective behavior.

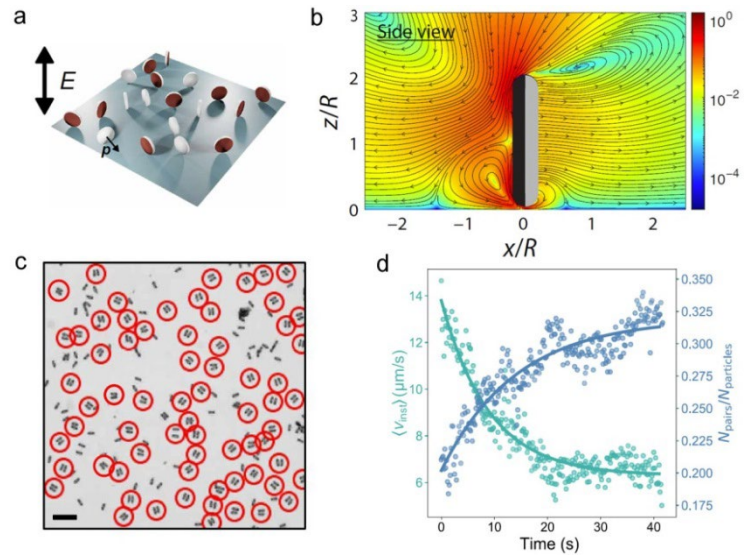


**Figure 2.** Hydrodynamically assisted bound state formation in ensembles of disk-shaped Janus particles. (a) Schematic of disk-shaped particles with axisymmetric coverage by a metal layer (brown). The particles stand up in an AC electric field. (b) Side view of the flow field in the vicinity of a Janus discoid. The color encodes the magnitude of the fluid flows. (c) Spontaneous pair formation of the Janus discoids resulting in arrested-motility state with a dramatic decrease of the activity demonstrated in (d). Scale bar is 40μm.

Guiding self-assembly of active colloids by temporal modulation of activity. Self-organization phenomena in ensembles of self-propelled particles open pathways to the synthesis of new dynamic states not accessible by traditional equilibrium processes. The challenge is to develop a set of principles that facilitate the control and manipulation of emergent active states. The majority of collective phenomena are observed in the systems with a constant (or nearly constant) energy injection rate. We suggested using temporal activity modulations as a tool to manipulate self-organized dynamic states. We revealed a novel self-assembled dynamic phase, dynamic alternating square lattices, in ensembles of active Quincke rollers energized by a spatially uniform but modulated in time electric field [3]. We demonstrate that the formation of dynamic structures is triggered by a momentarily decoupling between dominant inter-particle interactions – hydrodynamic velocity alignment and near field electrostatic repulsion as a result of a temporal

cessation of the energy injection. The lattices are reconfigurable with the control of the characteristic lattice constant by the particles' run time. Our results provide new insights into the collective behavior and control of active colloidal ensembles by means of a temporal modulation of activity. The reported mechanism should, in principle, be applicable to other active systems where the collective behavior is governed by the interplay of isotropic repulsions and hydrodynamic velocity alignment interactions.

### Future Plans

We plan to continue focusing our research on new approaches to discovery, synthesis and characterization of active colloidal materials.

In the next few years, we plan to explore a nontrivial interplay between chiral motion, shape, confinement and temporal activity modulations in the generation of a hidden order, dynamic state memory, and control of the system behavior. We plan to systematically investigate the dynamic behavior of active chiral fluids realized by rollers and spinners with spontaneous selection of chiral states and those with prescribed handedness. The study will stimulate discovery of new dynamic states in active fluids, expand our understanding of active chiral matter and provide new toolbox for the design and manipulation of self-assembled architectures. We will also aim to advance the fundamental understanding of the dynamic self-organized patterns, spontaneous flows, and topological defect transport fully synthetic active liquid crystalline materials powered by acoustic fields.

### References

1. B. Zhang, H. Yuan, A. Sokolov, M. Olvera de la Cruz, A. Snezhko, *Polar state reversal in active fluids*, Nature Physics **18**, 154 (2022).
2. J. Katuri, R. Poehnl, A. Sokolov, W. Uspal, A. Snezhko, *Arrested-motility states in populations of shape-anisotropic active Janus particles*, Science Advances **8**, eabo3604 (2022).
3. B. Zhang, A. Snezhko, A. Sokolov, *Guiding self-assembly of active colloids by temporal modulation of activity*, Physical Review Letters **128**, 018004 (2022).
4. B. Zhang, A. Snezhko, *Hyperuniform Active Chiral Fluids with Tunable Internal Structure*, Physical Review Letters **128**, 218002 (2022).
5. K. Han, A. Glatz, A. Snezhko, *Globally correlated states and control of vortex lattices in active roller fluids*, Physical Review Research **5**, 023040 (2023).

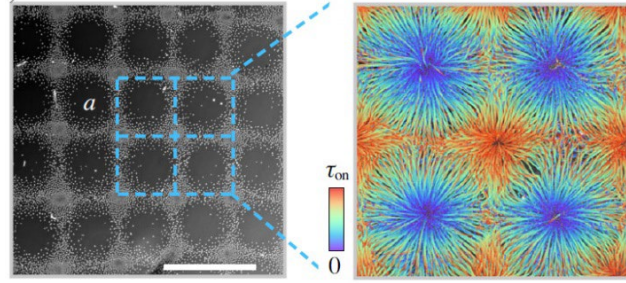


**Figure 3.** Dynamic square lattices emerge in response to activity modulations. Left panel: experimental snapshot of a dynamic square lattice formed by Quincke rollers with a temporally modulated activity. The blue squares mark four unit cells of the lattice. The scale bar is 0.5 mm. Right panel: Color-coded time evolution of particles positions during one cycle of activity modulation demonstrating switching of the active system between two equivalent lattice states.

## Publications

1. J. Katuri, R. Poehnl, A. Sokolov, W. Uspal, A. Snezhko, Arrested-motility states in populations of shape-anisotropic active Janus particles, *Science Advances* 8, eabo3604 (2022).
2. B. Zhang, H. Yuan, A. Sokolov, M. Olvera de la Cruz, A. Snezhko, Polar state reversal in active fluids, *Nature Physics* 18, 154 (2022).
3. B. Zhang, A. Snezhko, A. Sokolov, Guiding self-assembly of active colloids by temporal modulation of activity, *Physical Review Letters* 128, 018004 (2022).
4. B. Zhang, A. Snezhko, Hyperuniform Active Chiral Fluids with Tunable Internal Structure, *Physical Review Letters* 128, 218002 (2022).
5. K. Han, A. Glatz, A. Snezhko, Globally correlated states and control of vortex lattices in active roller fluids, *Physical Review Research* 5, 023040 (2023).
6. J. Katuri, A. Snezhko, A. Sokolov, Motility of acoustically powered micro-swimmers in a liquid crystalline environment, *Soft Matter* 18, 8641-8646 (2022).
7. B. Zhang, H. Karani, P. Vlahovska, A. Snezhko, Persistence length regulates emergent dynamics in active roller ensembles, *Soft Matter* 17, 4818 (2021).
8. N. Figueroa-Morales, M. Genkin, A. Sokolov, I. S. Aranson, Non-symmetric pinning of topological defects in living liquid crystals, *Communications Physics* 5, 301 (2022).
9. G. Kokot, H.A. Faizi, G.E. Pradillo, A. Snezhko, P.M. Vlahovska, Spontaneous self-propulsion and non-equilibrium shape fluctuations of a droplet enclosing active particles, *Communications Physics* 5, 91 (2022).
10. K. Han, A. Glatz, A. Snezhko, Emergence and dynamics of unconfined self-organized vortices in active magnetic roller liquids, *Soft Matter* 17, 10536 (2021).

*University  
Abstracts*

## **Bioinspired Active Transport and Energy Transduction using Liquid Crystals Beyond Equilibrium**

**Nicholas L. Abbott (Cornell University) and Juan J. de Pablo (University of Chicago)**

**Keywords:** Non-equilibrium, bioinspired, hierarchical, liquid crystals, solitons

### **Research Scope**

Biological systems function out of equilibrium, with structure and dynamics that arise from dissipative processes involving the interplay of advective and diffusive transport. The complex dynamic behaviors found in biology often reflect highly non-linear phenomena that lead to surprisingly localized responses to delocalized fields. These principles offer inspiration for new designs of soft materials that harvest and transduce non-localized sources of energy. In this project, we are exploring an emerging class of dynamic, cooperative phenomena that have been observed in liquid crystals (LCs) – solitary waves, or “solitons”, as the basis of new designs of active soft matter for achieving rapid and directed transport processes and new modes of energy transduction. These localized responses have analogies to many other physical and biological phenomena, and have only recently been shown to occur in LCs. In LCs, solitons consist of waves of localized orientational perturbations that can travel at high speed and over long distances. Through closely coupled simulations and experiments, this project is addressing open questions regarding the mechanisms by which solitons form in LCs and subsequently interact with fluid interfaces, with the long-term goal of creating fundamentally new ways to transduce soliton energy into new states of matter.

Recent progress in our project has established foundational knowledge related to soliton formation in LCs, focusing on electrically triggered solitons in nematic LCs confined by surfaces with precisely defined chemistries and topographies. The first numerical simulations of solitons in LCs have successfully identified the minimal conditions that give rise to solitons. In particular, the simulations identified surface heterogeneities (e.g., chemical patches) as playing a central role in formation of solitons, predictions that were validated by development of a new experimental system with precise control over surface anchoring of LCs. Additional complementary experiments and simulations have revealed the opportunity to engineer soliton formation and propagation via the tailoring of LC strain and Freedericksz transitions, including that solitons can reflect, refract, split and annihilate at LC domain boundaries. Finally, we have explored how solitons behave at interfaces between LCs and isotropic liquids, validating our hypothesis that soliton energies can be harnessed to trigger the “budding” of new phases in a manner similar to biological processes.

Overall, this project is leading to designs of active soft matter that are providing new modes of energy transduction, opening up the possibility of approaches to active transport with applications, for example, to nanoscale separations and assembly processes. The relevant physics arise at the mesoscale but can propagate at high speeds over macroscopic scales, and thus a complementary program of theory, simulation, and experiment is being adopted to interpret the results of our research and to design hierarchical materials systems with engineered behaviors.

## Recent Progress

We have recently addressed the question of what constitutes a minimal theory for soliton generation and propagation in a nematic LC. Past work has suggested that ionic impurities (which are unavoidable in experiments) may play a central role in soliton formation [1], but in our simulations, we were able to observe the formation of solitons without addition of salts. The model that we adopted consists of a continuum framework based on a Landau-de Gennes free energy functional for the tensorial order parameter  $Q=S(\mathbf{nn}-I/3)$  for uniaxial systems, where  $\mathbf{n}$  is the nematic director field and  $S$  is the largest eigenvalue of  $Q$ . The relaxational dynamics of  $Q$  are expressed in terms of a Ginzburg-Landau equation [2]

$$\mathbf{H} = - \left( \frac{\delta \mathcal{F}_{LdG}}{\delta \mathbf{Q}} - \frac{1}{3} \text{Tr} \frac{\delta \mathcal{F}_{LdG}}{\delta \mathbf{Q}} \right),$$

where  $\mathcal{F}_{LdG}$  is the free energy for a thermotropic nematic LC. The free energy includes a flexoelectric contribution, which is necessary to generate the soliton structure. In the presence of an externally applied electric field, flexoelectricity arises due to the interplay of nematic distortion and polarization [3]

$$f_{flex} = E_i P_i = \zeta_1 \frac{\partial Q_{ij}}{\partial x_j} E_i + \zeta_2 Q_{ij} \frac{\partial Q_{jk}}{\partial x_k} E_i.$$

We have used the above-described free energy to identify the key requirements needed to generate solitons in the absence of added charges. These include a surface inhomogeneity, consisting of an adsorbed particle or surface chemical patch capable of producing a twist in the LC, flexoelectricity, dielectric contrast, and an applied AC electric field that can couple to the LC director orientation. Figure 1a shows results from our simulations where solitons are nucleated above a homeotropic particle adsorbed on one of the surfaces of a slit channel. The free energy change upon formation of solitons is shown in Figure 2b. Upon application of the electric field, a butterfly is gradually formed via straining of the LC, which causes the energy of the LC to increase steadily. This process continues until the flexoelectric energy is too high and a bullet-like soliton is emitted, at which point the energy drops slightly and then starts to rise again, until another bullet is eventually generated. Overall, our numerical model has played a key role in interpreting a series of experimental observations obtained in the project by using surface chemical patches and immobilized microparticles to trigger formation of solitons.

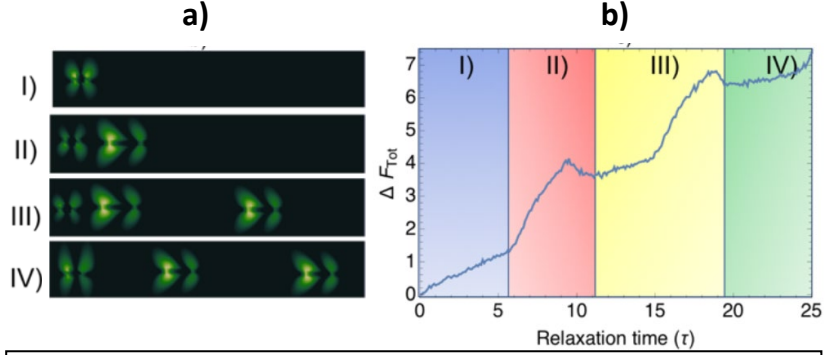


**Figure 1.** Simulations of soliton formation in the presence of a microparticle with homeotropic anchoring. (a) Simulation results (with increasing time down the column of calculated images) show the creation of a butterfly in the region above the particle, and the repeated ejection of bullets that move at similar speeds, in agreement with our experimental observations. (b) The calculated free energy increases over time until a bullet detaches from the butterfly, at which point the energy drops slightly before another bullet is ejected. In the simulations, we work with a dimensionless system where  $\tau$  is time/time relaxation and the  $F_{Tot}$  is the energy/(elastic constant \* coherent length).

A second focus over the past year has revolved around exploration of collisions between LC solitons and interfaces to isotropic fluids, and the discovery that the interactions can generate a range of interfacial hydrodynamic phenomena. Specifically, we have discovered that single solitons can either generate single droplets (Figure 2) or, alternatively, form jets of LC that subsequently break-up into organized assemblies of droplets. We have also shown that the influence of key parameters, such as electric field strength, LC film thickness and LC-oil interfacial tension, map onto a universal state diagram that characterizes the transduction of soliton flexoelectric energy into droplet interfacial energy. Overall, these results reveal that solitons in LCs can be used to focus the energy of non-localized electric fields to generate a new class of non-linear electrohydrodynamic effects at fluid interfaces, including jetting and emulsification.

### Future Plans

Our future efforts will be directed to experiments and simulations that provide insight into the behavior of solitons at interfaces, including interfaces between two LC domains that possess distinct orientations and interfaces between LCs and isotropic oils. For example, we seek to identify the microscopic factors that control the reflection, refraction, generation, splitting, and destruction of solitons that we have observed to occur at boundaries between patterned LC domains (Figure 3). One of our central hypotheses, which we will test in future experiments and simulations, is that out-of-plane director tilt within a soliton (i.e., phase of the soliton), at the instant it reaches the interface between distinct LC domains, selects for the observed behavior. Accordingly, our future experimental efforts will focus on using high-speed imaging to map director orientations, which fluctuate with the applied electric field, prior to impact.

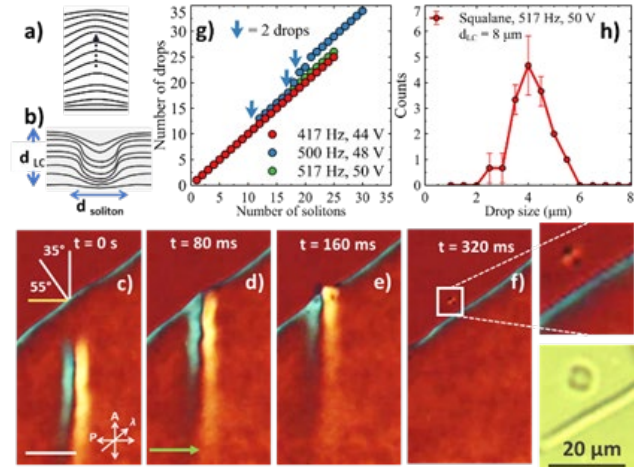


**Figure 2.** (a-b) Schematic illustration depicting the (a) azimuthal and (b) polar LC director orientations within a soliton propagating along the direction of the dotted arrow (c-f) Timed snapshots (crossed polars and a red plate compensator inserted at  $45^\circ$  from the polars) showing formation of a LC droplet following collision of a soliton with the LC-isotropic oil interface. Insets in (f) show bright-field and cross polar images of the LC droplet. The applied voltage is 517 Hz, 50 V. Green arrows indicate the direction of gold deposition. Scale bar  $30\ \mu\text{m}$  (g) Number of generated LC drops as a function of number of solitons hitting the interface at different applied electric fields. (h) Size distribution of generated LC drops.

A key future goal related to simulations will be to expand our models to include hydrodynamic interactions, which we believe are likely to play an important role in the dynamics of solitons at fluid interfaces (both LC-LC and LC-isotropic oil). Specifically, we will include nematohydrodynamic effects through a Beris-Edwards formulation of the form [4]

$$\left(\frac{\partial}{\partial t} + \mathbf{u} \cdot \nabla\right) \mathbf{Q} - \mathbf{S} = \Gamma \mathbf{H},$$

where  $\mathbf{S}$  is a generalized advective term that accounts for the response of the nematic order parameter to an applied stress and  $\mathbf{u}$  is the velocity field. In our initial efforts to incorporate hydrodynamic interactions, we will focus on boundaries between two LC domains. Subsequently, we will model interfaces between immiscible nematic and isotropic oils. To address that challenge a more sophisticated theory will be developed to handle the complexity introduced by multiple components and different phases of matter.

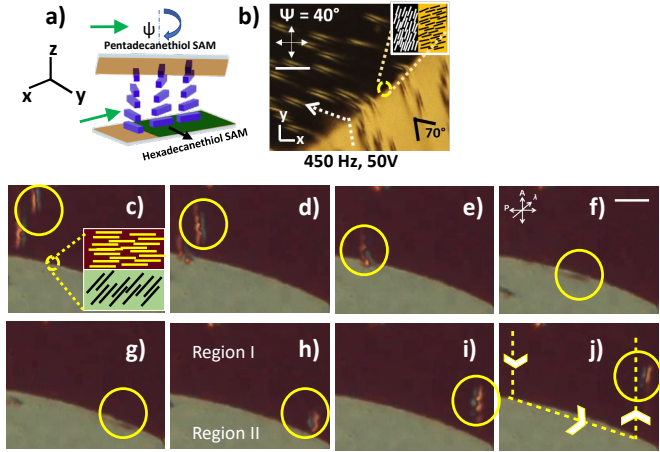


**Figure 3.** (a) Schematic illustration of LC alignment in optical cells patterned with self-assembled monolayers (SAMs) to create uniform and twisted regions. The top surface in (a) is rotated by  $\psi$  to create patterned LC regions of two different twists. (b) Soliton trajectories in a LC film created as shown in (a). (c-j) Optical micrographs of a soliton following a complex U-shaped trajectory in a spatially patterned optical cell. The dark region (Region I) corresponds to uniform planar LC alignment on  $C_{15}SH$  SAMs. The bright region (Region II) corresponds to twisted LC alignment between  $C_{15}SH$  and  $C_{16}SH$  SAMs. The soliton takes a U-turn, depicted by the yellow dotted line in (j), as it moves from Region I to Region II and back to Region I. The director alignment near the boundary at the mid-plane of the optical cell is illustrated in the inset of (c). The soliton is indicated by the yellow circles (500 Hz, 51 V). Images are taken 0.1s apart from each other. Scale bar 50  $\mu\text{m}$ .

## References

1. X. Li, R. L. Xiao, S. Paladugu, S. V. Shiyankovskii, and O. D. Lavrentovich, *Three-Dimensional Solitary Waves with Electrically Tunable Direction of Propagation in Nematics*, Nat. Commun. **10**, 1 (2019).
2. M. Sadati, J. A. Martinez-Gonzalez, Y. Zhou, N. T. Qazvini, K. Kurtenbach, X. Li, E. Bukusoglu, R. Zhang, N. L. Abbott, J. P. Hernandez-Ortiz, J. J. de Pablo, *Prolate and Oblate Chiral Liquid Crystal Spheroids*, Sci. Adv. **6**, (2020)
3. A. L. Alexe-Ionescu, *Flexoelectric Polarization and Second Order Elasticity for Nematic Liquid Crystals*, Phys. Lett. A **180**, 456 (1993).
4. A. N. Beris and B. J. Edwards, *Thermodynamics of Flowing Systems : With Internal Microstructure*, 683 (1994).

## Publications

1. S. Das, N. Atzin, X. Tang, A. Mozaffari, J.J. de Pablo and N.L. Abbott, Jetting and Droplet Formation Driven by Interfacial Electrohydrodynamic Effects Mediated by Solitons in Liquid Crystals, *Physical Review Letters* (2023), in press.
2. S. Das, S. Roh, N. Atzin, A. Mozaffari, X. Tang, J. J. De Pablo, and N. L. Abbott, Programming Solitons in Liquid Crystals Using Surface Chemistry, *Langmuir* **38**, 3575 (2022).
3. N. Atzin, A. Mozaffari, X. Tang, S. Das, N. L. Abbott, and J. J. de Pablo, A Minimal Model of Solitons in Nematic Liquid Crystals, <https://Arxiv.Org/Abs/2210.08666v1> (2022).
4. X. Tang, A. Mozaffari, N. Atzin, S. Das, N. L. Abbott, and J. J. de Pablo, Generation and Propagation of Solitary Waves in Nematic Liquid Crystals, submitted to *Soft Matter* (2023).
5. X. Wang, R. Zhang, A. Mozaffari, J. J. de Pablo, and N. L. Abbott, Active Motion of Multiphase Oil Droplets: Emergent Dynamics of Squirmers with Evolving Internal Structure, *Soft Matter* **17**, 2985 (2021).
6. B. Senyuk, A. Mozaffari, K. Crust, R. Zhang, J. J. de Pablo, and I. I. Smalyukh, Transformation between Elastic Dipoles, Quadrupoles, Octupoles, and Hexadecapoles Driven by Surfactant Self-Assembly in Nematic Emulsion, *Sci. Adv.* **7**, 377 (2021).
7. K. He, Y. Zhou, H. Ramezani-Dakhel, J. J. De Pablo, A. Fernandez-Nieves, and T. Lopez-Leon, From Nematic Shells to Nematic Droplets: Energetics and Defect Transitions, *Soft Matter* **18**, 1395 (2022).
8. M. Sadati, J. A. Martinez-Gonzalez, A. Cohen, S. Norouzi, O. Guzmán, and J. J. de Pablo, Control of Monodomain Polymer-Stabilized Cuboidal Nanocrystals of Chiral Nematics by Confinement, *ACS Nano* **15**, 15972 (2021).
9. Y. Yang, V. Palacio-Betancur, X. Wang, J. J. De Pablo, N. L. Abbott, Y. Yang, X. Wang, N. L. Abbott, V. Palacio-Betancur, and J. J. de Pablo, Strongly Chiral Liquid Crystals in Nanoemulsions, *Small* **18**, 2105835 (2022).
10. S. Das, J. J. De Pablo, and N. L. Abbott, Fréedericksz Transition and Soliton Formation in Thin Films of Nematic Liquid Crystals, in preparation (2023).

## Self-assembled adaptive materials via 3D printed active programmable building blocks

Igor Aronson and Ayusman Sen, Pennsylvania State University

**Keywords:** self-assembly, active matter, colloids, 3D-printing

### Research Scope

State-of-the-art materials inspired by living systems are at the heart of multiple emerging technologies, such as additive manufacturing, soft robotics, and nanofabrication. Another enabling technology inspired by the biological world is self-assembly, i.e., the tendency of simple building blocks (molecules, colloids) to form complex superstructures. In this research, we will harness the progress in self-assembly, soft materials, and additive manufacturing to design a new class of multi-responsive microscopic building blocks. The microblocks will be based on 3D-printed, self-propelled particles

that respond to chemical concentration gradients, light, and external magnetic or electric fields. Exploiting the progress in nanofabrication and characterization of functionalized, 3D-printed microscopic building blocks, we will target the most challenging question in active matter: *what are the fundamental principles controlling the hierarchical organization of materials out of equilibrium?*

### Recent Progress

Ultrasound manipulation and active nanorods. This study reports on the synergistic effect of acoustic and flow-induced focusing in microfluidic nozzles. In a microchannel with a nozzle, the balance between the acoustophoretic forces and the fluid drag due to streaming flows generated by the acoustic field controls the microparticle's dynamics. This study manipulates the positions and orientations of dispersed particles and dense clusters inside the channel at a fixed frequency by tuning the acoustic intensity. The main findings are: first, this study successfully manipulates the positions and orientations of individual particles and dense clusters inside the channel at a fixed frequency by tuning the acoustic intensity. Second, when an external flow is applied, the acoustic field separates and selectively extrudes shape-anisotropic passive particles and self-propelled active nanorods. Finally, the observed phenomena are explained by multiphysics finite-element modeling. The results shed light on the control and extrusion of active particles in confined geometries and enable applications for acoustic cargo (e.g., drug) delivery, particle injection, and additive manufacturing via printed self-propelled active particles [1].

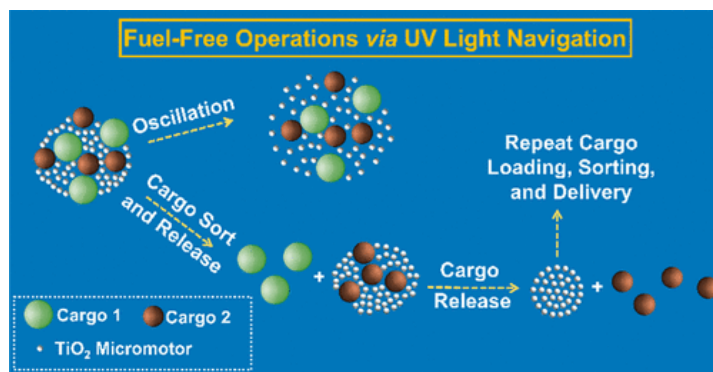


**Fig. 1.** Light-guided TiO<sub>2</sub> swarms undergo directed long-range migration without added chemical fuel. The swarms reversibly and controllably transport and release cargo, sorting them out by size [4].

Programming Motion of Platinum Microparticles: From Linear to Orbital. Self-powered catalytic micromotors that swim through a fluid by harvesting energy from their environment have received increasing attention because of their potential applications in nanomachinery, nanoscale assembly, and robotics. Through modeling and experiments, we demonstrate the general design strategy for single-component platinum micromotors that, in the presence of hydrogen peroxide, can execute a variety of motion trajectories from extremely linear to orbital. This is achieved via a simple shape design wherein the speed and directionality of a particle are determined by overall symmetry elements. Shape design gives high reproducibility and allows a wide range of adjustments to fine-tune the desired particle motion. We observe strong agreement between experimental data and numerical predictions, indicating that our model can serve to predict the directionality and speed of a particle prior to fabrication. Shape programming works on an individual-particle basis, thus enabling complex systems which require different modes of motion for the individual parts [2].

Multi-scale organization in communicating active matter. Despite its eminent importance, the role of communication in the collective organization of active systems is not yet fully understood. We report on the multi-scale self-organization of interacting self-propelled agents that locally process information transmitted by chemical signals. We show that this communication capacity dramatically expands their ability to form complex structures, allowing them to self-organize through a series of collective dynamical states at multiple hierarchical levels. Our findings provide insights into the role of self-sustained signal processing for self-organization in biological systems and open routes to applications using chemically driven colloids or microrobots [3].

Light-Powered, Fuel-Free Oscillation, Migration, and Reversible Manipulation of Multiple Cargo Types by Micromotor Swarms. We show that fuel-free photoactive  $\text{TiO}_2$  microparticles can form mobile, coherent swarms in the presence of UV light, which track the subsequent movement of an irradiated spot in a fluid-filled microchamber. Multiple concurrent propulsion mechanisms (electrolyte diffusion-osmotic swarming, photocatalytic expansion, and photothermal migration) control the rich collective behavior of the swarms, which provide a strategy to reversely manipulate cargo. The active swarms can autonomously pick up groups of inert particles, sort them by size, and sequentially release the sorted particles at particular locations in the microchamber, Fig. 1. Hence, these swarms overcome three obstacles, limiting the utility of self-propelled particles. Namely, they can (1) undergo directed, long-range migration without the addition of a chemical fuel, (2) perform diverse collective behavior not possible with a single active particle, and (3) repeatedly and controllably isolate and deliver specific components of a multiparticle “cargo”. Since light sources are easily fabricated, transported, and controlled, the results can facilitate the development of portable devices, providing broader access to the diagnostic and manufacturing advances enabled by microfluidics [4].

Forces that control self-organization of chemically-propelled Janus tori. We describe the interactions of chemically-propelled microtori near a wall. The results show that a torus hovers at a certain distance from the wall due to a combination of gravity and hydrodynamic flows generated by the chemical activity. Moreover, electrostatic dipolar interactions between the torus and the wall result in a spontaneous tilt and horizontal translation, in qualitative agreement with the experiment. Simulations of the dynamics of two and four tori near a wall provide evidence for the formation of stable self-propelled bound states. Our results illustrate that self-organization at the microscale occurs due to a combination of multiple factors, including hydrodynamic, chemical, electrostatic, and steric interactions [5].

## Future Plans

Enabled by the progress in colloidal out-of-equilibrium self-assembly, additive manufacturing, and computational modeling, we will target the most challenging questions in active matter: how do information exchange and decision-making lead to hierarchical self-assembled colloidal materials akin to living systems? How can we describe the emergent out-of-equilibrium behavior, and what theoretical tools do we need to develop? Experiments, computational modeling, and theory will be executed hand-in-hand to advance the goal. Besides the relevance for materials science, energy technology, and microrobotics, understating the collective behavior and long-range coherence among such communicating microscopic active elements will uncover fundamental rules of self-organization and self-assembly in living and synthetic active systems.

The main research thrusts will be: (i) Designing active communicating colloidal systems. We will fabricate self-propelled colloids undergoing chemical reactions. One system involves an aqueous suspension of silver salt microparticles under UV-Vis light illumination in the presence of an oxidant. Such systems exhibit periodic oscillations and excitable wave propagation due to competing oxidation and reduction of silver. Oscillatory and excitable systems will also be designed by employing enzyme-attached colloidal particles. Using appropriate enzymes or combinations of enzymes will lead to pH oscillations, resulting in particle assembly/disassembly or the propagation of waves through dense particle suspensions. (ii) Controlling hierarchical assembly. To create complex aggregates, we will design chemically-communicating particles of complex shapes that can respond to magnetic fields, light, and chemical gradients. Hierarchical particle assemblies based on chemotaxis will be designed using enzymes that are part of reaction cascades where the product of one enzyme is the substrate for the next. (iii) Theoretical approaches. We will apply a multi-scale approach to examine the self-assembled behavior of the chemically-communicating colloids. We will use complimentary computational and analytical tools: multi-particle collision dynamics (MPCD) for the microscopic simulations, agent-based modeling for the mesoscale analysis, and coarse-grained continuum description to assess the self-assembled behavior on the macroscale. Contrary to non-communicating colloids, the information propagation enables much faster aggregation and elevated robustness to fluctuations and heterogeneity. The resulting dynamic states, like vortices or pulsating clusters, will have hierarchical organization and higher sensitivity to external stimuli, making them much better candidates for self-assembled sensors and cargo manipulators.

## References

1. L.D., Rubio, M. Collins, A. Sen, and I.S. Aranson, Ultrasound Manipulation and Extrusion of Active Nanorods. *Small*, 2300028 (2023).
2. A. Unruh, A. M. Brooks, I. S. Aranson, A. and A. Sen, Programming Motion of Platinum Microparticles: From Linear to Orbital, *ACS Applied Engineering Materials* 1, 1126 (2023)
3. A. Ziepke, I. Maryshev, I. S. Aranson, and E. Frey. Multi-scale organization in communicating active matter. *Nature Communications*, 13, 1 (2022).
4. J. Zhang, A. Laskar, J. Song, O. E. Shklyaev, F. Mou, J. Guan, A. C. Balazs, A. Sen, Light-Powered, Fuel-Free Oscillation, Migration, and Reversible Manipulation of Multiple Cargo Types by Micromotor Swarms, *ACS Nano*, 17, 251 (2023)

5. J. Wang, M. J. Huang, R. D. Baker-Sediako, R. Kapral, R. and I. S. Aranson, Forces that control self-organization of chemically-propelled Janus tori. *Communication Physics* 5, 176 (2022)

## **Publications**

1. L. D., Rubio, M. Collins, A. Sen, and I. S. Aranson, Ultrasound Manipulation and Extrusion of Active Nanorods. *Small*, 2300028 (2023).
2. A. Unruh, A. M. Brooks, I. S. Aranson, and A. Sen, Programming Motion of Platinum Microparticles: From Linear to Orbital, *ACS Applied Engineering Materials* 1, 1126 (2023)
3. J. Zhang, A. Laskar, J. Song, O. E. Shklyaev, F. Mou, J. Guan, A. C. Balazs, A. Sen, Light-Powered, Fuel-Free Oscillation, Migration, and Reversible Manipulation of Multiple Cargo Types by Micromotor Swarms, *ACS Nano*, 17, 251 (2023)
4. A. Ziepke, I. Maryshev, I. S. Aranson, and E. Frey. Multi-scale organization in communicating active matter. *Nature Communications*, 13, 1 (2022).
5. J. Zhang, A. Laskar, J. Song, O. E. Shklyaev, F. Mou, J. Guan, A. C. Balazs, A. Sen, Light-Powered, Fuel-Free Oscillation, Migration, and Reversible Manipulation of Multiple Cargo Types by Micromotor Swarms, *ACS Nano*, 17, 251 (2023)
6. J. Wang, M. J. Huang, R. D. Baker-Sediako, R. Kapral, R. and I. S. Aranson, Forces that control self-organization of chemically-propelled Janus tori. *Communication Physics* 5, 176 (2022)
7. I. S. Aranson and A. Pikovsky, Confinement and collective escape of active particles, *Physical Review Letters* 128, 108001(2022)
8. J. Song, J. Zhang, S. Krishna Mani, and A. Sen, Droplet navigation by photothermal pumping in an optofluidic system, *Langmuir*, 38, 11486 (2022).
9. J. Zhang, F. Mou, S. Tang, J. E. Kauffman, A. Sen, and J. Guan, Photochemical micromotor of eccentric core in isotropic hollow shell exhibiting multimodal motion behavior, *Applied Materials Today*, 26, 101371 (2022).
10. R. K. Manna, K. Gentile, O. E. Shklyaev, A. Sen, and A. C. Balazs, Self-generated convective flows enhance the rates of chemical reactions, *Langmuir*, 38, 1432 (2022).

## **Protein Design Using Deep Learning**

**David Baker, Professor, University of Washington**

**Keywords:** protein design, machine learning, deep learning

### **Research Scope**

Proteins mediate the critical processes of life and beautifully solve the challenges faced during the evolution of modern organisms. Our goal is to design a new generation of proteins that address current-day problems not faced during evolution. In contrast to traditional protein engineering efforts, which have focused on modifying naturally occurring proteins, we design new proteins from scratch to optimally solve the problem at hand. Following the computation of new amino acid sequences predicted to fold into proteins with new structures and functions, we produce synthetic genes encoding these sequences, and characterize them experimentally.

### **Recent Progress**

The 2-photosystem Z-scheme of photosynthesis wastes a significant fraction of solar energy as heat, but de novo-designed proteins using alternative approaches to light harvesting and charge separation could greatly increase the overall efficiency. We have demonstrated precision design of chlorophyll "special pair" dimers, built light harvesting proteins containing multiple chlorophyll molecules and bilins, and assembled multi-component chlorophyll-binding supercomplexes.

Molecular systems with coincident cyclic and superhelical symmetry axes have considerable advantages for materials design as they can be readily lengthened or shortened by changing the length of the constituent monomers. We have developed a systematic approach to generating modular and rigid repeat protein oligomers with coincident C2 to C8 and superhelical symmetry axes that can be readily extended by repeat propagation. From these building blocks, we have shown that a wide range of unbounded fibers can be systematically designed by introducing hydrophilic surface patches that force staggering of the monomers; the geometry of such fibers can be precisely tuned by varying the number of repeat units in the monomer and the placement of the hydrophilic patches.

### **Future Plans**

Using a modular approach, we seek to integrate our designed proteins to make efficient photosystems powered by both visible and near-infrared light.

## Publications

1. Kim, David E., et al. "De novo design of small beta barrel proteins." *Proceedings of the National Academy of Sciences* 120.11 (2023): e2207974120.
2. Davila Hernandez, Fatima Angelica, et al. "Directing polymorph specific calcium carbonate formation with de novo protein templates." *bioRxiv* (2023): 2023-06.
3. Li, Zhe, et al. "Accurate computational design of 3D protein crystals." *bioRxiv* (2022): 2022-11.
4. Sheffler, William, et al. "Fast and versatile sequence-independent protein docking for nanomaterials design using RPXDock." *PLOS Computational Biology* 19.5 (2023): e1010680.
5. Watson, Joseph L., et al. "De novo design of protein structure and function with RFdiffusion." *Nature* (2023): 1-3.
6. Yang, Erin C., et al. "Computational design of non-porous, pH-responsive antibody nanoparticles." *bioRxiv* (2023): 2023-04.

## Controlling Physical and Chemical Dynamics of Heterogeneous Networks Constructed from Soft Macromolecular Building Blocks

**PI: Anna C. Balazs** (Univ. of Pittsburgh); **Co-PI: Krzysztof Matyjaszewski** (Carnegie Mellon University); **Co-Investigator: Tomasz Kowalewski** (Carnegie Mellon University)

**Keywords:** Macromolecular networks; Controlled radical polymerization; Orthogonal chemistry

### Research Scope

Inspired by the modular assemblies of biomacromolecules that form complex, dynamic architectures with sophisticated functions, this current program aims to contribute to the *energy-efficient manufacturing by employing* transformable “Structurally Tailored and Engineered Macromolecular (STEM)” gels<sup>1</sup> that mimic natural stem cells. We explored structural uniformity and properties of networks made by ATRP and RAFT, and further improved them by using PET RAFT and cocatalysts on ATRP. Subsequently we studied growth of materials in confined environment utilizing polymer networks as “nanoreactors” for promoting and controlling physical interactions or chemical reactions exogenous to the networks, using three examples, polyacrylonitrile photoluminescence, uranium harvesting and nanocrystals formation.

### Recent Progress

#### Comparison of RAFT and ATRP methods in network formation

We previously reported the synthesis of STEM gels by combining RAFT polymerization and ATRP.<sup>2</sup> However, there are substantial mechanistic differences between these two methods. In ATRP, a small-molecule catalyst (usually a Cu complex) transfers an atom (usually a halogen such as Br) with the polymer chain end. In comparison, RAFT polymerization is based on the degenerative transfer between different polymer chain ends, which changes between an active radical and a dormant chain transfer agent (CTA)-capped chain. Thus, the control in RAFT polymerization should be profoundly influenced by the viscosity of the media than that in ATRP. Herein, we found that the two RDRP methods produce comparable networks at a low primary chain length, but ATRP maintains better control at a higher primary chain length, as determined by rheological analysis. (Figure 1).<sup>13</sup>

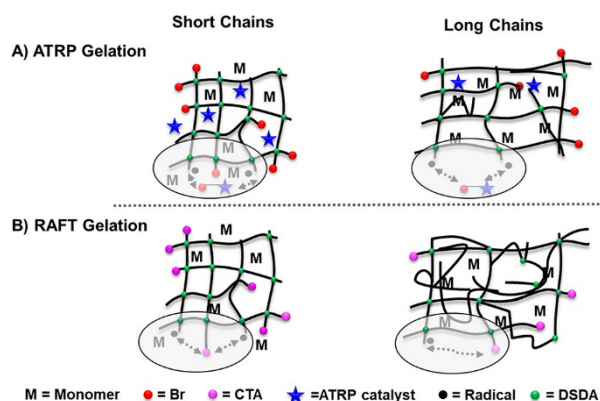


**Figure 1.** Scheme showing difference between polymers networks prepared by ATRP and RAFT polymerization. (A) The small-molecule catalyst in ATRP consistently mediates the polymerization under both short and long chain condition. (B) In RAFT gelation, the degenerative transfer is less feasible in the network with long chains.

Subsequently, we expanded this study to a conventional photoinitiated RAFT polymerization and photoinduced electron/energy transfer RAFT (PET-RAFT) polymerization (Figure 2).<sup>8</sup> Since PET-RAFT involves both RAFT exchange and reversible coupling with the CTA fragment, we

hypothesized that PET-RAFT has the potential to offer better control compared to conventional RAFT in network synthesis.

We also explored various chemical and photochemical cocatalysts used in copper-catalyzed ATRP.<sup>7</sup> For example, we studied the function of liquid metal (LM) micro/nanodroplets in ATRP, which will help develop LM-polymer nanocomposites for applications in stretchable electronics. Thus, eutectic Ga–In alloy (EGaIn) was employed in ATRP in organic solvents with low ppm (parts per million) loading of Cu catalysts (Figure 3).<sup>14</sup> ATRP in the presence of EGaIn produced well-defined polymers ( $D < 1.1$ ) that could be separated via centrifugation. Besides, no external forces or triggers, such as ultrasound sonication, were applied during the



**Figure 3.** A typical procedure of ATRP in the presence of EGaIn micro/nanodroplets.

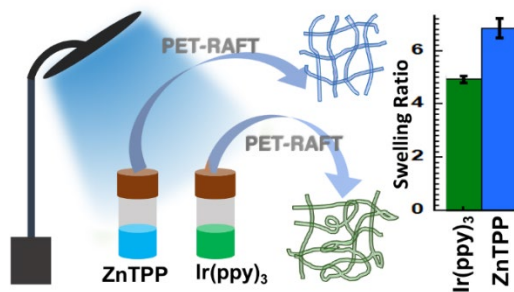


**Figure 2.** Influence of different PET-RAFT methods on the uniformity of the network structure.

polymerization. Control experiments showed that EGaIn micro/nanodroplets also activated dormant alkyl bromide species. However, this activation reaction was  $\sim 6$  orders of magnitude slower than the activation by  $\text{Cu}^I$  complexes, which is similar to SARA (supplemental activators and reducing agents) ATRP.

### Crosslinking and growth in confined space during ATRP

The project aims to study the effect of preparation methods on the structure of polymer networks. The confinement effect of mono- and divinyl monomers was studied by Monte Carlo simulations using the dynamic lattice liquid method.<sup>6</sup> The simulation was set up between two parallel walls with monomers and crosslinkers randomly distributed (Figure 4). Initiators were either randomly distributed or anchored to one wall. For anchored polymer brushes, the gel point depended on the slit width in addition to grafting density and initiator-to-crosslinker ratios. There was also a nonuniform density of crosslinks, with the highest density close to the wall, with nonuniformity decreasing at higher conversions.

This approach was employed to three systems with confined environment. The first one explored photoluminescent STEM networks based on the interactions between dangling polyacrylonitrile (PAN) chains facilitated by the congested environment of the network. We developed a one-step method based on hydrothermal reactions to produce water-soluble photoluminescent polymers from PAN ( $ht\text{-PLP}_{\text{PAN}}$ ).<sup>3</sup> To demonstrate the photoactivity of the photoluminescent polymer, we have applied  $ht\text{-PLP}_{\text{PAN}}$  in Cu-catalyzed ATRP

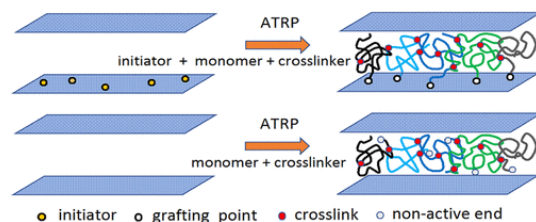


**Figure 4.** Schematic representation of different simulation conditions, one with tethered initiators, the other without.

mediated by blue or green light irradiation (Figure 5).<sup>12</sup> Such photoinduced ATRP reactions of (meth)acrylate monomers were performed in water or organic solvents, using parts per million (ppm) concentrations of the Cu<sup>II</sup> complex with tris(2-pyridylmethyl)amine (TPMA) as the catalyst and *ht*-PLP<sub>PAN</sub> as the photo-cocatalyst. The photo-cocatalyst in this study could be extended to designing gel-based photoactive materials from PAN, via similar hydrothermal pathways or non-covalent aggregation of grafted PAN segments.<sup>12</sup>

The second one employed a multi-scale computer-aided design and photo-controlled macromolecular synthesis to boost uranium harvesting from seawater (Figure 6). Using macromolecular materials that are capable of adsorbing uranium from seawater is a powerful strategy for U concentration. Finding the best copolymer composition for U adsorption is critical but requires a tremendous amount of synthesis using conventional experimental methods. In a recent study, we studied the relationship between adsorption capacity and copolymer composition by combining a dissipative

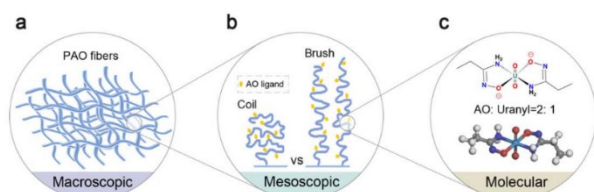


**Figure 6.** Scheme of factors influencing uranium adsorption by PAO. a. Morphology of PAO fibers at the macroscopic level. b. Spatial conformations of PAO chains at the mesoscopic level. c. Metal-ligand interaction at the molecular level.

particle dynamics (DPD) approach with a molecular dynamics (MD) study.<sup>10</sup> The designed polymers exhibited a record high adsorption capacity of uranium ( $11.4 \pm 1.2$  mg/g) in real seawater within 28 days. The established computation-aided protocol is generally adaptable for the target-oriented development of more advanced polymeric materials for other energy-related applications.

The third example involved engineering the dynamic hydrogen bonds in  $\pi$ -stacked supramolecular assemblies for hierarchical nanocrystal formation. We reported a novel crystalline polyphenol assembly hierarchically regulated by the interplay of  $\pi$ - $\pi$  stacking and reconfigurable hydrogen bonds (H-bonds).<sup>11</sup> By selectively engineering the dynamic hydrogen bonding between polyphenols, oriented structural reorganization of the crystalline assemblies to low-dimensional nanocrystals was achieved, accompanied by structural “self-correction”. Specifically, the crystalline polyphenol assemblies exhibited a shear-driven sliding of the H-bond interfaces, followed by an “end-to-end” molecular plane fusion, to form 1D ultrafine nanofibers. Introducing metal coordination (e.g., Zr<sup>4+</sup>, Fe<sup>3+</sup>) to disintegrate the dynamic H-bond networks resulted in unzipping of the lamellar polyphenol crystals to form 2D nanobelts (Error! Reference source not found.).

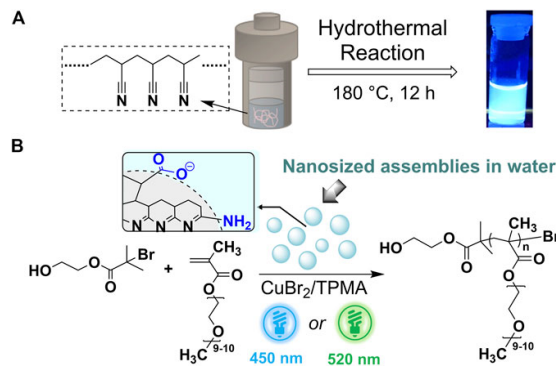


**Figure 5.** PAN-derived photo-cocatalyst. (A) Preparation of *ht*-PLP<sub>PAN</sub> from PAN. (B) Photoinduced ATRP using *ht*-PLP<sub>PAN</sub>.

The third example involved engineering the dynamic hydrogen bonds in  $\pi$ -stacked supramolecular assemblies for hierarchical nanocrystal formation. We reported a novel crystalline polyphenol assembly hierarchically regulated by the interplay of  $\pi$ - $\pi$  stacking and reconfigurable hydrogen bonds (H-bonds).<sup>11</sup> By selectively engineering the dynamic hydrogen bonding between polyphenols, oriented structural reorganization of the crystalline assemblies to low-dimensional nanocrystals was achieved, accompanied by structural “self-correction”. Specifically, the crystalline polyphenol assemblies exhibited a shear-driven sliding of the H-bond interfaces, followed by an “end-to-end” molecular plane fusion, to form 1D ultrafine nanofibers. Introducing metal coordination (e.g., Zr<sup>4+</sup>, Fe<sup>3+</sup>) to disintegrate the dynamic H-bond networks resulted in unzipping of the lamellar polyphenol crystals to form 2D nanobelts (Error! Reference source not found.).

The third example involved engineering the dynamic hydrogen bonds in  $\pi$ -stacked supramolecular assemblies for hierarchical nanocrystal formation. We reported a novel crystalline polyphenol assembly hierarchically regulated by the interplay of  $\pi$ - $\pi$  stacking and reconfigurable hydrogen bonds (H-bonds).<sup>11</sup> By selectively engineering the dynamic hydrogen bonding between polyphenols, oriented structural reorganization of the crystalline assemblies to low-dimensional nanocrystals was achieved, accompanied by structural “self-correction”. Specifically, the crystalline polyphenol assemblies exhibited a shear-driven sliding of the H-bond interfaces, followed by an “end-to-end” molecular plane fusion, to form 1D ultrafine nanofibers. Introducing metal coordination (e.g., Zr<sup>4+</sup>, Fe<sup>3+</sup>) to disintegrate the dynamic H-bond networks resulted in unzipping of the lamellar polyphenol crystals to form 2D nanobelts (Error! Reference source not found.).

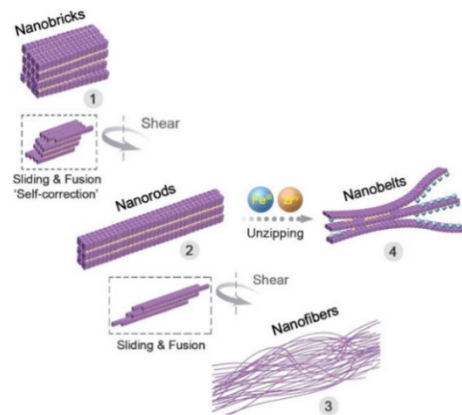


**Figure 7.** Scheme of the hierarchical crystalline polyphenol assemblies and the structural transformation induced by shear force and metal coordination.

To complement the experiments, we performed a number of computational studies to gain greater insight into the behavior of the STEM gels. In particular, we used theory and simulation to model the mechanical behavior of gels that encompass loops and dangling chain ends (schematic in Figure 8).<sup>1,4</sup> If the loops remain folded and dangling ends are chemically inert, then these topological features just serve as defects. If, however, the loops unfold to expose the hidden binding sites and the ends of the dangling chains are reactive, these moieties can form bonds that improve the gel's mechanical properties. For gels with a lower critical solubility temperature (LCST), we systematically switched on and off the possible unfolding and binding events. To quantify the resulting effects, we derived equations for the gel's equilibrium and dynamic elastic moduli. We also used a finite element approach to simulate the gel's response to deformation and validate the analytic calculations. We showed that the equilibrium moduli are highly sensitive to the presence of unfolding and binding transitions. The dynamical moduli are sensitive not only to these structural changes but also to the frequency of deformation. For

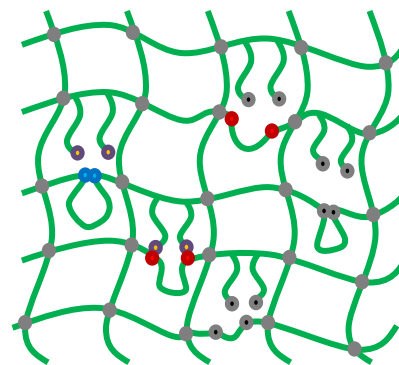


**Figure 8.** Polymer network (in green) containing loops and dangling chains. Loops in permanently folded state or permanently unfolded state (chemically inert) are shown by black solid circles. Loops with reactive labile bonds are shown in blue when bonded. Reactive ends of the dangling chains (yellow) can undergo binding with exposed ends of the loop (red). Ends of dangling chain drawn in black are chemically inert.

example, when reactive ends bind to exposed red sites (Figure 8) at  $T = 29^\circ\text{C}$  and relatively high frequency, the storage shear modulus is 119% greater than the corresponding equilibrium value, while the storage Young's modulus is 109% greater than at equilibrium. These findings provide guidelines for tuning the chemical reactivity of loops and dangling ends and the frequency of deformation to tailor the mechano-responsive behavior of polymer networks.

As a means to develop a deeper understanding of how STEM gels respond to mechanical force, we used dissipative particle dynamics (DPD) simulations to study the mechanical response of the modified STEM gels under compression for various values of the side chain length,  $n_{sc}$ .<sup>15</sup> We found that the mechanical properties can be tuned by varying the grafting density and  $n_{sc}$ . Increases in  $n_{sc}$ , lower the modulus of the networks up to certain saturation value; increasing  $n_{sc}$  beyond that point does not lead to any further softening of the sample. The latter findings agree with the experimental results.

## Future Plans

Synthetic methods used so far in the preparation of STEM networks were focused on controlled *radical* polymerizations such as ATRP and RAFT. We will now extend our studies to the combination of ATRP with ring-opening metathesis polymerization (ROMP). Since ROMP does not involve radical mechanisms and is orthogonal to ATRP, this combination will make it possible to further extend control over the structure and properties of materials. Work with Ir photocatalysts incorporated in functionalized networks will be expanded to explore their application to  $\text{H}_2$  evolution reaction, dehalogenation of toxic aromatics, and photoreduction.<sup>5</sup>

## References

1. J. Cuthbert, A. C. Balazs, T. Kowalewski and K. Matyjaszewski, *STEM Gels by Controlled Radical Polymerization*, Trends in Chemistry **2**, 341-353, (2020).
2. J. Cuthbert, T. Zhang, S. Biswas, M. Olszewski, S. Shanmugam, T. Fu, E. Gottlieb, T. Kowalewski, A. C. Balazs and K. Matyjaszewski, *Structurally Tailored and Engineered Macromolecular (STEM) Gels as Soft Elastomers and Hard/Soft Interfaces*, Macromolecules **51**, 9184-9191, (2018).
3. M. Sun, E. Gottlieb, R. Yuan, S. Ghosh, H. Wang, R. Selhorst, A. Huggett, X. Du, R. Yin, D. H. Waldeck, K. Matyjaszewski and T. Kowalewski, *Polyene-Free Photoluminescent Polymers via Hydrothermal Hydrolysis of Polyacrylonitrile in Neutral Water*, ACS Macro Letters **9**, 1403-1408, (2020).
4. Zhang, T.; Biswas S.; Cuthbert, J.; Kowalewski, T.; Matyjaszewski, K.; Balazs, A. C.; *Understanding the origin of softness in Structurally Tailored and Engineered Macromolecular (STEM) Gels: A DPD study*. Polymer **206**, 122909, (2020).
5. S. DiLuzio, T. U. Connell, V. Mdluli, J. F. Kowalewski and S. Bernhard, *Understanding Ir(III) Photocatalyst Structure–Activity Relationships: A Highly Parallelized Study of Light-Driven Metal Reduction Processes*, Journal of the American Chemical Society **144**, 1431-1444, (2022).

## Publications

1. P. Polanowski, J. K. Jeszka and K. Matyjaszewski, Crosslinking and Gelation of Polymer Brushes and Free Polymer Chains in a Confined Space during Controlled Radical Polymerization—A Computer Simulation Study, Macromolecules **56**, 2608-2618, (2023).
2. M. Sun, G. Szczepaniak, S. Dadashi-Silab, T.-C. Lin, T. Kowalewski and K. Matyjaszewski, Cu-Catalyzed Atom Transfer Radical Polymerization: The Effect of Cocatalysts, Macromolecular Chemistry and Physics **224**, 2200347, (2023).
3. J. Lyu, Y. Li, Z. Li, P. Polanowski, J. K. Jeszka, K. Matyjaszewski and W. Wang, Modelling Development in Radical (Co)Polymerization of Multivinyl Monomers, Angewandte Chemie International Edition **62**, e202212235, (2023).
4. S. V. Wanasinghe, M. Sun, K. Yehl, J. Cuthbert, K. Matyjaszewski and D. Konkolewicz, PET-RAFT Increases Uniformity in Polymer Networks, ACS Macro Letters **11**, 1156-1161, (2022).
5. Z. Liu, Y. Lan, J. Jia, Y. Geng, X. Dai, L. Yan, T. Hu, J. Chen, K. Matyjaszewski and G. Ye, Multi-scale computer-aided design and photo-controlled macromolecular synthesis boosting uranium harvesting from seawater, Nature Communications **13**, 3918, (2022).
6. Y. Liu, Z. Liu, J. Jia, G. Ye, Y. Xie, W. Wang, J. Chen, T. Hu and K. Matyjaszewski, Engineering the Dynamic Hydrogen Bonds in  $\pi$ -Stacked Supramolecular Assemblies for Hierarchical Nanocrystal Formation, Chemistry of Materials **34**, 3525-3535, (2022).
7. M. Sun, F. Lorandi, R. Yuan, S. Dadashi-Silab, T. Kowalewski and K. Matyjaszewski, Assemblies of Polyacrylonitrile-Derived Photoactive Polymers as Blue and Green Light Photo-Cocatalysts for Cu-Catalyzed ATRP in Water and Organic Solvents, Frontiers in Chemistry **9**, 734076 (2021).
8. J. Cuthbert, S. V. Wanasinghe, K. Matyjaszewski and D. Konkolewicz, Are RAFT and ATRP Universally Interchangeable Polymerization Methods in Network Formation?, Macromolecules **54**, 8331-8340, (2021).
9. Q. Wei, M. Sun, F. Lorandi, R. Yin, J. Yan, T. Liu, T. Kowalewski and K. Matyjaszewski, Cu-Catalyzed Atom Transfer Radical Polymerization in the Presence of Liquid Metal Micro/Nanodroplets, Macromolecules **54**, 1631-1638, (2021).
10. Biswas, S., Yashin, V.V., and Balazs, A.C., “Dynamic Behavior of Chemically Tunable Mechano-responsive Hydrogels” Soft Matter **17** 10664-10674 (2021)

## DNA Origami Templated Inorganic Nanostructures

Carlos E. Castro<sup>1,2</sup>, Michael G. Poirier<sup>1,3</sup>, Ralf Bundschuh<sup>1,3</sup>, Jessica O. Winter<sup>1,4,5</sup>

<sup>1</sup>Biophysics Program, <sup>2</sup>Department of Mechanical and Aerospace Engineering, <sup>3</sup>Department of Physics, <sup>4</sup>William G. Lowrie Department of Chemical and Biomolecular Engineering, <sup>5</sup>Department of Biomedical Engineering, The Ohio State University, Columbus, OH

**Keywords:** DNA origami, nanostructures, iron oxide, gold, perovskite

### Research Scope

This research investigates the use of deoxyribonucleic acid (DNA) origami nanostructures as templates for the formation of inorganic nanostructures to access shapes not achievable through solution-based chemistry. In particular, we are investigating gold and iron oxide metallic and perovskite nanostructures. Gold nanostructures exhibit surface plasmon resonance (SPR), the ability to convert light to thermal energy, that depends on their size and shape. Similarly, iron oxide nanostructures offer the ability to generate tailored magnetic fields, and perovskite materials form the cornerstone of advanced solar cells. However, material design approaches for these materials have primarily been limited to spherical or rod-shaped nanoparticles (NPs). Additional methods are needed to access nanostructures with unique geometries for tailored size and shape dependent properties.

Our research harnesses the power of previous DNA templating technologies that used double-stranded DNA and DNA origamis to template[1] or mold[2] gold and/or silver nanostructures to generate iron oxide and perovskite nanostructures (Figure 1). Complex DNA nanostructures, such as DNA origamis, can exhibit dynamic behaviors that enable reconfigurable materials with on-demand response to external (i.e., actuated materials) or environmental (i.e., sensing materials) triggers.

Coupled with inorganic nanomaterials, such structures could harvest electromagnetic energy converting it to dynamic motion and mechanical work or provide optical switching mechanisms. However, additional fundamental knowledge of the relationships between thermal effects, applied force and strain, material mechanical properties, and material structure are needed to enable this vision.

This research seeks to gain fundamental knowledge of energy conversions in inorganic-DNA origami composite materials, while developing synthesis and assembly methods to access several new materials architectures. In these approaches, DNA origamis are used to template inorganic thin films or mold nanostructure growth. However, this research requires pushing the bar in materials synthesis, as current DNA templates are nearly universally employed in aqueous solvents, whereas many inorganic syntheses occur in the organic phase. These advances provide access to shapes not achievable through solution chemistry, expanding the engineering design space for inorganic nanostructure properties. These templated materials can be scaled to useful

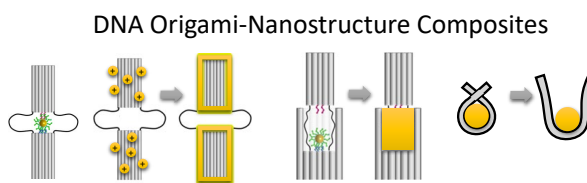


**Figure 1: Schematic.** DNA origami-nanostructure composites are constructed by (L to R) integrating NPs, templated film growth from metal ions, NP seeded growth in DNA origami cavities, or DNA origami folding on NP surfaces.

sizes through potential incorporation in polymer carrier matrices, enabling their translation toward commercial devices.

## Recent Progress

### *DNA Origami Molded Iron Oxide Nanostructures*

Initially, we attempted to use a molding strategy pioneered by Seidel et al. [2] to pattern gold nanostructures inside DNA origami boxes (Figure 2). However, in those early studies we found that the rigidity of the DNA origami box was crucial to obtaining the desired shape. With boxes consisting of fewer DNA barrels, we observed distortion of the DNA origami molds (Figure 2E-F). By increasing box rigidity (Figure 3), we were able to obtain nanostructures with greater shape fidelity. Using this approach, we fabricate molded iron oxide nanostructures (Figure 2G-H).

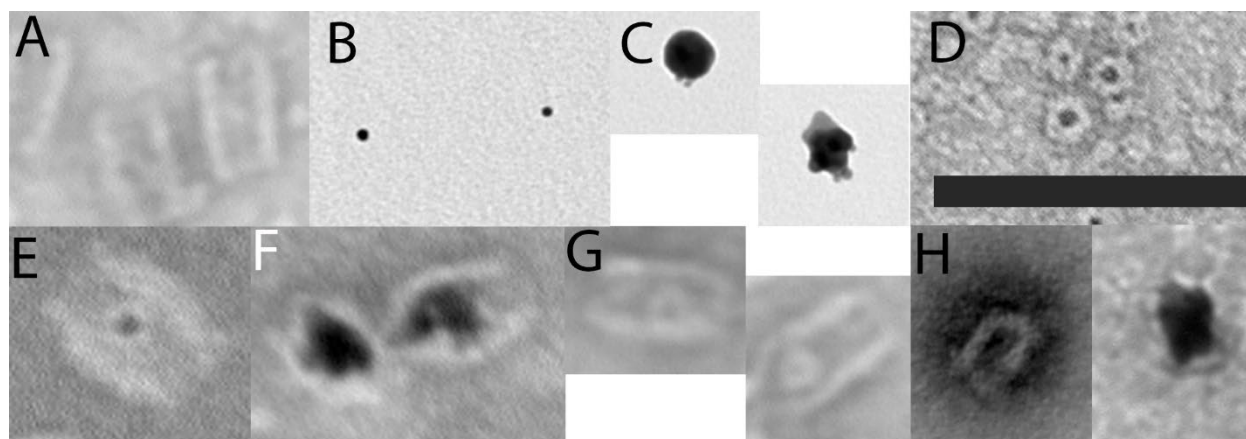


**Figure 2:** DNA origami molded cuboid nanostructures. A) Empty DNA origami cuboids, B) Purchased 5 nm citrate capped AuNPs, C) AuNPs grown using purchased AuNPs as seeds in the absence of a template, D) Purchased 5 nm amine coated SPIONs, E) DNA origami cuboid seeded with a single AuNP, F) Gold growth in DNA origami cuboids seeded with a single AuNP, G) DNA origami cuboids seeded with a single SPION, H) Iron growth in DNA origami cuboids seeded with a single SPION. Scale bar =100 nm.

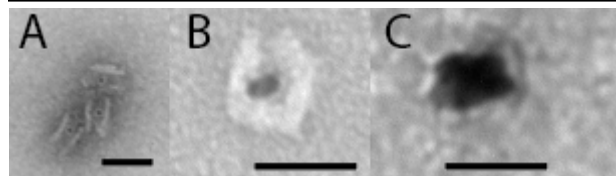


**Figure 3:** DNA origami boxes with thicker walls designed to control growth shape. A) These boxes were seeded with 5 nm gold nanoparticles before growth using acidic reduction using B) low and C) high concentrations of gold chloride. Scale bar is 100 nm.

### *DNA Origami Template Iron Oxide Thin Films*

Next, we adapted the templating approach of Ben-Yoseph et al. [1] to pattern iron oxide thin films on three different DNA origami structures (Figure 4): hinges, six bars, and NanoDyn force sensors. For the six bar structure, we examined the material in three different configurations. For each material, we investigated the relationship between increased iron concentration and coating thickness and integrity (Figure 5). We also showed that, provided the coating was sufficiently thin, DNA templated nanostructures main accessible ssDNA sticky ends that can be used for attaching

NPs (Figure 6) or for reconfiguration, consistent with recent reports for silica-coated nanostructures [3].

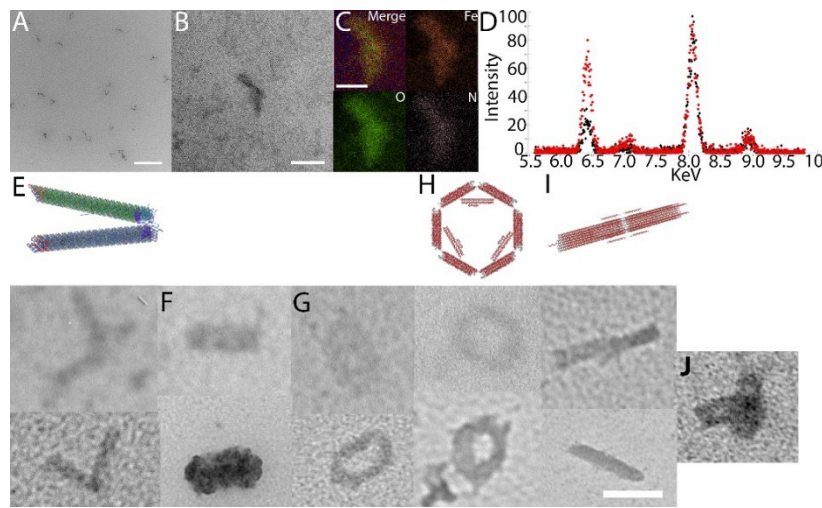


**Figure 4:** TEM images and schematics of uncoated and iron-coated DNA origami without stain. A) Wide field TEM image of iron coated origami hinges. Scale bar = 500 nm, B) TEM image of an individual iron-coated hinge, C) Composite and select elemental EDS images, D) Plot of EDS data for iron coated structure (red) and background signal (black), E-I) Schematics (top), uncoated (middle), and iron-coated (bottom) (E) hinges, 6 bars with (F) flat close, (G) rectangle, (H) and hexagon conformations, and (I) NanoDyNs. J) TEM image of 6 bar in flat close showing magnetic ordering. B-J scale bars = 100 nm.

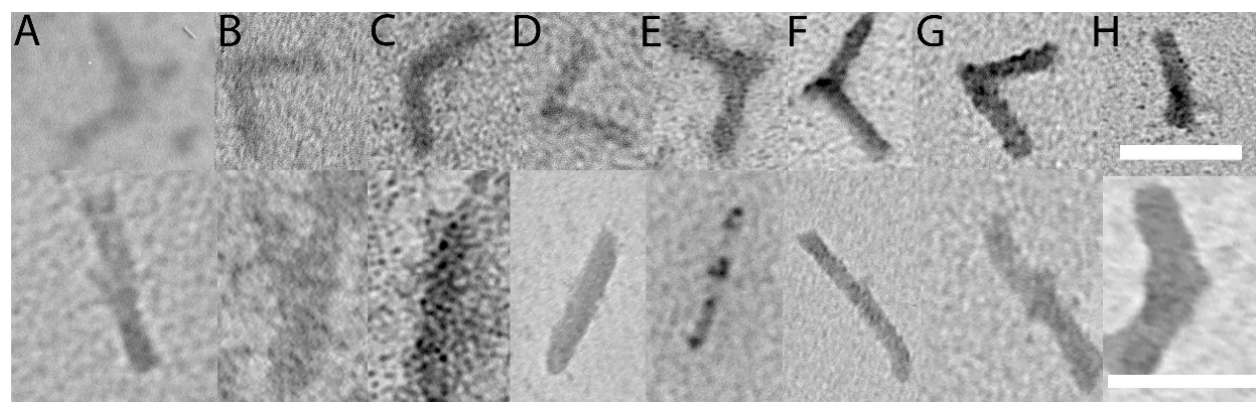


**Figure 5:** TEM images of individual hinges (top) and NanoDyNs (bottom) with A) 0, B) 50,000, C) 100,000, D) 250,000, E) 375,000, F) 500,000, G) 750,000, and H) 1,000,000 iron ions per origami structure. No stains were used in these images. Increased coating density is indicated by increasing contrast reflecting the electron density of the coated structure. Scale bar = 100 nm.

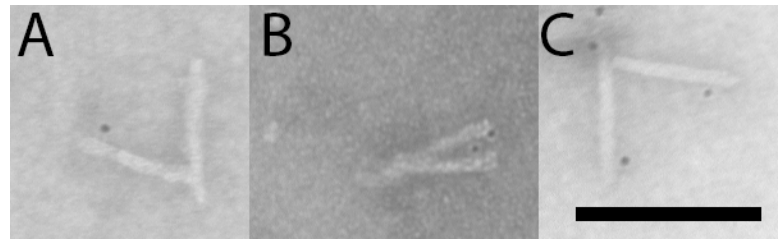


**Figure 6:** TEM images of individual, iron-coated DNA origami hinges with A, B) one AuNP bound in A) open B) closed configurations, and C) with two AuNPs bound. (Note, in B, an additional AuNP is adsorbed to the top arm of the hinge.) Scale bar = 100 nm

### *Expanding the Templating Approach to Organic Solvents: Case Study with Perovskites*

In the above examples, we explored materials that can be synthesized through simple nanoprecipitation reactions in aqueous solution. To broaden the impact of our work, we next adapted this approach to synthesis in organic solvents using perovskite materials as a model system. This work builds on previous work showing that, despite popular conception, DNA origami materials can be stable in organic solvents, including toluene [4]. Adapting a standard synthesis procedure for CsPbBr<sub>3</sub> perovskites [5] that uses toluene as a solvent, we preliminary showed that perovskite materials can be templated on DNA origami NanoDyn structures (Figures 7-8). Perovskites are widely pursued materials for their potential use in solar cells. One of the standard approaches for solar cell fabrication includes perovskite dispersal in a polymer matrix via spin coating, an approach readily adaptable to DNA templated nanostructures. The ability to generate perovskites with defined shapes may enhance their properties.

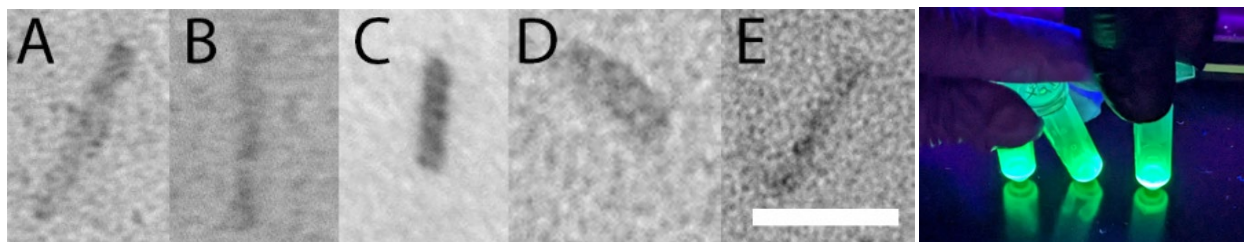


**Figure 7:** TEM images of NanoDyn structures coated with CsPbBr<sub>3</sub> perovskite. A) Uncoated NanoDyn in toluene, B) NanoDyn with Br precursor only (no crystal formation), (C-D) Perovskite-coated NanoDyNs with C) Pb precursor added first, D) Cs precursor added first, and E) Pb/Cs precursor added simultaneously. Scale

**Figure 8:** Fluorescence of perovskite-coated DNA origami nanostructures under UV light.

### **Future Plans**

We are currently measuring the effect of iron oxide coating on material rigidity and mechanical properties of these molded and templated nanostructures. Additionally, we are studying the effect of magnetic fields on ordering of iron oxide templated structures. Preliminarily, we have found that inherent and extrinsic magnetic fields may provide an additional method of self-assembly for these materials (Figure 4J). We are also refining coating and molding methodologies to improve uniformity. We are studying the relationship between DNA origami stability in harsh environments and coating, and we are studying the limitations of material actuation with coating thickness. We also hope to specifically interrogate structure-property relationships for specific geometries.

### **References**

1. E. Braun, Y. Eichen, U. Sivan and G. Ben-Yoseph, *Nature* **391**, 775-778 (1998).
2. S. Helmi, C. Ziegler, D. J. Kauert and R. Seidel, *Nano Letters* **14**, 6693-6698 (2014).
3. L. M. Wassermann, M. Scheckenbach, A. V. Baptist, V. Glembockyte and A. Heuer-Jungemann, *Advanced Materials* **35**, 2212024 (2023).
4. H. Kim, S. P. Surwade, A. Powell, C. O'Donnell and H. Liu, *Chemistry of Materials* **26**, 5265-5273 (2014).
5. S. Wei, Y. Yang, X. Kang, L. Wang, L. Huang and D. Pan, *Chemical Communications* **52**, 7265-7268 (2016).

## Publications

1. E. Jergens and J. O. Winter, *Nanoparticles caged with DNA nanostructures*, *Current Opinion in Biotechnology* **74**, 278-284 (2022).
2. E. Jergens, S. de Araujo Fernandes-Junior, Y. Cui, A. Robbins, C. E. Castro, M. G. Poirier, M. N. Gurcan, J. J. Otero and J. O. Winter, *DNA-caged nanoparticles via electrostatic self-assembly*, *Nanoscale* **15**, 9390-9402 (2023).
3. J. A. Johnson, V. Kolliopoulos and C. E. Castro, *Co-self-assembly of multiple DNA origami nanostructures in a single pot*, *Chemical Communications* **57**, 4795-4798 (2021).
4. K. Crocker, J. Johnson, W. Pfeifer, C. Castro and R. Bundschuh, *A quantitative model for a nanoscale switch accurately predicts thermal actuation behavior*, *Nanoscale* **13**, 13746-13757 (2021).
5. Robbins, H. Hildebolt, M. Neuhoff, P. Beshay, J. O. Winter, C. E. Castro, R. Bundschuh and M. G. Poirier, *Cooperative control of a DNA origami force sensor*, *bioRxiv* 2023.06.26.546608 (2023).
6. E. Akbari, M. Shahhosseini, A. Robbins, M. G. Poirier, J. W. Song and C. E. Castro, *Low cost and massively parallel force spectroscopy with fluid loading on a chip*, *Nature Communications* **13**, 6800 (2022).

## **Self-Assembly and Self-Replication of Novel Materials from Particles with Specific Recognition DE-SC0007991.**

**Paul M. Chaikin, David Pine, Dept. of Physics, New York University, Ruoji Sha, Marcus Weck, Dept. of Chemistry, New York University.**

**1. Weck - Keywords:** Colloidal machines, DNA-coated colloids, self-assembly

### **Research Scope**

Colloidal science has long focused on the assembly of spherical particles and explored this topic in great detail developing an understanding of the mechanism and dynamics of these assemblies. The challenge of making more complex colloidal superstructures and, potentially, colloidal machines, lies in the colloidal building blocks themselves, as isotropic colloids lack specific bonding directionality. Achieving structurally complex assemblies necessitates the use of chemically and structurally anisotropic building blocks. Using tunable anisotropic particles and geometrically tunable particles coupled with the DNA interactions, we target shape shifting colloidal assemblies as a first step towards colloidal machines and three-dimensional cage and cage-like structures.

### **Recent Progress**

We present a binary system of anisotropic particles composed of a responsive unit and a non-responsive unit that assemble based on DNA interactions into chains. We use DNA hybridization because it is composed of weak interactions including hydrogen bonding between subunits allowing for reversibility and correction within the system. The Weck group has proven that this type of site-specific DNA bonding enables assembly, disassembly, and restructuring when stimulated by temperature.<sup>1</sup> To stimulate the shape-shifting an organic solvent is introduced to the system resulting in the responsive units swelling while remaining chained. All components are characterized with SEM, holographic imaging, bright field and fluorescent microscopy. Specifically, holographic imaging is used to qualitatively measure the swelling after the solvent is introduced, in the responsive unit the holographic imaging shows both the size change but all the shape change (spherical to oblong). Fluorescent Microscopy is used to confirm the binary chains have assembled utilizing the fluorescent dye in the complementary DNA used.

### **Future Plans**

i) These shape-shifting chains can be incorporated into larger dynamic systems as gates, with the dynamic nature being a trigger to allow for a switch between open and closed states. The dynamic nature can be incorporated into sensors, delivery or electrical systems. This is just the beginning of dynamic assemblies, dynamic colloids such as those utilized here can be used to impart advanced functionality to colloidal assemblies, opening an avenue to create machine-like colloidal structures.

ii) We target advanced colloidal engineering methods to fabricate geometrically unique multi-component patchy particles that are both directional in bonding as well as solvent

responsive. We will characterize, assemble, and explore the dynamic nature of these particles and their assemblies in a flow cell, assisted by electron, confocal, and bright-field microcopies, followed by statistical elucidation of the assembled superstructures with computational image recognition.

## 2. Chaikin - Keywords: Self-replication, Nano Industrial Robots, Colloidal Micro-Machines

### Research Scope

We seek to extend the use of specific DNA recognition and hybridization from the nanoscale to the micro scale. We have exhibited self-replication of DNA origami motifs in one, two, and three dimensions and also shown mutation, and selection. A current goal is DNA assisted self-assembly and activation of colloidal micro-machines.

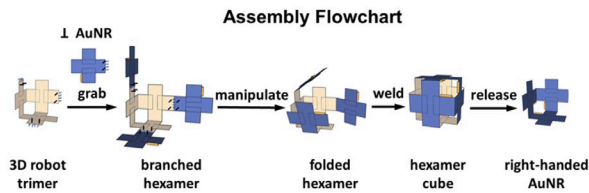


**Fig. 1** DNA Nano robot Flowchart for optically active Chiral structures Au NanoRod, AuNR, monomer plates. Start at 40C. Grab: anneal to 16C at 1 C/hr. Robot trimer hybridizes with three plates to form a branched hexamer. Manipulate: On further cooling, struts precisely fold the plates 90° to form a closed cube. Weld: UV chemically cross-links. Release: heat to 40C → chiral AuNr.

**3D DNA Industrial Nanorobots:** Nanoscale industrial robots have potential as manufacturing platforms, capable of automatically performing repetitive tasks to handle and produce nanomaterials with precision and accuracy. We demonstrate a DNA industrial nanorobot, that fabricates a 3D optically active, chiral structure from optically inactive parts. Our programmable robot,  $\sim (100\text{nm})^3$  in size, grabs different parts, positions and aligns them so that they can be "welded", releases the construct and returns to its original configuration ready for its next operation. Using robots for self-replication also solves the problem of 3D direct self-replication that's difficult to do by single-step templating (which requires an additional dimension and/or further assembly). Our introduction of multiple-axis precise folding and positioning as a tool/technology for nano manufacturing opens the door to more complex, useful nano-micro devices. The products that can be made depend on the nanorobot structure, but different products can be made from the same nanorobot by changing the programming, in particular the order of grabbing, folding and welding.

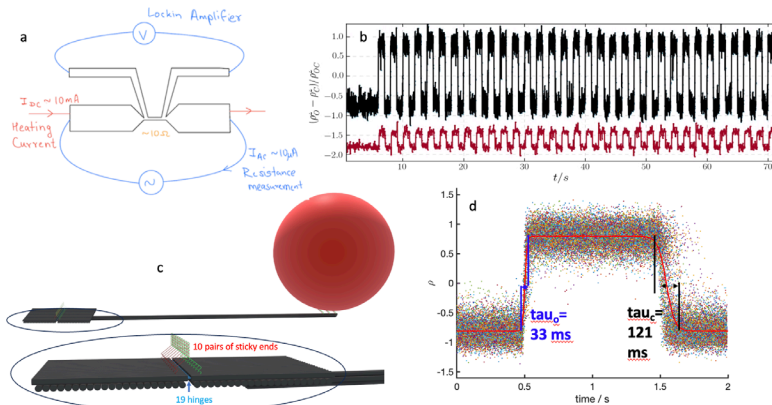


**Fig.2** a) Schematic of the thin film heater-thermometer. b) red-temperature (20-31C), black bead displacement from open to close. c) Two square origami connected by 19 2T ssDNA and 10 sticky end pairs. d) Open-close cycle repeated 100 times.

**Local Heating experiments with DNA molecular motors.** To make faster machines as well as investigate the intrinsic zipping and unzipping times for DNA hybridization we built a local heater that can potentially provide data up to the megahertz regime, Fig.2. Measuring the resistance makes the heater its own thermometer. To make our hinge motors more powerful and faster we want to put DNA sticky ends in parallel - enabled here since all are heated at the same time. Triggering the opening periodically we can also average over many cycles. Using this technique we were able to measure the opening and closing times, 33ms and 121ms.

**Future Plans** - competition and evolution, further DNA molecular machines and muscles.

**3. Pine - Keywords:** DNA-coated colloids, TIRM, electrophoresis

### **Research Scope**

DNA-coated colloids (DNACCs) offer unprecedented control over colloidal self-assembly, with the ability to dynamically assemble and disassemble new structures ranging from new 3-dimensional crystal structures to chains, colloidal micelles, and sheets. Our current DOE-sponsored work focuses on experiments to develop a detailed understanding of DNA-mediated interactions between DNACCs, which includes developing and using total internal reflection microscopy (TIRM) and video microscopy as well as electrophoresis and dielectric spectroscopy to characterize the nanostructure of DNA tethered to colloidal particles by polymer chains.

### **Recent Progress**

We developed and used TIRM to study the interactions between hybridizing DNA tethered by polyethylene oxide to micrometer-size colloidal particles. In the course of our research, we uncovered a fundamental limit to the spatial resolution with which TIRM can measure colloidal interactions, a limit that had not previously been appreciated in the 35 years of use (and misuse) of TIRM. In so doing, we developed an analytical description of the resolution limit, which comes about due to the quantum mechanical nature of photon counting statistics in the measurement of light intensity. We went on to use TIRM to measure the DNA-mediated interactions between colloids and, working with NYU theorists Dr. Sophie Marbach and Prof. Miranda Holmes-Cerfon, developed a detailed framework that quantitatively accounts for the experimentally measured dependence of the interaction potential on DNA grafting density and molecular weight as well as on DNA coding sequence, complementary fraction, and salt concentration. We made the model, which provides a quantitative and predictive approach for guiding material design, publicly available on GitHub.

### **Future Plans**

We are using colloidal electrophoresis and dielectric spectroscopy along with exact numerical solutions to the electrokinetic governing equations<sup>2,3</sup> to provide detailed nanoscale characterization of DNA polymer coatings on colloids. These measurements, together with the numerical solutions provided by our collaborator, Prof. Reghan Hill at McGill University, can distinguish differences of the polymer brush thickness of 2 nm and can measure the grafting density as well as the conformation of polymers within the brush (e.g. stretched vs. mushroom). It is even sensitive to

how charge is distributed along the grafted chain, exhibiting easily distinguishable changes in the salt-dependent electrophoretic mobility between charges evenly distributed along the chain vs. charge localized at the end of the chain. Initial results show remarkable agreement between theory and experiment. We plan to further develop this tool across a broad spectrum of particles sizes as well as adding dielectric spectroscopy to the toolset. When fully developed, we believe these tools, which are simple to implement, can be widely applied across the community of researchers studying DNA-coated colloidal particles and nanoparticles.

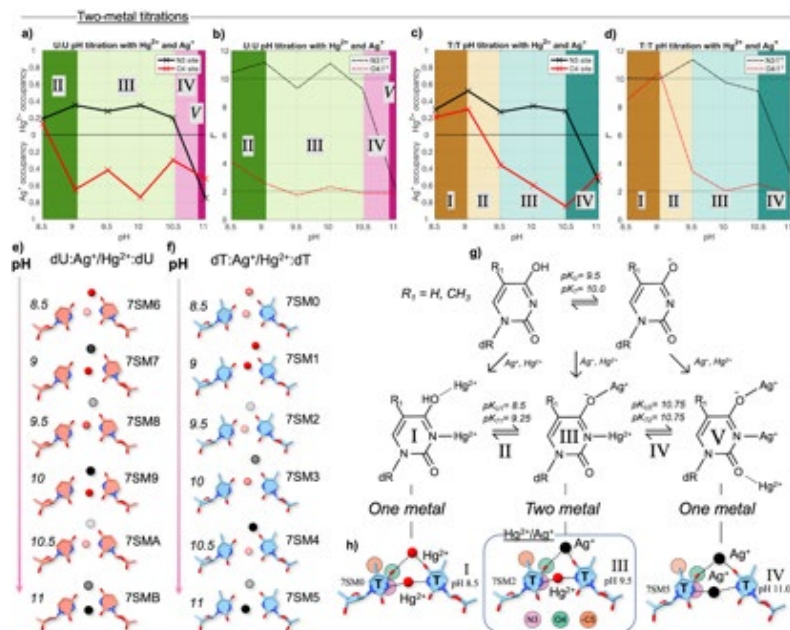
#### 4. Sha, Seeman - Keywords: Metal-mediated DNA, crystallography

##### Research Scope

Metal-mediated DNA (mmDNA) is a pathway towards engineering bioinorganic and electronic behavior into DNA devices. Many chemical and biophysical forces drive the programmable chelation of metals between pyrimidine base pairs. The precision self-assembly of heterometallic DNA chemistry at the sub-nanometer scale will enable atomistic design frameworks for more elaborate mmDNA-based nanodevices and nanotechnologies.

##### Recent Progress

Using the tensegrity triangle motif as a scaffold to drive B-form crystallization allowed us to develop a method of taking crystallographic snapshots for the structure determination of mmDNA base pairs. Motifs containing dT:Ag<sup>+</sup>:dT and dU:Ag<sup>+</sup>:dU show strong pH dependence, titrating from a crystallographic occupancy of 0.0 to 1.0 for a pH range of 8.0-10.0. Using this pH-dependent binding site, we further determined the structures of mmDNA homothymine and homouracil base pairs with silver(I) at the O4 position and mercury(II) at the N3 position and analyzed their behavior across pH values of 8.5-11.0, discovering three pH-dependent binding modes with tandem chelation of mercury(II) and silver(I). We additionally tested this method on cytosine and identified the pH-dependent incorporation of mercury(II) into homocytosine base pairs as well as a heterometal base pair with both silver(I) and mercury(II)<sup>4,5</sup>.



pairs as well as a heterometal base pair with both silver(I) and mercury(II)<sup>4,5</sup>.

##### Future Plans

i) Isothermal separation of DNA tiles for self-replication: The stability of DNA tiles is the issue when higher temperature is needed

Fig. 3. Crystallographic pH titrations for double metal (dT:Ag<sup>+</sup>/Hg<sup>2+</sup>:dT and dU:Ag<sup>+</sup>/Hg<sup>2+</sup>:dU) mmDNA base pairs in Tris buffer.

for separating newly generated materials from their templates. We

are developing a mechanism to dissociate DNA base pairs in room temperature by changing the ions and pH of the solution.

ii) Metal-ion-assisted DNA strand displacement with pyrimidine toeholds: We are trying to selectively initiate DNA single strand invasion in specific ion and pH conditions to affect the binding of replicating units and their template and it will enable us to study the mutation and selection processes in self-assembly and self-replication systems, which are induced by variation of ions and pH change.

## References

1. X. Zheng, Y. Wang, Y. Wang, D. J. Pine, M. Weck, , Thermal Regulation of Colloidal Materials Architecture through Orthogonal Functionalizable Patchy Particles. *Chem. Mater.* **2016**, *28*, 3984-3989.
2. R. J. Hill, D. A. Saville, W. B. Russel, Electrophoresis of spherical polymer-coated colloidal particles. *Journal of Colloid and Interface Science* **258**, 56–74 (2003).
3. R. J. Hill, Corona charge regulation in nanoparticle electrophoresis. *Proc. R. Soc. A.* **471**, 20150522 (2015).
4. J. Zheng, J. J. Birktoft, Y. Chen, T. Wang, R. Sha, P. E. Constantinou, S. L. Ginell, C. Mao and N. C. Seeman, From Molecular to Macroscopic Via the Rational Design of a Self-Assembled 3d DNA Crystal. *Nature* **461**, 74-77, (2009).
5. Y. Miyake, H. Togashi, M. Tashiro, H. Yamaguchi, S. Oda, M. Kudo, Y. Tanaka, Y. Kondo, R. Sawa, T. Fujimoto, T. Machinami and A. Ono, Mercuryii-Mediated Formation of Thymine-Hgii-Thymine Base Pairs in DNA Duplexes. *J. Am. Chem. Soc.* **128**, 2172-2173, (2006).

## Publications

1. Zhou, Feng, Ruojie Sha, Heng Ni, Nadrian Seeman, and Paul Chaikin. "Mutations in artificial self-replicating tiles: A step toward Darwinian evolution." *Proceedings of the National Academy of Sciences* 118, no. 50 (2021): e2111193118.
2. Liu, Mingzhu, Xiaolong Zheng, Veronica Grebe, Mingxin He, David J. Pine, and Marcus Weck. "Two-Dimensional (2D) or Quasi-2D Superstructures from DNA-Coated Colloidal Particles." *Angewandte Chemie International Edition* 60, no. 11 (2021): 5744-5748.
3. Zheng, Mengxi, Zhe Li, Cuizheng Zhang, Nadrian C. Seeman, and Chengde Mao. "Powering  $\approx 50 \mu\text{m}$  Motion by a Molecular Event in DNA Crystals." *Advanced Materials* 34, no. 26 (2022): 2200441.
4. Wang, Xiao, Rahul Deshmukh, Ruojie Sha, Jens J. Birktoft, Vinod Menon, Nadrian C. Seeman, and James W. Canary. "Orienting an Organic Semiconductor into DNA 3D Arrays by Covalent Bonds." *Angewandte Chemie International Edition* 61, no. 5 (2022): e202115155.
5. Lu, Brandon, Simon Vecchioni, Yoel P. Ohayon, James W. Canary, and Ruojie Sha. "The wending rhombus: Self-assembling 3D DNA crystals." *Biophysical journal* 121, no. 24 (2022): 4759-4765.
6. Cui, Fan, Sophie Marbach, Jeana Aojie Zheng, Miranda Holmes-Cerfon, and David J. Pine. "Comprehensive view of microscopic interactions between DNA-coated colloids." *Nature communications* 13, no. 1 (2022): 2304.
7. Ni, Heng, Xiao Fan, Feng Zhou, Galio Guo, Jae Young Lee, Nadrian C. Seeman, Do-Nyun Kim, Nan Yao, Paul M. Chaikin, and Yimo Han. "Direct visualization of floppy two-dimensional DNA origami using cryogenic electron microscopy." *Science* 25, no. 6 (2022).

8. Vecchioni, Simon, Brandon Lu, William Livernois, Yoel P. Ohayon, Jesse B. Yoder, Chu-Fan Yang, Karol Woloszyn et al. "Metal-Mediated DNA Nanotechnology in 3D: Structural Library by Templated Diffraction." *Advanced Materials* (2023): 2210938.
9. Zhao, Yue, Arun Richard Chandrasekaran, David A. Rusling, Karol Woloszyn, Yudong Hao, Carina Hernandez, Simon Vecchioni et al. "The Formation and Displacement of Ordered DNA Triplexes in Self-Assembled Three-Dimensional DNA Crystals." *Journal of the American Chemical Society* 145, no. 6 (2023): 3599-3605.
10. Lu, Brandon, Karol Woloszyn, Yoel P. Ohayon, Bena Yang, Cuizheng Zhang, Chengde Mao, Nadrian C. Seeman, Simon Vecchioni, and Ruojie Sha. "Programmable 3D Hexagonal Geometry of DNA Tensegrity Triangles." *Angewandte Chemie International Edition* 62, no. 6 (2023): e202213451.

# Energy-Efficient Self-Organization and Swarm Behavior in Active Matter

Paul Chaikin, Dept. of Physics, New York University

Jerome Delhommelle, Dept. of Chemistry, University of Massachusetts Lowell

Stefano Sacanna, Mark Tuckerman, Dept. of Chemistry, New York University

**Keywords:** active matter; nonequilibrium assembly; entropy production; colloidal synthesis; nonequilibrium simulations

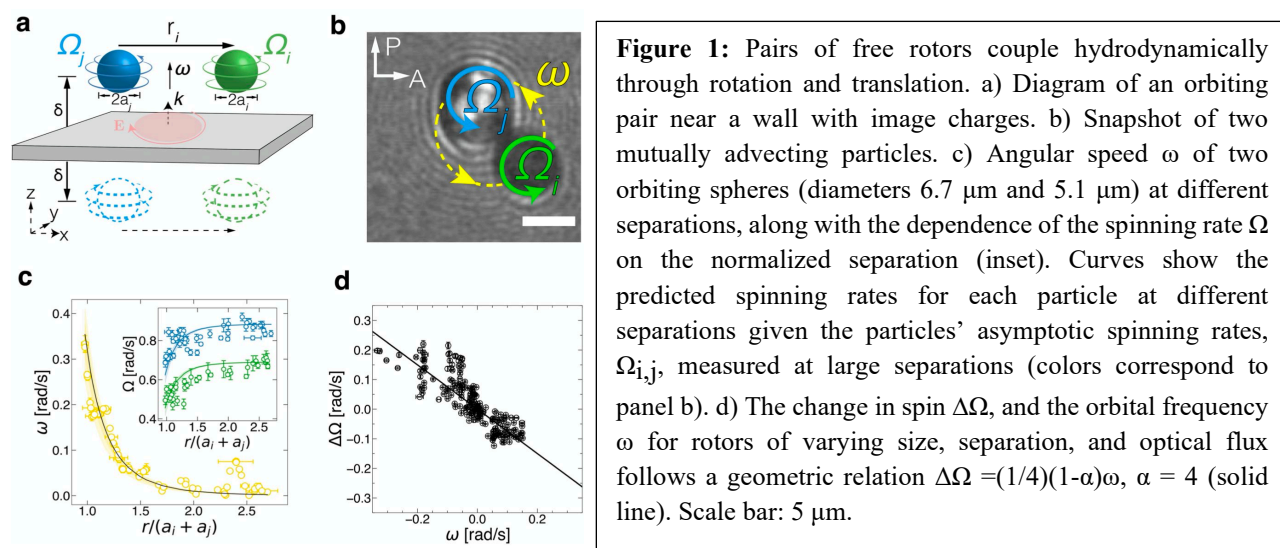
## Research Scope

Living systems have the unique ability to form hierarchical assemblies in which individual constituents can perform tasks cooperatively and emergently. Harnessing such properties is a long-standing challenge for the rational design of dynamic materials that can respond to their environment, communicate with one another, and undergo a rapid, reversible assembly. Recent developments in the design of smart and active colloidal building blocks have led to tremendous breakthroughs, such as the onset of synthetic photoactivated active assemblies. In this project, we combine experiments, theory, and computations to identify novel couplings between elemental active building blocks, elucidate diffusiophoretic cluster growth, shed light on how to program inverse assembly and assembly in active matter and determine local entropy production and extractable work in active matter.

## Recent Progress

### Hydrodynamic spin-orbit coupling in micro-rotors<sup>1</sup>

Direct observation of the hydrodynamic coupling between artificial micro-rotors has been restricted by the details of the chosen drive, either through synchronization (using external magnetic fields) or confinement (using optical tweezers). Here we present a new active system



that illuminates the interplay of rotation and translation in free rotors. We developed a non-tweezing circularly polarized beam that simultaneously rotates hundreds of silica-coated birefringent colloids. The particles rotate asynchronously in the optical torque field while freely diffusing in the plane. Neighboring particles orbit each other with an angular velocity that depends on their spins. We derive an analytical model in the Stokes limit for pairs of spheres. The geometrical nature of the low Reynolds fluid results in a universal hydrodynamic spin-orbit coupling,  $\Delta\Omega = (1/4)(1-\alpha)\omega$ , where the tangential flow from a spinning particle varies as  $u \sim 1/r^\alpha$ .

## Diffusiophoretic Cluster Growth<sup>2</sup>

Hematite is a photoactivated catalyst that decomposes  $\text{H}_2\text{O}_2$  into  $\text{H}_2\text{O}$  and  $\text{O}_2$ . A hematite cube on a surface, when illuminated by blue light, presents the system with  $\text{O}_2$  concentration gradients that cause diffusiophoretic migration of polystyrene (or TPM) particles toward the hematite and a three-dimensional crystalline cluster assembles. What is interesting about this attractive clustering is that the interaction between the hematite and the colloids is non-reciprocal (the hematite is not attracted, nor does it move towards the colloidal particles), and the interaction cannot be described in terms of a potential. Fig. 2 left) shows a schematic of the experiment and right) shows two clusters formed around two hematite cubes. The center) shows the time dependence of a typical cluster radius and the long-time saturation at steady state. Since this is a non-equilibrium problem, we look at forces and fluxes rather than thermodynamic energies. We equate the inward flux,  $c v_D$ , ( $c$  = concentration of colloids, drift speed  $v_D = -k/r^2$  determined as the gradient of the  $n \sim 1/r$  diffusion profile from the hematite,  $k$  = diffusiophoretic coefficient) to the flux from the colloid diffusion ( $-D\partial c/\partial r$ ) or  $-kc/r^2 = -D\partial c/\partial r$ . This has a solution of the form  $c = Ae^{k/rD}$  similar to an exponential atmosphere. While there is no cutoff, when  $r^2 D/k = a$  radius, the concentration drops by  $e^2$  in a diameter. The size of these clusters obeys this relationship as the intensity of the light is varied. The clusters vanish when the light is turned off.

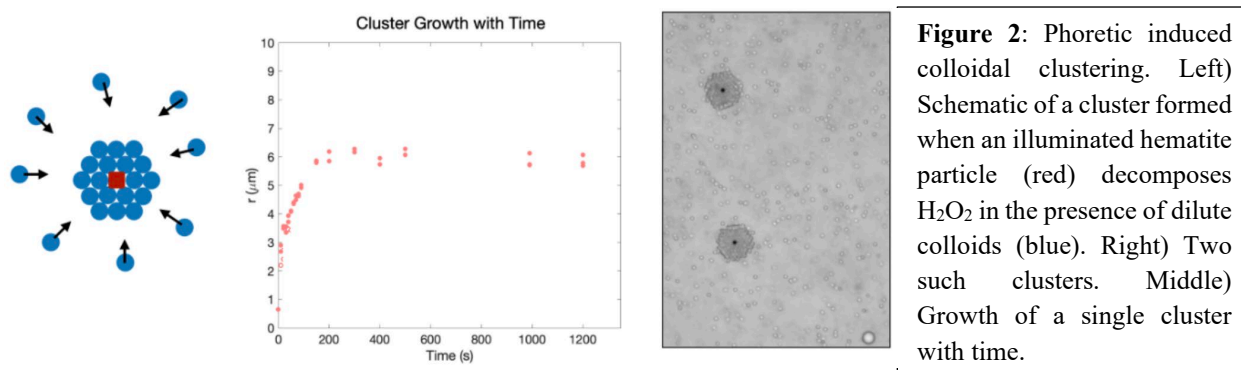


**Figure 2:** Phoretic induced colloidal clustering. Left) Schematic of a cluster formed when an illuminated hematite particle (red) decomposes  $\text{H}_2\text{O}_2$  in the presence of dilute colloids (blue). Right) Two such clusters. Middle) Growth of a single cluster with time.

## Programmable templated assembly and inverse assembly in active matter<sup>3</sup>

Microstructure can be constructed through the self-assembly of microscopic elemental building blocks. Here we leverage a specific property of active matter, *i.e.*, its ability to exhibit dynamics-dependent density distributions, to program the nonequilibrium assembly of photoactivated

synthetic microswimmers. Using simulations of Active Brownian Particles (ABP) and experiments on light-activated microswimmers, we examine how light patterns (see the top of Figure 3) can lead to inverse assembly, creating void regions within the fluid, or promote assembly, shaping clusters of particles that match the size and geometry of the pattern. This allows us to identify scaling relations that determine the characteristic time for both processes. For instance, the ratio of the pattern size ( $L_\theta$ ) over the persistence length of the active fluid ( $L_p$ ) determines the characteristic time for inverse assembly. The dynamics for forming larger clusters via light patterns are shown to occur in a two-step process, with particles initially thrust into the dark regions before undergoing a diffusive motion toward the center of the dark pattern.

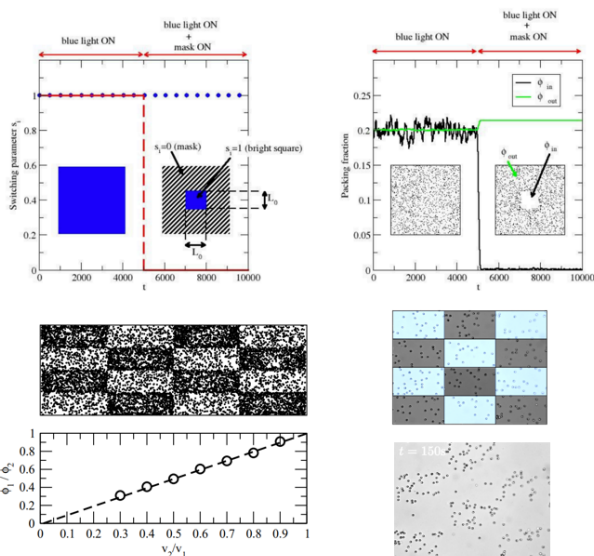


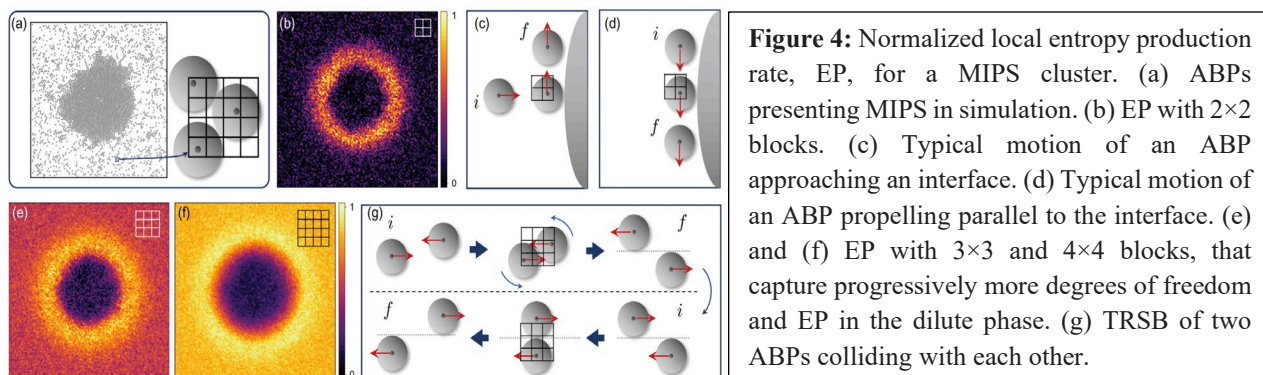
**Figure 3:** Inverse assembly and assembly programmed by light patterns. Top) Schematic of the application of the light pattern (left) leading to the onset of a void (right) in an initially uniform system. Bottom) Creation of a checkerboard motifs in ABP simulations (left) and experiments (right). The plot shows how the ratio of the densities in the bright ( $\phi_1$ ) and dark ( $\phi_2$ ) regions scales with the ratio of the self-propelled velocities in these two regions ( $v_1$  and  $v_2$ , respectively). In the experiments, the light mask is projected onto the system and gives rise to the formation of a checkerboard motif in the active suspension (the bottom picture shows the system 150s after the mask has been applied).

Combining inverse assembly and assembly processes to template complex structures in the active fluid, we precisely control the local packing fraction throughout the fluid by modulating the light intensity in the dark and bright regions and, thus, the relative velocities in the two regions. This behavior predicted by simulations is demonstrated experimentally (see bottom of Figure 3). This paves the way for novel nonequilibrium assembly strategies in active matter by programming a stimulus with a high-resolution spatio-temporal pattern.

### Local Entropy Production and Extractable Work in Active Matter<sup>4</sup>

Time-reversal symmetry breaking (TSRB) and entropy production (EP) are universal features of nonequilibrium phenomena. Despite its importance in the physics of active and living systems, the entropy production of systems with many degrees of freedom has remained of little practical significance because the high dimensionality of their state space makes it difficult to measure. Here we introduce a local measure of entropy production and a numerical protocol to estimate it. We establish a connection between the entropy production and extractability of work in a given region of the system and show how this quantity depends crucially on the degrees of freedom being tracked. We validate our approach in theory, simulation, and experiments by considering systems of active Brownian particles undergoing motility-induced phase separation, as well as active

Brownian particles in Figure 4. Our approach comes from an information theoretical treatment and lossless data compression. Locally one can measure a quantity such as density or velocity as a function of time. Compressing the sequence either forward or backwards in time yields the same compressed length. However, if the second half of the sequence is reversed then the compressed length remains the same only if all the forward paths match the time reversed paths. The difference is a measure of the time reversal symmetry breaking and the entropy production. Formally, entropy production in statistical mechanics can be related to the Kulback-Leibler divergence in information theory which we have developed in terms of the cross-parsing complexity of a sequence read half forward and half backwards.



## Future plans

Future studies will focus on the application of dynamic, both spatially and time-dependent, patterns instead of static, solely spatially dependent patterns to direct the motion of clusters of active particles. Our initial results have also enabled us to characterize the interplay between the properties of the active suspension and the characteristics of the dynamic pattern in line with the scaling relations we previously determined for static assembly. Furthermore, we will elucidate the coupling between active particles in the presence of another external field (such as shear) and identify the most efficient strategies to program active cluster assembly under such conditions. Finally, we will introduce a new model for local entropy production based on fluctuation theorems to complement the abovementioned approach. These results will lead to a deeper understanding of how information may be programmed and encoded into active matter.

## References

1. Zion, M. Y. B.; Modin, A.; Chaikin, P. M. "Hydrodynamic spin-orbit coupling in asynchronous optically driven micro-rotors" Nat. Commun. 2023, accepted for publication (preprint: arXiv:2203.11051)
2. Hauser, A.; Hardikar, A.; Chaikin, P. M.; Delhommelle, J.; Sacanna, S. "Non-Reciprocal Forces and Phoretic Colloidal Clustering, 2023, to be published
3. Desgranges, C.; Ferrari, M.; Chaikin, P. M.; Sacanna, S.; Tuckerman, M. E.; Delhommelle, J. "Microswimmers under the spotlight: interplay between agents with different levels of activity." 2023, under review
4. Ro, S.; Guo, B.; Shih, A.; Phan, T. V.; Austin, R. H.; Levine, D.; Chaikin, P. M.; Martiniani, S. "Model-free measurement of local entropy production and extractable work in active matter." Phys. Rev. Lett. 2022, 129, 220601

## Publications 2022-2023

1. Ro, S.; Guo, B.; Shih, A.; Phan, T. V.; Austin, R. H.; Levine, D.; Chaikin, P. M.; Martiniani, S. "Model-free measurement of local entropy production and extractable work in active matter." Phys. Rev. Lett. 2022, 129, 220601.
2. Essafri, I., Ghosh, B.; Desgranges, C.; Delhommelle, J. "Designing, synthesizing, and modeling active fluids." Phys. Fluids 2022, 34, 071301
3. Ghosh, A.; Radhakrishnan, J.; Chaikin, P. M.; Levine, D.; Shankar, G. "Coupled dynamical phase transitions in driven disk packings." Phys. Rev. Lett. 2022, 129, 188002.
4. Zion, M. Y. B.; Modin, A.; Chaikin, P. M. "Hydrodynamic spin-orbit coupling in asynchronous optically driven micro-rotors" Nat. Commun. 2023, accepted for publication (preprint: arXiv:2203.11051)
5. Desgranges, C.; Ferrari, M.; Chaikin, P. M.; Sacanna, S.; Tuckerman, M. E.; Delhommelle, J. "Microswimmers under the spotlight: interplay between agents with different levels of activity." 2023, under review
6. Desgranges, C.; Chaikin, P. M.; Sacanna, S., Tuckerman, M. E.; Delhommelle, J. "Directed assembly and motions of patterns in active matter." 2023, in preparation
7. Desgranges, C.; Tuckerman, M. E.; Delhommelle, J. "Assessing the accuracy of numerical integrators for active matter motion equations." 2023, under review
8. Wilken, S.; Guo, A. Z.; Levine, D.; Chaikin, P. M. "Random Close Packing is least random in three dimensions." 2023, under review (preprint: arXiv:2212.09913)

## **Design Principles of Biomolecular Metamaterials**

**Jong Hyun Choi, Purdue University**

### **Program Scope**

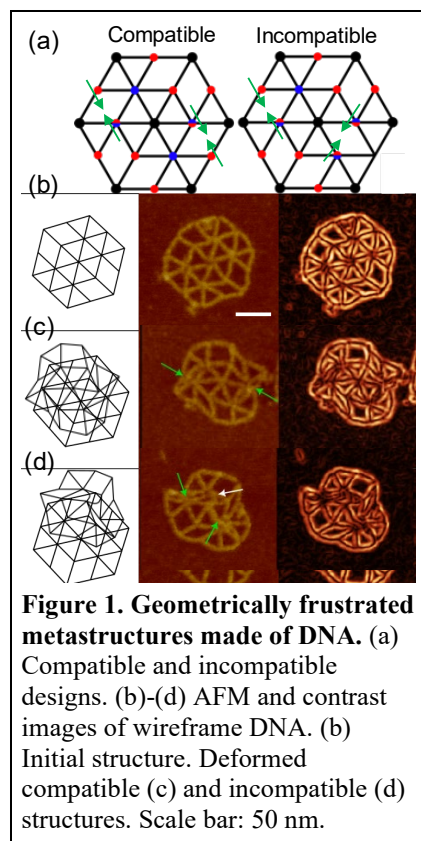
The goal of this program is to develop general principles for auxetic metastructures from DNA. Mechanical metamaterials show exotic structural properties and mechanical behaviors with negative Poisson's ratios, which may be exploited for energy absorption mechanisms and adaptative devices with enhanced toughness.<sup>1</sup> The fundamental idea of metamaterials is that their properties are determined by structure regardless of chemical composition.<sup>2</sup> This premise has yet to be tested at the molecular scale where chemistry may be critical. There is also a significant gap in lengthscale as nanoscale auxetics are difficult to realize due to the challenges in manufacturing.<sup>3</sup> DNA self-assembly is a programmable bottom-up approach that can ideally construct complex architectures at the macromolecular scale. In this research, we have used DNA origami to design and synthesize various two-dimensional (2D) auxetic metastructures and studied their mechanical properties and deformation behaviors. Our objectives include (1) demonstration of DNA auxetics and geometric frustration, (2) elucidation of structural mechanics and behaviors, and (3) establishment of design rules and novel mechanisms for deformable 2D metastructures. Our work also develops theoretical and computational basis for biomolecular auxetic nanomaterials.

### **Recent Progress**

#### **1. 2D auxetic nanomaterials and geometric frustration**

We have demonstrated several unique 2D architectures that exhibit auxetic behaviors, including re-entrant honeycomb, re-entrant triangle, rotating square, Hoberman flight ring, and geometrically frustrated metastructures. These may be classified into two types: periodic cellular and finite structures. In our approach, we simplified the designs such that a single wireframe DNA origami could represent the auxetic units and their behaviors. Edges are constructed with dsDNA bundles for structural integrity, while joints consist of ssDNA segments for deformability studied with AFM imaging and coarse-grained molecular dynamics (MD) simulations on the open-source oxDNA platform. In the experiment, we introduced 'jack' edges for structural transformation. Like a car jack, the jack length can be modulated by strand displacement (termed chemical deformation), which defines the overall conformation (e.g., compressed or extended states). This allowed us to demonstrate precise control in the shape-change process. In MD computation, direct mechanical deformations were performed without the jacks (termed mechanical deformation). The structures show negative Poisson's ratios ( $\nu$ ), as designed. For example, the DNA flight ring deploys between -1.67 and -2.0, while the centrosymmetric rotating square exhibits a constant value of  $\nu = -1$ .

We also have introduced the first geometric frustration at the nanoscale using DNA metastructures. Geometric frustration is a concept that the geometric arrangement of atoms in a crystal lattice leads to conflicting inter-atomic forces and related interesting physics. This concept was originally



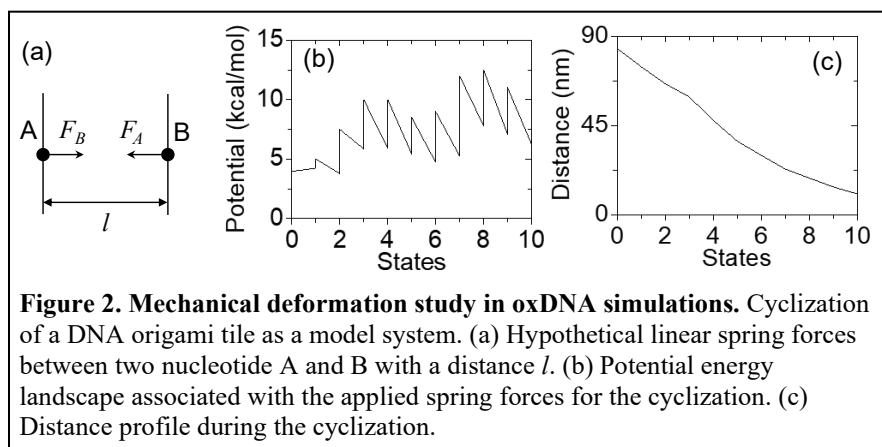
developed in magnetism, where nearest-neighboring spins may clash (thus become ‘frustrated’) due to the geometrical constraint. We drew an analogy between magnetic and mechanical frustrations. As shown in Fig. 1, compatible and incompatible structures were designed and subjected to identical external loads. They are complementary to each other, and the only difference between them is one of the loading spots (green arrows in Fig. 1a).

We have discovered that the compatible structure can accommodate external loads, whereas the incompatible one cannot due to the geometric constraint (Fig. 1b-d). As a result, the incompatible structure will experience buckling in one of the edges (indicated by a white arrow). MD simulations support this, showing that one of the edges in the incompatible design is irreversibly bent. In contrast, the compatible design may experience some fluctuations but can recover, avoiding any significant bending. Our DNA metastructures may serve as a novel platform to study traditionally difficult problems in geometric frustration in both mechanics and magnetism.

## 2. Mechanical behaviors and structural properties

We have studied the structural properties of DNA origami and investigated mechanical energy needed to deform the nanostructures. Figure 2 presents a simple case, where we used a single-layer DNA origami tile as a model system and studied its cyclization process. We applied linear spring forces in a series of deformation by mutual traps in oxDNA computation, and calculated the related energies based on the Hooke’s law by considering the conformation in each state. The potential energies are needed to overcome the initial conformation and induce cyclization. Figure 2a shows our scheme where a hypothetical spring connects nucleotide A and B with a force constant  $k$  and distance  $l$ . The potential can be modulated by varying  $k$  and  $l$  in each calculation from one state to the next. The conformation with minimum energy was chosen as the next state. Figure 2b presents the landscape of calculated energy via multiple steps, indicating the external work to complete a cyclization. The distance between two opposite ends of the tile (i.e., the origami conformation) can also be determined as shown in Fig. 2c. This work advances our understanding of mechanical behaviors of DNA assemblies and should be useful for designing energy driven processes.

Our studies strongly suggest that mechanical properties of a DNA architecture are correlated



with those of its component molecules. However, the structure shows complex behaviors which may not be predicted by components alone and the architectural design must be considered as well. Thus, one shall consider both structure and material for designing nanoscale auxetics. This work addresses the premise of the metamaterials as proposed and provides critical insights into the structure-property relationship.

### **3. Transformation mechanisms and design guidelines**

Architected metamaterials exhibit unique deformation behaviors in response to external loads. Traditionally, DNA mechanics have been studied with optical and magnetic tweezers. Given the complexity of 2D DNA metastructures, however, it is difficult to apply mechanical loading directly using these methods. In our experiment, we devised chemical loading methods by changing the length of the jack edges (thereby exerting forces at desired locations). Intercalation with chemical adducts may also be used as shown previously, however the effects will be global rather than local. In parallel, our MD simulations investigated direct mechanical loading, elucidating Young's modulus, yield strength, and related energetics. We found that the forces for mechanical deformations are approximately half of the chemical forces (for example,  $\sim 21$  and  $55$  pN per jack edge in the re-entrant triangle; about  $35$  and  $72$  pN per jack in the rotating square). This may be understood as mechanical forces are the minimum for reconfiguration, while chemical methods are the upper limit of excess forces.

This research has generated a set of design requirements for 2D DNA origami architectures. For example, an edge in wireframe DNA must have a thickness of at least 10% of its length to avoid significant curvature under considerable loading. A joint made of ssDNA should have some level of tension (not too tight and not too loose) to maintain the structural integrity with sufficient deformability. Our recommendation is that the joint stretch level defined as displacement over distance must be between 55 and 70%. In general, deformable structures may be classified into three groups. First, those with small deformations ( $<10\%$  relative changes) may be designed like static structures. Second, those with a greater extent of deformation (10-50% relative changes) must follow the design guidelines this work presented. Otherwise, the structure will not be able to accommodate the loading and structural transformation may not work as designed. For significant deformations ( $>50\%$ ), the properties of DNA components will be changed, thus full-fledged simulations must be accompanied with design and synthesis. Our work also provides insights on how to use different models for the structures (e.g., finite element vs coarse-grained models). Overall, this research laid the foundation for DNA-based metamaterials.

#### **Future Plans**

We will continue our efforts integrating DNA self-assembly with mechanics toward auxetic DNA metamaterials. Thus far, our work has focused on 2D architectures, and we plan to switch to 3D metastructures. Generally, 3D structures will be more complex than 2D designs since more components are involved. Given the increased structural complexity, we will revisit the design guidelines for 2D geometries and examine their applicability in 3D auxetic designs. Combined experiment and MD computation will help update the design strategies. In parallel, we plan to examine if elastic energy can be stored locally and released quickly for structural transformation. The new mechanisms will be explored for developing rapidly reconfiguring devices utilizing the stored mechanical energy.

## References

1. K. E. Evans, A. Alderson, *Advanced Materials* **12**, 617-628 (2000).
2. K. Bertoldi, V. Vitelli, J. Christensen, M. van Hecke, *Nature Reviews Materials* **2**, 17066 (2017).
3. J.H. Lee, J.P. Singer, E.L. Thomas, *Advanced Materials* **24**, 4782-4810 (2012).

## Publications (BES supported, last two years)

1. A.S. Madhvacharyula, R. Li, A.A. Swett, and J.H. Choi, *Geometrically Frustrated Metastructures from DNA*. In preparation
2. Y. Du, R. Li, A.S. Madhvacharyula, and J.H. Choi, Programmable and Reversible Reconfiguration of Auxetic Nanostructures by Sliding DNA. In preparation
3. A. Shrivastava, Y. Du, H.K. Adepu, R. Li, A.S. Madhvacharyula, A.A. Swett, and J.H. Choi, *Motility of Synthetic Cells from Engineered Lipids*, *ACS Synthetic Biology* (2023). Under review
4. R. Li, A.S. Madhvacharyula, Y. Du, H.K. Adepu, and J.H. Choi, *Mechanics of Dynamic and Deformable DNA Nanostructures*, *Chemical Science* (2023). DOI:10.1039/D3SC01793A
5. R. Li, M. Zheng, A.S. Madhvacharyula, Y. Du, C. Mao, and J.H. Choi, *Mechanical Deformation Behaviors and Structural Properties of Ligated DNA Crystals*, *Biophysical Journal* **121**, 4078-4090 (2022).
6. R. Li, H. Chen, and J.H. Choi, *Auxetic Two-Dimensional Nanostructures from DNA*, *Angewandte Chemie International Edition* **60**, 7165-7173 (2021).
7. R. Li, H. Chen, and J.H. Choi, Topological Assembly of a Deployable Hoberman Flight Ring from DNA, *Small* **17**, 2007069 (2021).
8. R. Li, H. Chen, H. Lee, and J.H. Choi, *Elucidating the Mechanical Energy for Cyclization of a DNA Origami Tile*, *Applied Sciences* **11**, 2357 (2021).
9. H. Qiu, F. Li, Y. Du, R. Li, J.Y. Hyun, S.Y. Lee, and J.H. Choi, *Programmable Aggregation of Artificial Cells with DNA Signals*, *ACS Synthetic Biology* **10**, 1268-1276 (2021).
10. R. Li, H. Chen, H. Lee, and J.H. Choi, Conformational Control of DNA Origami by DNA Oligomers, Intercalators and UV Light, *Methods and Protocols* **4**, 38 (2021).

# Porin-Inspired Ionomers with sub-nm Gated Ion Channels for High Ion Conductivity and Selectivity

Shudipto Konika Dishari, University of Nebraska-Lincoln

**Keywords:** ion conduction, ionomers, porin, biological ion channel, gating, permselectivity

## Program Scope

Biological channels or porins play a key role in various critical functions of natural living systems. These channels act like molecular filters, and are responsible for controlled transport of water, ions, and hydrophilic molecules across living cells as they self-assemble within biological membranes. Water and ion transport are also critical for clean energy technologies, like fuel cells, electrolyzers, flow batteries, as well as recycling and separation-related technologies. Bringing the capabilities of natural living systems within synthetic ion-conducting polymeric materials (ionomers) can thus revolutionize the design of next-generation energy conversion and storage devices. Taking inspiration from nature, this CAREER project incorporates hollow macrocyclic cavity-forming repeat units into ionomer chains. By hierarchical synthesis of an array of model, gated, calix[4]arene-based monomers and oligomers, and inducing predictive, but structure-driven ionomer alignment and self-assembly, this project aims to unravel new ways to gain unprecedented control over ionic conductivity and selective ion transport. The extremely narrow macrocycles ( $< 1$  nm) we utilized can stack up and create one-dimensional water channels. In addition to the traditional proton-hopping pathways (across the terminal sulfonic acids groups, external to cavities), the macrocycle-containing ionomers thus open up new possibilities of proton transport by leveraging the unique arrangement of one-dimensional water wire across narrow cavities. Not only that, but these cavity-forming ionomers can also act like voltage-responsive gates or ionic diodes and control the direction and selectivity of ion transport.

## Recent Progress

Sub- $\mu\text{m}$  thick ionomer layers often suffer from poor ionic conductivity at substrate/catalyst interface. The weak proton conductivity makes the electrochemical reaction at the cathode of proton exchange membrane fuel cells sluggish. At the early stage of this project, we proved that in sub- $\mu\text{m}$ -thick films, the macrocycle-containing oligomeric ionomers we designed can beat the performance of the current state-of-the-art ionomer, Nafion, used for proton transport in electrochemical devices.<sup>1</sup>

In the last 2 years, we designed a series of calix[4]arene-based ion-conducting monomers and oligomers to better understand how macrocyclic cavity-forming units play role in and elevate ion transport. Ion transport is often mediated by water. We have been able to develop a novel nuclear magnetic resonance (NMR)-based strategy to line up a proof showing that macrocycle-containing ionomers make water diffusion faster.<sup>2</sup> Using diffusion-ordered NMR (DOSY-NMR), we measured the water self-diffusion coefficient ( $D_{\text{self, water}}$ ) within  $\sim 300$  nm thick, hydrated films of Nafion and a representative macrocycle-containing ionomer (PS-calix).  $D_{\text{self, water}}$  of the Nafion film at 100% RH was  $2.5 \times 10^{-10}$  m<sup>2</sup>/s; while the  $D_{\text{self, water}}$  increased up to  $7.1 \times 10^{-9}$  m<sup>2</sup>/s for the styrene-calix[4]arene-based ionomer (PS-calix) (Figure 1a). These macrocycle-containing ionomers also showed ionic conductivity ( $\sigma$ ) more than an order of magnitude higher than Nafion in sub-micron thick films.<sup>2</sup> Simultaneous observation of very high  $D_{\text{self, water}}$  (water transport), and

$\sigma$  (proton conductivity) of PS-calix suggested that the macrocycle-containing ionomers likely have the capabilities to create unique and faster water and ion-transport pathways,<sup>2</sup> in agreement with our prior work.<sup>1</sup> Not only that, in some cases, the values of  $D_{\text{self, water}}$  in PS-calix films were even higher than what is reported for bulk water ( $2.3 \times 10^{-9} \text{ m}^2/\text{s}$ ). Using carbon nanotubes (CNTs), Noy<sup>3</sup> showed that “faster-than-bulk” water transport behavior can be achieved when the diameter of CNT is narrowed down to sub-nm (shown in Figure 1a for comparison). The sub-nm-sized constrictions have also been found beneficial to make water move very fast through a range of natural (Gramicidin A (4 Å)) and artificial channels as angstrom-scale conduits can compel water to align into a single file (1D water wire) and enable their frictionless “slip” flow. Noy also showed that the sub-nm-sized CNTs conduct protons faster than their larger-than-1-nm counterparts.<sup>4</sup> From these works, they inferred that sub-nm-sized hydrophobic channels may enhance the proton transport rate due to the 1D water wire.<sup>4</sup> Our macrocycle-based ionomers also have similar features (sub-nm sized cavities made of bridged aromatic rings, creating a hydrophobic interior and confining water into 1D sub-nanospace). While it is difficult to experimentally quantify the relative contribution of macrocycles and  $-\text{SO}_3\text{H}$ -water-based conventional proton hopping pathways

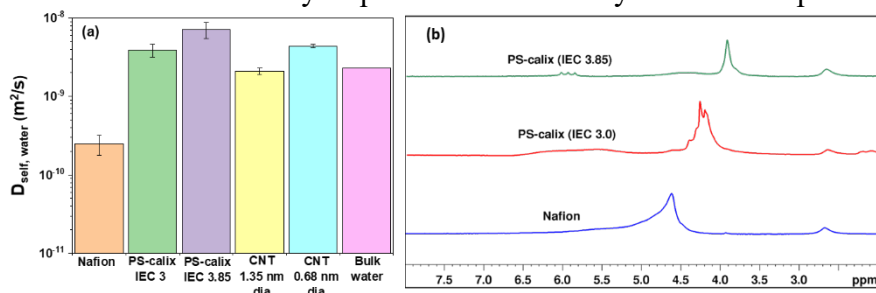


**Figure 1.** (a) Water self-diffusion coefficients ( $D_{\text{self, H}_2\text{O}}$ ) of Nafion, PS-calix (IEC 3, 3.85), CNTs with  $>1$  nm and sub-nm diameters, and bulk water. Nafion and PS-calix data were obtained for  $\sim 300$  nm-thick films at 100% RH using DOSY-NMR for this work. CNT and bulk water data were taken from literature for comparison.<sup>3,5</sup> (b)  $^1\text{H}$  NMR of  $\sim 300$  nm thick Nafion and PS-calix (IEC 3, 3.85) films.

(exterior to macrocyclic units) on the overall  $\sigma$ , we showed that a non-macrocycle-containing analog of a macrocycle-containing ionomer could have several orders of magnitude weaker proton conductivity.<sup>1</sup> We also showed the possible presence of H-bonded 1D water wire across macrocyclic calix[4]arene cavities in another ionomer *via* molecular dynamics simulations.<sup>1</sup> Furthermore, the water peak in  $^1\text{H}$  NMR shifted to lower ppm and became narrower for PS-calix as compared to Nafion in thin films at 100% RH (Figure 1b). This suggested improved mobility of protons and relatively looser H-bonding of water molecules in calix[4]arene-containing ionomers. The experimental evidence thus suggested that sub-nm-sized macrocycles, a missing feature in Nafion, may have played an important role in making both water and proton transport faster in styrene-calix[4]arene-based ionomers films.

Some of the oligomeric ionomers (e.g., calix-2, Figure 2a) we designed form ellipsoidal aggregates, while the state-of-the-art ionomer Nafion does not form such features. Therefore, if Nafion-calix-2 composite films are made, the ellipsoidal features made of macrocyclic ionomers can be easily identified or located using fluorescence imaging when the films are stained with photoacid dye (HPTS), sensitive to local proton transport environment. Using confocal microscopy, we were able to locate and measure proton conduction properties across Nafion-rich and calix-2-rich regions within a film (Figure 2b). We saw that the proton conduction was better at places within a film where macrocycles were located (bright reddish orange fluorescence from ellipsoidal, calix-2-rich features, Figure 2b, inset).<sup>1</sup> The proton conduction profile along z-direction (Figure 2b) also showed that the deprotonation ratio ( $I_d/I_p$ ) at a point over the ellipsoidal feature (calix-2 rich) was ~3 times higher than that at a point outside of the ellipsoidal feature (i.e., Nafion-rich region). This indicated that the macrocyclic units are playing a role in enhancing proton conductivity of calix-2-containing films. If such macrocycle-based ionomer design approaches are adopted, interfacial ion transport limitations can be effectively addressed and alleviated.

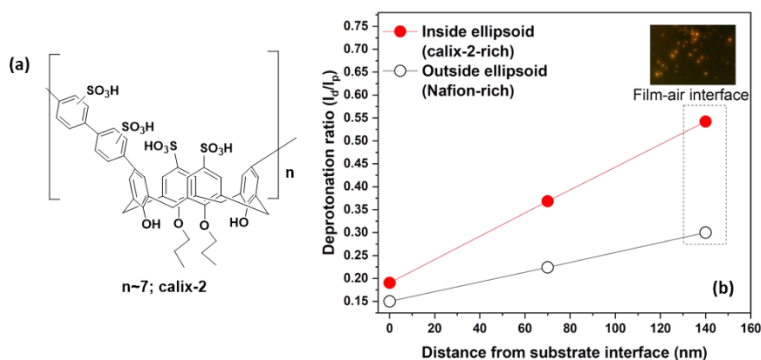


**Figure 2.** (a) Chemical structure of calix-2, an ionomeric oligomer. (b) Through-plane proton conduction ( $I_d/I_p$ ) profile of a Nafion-calix-2 composite film (~140 nm thick) at 80%RH. An increase in  $I_d/I_p$  at a certain location indicates an increase in proton transport in that location or depth within the ionomer film. The inset shows the CLSM image of the film at the film-air interface (scale bar 1  $\mu\text{m}$ ). The  $I_d/I_p$  values at this film-air interface are shown within the dotted black box.

To achieve directionality in ion transport, we first mixed the macrocyclic ionomers (calix-2) having asymmetric charge distribution with ionomers lacking that functionality (Nafion) (Figure 3, left). In Nafion-calix-2 mixed membranes, the macrocycles had cup-like stacking (i.e., lower rim of one macrocycle was facing the upper rim of the next one) within ellipsoidal features. This cup-like stacks in an aggregate created continued pathways with asymmetric charge distribution which was congenial for voltage gating and inhibiting local ion accumulation. However, these ellipsoidal features were randomly

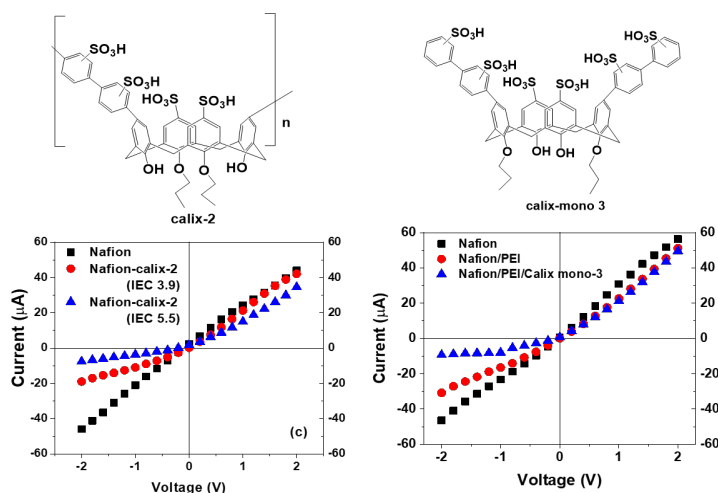


**Figure 3.** I-V curves of pure Nafion and Nafion-calix-2 (IECs 3.9, 5.8, 1: 0.05 w/w) mixed composite membranes (bottom, left). I-V curves of pure Nafion and Nafion membrane coated with PEI/calix mono-3 on one side of the membrane (bottom, right). The I-V data were recorded in 0.1 M KCl in DI water.

distributed within Nafion matrix in mixed membrane. This suggested that in the mixed membrane, the observed voltage gating or preferential ionic current was a collective and resultant effect of local ionic movement across different calix-2 aggregates oriented in different directions within the membrane. To achieve more consistent orientation of calix units and charged groups, we adopted a LBL self-assembly approach. A cationic polyelectrolyte layer (polyethylene imine (PEI)) layer in between sulfonated Nafion and sulfonated calix-monomer (calix mono-3) allowed the order and achieved ionic rectification (Figure 3, right). This LBL-self-assembly strategy thus helped us to reliably assess the effect of asymmetric charge distribution of more uniformly oriented macrocycles on voltage gating.

## Future Plans

Based on the work done so far, creating asymmetry in charge distribution across macrocycles, comparison of cavity-forming ionomers to non-cavity forming ones, and leveraging their self-assembly appear to be great tools to unravel the contribution of macrocycles in ion transport. These aspects will be explored more through designing innovative experiments in coming years.

## References

1. Chatterjee, S.; Zamani, E.; Farzin, S.; Obewhere, O. A.; Johnson, T.; Dishari, S. K. Molecular-Level Control Over Ionic Conduction and Ionic Current Direction by Designing Macrocycle-Based Ionomers. *JACS Au* **2022**, *2*, 1144–1159. <https://doi.org/10.1021/jacsau.2c00143>.
2. Chatterjee, S.; Obewhere, O. A.; Zamani, E.; Keloth, R.; Farzin, S.; Morton, M. D.; Sarella, A.; Dishari, S. K. Advancing Ionomer Design to Boost Interfacial and Thin-Film Proton Conductivity via a Styrene-Calix[4]Arene-Based Ionomers. *Cell Rep. Phys. Sci.* **2023**, *4*, 1–20.
3. Tunuguntla, R. H.; Zhang, Y.; Henley, R. Y.; Yao, Y. C.; Pham, T. A.; Wanunu, M.; Noy, A. Enhanced Water Permeability and Tunable Ion Selectivity in Subnanometer Carbon Nanotube Porins. *Science* **2017**, *359*, 792–796. <https://doi.org/10.1126/science.aan2438>.
4. Tunuguntla, R. H.; Allen, F. I.; Kim, K.; Belliveau, A.; Noy, A. Ultrafast Proton Transport in Sub-1-Nm Diameter Carbon Nanotube Porins. *Nat. Nanotech.* **2016**, *11*, 639–644. <https://doi.org/10.1038/nnano.2016.43>.
5. Holz, M.; Heil, S. R.; Sacco, A. Temperature-Dependent Self-Diffusion Coefficients of Water and Six Selected Molecular Liquids for Calibration in Accurate 1H NMR PFG Measurements. *Phys. Chem. Chem. Phys.* **2000**, *2*, 4740–4742. <https://doi.org/10.1039/b005319h>.

## Publications Supported by BES (2021-2023)

1. Dishari, S. K. Ionomers with Macrocyclic Moieties for Ion conductivity and Permselectivity (2021) (Patent, PCT/US21/70432).
2. Chatterjee, S.; Zamani, E.; Farzin, S.; Evazzade, I.; Obewhere, O. A.; Johnson, T. J.; Alexandrov, V.; Dishari, S. K. *Molecular-Level Control over Ionic Conduction and Ionic Current Direction by Designing Macrocycle-based Ionomers*. *JACS Au* **2**, 1144-1159 (2022).
3. Chatterjee, S.; Obewhere, O. A.; Zamani, E.; Keloth, R.; Farzin, S.; Morton, M. D.; Sarella, A.; Dishari, S. K. *Advancing Ionomer Design to Boost Interfacial and Thin-Film Proton Conductivity via a Styrene-Calix[4]arene-based Ionomers*. *Cell Rep. Phys. Sci.* **4**, 1-20 (2023).
4. Acurio Cerda, K.; Kathol, M.; Purohit, G.; Zamani, E.; Morton, M. D.; Khalimonchuk, O.; Saha, R.; Dishari, S. K. *Cationic Lignin as an Efficient and Biorenewable Antimicrobial Material*. *ACS Sustainable Chem. Eng.* (2023).

5. Obewhere, O.A.; Acurio Cerda, K.; Dishari, S. K. *Creating Order in Macrocycles for Precise Ion Transport Pathways*, to be submitted.
6. Obewhere, O.A.; Keloth, R.; Dishari, S. K. *Role of Cavity-Forming Units in Systematic Ion Transport*, to be submitted.

## Active interfaces driven by microtubule-based active matter

Zvonimir Dogic, Christina Marchetti – University of California at Santa Barbara

**Keywords:** active matter, interfaces, liquid-liquid phase separation, wetting transitions.

### Research Scope

Controlling interfacial structure and dynamics is key to creating diverse functional soft materials, ranging from lipid vesicles and lamellar phases to phase-separated systems and emulsions. Traditionally, interfacial control is accomplished through surface-modifying agents, such as surfactants and block copolymers. The goal of this project is to explore an entirely different non-equilibrium mechanism for

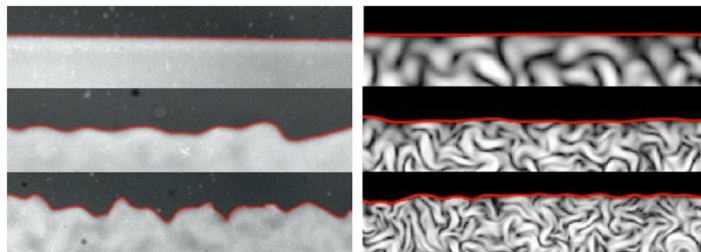


**Fig. 1.** (left) PEG-Dextran active interface with increasing kinesin concentration. (right) Conformation of interface obtained from a numerical model.

controlling and shaping soft interfaces. By merging a phase-separating mixture of a microtubule-based active isotropic fluid and a passive fluid, we aim to explore how activity provides a unique new handle for interfacial control. To gain a quantitative understanding of active interfaces we are pursuing several research aims. First, we are studying a model system of 1D active interfaces and associated liquid-liquid phase separation in quasi-2D geometries. We also generalized these studies to 2D interfaces that separate 3D bulk phases. We study the behavior of active droplets and their interaction with a planar hard wall, with a particular focus on using active stresses to control droplet shape and wetting properties. We also modify the coupling between the active fluid and the interface by directly linking the stress-generating elements of the active fluid to the interface-bound components. Our goals are unified by several synergistic features. First, they all explore the common theme of how bulk active fluids couple to soft interfaces to generate new phenomena and new life-like materials. Second, they rely on the unique properties of microtubule-based model experimental systems including the ability to assemble millimeter-scale samples and sustain their non-equilibrium dynamics for tens of hours. Third, all the aims merge experimental work with numerical simulations and theoretical modeling which are pursued jointly by the two investigators. We combine the unique features of our model systems with state-of-the-art microscopy techniques to visualize conformations of centimeter-sized interfaces, as well as the instantaneous configuration of the underlying active fluid with single-filament resolution. Combining such multiscale experimental data with theoretical modeling has the potential to decisively advance our understanding of how to shape and control soft interfaces through activity.

### Recent Progress

In a significant recently published accomplishment, we combined experiments theory and computer simulations to describe a novel system that reveals several unique and unexpected features of liquid-liquid phase separation (LLPS) the associated and active interfaces. We started with a phase-separated mixture of dextran and poly(ethylene glycol) (PEG) confined to a quasi-2D geometry. The active components including microtubules and kinesin partition into one of the two phases, creating an active LLPS with one active and one passive phase. Matching the

magnitude of the fluid-generated active stresses to interfacial energies generated a rich and till now entirely unexplored phenomenology that involves a close interplay between surface deformations and dynamics and mechanics of the underlying bulk fluid. We uncovered four universal features of out-of-equilibrium active flows on soft interfaces. First, active stresses drove giant interfacial fluctuations that were visible to the naked eye (Fig. 1). Forming an equilibrium interface with comparable roughness would require  $\sim 10^{11}$  K temperature. Second, the interfacial fluctuation energy was mainly carried by activity-dependent non-inertial propagating waves that arise from the coupling between surface deformations and nematic alignment of the underlying fluid. This is in contrast to conventional liquid interfaces, where propagating capillary waves require the presence of inertia. Third, interfacial motility could both enhance and arrest phase separation dynamics. In particular, for a well-defined regime of activities, we observed an emulsion-like dynamical steady state, consisting of finite-sized droplets which continuously exchange content by undergoing fusion and fission events (Fig. 2). For comparison, phase separation in conventional fluids proceeds in only one direction, yielding bulk phase-separated samples. Finally, active interfacial waves and stresses dramatically changed liquid spreading, leading to the formation of an active wetting layer that, reminiscent of superfluidity, can climb along a wall and thus work against gravity (Fig. 3).

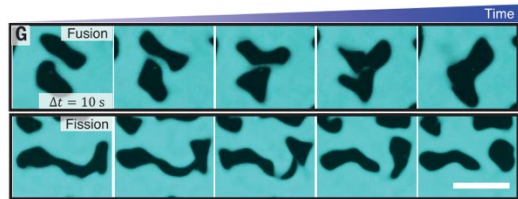


**Fig. 2.** Spontaneous fusion and fission event of active droplets.

Motivated by the above-described experiments we have developed a continuum hydrodynamics model of active interface and active LLPS. Numerical solutions of the hydrodynamic equations qualitatively reproduced all four experimental observations, demonstrating their universal features. Furthermore, the analytical model provided additional insight into a mechanism that generates traveling non-inertial waves of active interfaces and the active wetting transitions. In particular, the traveling waves are explained by time-delayed coupling between the height fluctuations of the active-passive interface and the surface-induced nematic alignment of adjacent microtubules. Similarly, the active wetting transition can be understood by the wall-induced nematic order of extensile microtubule bundles which in turn exert additional force onto the contact point raising it higher.

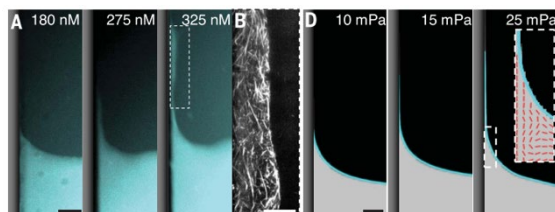


**Fig. 3.** Active wetting transitions in which the fluid climbs along a wall are observed both in experiments and numerical simulations of the hydrodynamics model.

Our initial work examined the behavior of active LLPS in quasi-2D confinements. Subsequently, we have explored the relevance of the above-described principles to 3D active and passive phases that are separated by a 2D interface. To characterize this system, we have developed an ultra-fast light-sheet imaging technique that allows for visualizing the entire 2D interface while also measuring the structure and dynamics of the underlying microtubule-based active fluid. These advances have demonstrated that the active interfacial fluctuations and active wetting transitions are even more pronounced for bulk 3D samples, which is primarily due to the lack of frictional interactions with the confining walls. We have quantified in extensive detail the properties of activity-induced deformations of the 2D interface. First, these efforts have revealed how the

magnitude of the fluctuations of the 2D interface increases over time, while in contrast the structure and the dynamics of the underlying active fluid remain time invariant. This suggests that active interfaces may behave like driven interfaces, perhaps described by a generalization of the well-known Kardar-Parisi-Zhang (KPZ) equation used for instance to model the growth of the edge of a bacterial colony. The KPZ equation relies on a single nonlinear term to describe driven interfacial growth. Further theoretical work will be needed to determine the additional nonlinearities induced by activity that are needed to account for the observed growth of interfacial fluctuations. Second, we also studied how at high activities the active interface starts to disintegrate and one observes invagination events where entire passive droplets are enveloped by the active phase, thus producing a heterogeneous perforated material. Finally, we examined active wetting phenomena which are significantly more dynamic in 3D. In particular, one observes pulsatile traveling wave-like densities climbing along the wall and then slowly falling back down under the influence of gravity. This is likely due to the coupling of the wall-induced wetting with traveling waves. Such experimental characterization demonstrates the need to develop a robust theoretical model of active wetting, an effort that is currently underway in our group.

To explore the influence of direct mechanical coupling between the active fluid and the droplets we developed an active-LLPS system that merges associating DNA nanostars with MT-based active fluids (Fig. 4). The DNA droplets were decorated with the kinesin motors which interacted with the background active fluid. Experiments demonstrated that such coupling changes the fundamental features of the liquid-liquid phase separation. Most importantly we found that activity lowered the temperature of the nanostar critical point while also narrowing the coexistence width of the liquid-liquid phase separation. Importantly, these experimental features could not be explained by the existing theoretical models of active LLPS. Motivated by the knowledge gap we have introduced a new theoretical model that tightly couples the active and passive coexisting phases and that is capable of describing the observed experimental phenomenology. This combined work that seamlessly merged experiments with theory revealed conditions under which active stresses act as an effective non-equilibrium thermodynamic parameter that controls the phase diagram.

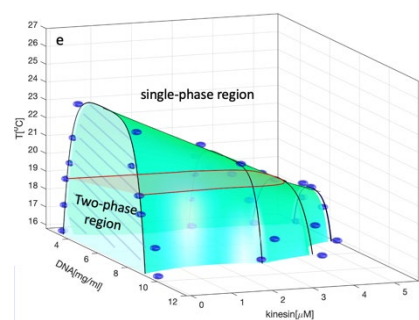


**Fig. 4.** A 3D diagram illustrating how activity suppresses phase separation of DNA nanostars.

In a complementary direction, we have also examined how 2D active nematics couple to rigid interfaces and the possibility of extracting useful work from such interactions (Fig. 5). In bulk solutions, such materials exhibit chaotic dynamics driven by continuous generation and annihilation of motile topological defects. We perturb this system by adding inclusions of different shapes. Our experiments reveal a complex interplay between force-generating active nematics and the motion of the embedded inclusion. On the one hand, the inclusion's boundaries transform the chaotic defect dynamics into quasiperiodic cycles consisting of the nucleation and annihilation of topological defects. In return, these defects exert an active force and torque on the inclusion powering their motion. For certain shapes the motion is random, but for other chiral shapes, we observe persistent long-term rotations with handedness that is determined by the inclusion chirality.

## Future Plans

The above-described advances motivated several future efforts that are being pursued by using a synergistic combination of experiments, theory, and numerical modeling.

Active interfaces provide a unique method to measure active stresses that are generated by the active fluid. Active stresses are the defining feature of active fluids, yet their measurement has proven highly elusive. Using a bulk-phase separated macroscopic 2D interface we have simultaneously quantified the motion of bulk active fluid and the deformations of the interface. Throughout the experiments, the properties of the active fluid remain unchanged yet the interface continues to increase in deformation. Similarly, the importance of active wetting increases over time. These observations cannot be explained by the current widely-adopted theoretical models of active fluids, which points to an unexpected gap in our fundamental understanding. Motivated by these findings we are developing a new model of the active interfaces that can account for such features. Experimentally, one of the primary goals is to quantitatively measure the surface-induced alignment of microtubule bundles as this is essential for a more rigorous comparison to existing theories.

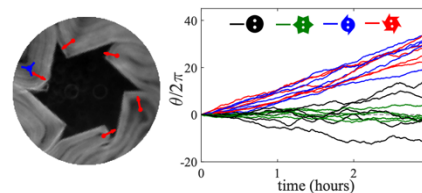


**Fig. 5.** (left) Inclusion controls local defect positions. (right) Rotational position of different defect shapes.

## Publications from DOE work:

1. A. M. Tayar, F. Caballero, T. Anderberg, O. A. Saleh, M. C. Marchetti, Z. Dogic, *Controlling liquid-liquid phase behavior with an active fluid*, Nature Materials, in press (2023)
2. S. Ray, J. Zhang, and Z. Dogic, Rectified Rotational Dynamics of Mobile Inclusions in Two-Dimensional Active Nematics, Physical Review Letters **130**, 238301 (2023).
3. M. Serra, L. Lemma, L. Giomi, Z. Dogic, L. Mahadevan, *Defect-mediated dynamics of coherent structures in active nematics*, Nature Physics (2023)
4. R. Adkins, I. Kolvin, Z. You, S. Witthaus, M. C. Marchetti, Z. Dogic, *Dynamics of active liquid interfaces*, Science **377**, 768 (2022).
5. P. Chandrakar, J. Berezney, B. Lemma, B. Hishamunda, A. Berry, K. Wu, R. Subramanian, J. Chung, D. Needleman, J. Gelles, Z. Dogic, *Engineering stability, longevity, and miscibility of microtubule-based active fluids*, Soft Matter **18**, 1825 (2022).

## Reactive, Functional Droplets in Bio-inspired Materials and Smart Interfaces

Todd Emrick, Polymer Science & Engineering Department, University of Massachusetts,  
Amherst, MA 01003 tsemrick@mail.pse.umass.edu

**Keywords:** Smart droplet, biomolecular materials, fluid interface, functional zwitterion, dendritic cell

### Research Scope

The scope of our project lies at the intersection of macromolecular synthesis and bio-inspired processes, with the overarching objective of producing smart, functional structures, droplets, and interfaces. This work builds upon biological inspiration spanning across fundamental recognition processes of living cells, biomacromolecular structures, and systems that work in conjunction with the immune system, *i.e.*, cells that identify disease and infection and in turn impart protective and healing measures via recognition and signaling. These and related biological processes, such as bone-absorption and secretion, and the structure and function of dendritic cells, inspire our preparation of new materials tailored to reflect these concepts in advanced materials designs.<sup>1</sup> The sheer biological complexity of such processes inspires us to seek *simpler synthetic tools* that may be implemented within non-biological environments. Making strides to achieve such objectives requires building new knowledge of the key interfacial interactions associated with synthetic materials and the principles of encapsulation that direct structures (*e.g.*, polymers, colloids, and droplets) to desired locations within materials systems. In essence, the effective translation of such fundamental biological principles to materials systems is vital for advancing the energy efficiency and versatility of modern materials (*i.e.*, in coatings, self-healing systems, and the like). Notably, *critically important challenges stem from experimentally realizing synthetic constructs that mimic complex biological processes and which are readily accessible and scalable*. Overall, as described below, the scope of this project centers on the synthesis of designer functional materials and complex, multi-length scale structures; autonomous, bio-inspired materials that promote energy efficiency; and new materials with precise localization and reactivity at interfaces.

### Recent Progress

Our recent progress has resulted from focus on fundamental studies of polymeric and mesoscale structures confined to fluid-fluid and solid-fluid interfaces. For example, building from our original experiments on droplet-based materials repair (*i.e.*, “repair & go”),<sup>2</sup> we created new droplet architectures with extending appendages—in the form of mesoscale polymer-based arms—that impart extensive reach to droplets and as such open a new opportunity to design structures that resemble the morphological and interactive features of dendritic cells. In another example, our syntheses of novel polymer zwitterions deepened the knowledge base of zwitterionic chemistry, as inspired by key structural components of cellular and intracellular compartments. These syntheses afford zwitterionic moieties with new properties and functional capabilities that arise when advances in synthetic chemistry are merged with biological lessons of Nature.

*Mesoscale polymer surfactants and designer droplets.* Stabilization of fluid droplets, as oil-in-water or water-in-oil emulsions, is typically conducted using molecular surfactants or small particulates that localize at oil-water interfaces. Our new design, inspired by the multi-armed

morphologies of dendritic cells, uses photolithographic methods to prepare to ribbon-like objects, which, in turn, adsorb to fluid interfaces where they extend as appendages from the droplet surface (Figure 1).<sup>3</sup> These mesoscale polymer surfactants (MPSs) were prepared from thin polymer films containing reactive and functional moieties which contain 1) coumarin for (reversible) photocrosslinking; 2) triphenylsulfonium as a photoacid generator (PAG); and 3) *tert*-butyl ester

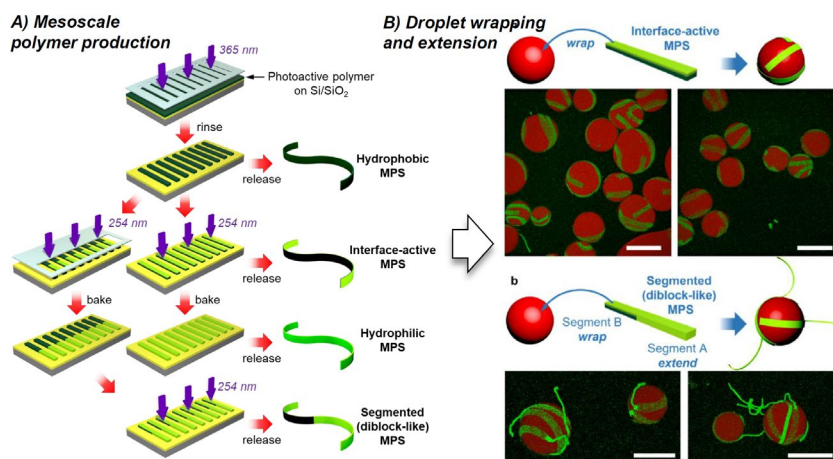


**Figure 1.** A) Photolithographic process designed to convert copolymer films to mesoscale polymer surfactants (MPSs), including hydrophobic, hydrophilic, interface-active, or segmented (diblock-like) structures.; B) Illustrations and confocal fluorescence microscopy images showing droplets that are wrapped by interface-active and segmented MPS structures. Scale bars = 500  $\mu$ m.

pendent groups to enable triggered hydrophobic-to-hydrophilic switching. The photolithographic techniques we employ represent a new, scalable approach to robust, filamentous structures of a variety of configurations, from straight filaments to helices. These structures are then utilized as mesoscale surfactants that adhere to the fluid interfaces of emulsion droplets, affording a kind of ‘dendritic droplet’ design in which the MPS wraps around the circumference of the droplet and extends from the interface as appendages. Droplets of this type may be considered for a variety of uses, such as capture or exchange of reagents from solution, or retraction and release, or potentially to drive droplet motion.

*Droplet stability and mesoscale chemistry.* To enhance the stability of these wrapped droplets for further manipulation, small molecule surfactants were added during the emulsification step. Using either ionic (SDS) or nonionic (Triton X-100) surfactant, the resultant droplets remained stable without coalescence for at least one week. Interestingly, when using high concentrations of non-ionic surfactants, fluorescence microscopy revealed that wrapping was prohibited, as oil-water interfacial coverage by the small molecule competes favorably over the MPSs for the fluid interface. Assessing the stability of MPS-wrapped droplets in fluids, and under flow, was performed in a chamber containing glass top and bottom covers that allow fluorescence visualization, with connection to a peristaltic pump to drive flow. Preliminary results show that the arms adhered capably to the droplets at flow rates at least up to 24 mL/min flow rate in this device. We also examined the potential of chemical versatility to augment MPS structure and bring new capabilities to wrapped droplets in “diblock-like” or segmented architectures. For example, building from *tert*-butyl ester/carboxylic acid and boc/amine chemistry, we successfully fabricated MPS diblock-like structures with hydrophilic segments rich in carboxylate, amine, or carboxybetaine, all of which successfully wrapped oil-in-water droplets with their hydrophobic segments, leaving the hydrophilic portion extended into the aqueous phase. This versatile chemistry is useful for building a toolbox of reactive and pH-responsive droplet arms that will give access to materials strategies in capture, repair, and reconfiguration.

*Building functional biomolecular materials with new zwitterion syntheses.* Our efforts in reactive and functional zwitterions produced new zwitterionic compositions, with a particularly compelling example based on inversion of the classic phosphorylcholine (PC) moiety to yield choline phosphate (CP) zwitterions with covalently attached functionality. In a recent example, illustrated in **Figure 2**, merging the CP zwitterion with fluorinated groups forces these strongly disparate chemistries (hydrophilic and fluorophilic) into close proximity within the zwitterionic framework. When performing this chemistry on a methacrylate framework, the resultant fluorinated choline phosphate (FCP) monomers were amenable to controlled free radical polymerization to produce a series

of novel FCP polymers, with polymerization chemistry that proved amenable to both solution and surface-grafting techniques.<sup>4</sup> Interestingly, grafting of FCP polymers from appropriately functionalized Au substrates produced non-fouling surfaces with wetting properties indicative of a dynamic surface structure. Testing FCP-functionalized surfaces with contact angle probe fluids revealed wetting properties intermediate between those of purely zwitterionic (hydrophilic) and fluorinated (hydrophobic) surfaces. Notably, the FCP surfaces were

hydrophobic in air, fluorophobic in water, and exhibited remarkably high contact angle hysteresis values. This dynamic wetting behavior suggests a reorganization of fluorinated and zwitterionic units in response to the contacting fluidic environment, as illustrated in **Figure 2**. Remarkably, FCP-grafted surfaces afforded comparable or better protein resistance against serum albumin (BSA) and lysozyme relative to PC- and fluorocarbon-modified surfaces, suggesting significant potential of this class of polymers for advancing the science of surface modification, wetting control, and self-cleaning substrates with tailored surface energies.

*Cysteine-like zwitterions: synthesis and assembly opportunities.* Our ongoing work on functional polymer zwitterions with embedded thiols represents a unique fusion of bio-inspired structures and biochemical motifs. With components found abundantly in Nature (*i.e.*, zwitterions and thiols), their strategic combination produces materials that augment fluid interfaces with enzyme-like functionality. Our synthetic approach, illustrated in **Figure 3**, utilizes our original functional CP concept with ultimate integration of aromatic or aliphatic thiols into the zwitterionic subunit. The potential advantages of these thiols within the polymer structure are numerous, which we are pursuing through routes to reversible (*i.e.*, disulfide) and irreversible (*i.e.*, thiol-Michael) droplet assemblies, including droplet sheets and networks. For example, vinyl-sulfone modification of emulsion droplets stabilized by thiol-bearing polymer zwitterion surfactants will allow selective reactions between thiol- and vinyl sulfone-bearing emulsion droplet populations at biologically relevant pH values.

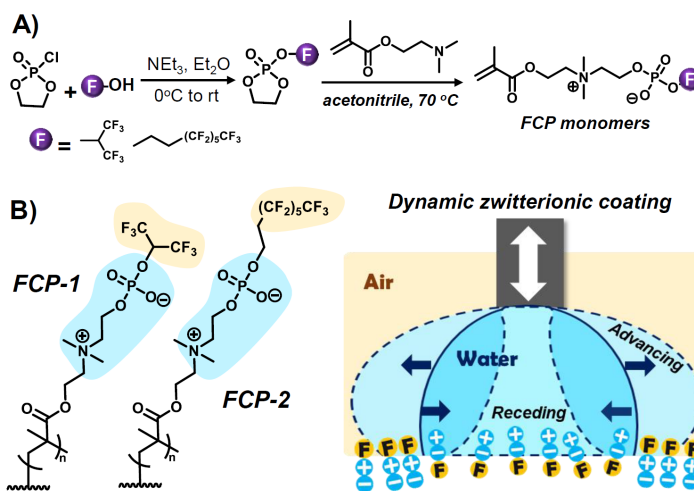


**Figure 2.** A) Synthesis of FCP monomers used in solution and surface-initiated polymerizations; B) illustration of dynamic FCP surface reorganization in response to a contacting fluid.

## Future plans

Going forward, we envisage rich opportunities to deepen understanding of biomolecular materials that mimic cell structure and functionality, and that propel the invention of new synthetic macromolecular materials. In essence, the concept of droplets with extended appendages offers routes to enticing targets central to ongoing and future objectives, including:

- *Targeted capture and release.* Carboxylate, amine, and/or zwitterion groups on droplet appendages offer particle and/or CO<sub>2(g)</sub> capture/absorption and expand the concepts of materials repair and remediation beyond what conventional surfactant-stabilized droplets may accomplish.
- *Building structures with droplets.* As we gain control over the functionality and stability of MPS-droplets, inter-droplet designs become feasible, wherein multiple droplets collect either for the purpose of triggered coalescence or building droplet-based structures and channels for transport.
- *Retractable arms.* Building responsive chemistry into MPS appendages opens routes to retractable and expandable arms on demand, including coiled and uncoiled morphologies, which would allow MPS arms to extend, capture, and retrieve objects to engulf into the encapsulated phase.
- *Arm digestion and release.* Building on our seminal nanoparticle pickup and drop-off experiments as an *in situ* method for materials repair,<sup>5</sup> inspired by theoretical findings of Balazs, droplet appendages may yield considerable advances in droplet reuse and repurposing in related particulate capture scenarios. Controllable dissolution (unzipping or uncrosslinking) of MPS segments in contact with droplet interfaces would allow digestion into the droplet, while the remaining MPS segment (containing captured material) is collected as the droplet becomes available for additional rounds of MPS wrapping, capture, and release.

## References

1. T. A. Patente, M. P. Pinho, A. A. Oliveira, G. C. M. Evangelista, P. C. Bergami-Santos, J. A. M. Barbuto, *Human Dendritic Cells: Their Heterogeneity and Clinical Application Potential in Cancer Immunotherapy*, *Front. Immunol.* **9**, 3176 (2019).
2. K. Kratz, A. Narasimhan, R. Tangirala, S. Moon, R. Revanur, S. Kundu, H. S. Kim, A. J. Crosby, T. P. Russell, T. Emrick, G. Kolmakov, A. C. Balazs, *Probing and Repairing Damaged Surfaces with Nanoparticle-containing Microcapsules*, *Nat. Nanotechnol.* **7**, 87 (2012).
3. Z. Yang, D. Snyder, J. N. Pagaduan, A. Waldman, A. J. Crosby, T. Emrick, *Mesoscale Polymer Surfactants: Photolithographic Production and Localization at Droplet Interfaces*, *J. Am. Chem. Soc.* **144**, 22059 (2022).
4. L. Zhou, Z. Yang, J. N. Pagaduan, T. Emrick, *Fluorinated Zwitterionic Polymers as Dynamic Surface Coatings*, *Polym. Chem.* **14**, 32 (2023).
5. A. Sathyan, Z. Yang, Y. Bai, H. Kim, A. J. Crosby, T. Emrick, *Simultaneous "Clean-and-Repair" of Surfaces Using Smart Droplets*, *Adv. Funct. Mater.* **29**, 1805219 (2019).

## Publications

1. Z. Yang, D. Snyder, J. N. Pagaduan, A. Waldman, A. J. Crosby, T. Emrick, Mesoscale Polymer Surfactants: Photolithographic Production and Localization at Droplet Interfaces, *J. Am. Chem. Soc.* 144, 22059 (2022).
2. L. Zhou, Z. Yang, J. N. Pagaduan, T. Emrick, Fluorinated Zwitterionic Polymers as Dynamic Surface Coatings, *Polym. Chem.* 14, 32 (2023).
3. Z. Yang, D. Snyder, A. Sathyan, A. C. Balazs, T. Emrick, *Smart Droplets Stabilized by Designer Surfactants: from Biomimicry to Active Motion to Materials Healing*, *Adv. Funct. Mater.* submitted (2023).
4. D. Snyder, T. Emrick, *Thiol-functionalized Polymer Zwitterions: Synthesis and Integration into Biomacromolecular Materials*, in preparation for *J. Polym. Sci.* (anticipated August 2023 submission).

## Early Formation Stages and Pathway Complexity in Functional Bio-Hybrid Nanomaterials

PI: Lara A. Estroff; Co-PI: Ulrich Wiesner

Department of Materials Science and Engineering, Cornell University, Ithaca, NY 14853

**Keywords:** Organic-inorganic hybrids, self-assembly, nanostructured materials, interfaces, crystallization

### Program Scope

Inspired by unmatched control in structure and function of biological organic-inorganic hybrid materials systems, we have built a program to understand how organic molecule self-assembly directs the formation of nanostructured amorphous as well as crystalline inorganic materials. The ultimate goal is to help establish a synthesis science for hierarchically-organized functional hybrid materials where the design of the final material is based on deep understanding of the underlying formation mechanisms starting at the earliest time points in the assembly all the way to the final product. To reach this goal, we have been studying several synthetic systems with increasing complexity. In a first set of experiments, we investigate how sol-gel derived 1-2 nm sized amorphous silica clusters assemble into nanostructures and how surfaces of small molecule organic cationic -surfactant micelle-assemblies in aqueous solutions direct inorganic silica cluster assembly. This leads to ultrasmall silica particles with sizes below 10 nm that can act as optical super-resolution microscopy (OSRM) probes as well as nanostructures with complex topologies, including rings and cages, respectively. The latter allows assessment of the impact of topology on materials properties. In a second set of experiments, we are evolving our understanding how the formation of crystalline inorganic materials is affected by either particle impurities that get incorporated into the crystals, or by nanostructured macromolecular surfaces that direct nucleation and growth. In the latter case, we are particularly interested to understand how solution-solid interfaces help direct the growth of crystalline inorganic materials. This approach uses nanostructured block copolymer (BCP)-derived surfaces to study the combined effects of nanoscopic confinement and surface chemistry on nucleation and growth of inorganic crystals. In all cases we are probing molecular processes and materials behavior with a combination of advanced characterization techniques including OSRM and *in situ* fluid cell (3D) AFM.

### Recent Progress

We have worked on projects originally proposed as well as new directions based on recent developments and discoveries. A major focus of our efforts has been on growing our characterization toolbox for enhancing our understanding of nanoscale structural and chemical details of fully solvated block copolymer thin films.

***Triblock Terpolymer Thin Film Nanocomposites Enabling Two-color Optical Super-Resolution Microscopy.*** This work describes self-assembled poly(isoprene-*block*-styrene-*block*-N,N-dimethyl aminoethyl methacrylate) (PI-*b*-PS-*b*-PDMAEMA or ISA) triblock terpolymer thin films with all three blocks exposed at the top surface (Fig. 1).<sup>1</sup> Structural characterization of neat films with standard techniques, including grazing-incidence small-angle X-ray scattering (GISAXS), atomic force microscopy (AFM), and electron microscopy (EM), revealed co-continuous network structures in the bulk of the films and hexagonally ordered top surface structures. Using two

chemically and optically orthogonal core-shell optical nanoparticle probes, which were developed as part of this project,<sup>2</sup> nanocomposite thin films were fabricated using simple physical mixing and evaporation-induced self-assembly (EISA). These composite thin films retained the hexagonally ordered surface morphology whilst enabling two-color optical super-resolution microscopy (OSRM) imaging of different block copolymer nanodomains. This approach suggests that fine-tuned organic ligand shells enable labeling of different blocks based on shell polarity, promising a straightforward physical mixing pathway to multicolor OSRM on chemically distinct nanodomains of organic-inorganic nanocomposites.

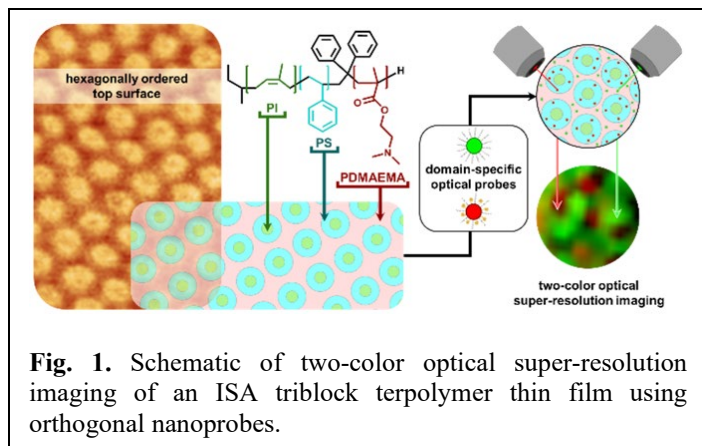


**Fig. 1.** Schematic of two-color optical super-resolution imaging of an ISA triblock terpolymer thin film using orthogonal nanoprobe.

### Interfacial Energy Driven Surface Reconstruction in Amphiphilic Block Copolymer Thin Films Probed by In-situ Atomic Force Microscopy.

Here, we used fluid cell AFM to characterize the “surface reconstruction” occurring upon hydration of BCP surfaces and found that the polymer chains rearrange, driven by entropic and enthalpic contributions.<sup>3</sup> Using Amplitude Modulation AFM (AM-AFM) Force Curve Analysis, we explored the mechano-responsive nature of these dynamic top surfaces in water and showed that there is surface rearrangement in aqueous environments upon minimal tip-sample stimulation (Fig. 2). From this data, we evaluated the swelling and surface reorganization behavior of an amphiphilic, non-ionizable BCP thin film (PS-*b*-PEO) as the baseline for the behavior of thin films of the more complex iSTAMP0, PS-*b*-P(AGE-*co*-EO). By calculating, for a hexagonal surface pattern, the enthalpic and entropic interfacial free energy contributions associated with chains of the PEO cylinder block swelling and crawling across the solid matrix PS block based surface area, we created a model successfully explaining the observed surface reconstructions.<sup>3</sup> In this model PEO chain rearrangements are driven by

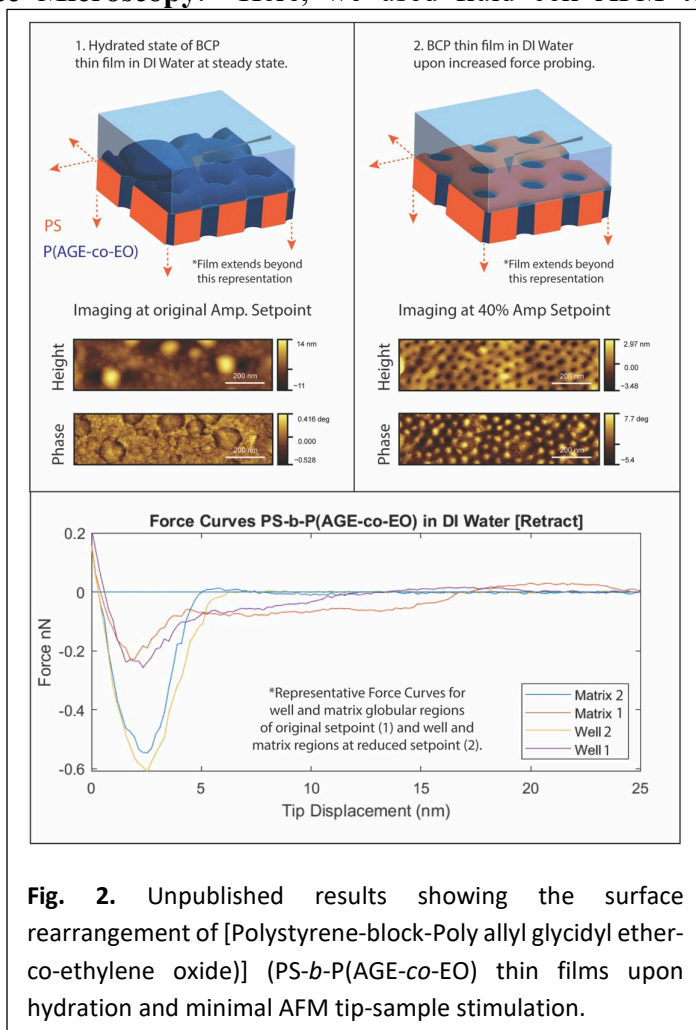


**Fig. 2.** Unpublished results showing the surface rearrangement of [Polystyrene-block-Poly allyl glycidyl ether-co-ethylene oxide] (PS-*b*-P(AGE-*co*-EO)) thin films upon hydration and minimal AFM tip-sample stimulation.

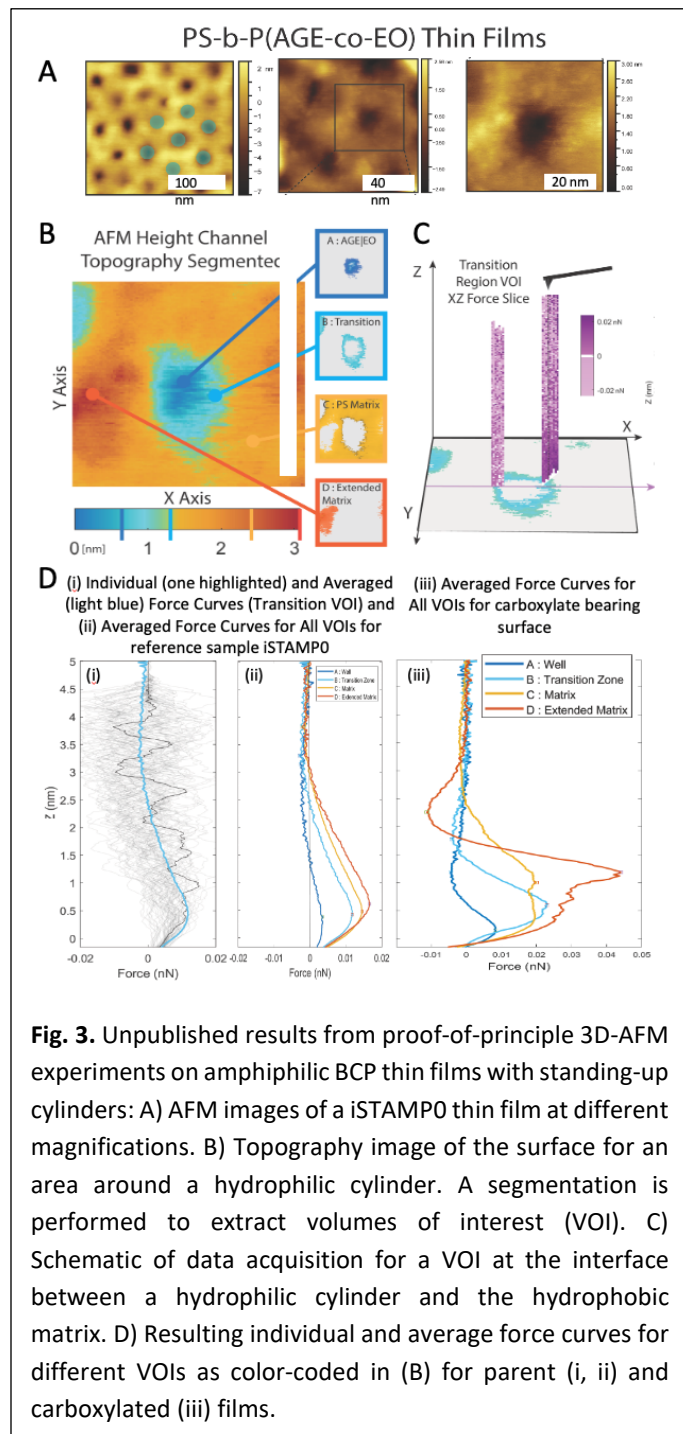


**Fig. 3.** Unpublished results from proof-of-principle 3D-AFM experiments on amphiphilic BCP thin films with standing-up cylinders: A) AFM images of a iSTAMPO thin film at different magnifications. B) Topography image of the surface for an area around a hydrophilic cylinder. A segmentation is performed to extract volumes of interest (VOI). C) Schematic of data acquisition for a VOI at the interface between a hydrophilic cylinder and the hydrophobic matrix. D) Resulting individual and average force curves for different VOIs as color-coded in (B) for parent (i, ii) and carboxylated (iii) films.

elimination of unfavorable PS-water interfaces, leading to a substantial change in top surface hydrophilicity of the thin films after exposure to water. Because of these rearrangements, the surface topography and spatial distribution of functional groups of the hydrated thin film differed significantly from the dry state.

**Visualizing the Local Nanoscale Chemistry and Topography of Water-Block Copolymer Interfacial Regions with 3D-AFM.**

To further understand the energetic landscapes presented by hydrated BCP thin films, we used 3-D atomic force microscopy (3D AFM). 3D AFM is an emerging technique that allows for nanometer resolution in the lateral and vertical directions, while maintaining a near native state for many of these interesting systems. Most importantly, this technique allows for capture of topography, phase, and force simultaneously with spatial correlation, enabling quantification of interphase interactions at these scales. We used 3D AFM to characterize the polymer-water interface of amphiphilic block copolymer (BCP) thin films, specifically poly(styrene-*block*-ethylene oxide and poly(styrene-*block*-allyl glycidyl ether-*co*-ethylene oxide). These BCPs assemble into standing up or lying down cylinders while the BCP containing the allyl glycidyl ether block can be functionalized using click-chemistry to introduce additional organic functional groups. Using 3D AFM, observables such as amplitude and phase shift were recorded, which were then converted into more physically intuitive

quantities such as force. The result is a three-dimensional map of the forces experienced by the probe as it navigates the interfacial region, which in principle corresponds to the solution structure (Fig. 3). From these initial experiments, we saw a strong dependence of the shape of the average force curves for both the parent and carboxylated thin films on chemistry (i.e., hydrophobic versus hydrophilic) and curvature of the domains, suggesting that at around 1 nm away from the substrate the water structure is still substantially influenced by what is on the surface (see averaged force curves for different VOIs, Fig. 3D).<sup>4</sup> Comparing the average force curves for parent and

carboxylate functionalized films, we saw substantial differences in both the force curve shapes and magnitudes (Fig. 3D). These results demonstrate our ability to successfully perform such experiments on non-crystalline polymeric substrates. Future work will build on these promising initial results and investigate the connection between solution composition, substrate chemistry and structure, and the molecular-scale interfacial structure.

**Future Plans.** Building on our successes, our future work is focused on understanding how nanostructured organic and inorganic interfaces guide assembly and crystallization pathways, resulting in materials with precisely controlled structures across length scales, from the near-molecular all the way to the macroscopic scale. *The work focuses on three materials platforms to elucidate solution-based assembly pathways, with an increasing focus on the role of solid-liquid interfaces composed of solvent molecules, polymer chains, and inorganic materials precursors and clusters.* In the first materials system, using surfactant self-assembly directed pathways we will probe the earliest assembly stages in the formation of spherical amorphous silica nanoparticles by elucidating the role of “magic cluster” numbers in initial particle aggregation events. We will control surface chemistry by introducing hydrophobic patches and manipulate particle topology to access rings, cages, and hollow particles. In the second system, we will investigate the role of the solid-liquid interface in directing the incorporation of secondary (nanoparticle) phases during crystallization. Studies will be performed as a function of silica nanoparticle surface chemistry (“patchiness”) and topology, thereby connecting to the first materials system. Finally, in the third system, by inverting the approach taken in the second system, we will develop methods to elucidate the energy landscape associated with block copolymer self-assembly based nanostructured substrates in controlling nucleation and growth of crystalline inorganic materials. This will be accomplished by elucidating the role of the solid-liquid interface during such growth phenomena. In all cases, we are interested in revealing the earliest stages in structure formation. We also will strive to understand the “active” role of the solvent in directing hybrid assembly pathways, and importantly in mediating the “cross-talk” (information transfer) between organic templates and growing inorganic materials.

Understanding the molecular structure of solid-liquid interfaces of nanoparticles, crystalline structures, and polymeric/organic substrates is essential for rationally designing assembly pathways to obtain hybrid materials with well-defined materials structures and resulting properties. When successful, this project will help develop a “synthesis science” associated with multicomponent organic and inorganic systems, *i.e.*, mapping out key synthetic parameters governing synthesis outcomes in amorphous and crystalline organic-inorganic hybrids. To that end, we will make use of significant recent advances in synthesis protocols as well as introducing and further developing advanced characterization techniques to provide insights into assembly pathways of hybrid materials not previously achievable. These techniques include the development of novel high-performance liquid chromatography (HPLC) methods to provide insights into surface chemical heterogeneity and cluster structure of amorphous silica nanoparticles, the application of advanced optical probes for optical super-resolution microscopy studies of the incorporation of secondary phases into growing crystals, the characterization of hydration and surface forces at crystalline interfaces, and the use of emerging 3D-AFM techniques to elucidate the molecular-scale structure of block copolymer-water interfaces.

## References.

1. Lee, W. Y.; Chapman, D. v.; Yu, F.; Tait, W. R. T.; Thedford, R. P.; Freychet, G.; Zhernenkov, M.; Estroff, L. A.; Wiesner, U. B. Triblock Terpolymer Thin Film Nanocomposites Enabling Two-Color Optical Super-Resolution Microscopy. *Macromolecules* 55, 9452–9464 (2022).
2. Chapman V, D.; Hinckley, J. A.; Erstling, J. A.; Estroff, L. A.; Wiesner, U. B. Orthogonal Nanoprobes Enabling Two-Color Optical Super-Resolution Imaging of the Two Domains of Diblock Copolymer Thin Film. *Chem. Mater.* 33, 5156–5167 (2021)
3. Hedderick, K. R.; Chapman, D. V.; Tait, W.; Oleske, K. W.; Tao, J.; Nakouzi, E.; Wiesner, U. B.; Estroff, L. A. Interfacial Energy Driven Surface Reconstruction in Amphiphilic Block Copolymer Thin Films Probed by In-situ Atomic Force Microscopy to be submitted (2023)
4. Hedderick, K.; Nakouzi, E.; Tao, J.; Wiesner, U. B.; Estroff, L. A. Visualizing the Local Nanoscale Chemistry and Topography of Water-Block Copolymer Interfacial Regions with 3D-AFM in prep (2023).

## Publications Supported by BES 2021-2023

1. Palin, D., Style, R.W., Zlopasa, J., Petrozzini, J.J., Pfeifer, M.A., Jonkers, H.M., Dufresne, E.R., **Estroff, L.A.** “Forming Anisotropic Crystal Composites: Assessing the Mechanical Translation of Gel Network Anisotropy to Calcite Crystal Form”, *J. Am. Chem. Soc.*, **2021**, 143, 3439-3447. <https://doi.org/10.1021/jacs.0c12326>
2. Thedford, R.P., Beaucage, P.A., Susca, E.M., Caho, C.A., Nowack, K.C., Van Dover, R.B., Gruner, S.M., **Wiesner, U.**, "Superconducting Quantum Metamaterials from High Pressure Melt Infiltration of Metals into Block Copolymer Double Gyroid Derived Ceramic Templates", *Adv. Funct. Mater.*, **2021**, 31, 2100469. <https://doi.org/10.1002/adfm.202100469>.
3. Krounbi, L., Hedderick, K., Eyal, Z., Shimoni, E., **Estroff, L.A.**, Gal, A. “Surface-induced coacervation facilitates localized precipitation of mineral precursors from dilute solutions” *Chem. Mater.* **2021**, 33, 3534. <https://doi.org/10.1021/acs.chemmater.0c04668>
4. Chapman, D.V., Hinckley, J.A., Erstling, J.A., **Estroff, L.A.**, **Wiesner, U.B.** “Orthogonal Nanoprobes Enabling Two-Color Optical Super- Resolution Microscopy Imaging of the Two Domains of Diblock Copolymer Thin Film Nanocomposites”, *Chem. Mater.* **2021**, 33, 5156–5167. <https://doi.org/10.1021/acs.chemmater.1c01204>.
5. Yu, F., Thedford, R.P., Hedderick, K.R., Freychet, G., Zhernenkov, M., **Estroff, L.A.**, Nowack, K.C., Gruner, S.M., **Wiesner, U.B.** “Patternable Mesoporous Thin Film Quantum Materials via Block Copolymer Self-Assembly: An Emergent Technology?” *ACS Appl. Mater. Interface*, **2021**, 13 (29), 34732–34741. <https://doi.org/10.1021/acsami.1c09085>
6. Tait, W. R. T.; Thedford, R. P.; Chapman V, D.; Yu, F.; Freidl, J. W.; Sablina, E. S.; Batsimm, G. M.; Wiesner, U. B. One-Pot Structure Direction of Large-Pore Co-Continuous Carbon Monoliths from Ultralarge Linear Diblock Copolymers. *Chemistry Of Materials*, **2021**, 33 (19), 7731–7742.
7. Lee, W. Y.; Chapman, D. v.; Yu, F.; Tait, W. R. T.; Thedford, R. P.; Freychet, G.; Zhernenkov, M.; Estroff, L. A.; Wiesner, U. B. Triblock Terpolymer Thin Film Nanocomposites Enabling Two-Color Optical Super-Resolution Microscopy. *Macromolecules* **2022**, 55 (21), 9452–9464. <https://doi.org/10.1021/acs.macromol.2c01017>.
8. Palin, D.; Kunitake, J. A. M. R.; Chang, M. P.; Sutter, S.; Estroff, L. A. Gel-Mediated Chemo-Mechanical Control of Calcium Carbonate Crystal Formation. *J Cryst Growth* **2023**, 602, 126943. <https://doi.org/10.1016/j.jcrysgro.2022.126943>.

## Programmable Dynamic Self-Assembly of DNA Nanostructures

Elisa Franco, UCLA

Rebecca Schulman, Johns Hopkins University

**Keywords:** actuators, DNA nanotechnology, force generation, polymerization, DNA nanotubes

### Research Scope

Biological cells take in energy from the environment and use it to perform a variety of multi-step physical operations in parallel. Cell division, growth, motility, and development require the coordinated temporal and spatial activation of different types of cytoskeletal filaments (actin and microtubules), bundles or networks of filaments at different times and locations. In all cases, multiple chemical reactions take in and store energy, distribute such energy into polymerizing structures, and finally dissipate energy to generate dynamic pulling and pushing forces. This coordinated architecture is advantageous because it makes it possible to achieve adaptive, repeated behaviors using a finite number of physical parts whose collective behavior is orchestrated by specific sets of chemical reactions.

Harnessing the cellular approach of coordinating and timing how multiple parts perform tasks holds enormous potential for developing artificial biomaterials that can generate microscopic motion, direct transport, and self-repair. While natural materials illustrate important design principles, we need to learn how to design artificial active biomolecular materials with tailored properties that may be customized to work under different physical and chemical conditions, across different length and time scales, and can be used to accomplish a variety of useful tasks.

Taking inspiration from cellular scaffolds, such new materials should comprise molecular components that can 1) assemble and reorganize into different configurations 2) harvest and dissipate energy to direct how these components dynamically disassemble and reassemble and 3) adapt their use of energy and the reorganization of components in response to a changing environment to achieve a specific function. Toward addressing this grand challenge of building active, reconfigurable materials, the central goal of this proposal is to develop design rules and experimental methods for building multicomponent, customizable artificial polymeric systems that use chemical energy to generate adaptive structural networks with the ability to perform mechanical work.

During the previous funding cycles we have developed strategies for building robust, programmable DNA and RNA filaments with well-understood and customizable structural features (**Fig. 1**). We have engineered these filaments so they can be assembled and disassembled based on an array of input signals and so that this organization can be orchestrated by a range of biochemical reaction networks, including those that mimic biological gene networks. We have

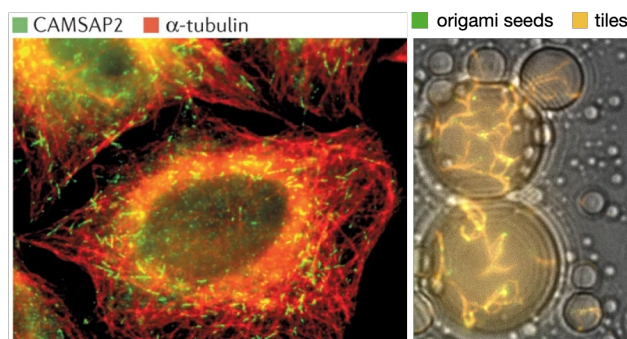


**Figure 1:** Left: actin filaments (red) organized by CAMSAP2 proteins (green) in HeLa cells [1]. Right: DNA filaments (orange) growing from origami seeds (green) in emulsion droplets (unpublished).

further devised methods to precisely route energy or information-storing molecules (fuel) to control the nucleation, growth rate, and dissolution rates of these filaments. We have also established approaches for storing and releasing these fuel molecules from compartments like droplets, vesicles and hydrogels. We have designed and synthesized nanostructures that organize how these filaments assemble to form filament networks, and can be selectively activated and deactivated. And we have developed the means to encapsulate filaments and the components of the biochemical reaction networks that control them within isolated or communicating droplets, mimicking the compartmentalization provided by cellular membranes. Building on our previous work, we are taking advantage of this suite of nucleic acid components to create microscopic materials that can self-organize, move, or deform target substrates such as particles or membranes. We achieve these behaviors by dissipating energy harvested from the environment to control the collective interaction of components that sense, signal, and assemble.

## Recent Progress

### Synthetic polymerization ratchets:

Filaments can play key roles in inducing motion within biological cells and systems. For example, actin filaments can exert pushing forces on plasma membrane through polymerization to induce membrane protrusion, a phenomenon known as a

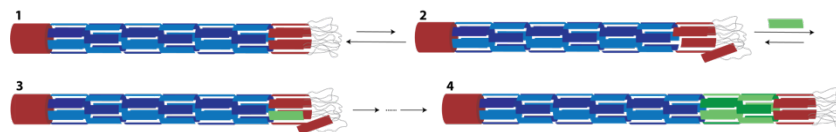


**Figure 2: Insertion polymerization and cap displacement.** (1) A seeded and capped nanotube; (SC nanotube) (2) A piece of the cap domain detaches and provides an unoccupied binding site; (3) A piece of tile monomer attaches to the site and pushes the falling cap domain away; (4) The above process happens repetitively and then the cap is being displaced and pushed further away towards the direction of insertion.

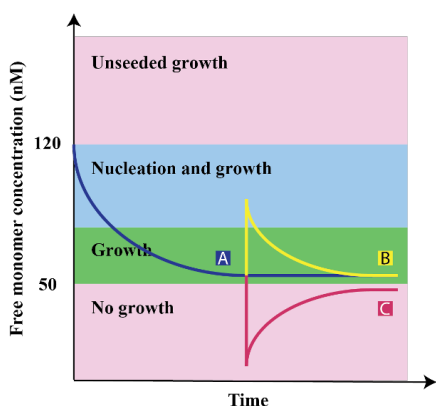


**Figure 3: Free monomer concentration profile for different motor actions.** (A) Nanotube nucleation and growth. (B) insertion polymerization. (C) shrinking depolymerization.

We have developed a synthetic, programmable polymerization ratchet that acts as a linear actuator using the dynamic growth and shrinkage of DNA nanotubes. This actuator consists of a DNA nanotube with an attached capping structure [3] that can be displaced by polymerization or depolymerization of DNA tiles (Figure 2). To characterize the displacement of capping structures within an ensemble of linear actuators, we developed an assay in which we first grow DNA nanotubes using DNA tiles labeled with one type of fluorophore, cap them, and then add tiles labeled with a different type of fluorophore to the surrounding solution. The amount of positive displacement of the capping structure is then observable through the length of the nanotube containing tiles with the second type of fluorophore. Epifluorescence microscopy is performed to visualize insertion polymerization mediated displacement of the cap. We observed that for a free monomer concentration is higher than the critical concentration of 50nM, new tiles are inserted by 33% at nanotube-cap interfaces where the cap is connected to the nanotube by flexible connections, as designed, while no insertion occurs at the nanotube-seed interfaces with rigid interconnects. Conversely, depolymerization happens at nanotube-cap interfaces with flexible interfaces when the free monomer concentration becomes lower than 50 nM: we

observed that nanotubes became shortened by 25%. Since the kinetics of nanotube tile self-assembly, which drives the displacement, are quite sensitive to monomer concentration, at a specific temperature we predict we can tune the rates of nanotube polymerization and depolymerization by tuning the free monomer concentration (Figure 3). The DNA nanostructures we are building are programmable active elements whose motion could be sensitive to stimuli from the environment by coupling these stimuli to the modulation of monomer concentration. Insertion polymerization could also occur at multiple sites within DNA nanotube chains, so that larger structures could enable faster displacement.

**Temporal coordination of distinct nanotube populations through interconnected gene networks.** We have demonstrated that *in vitro* gene networks can be used to direct DNA nanotubes [4]

and we have now expanded this approach to control distinct populations of DNA nanotubes simultaneously (Figure 5). For this purpose, we built modular cascades of genes communicating via DNA gate connectors (Figure 5A). Each gene in the cascade transcribes a distinct RNA output that activates or deactivates a particular type of tile through toehold-mediated strand displacement. As a result, cascaded events in the gene network generate sequential RNA production events that

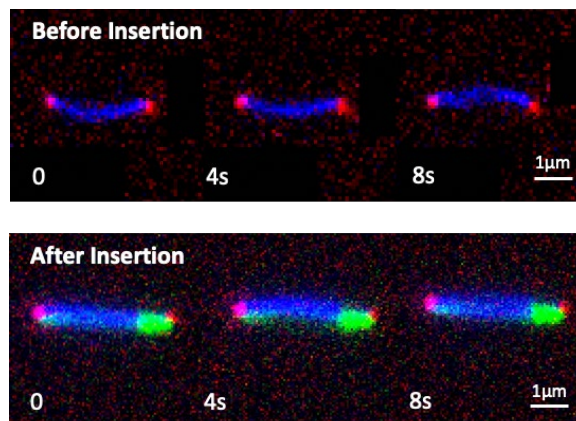
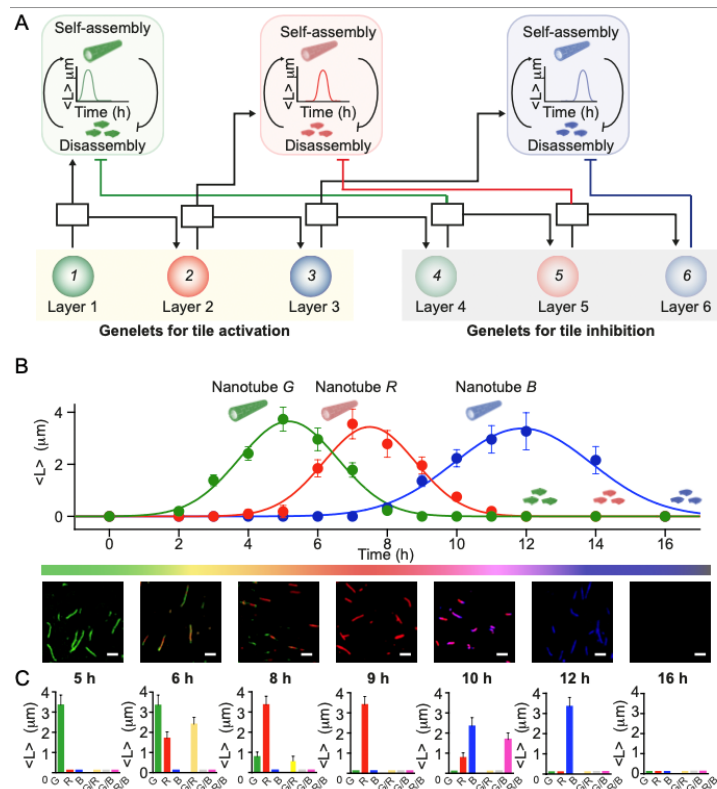


**Figure 4: Micrographs of nanotubes before and after insertion polymerization.** (Left) Before insertion, the nanotubes (blue) have a seed on one side and caps on the other (both show in red). (Right) After incubating 48 hours for insertion polymerization by adding more tile monomers (green), the nanotubes have a new section of nanotube inserted at the nanotube-cap interface which can displace the cap structure.



cause a temporal sequence of nanotube formation (Figure 5 B). We showed that the timing of tile activation (delay and speed) can be tuned by modulating the relative concentration of genes and the speed of connectors (which is controlled by toehold length). Further, by using tiles that can interact and controlling the timing of their activation/deactivation, we can control the characteristics of the polymer composition (random or block polymers) (Figure 5C). These

**Figure 5: Directing the assembly of multiple nanotube populations using cascaded gene networks.** (A) Schematic of the genetic cascade. (B) Temporally coordinated formation of DNA nanotubes from tiles having distinct fluorescent labels, with example microscopy images. (C) Bar chart of nanotube length including the presence of nanotubes with mixed tile color, which have interacting sticky ends but distinct regulators

experiments will enable us to activate distinct nanotube populations used to build polymerization motors, as well as networks within emulsion droplets and vesicles, making it possible to follow specific network developmental pathways that optimize force generation.

## Future Plans

One advantage of nanotube linear actuators is that they may be combined to increase the rate of displacement or displacement force. We have assembled chains of linear actuators and in the coming year, we plan to measure the insertion polymerization and depolymerization performance at multiple sites within nanotube chains to determine whether we observe faster displacement in chains than in single actuators (Figure 6). We will also investigate whether the scale of the forces generated by the nanotube linear actuators can displace a load, such as a polystyrene bead or nanoparticle and characterize the displacement under load and the stall force of linear actuators.

We further plan to investigate significant increases to the effective efficiency of polymerization motors. In principle, polymerization motors' efficiency can approach 100%, because unlike light or heat, the chemical potential not used by the motor is preserved as high-energy molecules rather than being dissipated. However, in practice one generates the chemical potential to drive motors everywhere in solution when the chemical potential is only needed at the location of the growth front. We are developing concentration *fields* that can direct growth only in a small region and will investigate our ability to focus chemical energy at sites needed by polymerization motors.

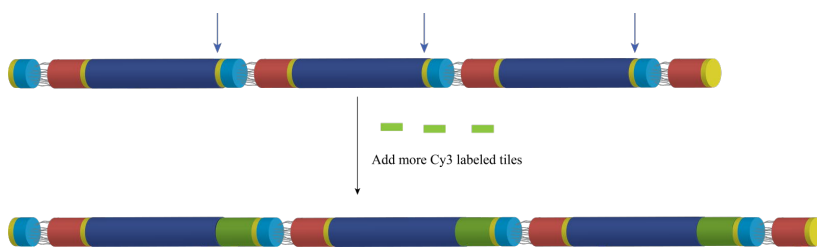


**Figure 6:** Nanotube chains could enable faster displacement using insertion polymerization.

In parallel, we will take advantage of our *in vitro* genetic programs to generate molecular signals that coordinate temporally the assembly and disassembly of tiles into specific nanotube types, thereby governing when a particular motor component is forming or dissolving, resulting in push or pull forces in the synthetic motors. We will also continue our characterization of encapsulated nanotube networks (Figure 1, right), first in droplets and then in lipid vesicles, with the goal of generating forces sufficient to deform vesicles based on the conversion of chemical inputs into polymerized components. To guide experiments, we will use computational simulations to analyze temporal pathways of nanotube self-assembly processes. We are developing a new coarse-grained molecular dynamics framework that can include relevant physical details of nanotube assembly (including binding energy and bending energy), as well as the ability of the framework to incorporate the ability to add temporal sequencing to the addition of distinct subunits. This is embedded in a molecular model of a vesicle that allows for deformation, as a way to probe the potential of force deformation in confinement.

## References

1. A. Akhmanova and M. O. Steinmetz, “Control of microtubule organization and dynamics: two ends in the limelight,” *Nat. Rev. Mol. Cell Biol.*, **16**, pp. 711–726, (2015).
2. C. S. Peskin, G. M. Odell, and G. F. Oster, “Cellular motions and thermal fluctuations: the Brownian ratchet,” *Biophys. J.*, **65**, pp. 316–324 (1993).
3. D. K. Agrawal, R. Jiang, S. Reinhart, A. M. Mohammed, T. D. Jorgenson, and R. Schulman, “Terminating DNA Tile Assembly with Nanostructured Caps,” *ACS Nano*, **11**, pp. 9770–9779 (2017).
4. L. N. Green, H. K. K. Subramanian, V. Mardanlou, J. Kim, R. F. Hariadi, and E. Franco, “Autonomous dynamic control of DNA nanostructure self-assembly,” *Nat. Chem.*, **11**, pp. 510–520 (2019).

## Publications

5. S. Agarwal, M.A. Klocke, P.E. Pungchai, and E. Franco. *Dynamic self-assembly of compartmentalized DNA nanotubes*, Nature Communications **12**, 1 3557, 2021.
6. S. Gentile, E. Del Grosso, P.E. Pungchai, E. Franco, L.J. Prins and F. Ricci. *Spontaneous reorganization of DNA-based polymers in higher ordered structures fueled by RNA*. Journal of the American Chemical Society **143**, 48 pp.20296-20301 (2021).
7. S. Schaffter, K. L. Chen, J. O’Brien, M. Noble, A. Murugan, R. Schulman, *Standardized excitable elements for scalable engineering of far-from-equilibrium chemical networks*, Nature Chemistry **14**, 11 pp.1224-1232 10.7281/T1/UBSZF1 (2022).
8. Y. Li, C. Maffeo, H. Joshi, B. Ménard, A. Aksimentiev, and R. Schulman, *Leakless transport of small molecules through micron-length DNA nanochannels*, Science Advances **8**, 26 10.1126/sciadv.abq4834 (2022).
9. P. G. Moerman, M. Gavrilov, T. Ha., R. Schulman, *Catalytic DNA Polymerization Can Be Expedited by Active Product Release*, Angew. Chem. Int. Ed. **61** 24 e202114581 10.1002/anie.202114581 (2022).
10. Liu, A.P., Appel, E.A., Ashby, P.D., Baker, B.M, Franco, E., Gu, L., Haynes K., Joshi, N.S., Kloxin, A.M., Kouwer, P.H.J., Mittal J., Morsut, L., Noireaux, V., Parekh, S., Schulman, R., Stephanopolous, N., Tang, S.K.Y., Valentine, M.T., Vega, S.L., Weber, W., Chauduri, O, *The living interface between synthetic biology and biomaterial design*, Nat. Mater. **21**, 4 pp.390–397 10.1038/s41563-022-01231-3 (2022).
11. J. Le, D. Osmanovic, M.A. Klocke, and E. Franco, *Fueling DNA Self-Assembly via Gel-Released Regulators*, ACS nano, **16**, 10 pp.16372-16384 (2022).
12. M. Rubanov, J. Cole, H.J. Lee. R. Schulman, *Multi-domain Automated Patterning of DNA-Functionalized Hydrogels*, Under review, *protocols.io*, 10.17504/protocols.io.j8nlkw2ywl5r/v1 (2023).

# Controlling Lattice Organization, Assembly Pathways and Defects in Self-Assembled DNA-Based Nanomaterials

Oleg Gang<sup>1,2</sup> and Sanat K. Kumar<sup>1</sup>

<sup>1</sup> Department of Chemical Engineering and <sup>2</sup> Department of Applied Physics and Applied Mathematics, Columbia University, New York, NY

**Keywords:** self-assembly, nanoparticles, inverse design, DNA nanotechnology, nanomaterials

## Research Scope

Our effort is focused on establishing approaches for assembling prescribed nanoscale architectures and uncovering the principles required for creating such systems. Using DNA-based assembly approaches, we develop platform methods for creating diverse large-scale and mesoscale 3D architectures for organizing nano-objects of several types (nanoparticles and proteins). By utilizing liquid robotics, advanced characterizations, computational developments, and machine learning methods, we explore how to design and control efficiently and with low defects assembly of prescribed complex periodic nano-architectures, how to steer the system's assembly pathway, and how to control a lattice growth using thermodynamic factors and bond design. By combining assembly with detailed characterization and analysis, the program will develop approaches for creating designed nanoparticle-based materials where their organization is controlled by DNA-programmable assembly.

## Recent Progress

### 1. Encoding Hierarchical 3D Architecture through Inverse Design of Programmable Bonds.

Advances in the fabrication of materials and devices at small scales, largely based on a progress in lithographic and additive manufacturing methods. However, the growing need to structure 3D nanoscale matter for emergent functions requires new means of material fabrication. We developed a new concept of the encoded assembly of nanoparticles into prescribed, hierarchically ordered 3D organizations using DNA programmable bonds<sup>1</sup>. Our inverse design approach allows for the encoding of targeted 3D hierarchical architectures with programmable bonds by identifying repeating mesoscale motifs and their elemental blocks, nanoscale voxels, that can also carry encoded nano-cargo. Using intrinsic symmetries of mesoscale motifs in targeted 3D architectures, we reduce the amount of information required for encoding bonds and incorporate this principle into the inverse design assembly strategy.

This design strategy considers the unique bond identities needed to achieve a desired structure through the inherent symmetry of the targeted structure. First, we consider an arbitrarily defined, hierarchically ordered 3D structure that contains many functional nanocomponents as the target material. The elementary building block is a DNA voxel that may contain a functional nano-object or remain empty. In this example, the material voxel is an octahedral cage<sup>2</sup> that can interact with six other voxels. This defines a 3D cubic grid in which nano-objects can be placed. Interactions between voxels are specified using orthogonal DNA chromatic binding sequences.

As examples of this approach, we assemble spatially ordered, low-dimensional arrays with coupled plasmonic and photonic scales, a nanoscale analog of face-perovskite lattice (Fig. 1), and a hierarchically organized lattice of spiral motifs. Detailed x-ray scattering and electron microscopy methods confirm the correspondence between the designed and realized architectures.

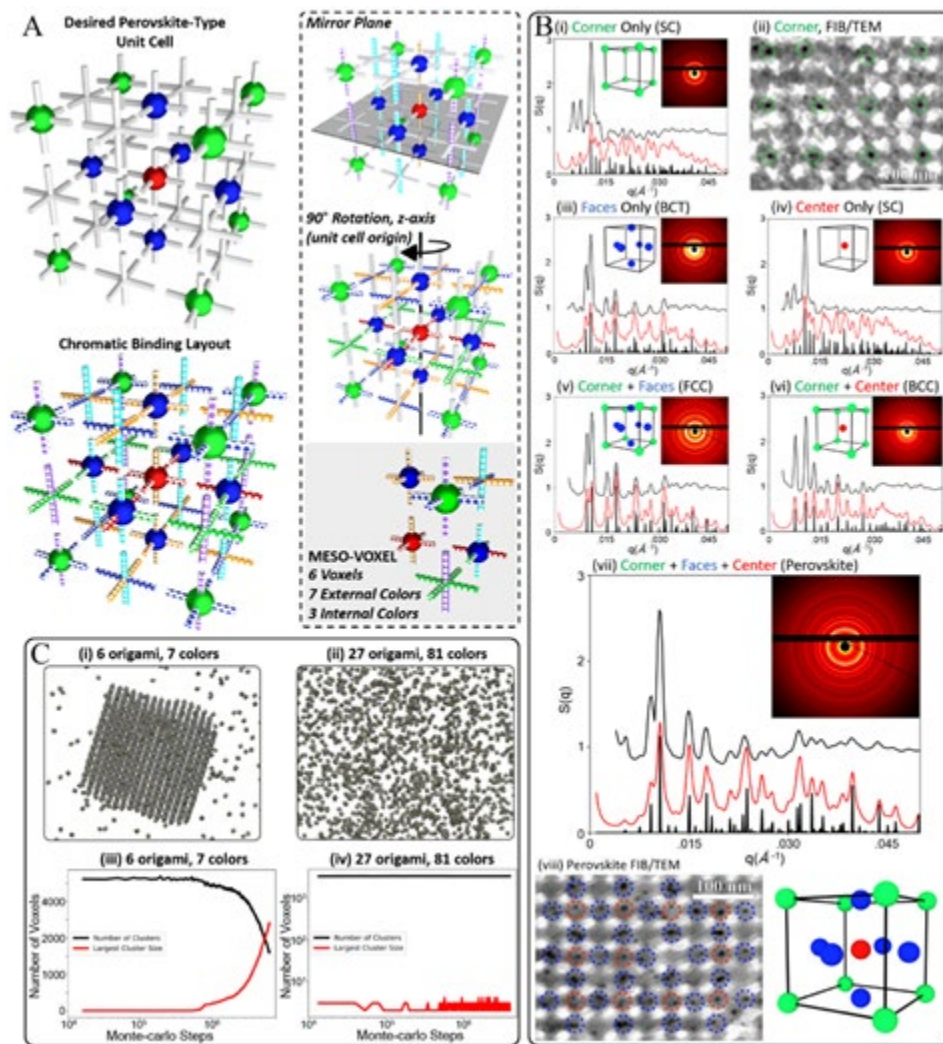


**Figure 1. Formation and selective filling of a perovskite lattice.** A perovskite-type unit cell has three NP-shell types – center (red), face (blue), and corner (green). (A) 3 internal origami colors, based on particle type, are mapped into a perovskite unit cell of 27 origami using a meso-voxel of 6 origami frames (B) Each of the individual particles can be added to form distinct lattices and subphases from the fully-filled perovskite unit cell. As measured by SAXS, with experimental  $S(q)$  shown in black plots and modelled  $S(q)$  shown in red with associated Bragg peak locations and inset diffraction patterns, the three ‘types’ of particles added individually yield SC or BCT phases, where combinations of two particle types yield either FCC or BCC, and addition of all three types yield a perovskite. TEM imaging of a prescribed partially-filled and fully-filled perovskite lattice with functionalized particles yields representative images, in real space, of the desired particle crystals. The model  $S(q)$  for each sample are shown in red. (C) Crystal growth is affected by entropic penalties associated with increased chromatic complexity. Modeled crystal growth of a DNA scaffold demonstrates lattice crystallization using the hierarchical perovskite meso-voxel.

## 2. The effect of anisotropic bonds on the morphology of the self-assembled lattices.

We have explored a design strategy for the self-assembly of nanomaterials with controlled morphology. To understand the thermodynamic underpinnings of the self-assembly of DNA-grafted nanoparticles, our recent work investigated the self-assembly behavior of octahedral hard particles with interacting vertices via theory and computer simulations. We demonstrated via computer simulations that assemblies with different 3D crystalline morphologies can be formed depending on the relative strength of vertex-to-vertex interactions in different directions as shown in the morphology diagram (Fig. 2). We developed a simple theory based on the calculation of the second-virial coefficient of patchy particles adequately summarizing the simulation results.

Complementing the theory and simulations, experimental studies were performed to investigate the assembly of octahedral DNA origami frames with varying binding energies. SAXS and electron microscopy imaging of the assembled domains validated the theoretical predictions and showed the correspondence of the distinct morphologies to the DNA interaction strengths in the three orthogonal directions. To further explore the controllability of the final assembly morphology via manipulating the directionality of inter-vertex interactions, we are currently investigating octahedral nanoparticles with ‘asymmetric’ inter-vertex interactions.

### Future Plans

An increased complexity of DNA-based systems it becomes more difficult to fabricate and characterize due the diversity of nano-components to be assembled and wide hierarchical range to be characterized. Our 3D imaging methods based on hard x-ray tomographic imaging<sup>3</sup> reflect state of the art in depth of focus and resolution on the nanoscale for revealing complex material organization and imperfections. Future designed nanoparticles arrays will require physics-informed models for tomographic reconstruction as sampling requirements increase to the limits of synchrotron light source capabilities. We will build multicomponent systems for characterization using hard x-ray tomography and will complements it with serial sectioning with SEM to investigate structural and compositional disorder of nanoparticles assembled by discussed above DNA color-encoded approaches. In parallel, we are developing high-throughput methods for creating targeted organization using liquid robotics with online characterization capabilities

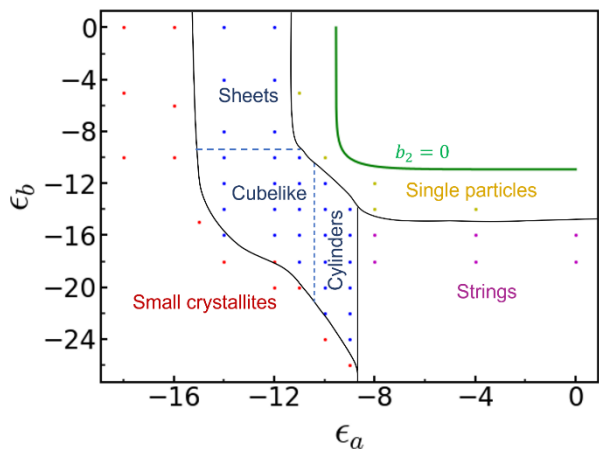


**Figure 2. Crystal morphology diagram in the interaction energy, ( $\epsilon_a$ ,  $\epsilon_b$ ), space. The green line is the boundary between the regions of negative and positive second virial coefficient. Crystalline domains of three distinct morphologies: sheet-like, cube-like, and cylinder-like, all shown by the blue dots, where regions of different morphologies separated by dashed lines, are formed.**

(fluorescence, UV-Vis-absorption, optical microscopy). The combination of physics-informed models and ML methods will be explored to guide the system design and assembly pathways.

## References

1. Kahn, J. S., Minevich, B., Michelson, A., Emamy, H., Kisslinger, K., Xiang, S., Kumar, S. K. & Gang, O. Encoding Hierarchical 3D Architecture through Inverse Design of Programmable Bonds. *ChemRxiv* (2023). <https://doi.org:10.26434/chemrxiv-2022-xwbst>
2. Tian, Y., Lhermitte, J. R., Bai, L., Vo, T., Xin, H. L. L., Li, H. L., Li, R. P., Fukuto, M., Yager, K. G., Kahn, J. S., Xiong, Y., Minevich, B., Kumar, S. K. & Gang, O. Ordered three-dimensional nanomaterials using DNA-prescribed and valence-controlled material voxels. *Nature Materials* 19, 789-+ (2020).
3. Michelson, A., Minevich, B., Emamy, H., Huang, X. J., Chu, Y. S., Yan, H. F. & Gang, O. Three-dimensional visualization of nanoparticle lattices and multimaterial frameworks. *Science* 376, 203-+ (2022).

## Publications

1. Michelson, A., Flanagan, T. J., Lee, S.-W. & Gang, O. High-strength, lightweight nano-architected silica. *Cell Reports Physical Science*, 101475 (2023). <https://doi.org:https://doi.org/10.1016/j.xcrp.2023.101475>
2. Kahn, J. S., Minevich, B., Michelson, A., Emamy, H., Kisslinger, K., Xiang, S., Kumar, S. K. & Gang, O. Encoding Hierarchical 3D Architecture through Inverse Design of Programmable Bonds. *ChemRxiv* (2023). <https://doi.org:10.26434/chemrxiv-2022-xwbst>
3. Srivastava, S., Chhabra, A. & Gang, O. Effect of mono- and multi-valent ionic environments on the in-lattice nanoparticle-grafted single-stranded DNA. *Soft Matter* 18, 526-534 (2022). <https://doi.org:10.1039/d1sm01171e>
4. Mostarac, D., Xiong, Y., Gang, O. & Kantorovich, S. Nanopolymers for magnetic applications: how to choose the architecture? *Nanoscale* 14, 11139-11151 (2022). <https://doi.org:10.1039/d2nr01502a>
5. Michelson, A., Minevich, B., Emamy, H., Huang, X. J., Chu, Y. S., Yan, H. F. & Gang, O. Three-dimensional visualization of nanoparticle lattices and multimaterial frameworks. *Science* 376, 203-+ (2022). <https://doi.org:10.1126/science.abk0463>
6. Kahn, J. S. & Gang, O. Designer Nanomaterials through Programmable Assembly. *ANGEWANDTE CHEMIE-INTERNATIONAL EDITION* 61 (2022). <https://doi.org:10.1002/anie.202105678>
7. Xiong, Y., Lin, Z. W., Mostarac, D., Minevich, B., Peng, Q. Y., Zhu, G. L., Sanchez, P. A., Kantorovich, S., Ke, Y. G. & Gang, O. Divalent Multilinking Bonds Control Growth and Morphology of Nanopolymers. *NANO LETTERS* 21, 10547-10554 (2021). <https://doi.org:10.1021/acs.nanolett.1c03009>
8. Wang, S. T., Minevich, B., Liu, J. F., Zhang, H. H., Nykypanchuk, D., Byrnes, J., Liu, W., Bershadsky, L., Liu, Q., Wang, T., Ren, G. & Gang, O. Designed and biologically active protein lattices. *NATURE COMMUNICATIONS* 12 (2021). <https://doi.org:10.1038/s41467-021-23966-4>
9. Shani, L., Tinnefeld, P., Fleger, Y., Sharoni, A., Shapiro, B. Y., Shaulov, A., Gang, O. & Yeshurun, Y. DNA origami based superconducting nanowires. *Aip Advances* 11 (2021). <https://doi.org:10.1063/5.0029781>
10. Majewski, P. W., Michelson, A., Cordeiro, M. A. L., Tian, C., Ma, C. L., Kisslinger, K., Tian, Y., Liu, W. Y., Stach, E. A., Yager, K. G. & Gang, O. L. Resilient three-dimensional ordered architectures assembled from nanoparticles by DNA. *Science Advances* 7 (2021). <https://doi.org:10.1126/sciadv.abf0617>

## **A reduced-order dynamical systems approach to modeling, sensing and control of active fluids**

**Piyush Grover (PI) and Jae Sung Park (co-PI), Mechanical and Materials Engineering, University of Nebraska-Lincoln**

**Michael M. Norton (Co-PI), School of Physics and Astronomy, Rochester Institute of Technology**

**Keywords:** Active fluids, active turbulence, nonequilibrium steady states, pattern formation, reaction-diffusion

### **Research Scope**

The project aims to develop a reduced-order modeling framework for understanding and controlling active fluid flows. Active fluids are viscous suspensions of constituents that consume chemical energy and convert it into mechanical work by generating stresses on the microscale, resulting in spontaneous coherent flows, dynamical vortex patterns, and chaotic hydrodynamics (i.e., low Reynolds number 'active/mesoscale turbulence'). These systems are governed by fully nonequilibrium dynamics. We focus on *active nematics* [1], which are suspensions of active, rod-like, and apolar components. Our interest is in part motivated by the potential of exploiting the rich phenomenology of active nematics for design of smart materials.

To achieve our objectives, we employ theoretical and computational techniques from nonlinear dynamics to expose the global phase space of flow and director fields of active nematics. Our framework does not require close-to-equilibrium or 'equilibrium-like' assumptions, such as linear response or the existence of a local free energy functional. This infinite dimensional phase space is found to be populated by *Exact Coherent Structures* (ECS), which are exact solutions of the physical dynamics with distinct and regular spatiotemporal structure; examples include stable and *unstable* equilibria, periodic orbits, and traveling waves. These ECSs are interconnected by invariant manifolds, which act as dynamical pathways. Our main hypothesis is that active/mesoscale turbulence corresponds to a trajectory meandering in this phase space, transitioning between neighborhoods of the unstable ECSs by traveling on the invariant manifolds. The project aims to:

- 1). Develop reduced-order, predictive models by identifying the dominant ECSs and the transition dynamics between them. Besides improving fundamental understanding of mesoscale turbulence in active nematics, this analysis will illuminate the mechanisms driving such systems into, and out of, the turbulent state. This strategy is motivated by recent successes of ECS-based techniques in characterizing the routes to high Reynolds number turbulence in regular fluids. In experiments, the reduced-order representation can be exploited by applying external vorticity, light activation or pressure modulation to reach and/or stabilize otherwise inaccessible/unstable spatiotemporal states.
- 2). Develop designs of endogenously controlled non equilibrium systems. We take a bioinspired approach and seek to identify reaction-diffusion systems that, when coupled to an active nematic, produce desired spatiotemporal behaviors. We aim to both identify broadly applicable principles while inspiring novel experiments through collaboration.

**Recent Progress: Exact coherent structures and connecting manifolds in the phase space of 2D active nematic channel flow:** We have developed computational algorithms and an open-source computational toolbox (ECSAct) for efficient computation of various type of ECS for the 2D active nematic [1,2]. The toolbox also computes the stability of each ECS and enables the computation of connecting orbits between various pairs of ECS. A connecting orbit is a dynamical trajectory which departs from one ECS and lands onto another ECS. It is often observed that natural dynamical pathways between a pair of stable steady states are mediated by unstable states. Hence, our computation of unstable structures leads to new insight into the origin of stable structures, and the dynamical paths between them.

In the pre-turbulent regime at a single medium activity value, we have computed over 50 ECS, and found three co-existing attractors (stable ECS), some of which are shown in Fig. 1. In the turbulent regime at high activity, we computed over 200 ECS, all of whom are unstable.

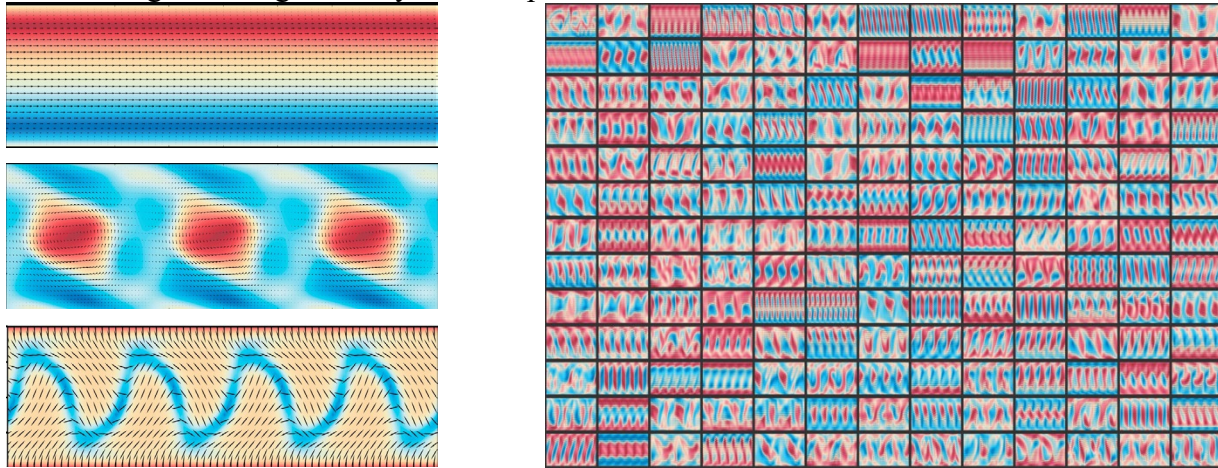


**Fig. 1.** Left: Snapshots of the velocity fields of three ECS (out of about 50) computed in the pre-turbulent regime. The unidirectional equilibrium (top, unstable), a time-periodic three vortex lattice (middle, stable), and a travelling wave (bottom, unstable). Right: A mosaic of snapshots of a subset of ECS computed in the turbulent regime at *single value of activity*, all unstable. The color is vorticity (red + /blue -).

In experiments, one might wish to direct the system toward a specific attractor. Our framework allows for more complex control objectives involving unstable ECS, which is a necessary prelude to controlling turbulent active nematic flows. This capability is provided by the reduced-order representation of the phase space in terms of a directed graph (Fig. 2), in which ECS are nodes, and dynamical connections are edges. This representation uncovers nontrivial relationships in phase space, which can be exploited to induce desired transitions using minimal external control input. For instance, such methods have been used to discover low-energy dynamical channels forming an 'interplanetary superhighway' in the solar system [3].

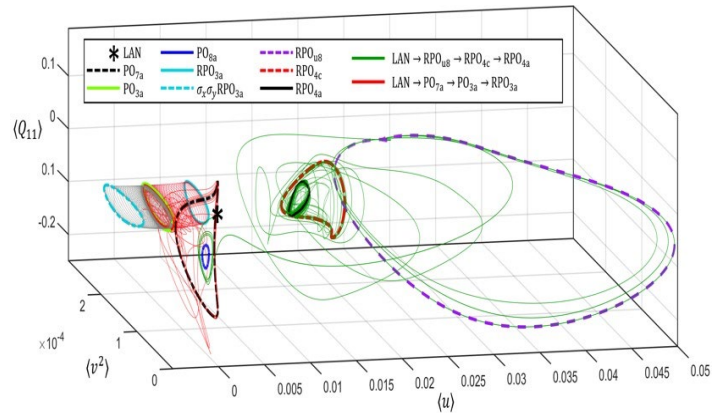
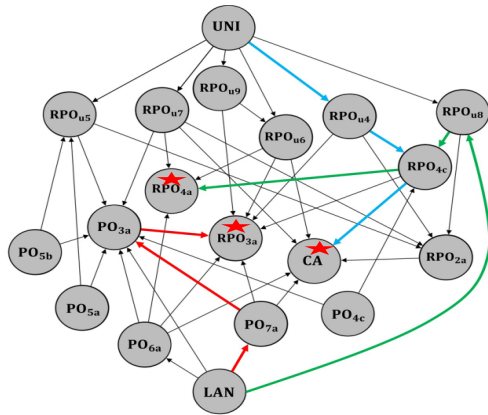


**Fig. 2.** Left: Directed graph representation of the phase space, with ECS (and the chaotic attractor) as nodes and dynamical connections as edges. The 3 attractors (★) only have incoming edges. The colored arrows (red, green, blue) highlight three multistep connections, some of which are visualized in the right figure in more detail. UNI/LAN are equilibria, POxx are the various vortex-lattice periodic orbits, RPOxx are the various relative periodic orbits, and CA is the chaotic attractor. Right: Three connecting orbits obtained from the graph representation shown in a reduced phase space. Such orbits can be constructed for a pair of ECS if a directed path exists between them in the graph. Each orbit is formed by patching together dynamical connections between successive ECS along the path using small perturbations.

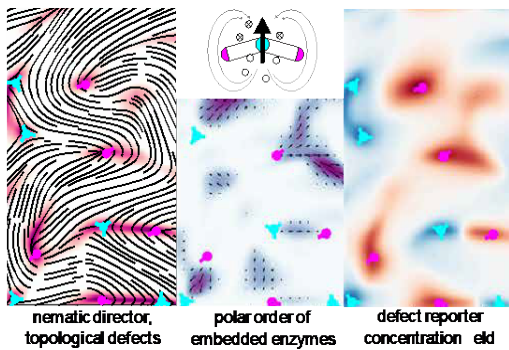


**Fig. 3.** Defect sensing in an active nematic. (left) active nematic with defects labeled, (middle) degree and direction of polar order of embedded enzymes, (inset) cartoon of bend-activated enzyme, (right) concentration field created by dipoles.

**A proposal for endogenous defect sensing :** A key feature of biological systems are feedback loops that connect mechanics and geometry to reaction-diffusion processes. Towards engineering materials with biologically inspired autonomy, we have developed [4] a continuum model of a non-equilibrium enzymatic process that chemically responds to the topology of an embedding active nematic. Specifically, we propose a PDE system that creates a concentration field with local minima and maxima coinciding with +/- 1/2 defects, a process that we call “defect sensing.” We chose to focus on sensing because feedback is a well-known process for stabilizing desirable dynamics. However, doing so in the context of active nematics requires, as a first step, converting structural information into a chemical signal, which has *not* been previously addressed. We are further motivated by the apparent functional roles taken

by topological defects in so-called living active nematics: bacterial colonies and animal tissues. A striking example is the hydra microorganism, wherein defect patterns in the animal’s supracellular actomyosin network locate its limbs, mouth, and foot [5]. These observations from biology suggest the existence of a variety of feedback mechanisms between topological information and biochemistry and, more broadly, diverse strategies for sensing geometry and controlling form.

In our minimal model, we embed within the nematic a field of reaction dipoles (middle inset of Fig. 3) that produce a chemical signal on the concave side, that is destroyed on the convex side. These dipoles become chemically active only when bent beyond a critical deformation by the nematic. Consequently, they are activated near defects in the nematic. These activated dipoles are organized into large regions of polar order (Fig. 3 middle panel) that produce concentration sources and sinks at their poles, in analogy with the electrostatic polarization charge density (Fig. 3 right panel). The result is a concentration field with minima/maxima that coincide with defect locations. Our model lays the groundwork for highly-coupled chemo-mechanical systems in which complex spatiotemporal patterns are robustly encoded in reaction-diffusion networks.

## Future Plans

The next steps for the ECS work include the extension to computation and feedback control of ECS in an experimentally realizable setting, e.g., the light-activated active nematic system in a 2D annulus, as well as reduced-order graph representation of the system in the active turbulence regime.

The next direct step for the defect sensing work is to “close the loop” by using resulting concentration fields to modulate activity. The resulting spatiotemporal structures can then be analyzed through the ECS framework and contrasted with the uncontrolled system. Further, while this work precedes current experimental capabilities, the proposed model can serve as an inspiration for the engineering of constituent molecules that couple nematic geometry and chemical dynamics.

## References

1. C.G. Wagner, M.M. Norton, J.S. Park, and P. Grover, Exact coherent structures and phase space geometry of preturbulent 2D active nematic channel flow, *Physical Review Letters*, **128**.2: 028003 (2022)
2. C.G. Wagner, R.H. Pallock, M.M. Norton, J.S. Park, and P. Grover, Exploring regular and turbulent flow states in active nematic channel flow via Exact Coherent Structures and their invariant manifolds, arXiv:2305.00939 (2023)
3. W.S. Koon, M.W. Lo, J.E. Marsden, and S.D. Ross, Heteroclinic connections between periodic orbits and resonance transitions in celestial mechanics. *Chaos: An Interdisciplinary Journal of Nonlinear Science*, **10**(2), 427-469 (2000).
4. M. M. Norton, and P. Grover, Mechanochemical Topological Defects in an Active Nematic, arXiv:2210.03796 (2022)
5. Maroudas-Sacks, Y., Garion, L., Shani-Zerbib, L. *et al.* Topological defects in the nematic order of actin fibres as organization centres of *Hydra* morphogenesis. *Nat. Phys.* **17**, 251–259 (2021).

## Publications

1. C.G. Wagner, R.H. Pallock, M.M. Norton, J.S. Park, and P. Grover, Exploring regular and turbulent flow states in active nematic channel flow via Exact Coherent Structures and their invariant manifolds, arXiv:2305.00939 (2023)
2. C.G. Wagner, M.M. Norton, J.S. Park, and P. Grover, Exact coherent structures and phase space geometry of preturbulent 2D active nematic channel flow, Physical Review Letters, **128.2**: 028003 (2022)
3. M. M. Norton, and P. Grover, Mechanochemical Topological Defects in an Active Nematic, arXiv:2210.03796 (2022)
4. T. E. Bate, M. E. Varney, E. H. Taylor, J. H. Dickie, C.-C. Chueh, M. M. Norton, and K.-T. Wu., Self-mixing in microtubule-kinesin active fluid from nonuniform to uniform distribution of activity. Nature Communications **13**, 6573 (2022)
5. Exact Coherent Structures for Active Matter (**ECSAct v1.0**): Open-source library available at <https://github.com/DynamicalSystemsLab-UNL/ECSActV1.0> (2022)

# Bioinspired Design of Electrically Fueled Dissipative Self-assembly of Supramolecular Materials

Zhibin Guan, University of California, Irvine, Irvine, CA 92697 (zguan@uci.edu)

**Keywords:** dissipative self-assembly, active materials, electrical fuel, supramolecular materials, hydrogels

## Program Scope

The overall objective of this project is to mimic nature's out-of-equilibrium self-assembly processes to develop dissipative self-assembly of active materials using redox chemistry. Fuel driven dissipative, out-of-equilibrium assemblies, such as microtubule and actin filaments, are at the heart for many cellular processes, including cellular transport, cell motility, proliferation, and morphogenesis. Such dissipative processes in nature have inspired the design of synthetic self-assembled systems driven by chemical fuels. Nevertheless, the currently reported chemical-fueled dissipative assembly have several major limitations such as the use of harsh and toxic fuels, the creation of wastes, the relatively low fueling efficiency due to nonproductive background reactions, and the lack of precise spatiotemporal control of the active assemblies. These limitations critically hinder further development of active materials for real applications. With the DOE support, this project is aimed to address several of these key issues by developing out-of-equilibrium self-assembly system using mild chemical redox reaction network. During this review period, we have developed a fully electrically fueled dissipative self-assembly system that is waste-free, highly sustainable, and can provide precise spatiotemporal control. In addition, by combining light and electricity as two non-invasive, spatiotemporally addressable energy fuels, we show precise control of dissipative self-assembly of supramolecular materials.

## Recent Progress

### 1. Waste-free, fully electrically fueled dissipative self-assembly of supramolecular materials

During the previous report period, we developed a half electrically fueled dissipative self-assembly system in which electrochemical oxidation of a cysteine derivative (CSH) into its disulfide dimer (CSSC) initiates supramolecular polymerization to form long nano-fibers that grow directionally from the working electrode surface toward the counter electrode. Chemical reduction of CSSC back to CSH causes dissipative assembly of the fibers (*J. Am. Chem. Soc.* **2022**, *144*, 7844–7851). Although this half electrically-fueled dissipative self-assembly system demonstrates several advantageous features including the directionality of fiber assembly and spatiotemporal control of the assembly, it still generates chemical waste because the reduction still proceeds through chemical reduction process. Because of the waste accumulation with time, the system continues changing and cannot sustain for a long time (**Fig. 1a**).

To solve this major problem for all chemically fueled dissipative material systems, during this review period we developed a waste-free, fully electrically fueled dissipative self-assembly system. To achieve, we coupled two electrocatalytic cycles – one creating a catalytic oxidant at anode and the other generating a catalytic reductant at cathode, both electrochemically – to drive both the assembly and disassembly simultaneously by electricity (**Fig. 1b**). After carefully screening many electrochemical reductive catalysts, we chose methyl viologen ( $[MV]^{2+}$ ) as the

mediator for electrochemical reduction at the cathode. While anodic oxidation generates  $[\text{Fe}(\text{CN})_6]^{3-}$  catalytic oxidant as positive fuel that oxidized CSH into CSSC initiating self-assembly of fibers, cathodic reduction of  $[\text{MV}]^{2+}$  produced a catalytic reductant ( $[\text{MV}]^{+}$ ) as negative fuel that reduced CSSC back to CSH and triggered disassembly (**Fig. 2a**). By integrating the anodic and cathodic half cycles into one system, we accomplished a fully electrically fueled active self-assembly system that is completely waste free, with spatiotemporal control, and could sustain over an extended period.

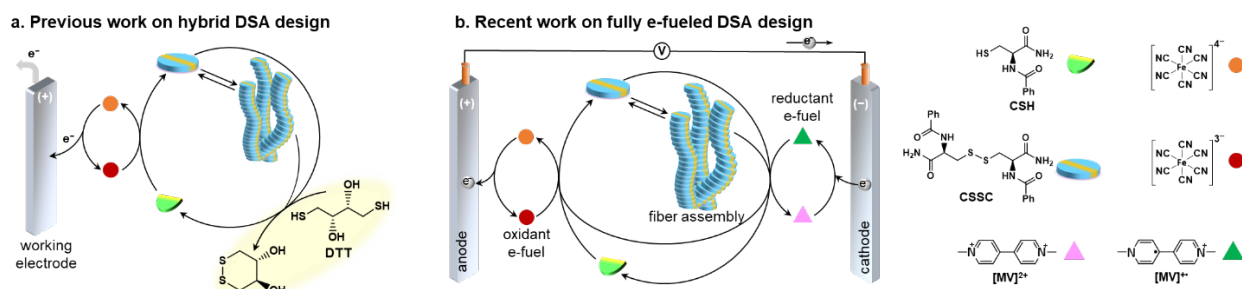


**Figure 1.** (a) Hybrid design combining electrical fuel for CSH oxidation and chemical fuel DTT for CSSC reduction showing generation of chemical waste. (b) Fully electrically fueled dissipative self-assembly design mediated by dual electrocatalytic cycles. When electric field is applied, anodic oxidation of  $[\text{Fe}(\text{CN})_6]^{4-}$  forms  $[\text{Fe}(\text{CN})_6]^{3-}$  that further oxidizes CSH into CSSC for fiber assembly, and simultaneously  $[\text{MV}]^{2+}$  is electrochemically reduced to  $[\text{MV}]^{+}$  at cathode that further reduces CSSC to CSH for disassembly.

By coupling the synchronous electrocatalytic formation of oxidant and reductant with redox-controlled interconversion between CSH and CSSC, we achieved the first fully electrically fueled dissipative self-assembly system. Transient fiber assembly was shown by repetitively turning on and off the electrical voltage. Through balancing CSH oxidation by positive fuel for fiber assembly and CSSC reduction by negative fuel for fiber disassembly, dynamic active self-assembly was sustained by electrical potential (**Fig. 2b**). Compared to chemical-fueled synthetic dissipative self-assembly systems, the fully electrically fueled dissipative self-assembly system demonstrated here has several advantageous features. First, due to the complete electrocatalytic reaction cycles, no chemical waste is produced in the entire process. Second, the absence of waste generation allows us to achieve a homeostatic active dissipative self-assembly system that can be sustained for an extended period of time (**Fig. 2c**), which was not possible for any previous synthetic closed-system active materials. Such fully electrically fueled, waste-free, and sustainable active material platform will be employed to investigate other redox active supramolecular self-assembly systems which may open door to potential bioelectronic applications in the future.

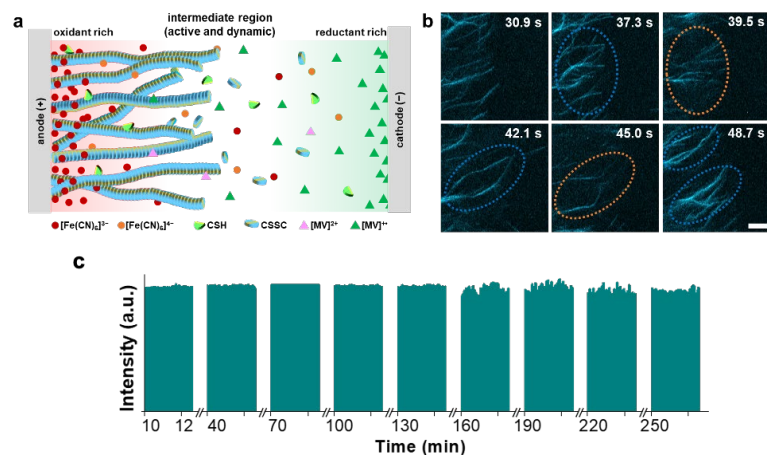


**Figure 2.** (a) Schematic illustration showing generation of catalytic oxidant and reductant upon electrically fueled activation inducing CSH  $\leftrightarrow$  CSSC interconversions to achieve active self-assembly. (b) CLSM snapshots of fully electrically fueled system displaying active and dynamic features undergoing rapid growth and shrinkage of CSSC fibers. (c) The corresponding average fluorescence intensity profiles derived from CLSM image frames showing the sustainable active assembly system for up to 250 min of electrical fueling.

## 2. Precise control of dissipative self-assembly by using both light and electricity

In another study, we successfully combined light and electricity as two clean, and spatiotemporally addressable fuels to provide precise control over the morphology for dissipative self-assembly of a perylenebisimide glycine (PBIg) building block in a self-contained solution. In this design, electrochemical oxidation provides the positive fuel to activate PBIg self-assembly while photoreduction supplies the negative fuel to deactivate the system for disassembly. Through programming the two counteracting fuels, we demonstrated the control of PBIg self-assembly into a variety of assembly morphologies in a self-contained system (**Fig. 3**). In addition, by exerting light and electrical dual fuels simultaneously, we could create an active homeostasis exhibiting dynamic instability, leading to morphological change to asymmetric assemblies with curvatures. Such precise control over self-assembly of self-contained systems may find future applications in programming complex active materials as well as formulating pharmaceutical reagents with desired morphologies.

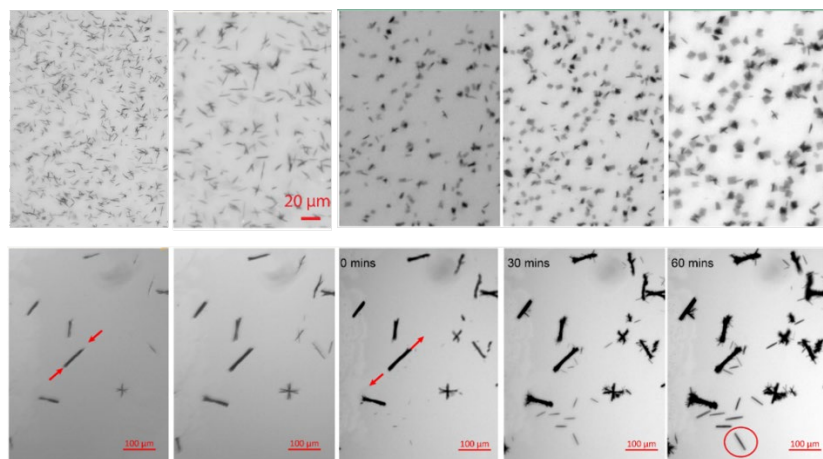


**Figure 3.** Programmable self-assembly of PBIg by controlling the application of UV light and electrical potential. Through judicious programming light and electricity as two clean and spatiotemporally addressable fuels, we can control the morphology of PBIg assembly.

This is the first example of using both light and electricity to fuel a dissipative self-assembly system. By programming the sequence of photoreduction and electrochemical oxidation, we could obtain a diverse range of aggregate morphologies for the same building block without altering the solution composition. Excitingly, the dual fuel-sustained active system displayed a morphological change of the aggregates to asymmetric assemblies with curvatures. Such precise control over

supramolecular assemblies in self-contained systems may find future applications in programming complex active materials as well as formulating pharmaceutical reagents with desired morphologies.

### **Future Plans**

In our further study, we will continue developing new strategies for energy-fueled dissipative self-assembly platforms while simultaneously exploring potential functional applications of such active material systems. For example, we plan to investigate our electrically fueled dissipative assembled materials for dynamic structural color changing device and for dynamic resistive switch devices for neuromorphic computing. In addition, we will collaborate with theoretical researchers to gain fundamental understanding of the active self-assembly process and develop kinetic models for the dissipative self-assembly systems.

### **Publications in year 2021-2023 (which acknowledge DOE support):**

1. Selmani, S.; Schwartz, E.; Mulvey, J.; Wei, H.; Grosvirt-Dramen, A.; Gibson, W.; Hochbaum, A. I.; Patterson, J. P.; Ragan, R.; Guan, Z. “Electrically fueled active supramolecular materials” *J. Am. Chem. Soc.* 2022, 144, 7844–7851. <https://pubs.acs.org/doi/10.1021/jacs.2c01884>
2. Barpuzary, D.; Hurst, P.; Patterson, J.; Guan, Z. “Waste Free Fully Electrically Fueled Dissipative Self-assembly System” *J. Am. Chem. Soc.* 2023, 145, 3727–3735. <https://pubs.acs.org/doi/10.1021/jacs.2c13140>
3. Chen, C.; Guan, Z. “Precise Control of Dissipative Self-assembly by Light and Electricity” *Chem. E. J.* 2023, 29, 9, e202300347. <https://doi.org/10.1002/chem.202300347>
4. Jo, H.; Selmani, S.; Sim, S.; Guan, Z. “Sugar-Fueled Dissipative Living Materials”, *J. Am. Chem. Soc.* 2023, 145, 811–1817. <https://pubs.acs.org/doi/full/10.1021/jacs.2c11122>
5. Tretbar, C. A.; Castro, J.; Yokoyama, K.; Guan, Z. “Fluoride-Catalyzed Siloxane Exchange as a Robust Dynamic Chemistry for High-Performance Vitrimers”, *Adv. Mater.* 2023, 2303280. <https://onlinelibrary.wiley.com/doi/10.1002/adma.202303280>

## Machine learning approaches to understanding and controlling 3D active matter

Michael F. Hagan, Brandeis University (Principal Investigator)

Seth Fraden, Brandeis University (Co-Investigator)

Pengyu Hong, Brandeis University (Co-Investigator)

Zvonimir Dogic, University of California Santa Barbara (Co-Investigator)

**Keywords:** Active matter, Machine learning, data-driven methods, optimal control, deep learning

**Research Scope:** In Aim 1, we are developing model-free control protocols that redirect active materials to arbitrary new states. To enable precise control even in the absence of accurate theoretical models, we will combine large experimental data sets, Deep Learning (DL), and reinforcement learning (RL) to develop a model-independent framework that predicts and controls the dynamics of 3D active materials. The framework will not require the knowledge of the underlying microscopic mechanisms, but will leverage the symmetries of the system. In Aim 2, we develop model-predictive control protocols that target preset dynamics. We use optimal control theory to identify spatiotemporal sequences of light-generated activity or crosslinks that direct the dynamics of 3D active matter toward a predetermined steady state. We use the identified control protocols and their efficacy to understand the statistical properties of active stresses and their causal influence on the emergent dynamics. In Aim 3, we combine data-driven approaches with large experimental datasets to improve physics-based models of active materials. These models can describe experiments with higher accuracy, while also revealing how active stresses cascade across scales to generate collective dynamics and functionalities, without a priori knowledge of the microdynamics.

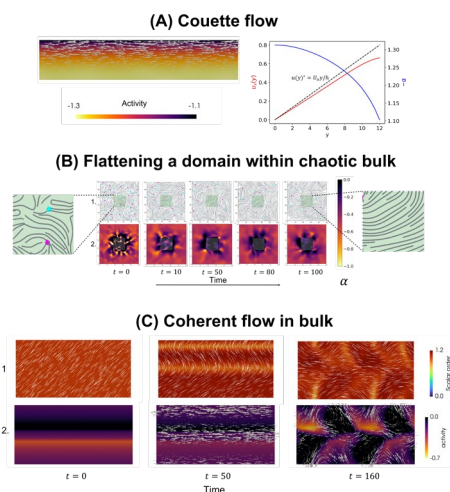


**Fig. 2.** Optimal control of light driven active nematic : (A) Activity pattern that drives a Couette like flow in a channel geometry. (B) Activity patterns that flatten a square domain into an aligned state. (C) Activity patterns that drive coherent flow along a strip or "channel" within a bulk system.

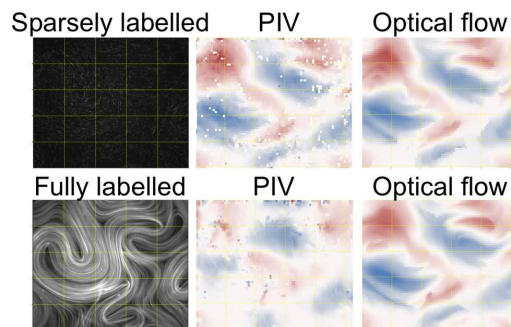


**Fig. 1.** Velocity (in pixels per frame) obtained by PIV and Optical Flow for sparsely and fully labelled active nematics. PIV is adequate for sparse labeling but fails for full labeling. Optical Flow performs well in both cases.

### Recent Progress:

Deep learning (DL) techniques to automatically generate director fields and identify defects from experimental fluorescence data:

We developed a

robust DL tool to extract director fields and defects from experimental images. This dramatically outperforms existing tools and eliminates the need for quantitative polarization microscopy, which dramatically increases the range of possible experiments. Applying traditional Particle Imaging Velocimetry (PIV) techniques to our 3D systems produces velocity profiles with too low resolution for data-driven methods. Therefore, we adapted a DL-based unsupervised optical flow model that robustly extracts flow fields from image sequences of active nematics. The framework yields velocity profiles with significantly higher resolution and

accuracy than PIV (Fig. 1). The method works well for all conditions, while PIV requires tuning parameters for different conditions. We anticipate that this will become a widely used ML-based tool in soft matter and beyond.

**Aim 1: Model-free forecasting.** Previous work [1,2] constructed Long-Short Term Memory (LSTM) neural networks that predict the future dynamics of an active nematic system including key physical events such as defect nucleation and annihilation. We have extended the model to learn a discrete latent space capable of reproducing fluorescence images of active nematics. All frames in 2D nematic videos are then encoded in the embedding space, and a large transformer model is trained to learn the dynamics in the latent space. These predictions are then decoded into the pixel space. Initial results suggest that the discrete latent space model outperforms our previous approaches, and the dimensionality reduction should significantly enhance human interpretability.

**Aim 2 (Optimal control):** To complement the model-free machine learning techniques, we are using optimal control theory to perform model-predictive control on active fluids. As first steps,

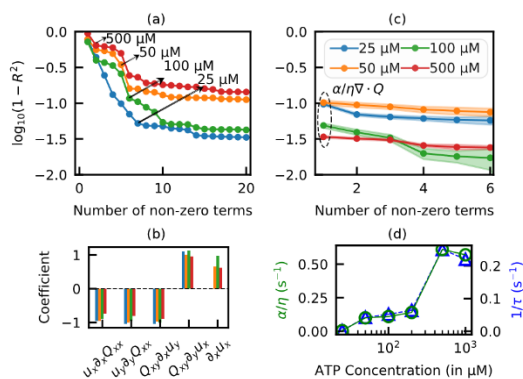


**Fig. 3. Discovering the optimal hydrodynamic theory from 2D active nematic experiments [3].**

(a) Optimality curves,  $\log(1 - R^2)$  vs. number of non-zero terms,  $n$ , for the alignment equation with indicated ATP concentrations. (b) C coefficients of key flow-coupling terms appearing in the optimal models for various ATP concentrations. (c) Optimality curves for the flow equation. (d) The fit coefficient of the activity term,  $\alpha / \eta$ , as a function of the ATP concentration (green circles).

we investigated 2D polar active fluids and active nematics. For the polar case, we computed protocols that move asters along a predetermined distance and direction, flip the direction of polar flocks, and transform a polar flock state into an aster state. For active nematics, we robustly demonstrate the controllability of the director field and velocity field for a number of target states. Fig. 2 shows several examples: (A) Mimicking a Couette flow structure in a channel geometry; (B) A flat, defect-free director field. This is the ideal starting point for any control target but currently is impossible to achieve experimentally. (C) Coherent flow along a strip or “channel”, where the “walls” of the channel are themselves light gradients. We extensively tested convergence and robustness and identified strategies when the target state is far from the initial state leading to a highly rugged landscape for the optimal control theory loss function.

**Aim 3: Data-driven model discovery:** We adapted Sparse Identification of Nonlinear Dynamics (SINDy), to automatically determine the equations of motion that most accurately capture the system’s time evolution, from both experiments and simulations. We first implemented SINDy in 2D [Ref. 3]. This testing in 2D is an essential step toward 3D, due to the complexity and extremely large size of 3D data sets. We determined several sources of experimental error and developed two powerful noise mitigation strategies. The equations discovered from the experimental data show that the dynamics are described by a surprisingly minimal model, with flow coupling, viscous damping, and the lowest order active stress term; elastic energy, substrate friction, and inertial terms are negligible. The model quantitatively describes the experiments without fit parameters (Fig. 3) and estimates parameters that cannot be directly measured in experiments. Next, we obtained preliminary equations for dry active nematics with negligible hydrodynamic interactions, using data from particle-based simulations. This is a significant test because appropriate governing equations are unknown, but are more complicated than those for wet active nematics. To extend these approaches to 3D, we developed an algorithm to automatically generate (in 3D) all combinations of variables and their gradients that satisfy physical constraints, and avoid co-linear terms.

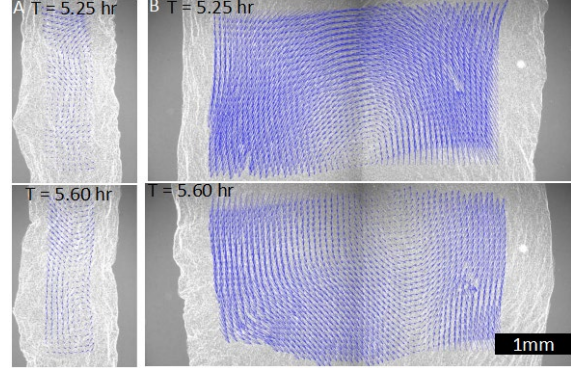


**Fig. 4:** Self-organized oscillation of active elastic sheets. Images of membranes undergoing in-plane dynamics. Chamber width, (A) 2.5 mm (B) 8 mm.

**Experiments: (1) Optogenetic motors:** We characterized optically responsive kinesin motors that allow for robust and repeatable spacetime control of their active stress with temporal resolution of tens of seconds. We used the unique features of this system to control the temporal and spatial evolution of the bend instability [4], which is the foundational property of active fluids. These results form the basis for experimental implementation of optimal control that is currently underway. **(2) Experimental Light Control:** We characterized two-dimensional (2D) microtubule-based active nematics driven by light-responsive opto-K365 kinesin motor clusters. The steady-state nematic flow and defect densities are set by the applied light intensity across centimeter-sized samples. Measurements reveal an order of magnitude improvement in the contrast of nematic flow speeds between maximally- and minimally-illuminated states for opto-K365 motors compared to the prior opto-K401 motors. This work establishes an experimental platform to test theoretical frameworks that exploit spatiotemporally-heterogeneous patterns of activity to generate targeted dynamical states. **(3) Active composites:** We developed novel active-solid composites based on bundled actin filaments and the microtubule-based active fluid. These materials exhibit several unique features including self-organized system-sized spontaneous oscillations. Using large scale data-sets and quantitative image analysis we quantified across all relevant length and time scales how active fluids imprint the shape, structure, mechanics and non-equilibrium dynamics of self-organized elastic membranes (Fig. 4).

**Future Plans:** Future plans include the following. **Aim 1:** We will extend the DL director field extractor, optical flow techniques, and forecaster to 3D. **Aim 2:** We will apply our active nematics model to the experimental system with optogenetic kinesins, where activity is controlled by light intensity. We will use the light control optics and open system flow cell to measure defect

distributions in active nematics in an activity gradient. Using these results, we will create data driven controllers that aim for activity patterns leading to behaviors such as shown in the figures. **Aim 3:** To progress our 3D SINDy implementation despite the low resolution and accuracy of PIV data, we will extend our optical flow framework to 3D, and use that framework to obtain velocity fields from the experimental 3D data. We will then apply our 3D SINDy framework to 3D active isotropic and active nematic systems. **Experiments:** We completed development of a dielectric tensor tomography setup that will allow us to image the director of 3D active nematics with improved spatial resolution and temporal resolution of 30 ms, which is about two orders of magnitude faster than what was possible previously. We will use this technique to image dynamics of 3D active nematics with sufficient spatiotemporal resolution to develop quantitative models of their non-equilibrium dynamics. At the same time, we plan to apply SINDy to light-activated systems. We will begin with systems with uniform light activation, at differing intensity levels. Subsequently, we will apply SINDy to systems with gradients of light. For active composites, we will quantitatively characterize the structure, mechanics, and non-equilibrium dynamics of self-organized elastic actin sheets at all relevant length and time scales. In particular, we will develop machine learning tools to characterize the microscopic network structure of the actin membranes and related this structure to its mechanical properties and dynamics. This will be essential information to inform the quantitative models that we are developing in parallel.

## References

1. Colen, J., Han, M., Zhang, R., Redford, S. A., Lemma, L. M., Morgan, L., Ruijgrok, P. V., Adkins, R., Bryant, Z., Dogic, Z., Gardel, M. L., de Pablo, J. J. & Vitelli, V. Machine learning active-nematic hydrodynamics. *Proc. Natl. Acad. Sci. U. S. A.* **118**, e2016708118 (2021).
2. Zhou, Z., Joshi, C., Liu, R., Norton, M. M., Lemma, L., Dogic, Z., Hagan, M. F., Fraden, S. & Hong, P. Machine learning forecasting of active nematics. *Soft Matter*, doi:10.1039/D0SM01316A (2020).
3. Joshi, C., Ray, S., Lemma, L. M., Varghese, M., Sharp, G., Dogic, Z., Baskaran, A. & Hagan, M. F. Data-Driven Discovery of Active Nematic Hydrodynamics. *Phys. Rev. Lett.* **129**, 258001, (2022).
4. Lemma, L. M., Varghese, M., Ross, T. D., Thomson, M., Baskaran, A. & Dogic, Z. Spatio-temporal patterning of extensile active stresses in microtubule-based active fluids. *PNAS Nexus* **2**, doi:10.1093/pnasnexus/pgad130 (2023).

## Publications

1. Joshi, C., Ray, S., Lemma, L. M., Varghese, M., Sharp, G., Dogic, Z., Baskaran, A. & Hagan, M. F. Data-Driven Discovery of Active Nematic Hydrodynamics. *Phys. Rev. Lett.* **129**, 258001, (2022).
2. Lemma, L. M., Varghese, M., Ross, T. D., Thomson, M., Baskaran, A. & Dogic, Z. Spatio-temporal patterning of extensile active stresses in microtubule-based active fluids. *PNAS Nexus* **2**, doi:10.1093/pnasnexus/pgad130 (2023).

## Propulsion of synthetic protocells and coacervates driven by biochemical catalysis

Daniel A. Hammer<sup>1,2</sup> (PI), Daeyeon Lee<sup>2</sup> (co-I), Matthew C. Good<sup>1,3</sup> (co-I), Departments of <sup>1</sup>Bioengineering, <sup>2</sup>Chemical and Biomolecular Engineering and <sup>3</sup>Cell and Developmental Biology, University of Pennsylvania, Philadelphia, PA 19104

**Keywords:** Protocells, Enzyme Propulsion, Urease, Coacervating Proteins, Surfactants,

### Research Scope

An important area in the design of biomolecular materials is the recapitulation of cellular activities through the assembly of molecular components into functional synthetic cells, or protocells. By building cell-like structures that mimic the organization and size of natural cells but incorporate novel, responsive components, we can augment their capabilities beyond biological limitations, including the ability to convert chemical and radiant energies to mechanical energy. The scope of this project is to make uniform, enzyme functionalized capsules by microfluidic assembly. We propose to ultimately drive the motility of these protocells with a wide range of enzymatic systems and use both surface and intra-protocell cascades to drive directed motion of protocells using gradients of substrates, heterogeneously applied stimuli, or asymmetric distributions of enzymes on the capsule surface. We will also leverage our novel protein coacervation system to make motile coacervates, and to use coacervates to make as membrane-less organelles which will serve as hubs for enzymatic activity that drive protocells motion.

**Relevance to DOE mission.** Our research on synthetic cells (protocells) fits the goals of the DOE BES Biomolecular Materials program, specifically to use *biological cells as a blueprint* for assembling functional protocells. The work we propose is a fundamental exploration of the design of protocells and coacervates as *adaptive, motile matter*, whose *morphology, content, behavior and performance* can be controlled through directed biochemical catalysis through the reconstitution and activation of enzymes, thus leading to the conversion of chemical to mechanical energy. The aims of the current research are to: (1) Measure the motility of single uniform protocells, in which we have developed innovative methods for synthesis of uniform cell-like microcapsules to quantify the effects of enzymatic activity on capsule motion. (2) Measure the effect of particle-particle interactions on the collective motion of groups of particles. It has been predicted that motile systems will display hydrodynamic coupling over length scales much longer than the particle size [R1]. We are measuring the effect of particle concentration (volume fraction) on the collective motion of motile particles. (3) Develop coacervates that act as membrane-less organelles in protocells to harvest enzymatic motion. Our goal is to use coacervating proteins as microcompartments in protocells to create regulatory hubs that guide protocell motion. We have embedded active enzymes within or on coacervates. We are also developing multiple orthogonal condensate systems so that we can build multifunctional cascades in protocells.

## Recent Progress

In a previous period we demonstrated the motility of polymersomes over surfaces driven by catalase [R2]. In this period, we have successfully made motile, uniform capsules from poly (lactic-co-glycolic acid) (PLGA) shells functionalized with the enzyme urease [P1]. Urease-powered micromotors are assembled from 75:25 PLGA polymers with a molecular weight range of 85 to 115kD (**Figure 1**). The inner phase consists of a dilute NaCl solution for osmotic balance; the outer phase contains either poly(vinyl alcohol) (PVA) or poly(ethylene-alt-maleic anhydride) (PEMA), which stabilize the oil-water interface and integrate into the particle. Asymmetry is thought to facilitate microswimmer motion [R2]. To systematically build in asymmetry and surface roughness, we added hydrophobic silica ( $\text{SiO}_2$ ) nanoparticles at 0.2 or 0.4 wt % in the middle phase. Microcapsules range from 30 - 60  $\mu\text{m}$  in diameter, and to prepare capsules are similar in size to leukocytes (10 - 20  $\mu\text{m}$ ), we annealed the particles in a high NaCl solution. At low nanoparticle concentrations, the dilute nanoparticles pack during solvent extraction to produce **smooth** microcapsules (**Figure 1b**). At high concentration of  $\text{SiO}_2$  nanoparticles, a dense packing of nanoparticles causes the interface to buckle upon drying (**Figure 1b**), creating **rough** particles. Microcapsules are formed upon solvent evaporation.

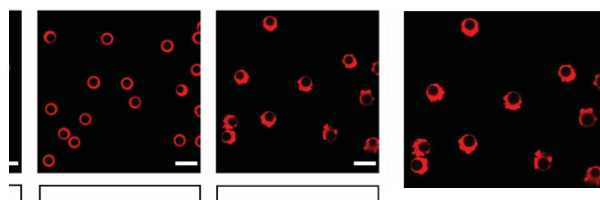


**Figure 2.** Rough PLGA microcapsules made with PEMA surfactant and 0.4 vol%  $\text{SiO}_2$  particles. The polymer layer is stained with Nile Red (left) (scale bar 10  $\mu\text{m}$ ), mean particle diameter is 16.5  $\mu\text{m}$  (middle), and SEM shows substantial surface roughness (right; scale bar 5  $\mu\text{m}$ ).

when the  $\text{SiO}_2$  concentration is high. These particles have the shape and surface roughness of biological cells, such as leukocytes. This procedure leads to particle diameters about 15  $\mu\text{m}$  in diameter; for example, rough PEMA-PLGA microcapsules are 16.5  $\mu\text{m}$  (see **Figure 2**).

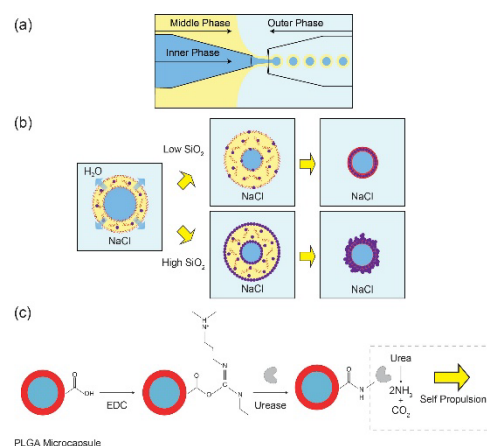


**Figure 1:** Overview of micromotor fabrication. Schematic illustrations of (a) microfluidic fabrication of water-in-oil-in-water (W/O/W) double emulsion droplets in a capillary microfluidic device, (b) size reduction of smooth (low  $\text{SiO}_2$ ) and rough (high  $\text{SiO}_2$ ) microcapsules by osmotic annealing in high salt solutions, and (c) urease functionalization using carbodiimide chemistry.

These capsules display active motion at a concentration of 100 mM urea. The avidity of the motion follows the qualitative trend Rough-PEMA>>Smooth-PEMA>Smooth PVA. **Figure 3** illustrates the trajectories of Smooth-PEMA (Fig. 3a) and Rough-PEMA (Fig. 3b) particles over 150 seconds (scale bar 100  $\mu\text{m}$ ). MSD plots show substantially more motion for Rough-PEMA particles (Fig. 3c), with a substantially higher value of  $\alpha$  (fit with  $\text{MSD} = bt^\alpha$ ) and a speed three times as high (**Fig. 3**). A paper has been submitted [P6].

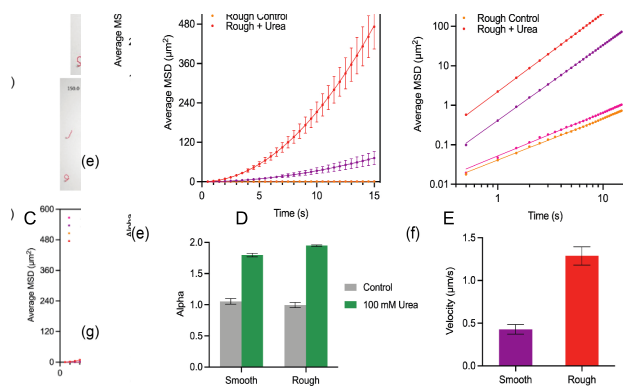


**Figure 3.** Panels A and B are representative trajectories of Smooth-PEMA and Rough-PEMA particles over 150 seconds in 100 mM urea. Panel C illustrates the MSD of Smooth-PEMA and Rough-PEMA in the presence and absence of 100 mM urea. (D) Both smooth and rough PEMA particles show active motion with values of  $\alpha$  close to 2. E. The velocity of rough-PEMA particles is almost three times that of smooth PEMA particles.

than their size, and that the mechanism of enzyme motion is through hydrodynamic streaming (due to osmotic flow).

We have also made substantial progress in the design of condensates (aim 3). Our design strategy is to make designer condensates using molecular biology through the multimeric assembly of the RGG domain of Laf-1, a protein that regulates RNA translation in *C. elegans* [R5]. By making multimers of RGG, we can regulate the phase behavior of the protein. We have shown that we can assemble multimers of RGG using small coiled-coil peptide binders, such as designed by the Jerala laboratory [R3, P2]. Furthermore, we can insert protease cleavable domains and light cleavable molecules (such as PhoCI) to reverse phase separation.

In this period, we highlight two major accomplishments. The first is that we have sequestered an active enzyme, NanoLuciferase (NLuc) within RGG droplets by placing the NLuc between two RGG domains. This active enzyme self-assembled into droplets and emits light. NLuc is also available as a split enzyme – LargeBit and SmallBit. To assemble these pieces, we placed LargeBit between two RGG domains and then triggered the release of RGG-SmallBit-RGG from a larger protein containing the maltose binding protein (MBP) solubility tag using a protease. When the protease is added, the RGG-smallBit-RGG is released and it assembled with its LargeBit counterpart in a coacervate, leading to the formation of a functional enzyme and the emission of light in response to furamizine, thus demonstrating assembly of a functional enzyme on cue [P5].

We have also made significant progress in assembling orthogonal condensates, which would allow us to build cascades of enzymes in two compartments. We have found that in addition to RGG condensates, we can assemble condensates from the low complexity domain of FUS (FUS

LC) and they are orthogonal to RGG condensates. The two phases will wet each other in suspension, but not fully mix. Separately, using mutation, our group has worked out the critical features of sequence that are responsible for this orthogonality [P4]. We have made novel protein surfactants to link together immiscible RGG and FUS LC condensates in unique ways. We made an RGG-mScarlet-FUS LC to link the two phases together. In **Figure 4** we illustrate that we can use this surfactant to coat either RGG droplets (Fig 4, left) or coat FUS LC droplets (Fig 4, left center). If we make RGG (labeled green with *gfp*) and FUS LC droplets (labeled blue with *bfp*), they wet, and upon addition we can form a novel three phase system (Fig. 4, right center). If we premake FUS LC droplets, and add RGG and surfactant, we can completely engulf the FUS LC droplets in RGG droplets (make a phagosome, Fig. 4 right). Thus, using engineered condensation, we can make assemblies reminiscent of basic biological processes.

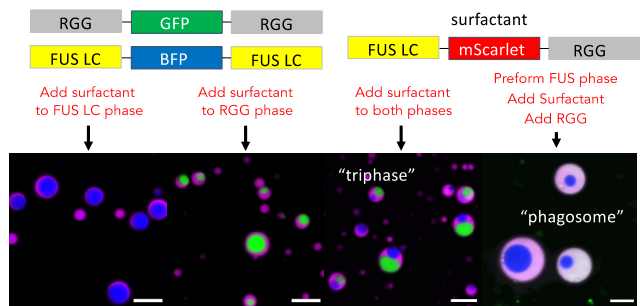


**Figure 4.** RGG and FUS LC are non-mixing phases. We used a surfactant (FUS LC-mScarlet-RGG) to assemble the two phases into various structures. The surfactant will coat either phase. When the two phases are mixed, and surfactant is added, a triphase is made. When FUS LC is added, then surfactant, then RGG, the FUS LC is trapped in the interior of the droplet, leading to a phagosome. Scale 10µm.

## Future Plans

In the near term, we will measure the collective behavior of active urease capsules over a range of volume fractions and urea concentrations, as well as blend active and inactive particles at different ratios to determine if active particle can cause streaming of inactive particles. We have also made Janus capsules by microfluidics with PLGA and polycaprolactone lobes, and we will examine the motility of asymmetric Janus particles. For our condensates, we are examining further ways that we can assemble orthogonal materials, using multimers of coiled-coil domains and light activated switches. Furthermore, we plan to measure the motility of condensates that are propelled by enzymes sequestered in a patch.

## References

1. Kolmakov, G.V., V.V. Yashin, S.P. Levitan, and A.C. Balazs, *Designing communicating colonies of biomimetic microcapsules*. Proceedings of the National Academy of Sciences of the United States of America, **107**(28):12417 (2010).
2. Jang, W.S., H.J. Kim, C. Gao, D. Lee, and D.A. Hammer, *Enzymatically Powered Surface-Associated Self-Motile Protocells*. Small **14**(36):8 (2018).
3. Parmar, J.; Vilela, D.; Villa, K.; Wang, J.; Sánchez, S. Micro-and nanomotors as active environmental microcleaners and sensors. *Journal of the American Chemical Society* **140**, 9317(2018).
4. Lebar, T., D. Lainscek, E. Merljak, J. Aupic, and R. Jerala, *A tunable orthogonal coiled-coil interaction toolbox for engineering mammalian cells*. Nature Chemical Biology, 2020. **16**(5):513.
5. Schuster, B.S., E.H. Reed, R. Parthasarathy, C.N. Jahnke, R.M. Caldwell, J.G. Bermudez, H. Ramage, M.C. Good, and D.A. Hammer, *Controllable protein phase separation and modular recruitment to form responsive membraneless organelles*. Nature Communications, 2018. **9**:12.

## Publication (2 year)

1. Garabedian MV, Wang W, Dabdoub JB, Tong M, Caldwell RM, Benman W, Schuster BS, Deiters A, Good MC. *Designer membraneless organelles sequester native factors for control of cell behavior*. *Nature Chemical Biology* **17**:998-1007 (2021).
2. Garabedian MV, Su Z, Dabdoub J, Tong M, Deiters A, Hammer DA, Good MC. *Controlled Multimerization of Intrinsically Disordered Sequences*. *Biochemistry* **61**:2470-2481 (2022).
3. Qi Xiao, Naomi Rivera-Martinez, Calvin J. Raab, Jessica G. Bermudez, Matthew C. Good, Michael L. Klein, Virgil Percec, *Coassembly of liposomes, dendrimersomes and polymersomes with amphiphilic Janus dendrimers conjugated to mono- and Tris-nitrilotriacetic acid (NTA, Tris NTA) enhances protein recruitment*. *Giant* **9** 100089 (2022).
4. Welles RM, Sojitra KA, Garabedian MV, Xia B, Regy RM, Gallagher ER, Mittal J, **Good MC**. *Determinants of Disordered Protein Co-assembly into Discrete Condensates Phases* bioRxiv. Mar 12:2023.03.10.532134 (2023)
5. Guan, Muyang, Mikael V. Garabedian, Marcel Leutenegger, Benjamin S. Schuster, Matthew C. Good and Daniel A. Hammer, *Incorporation and Assembly of a Light-Emitting Enzymatic Reaction into Model Protein Condensates* *Biochemistry* **60** 3137-3151 (2021).
6. O'Callahan, Jessica C., Daeyeon Lee, and Daniel A. Hammer, *Urease-Powered Micromotors from Double-Emulsion-Templated Microcapsules*, submitted, *ACS Applied Materials and Interfaces*, (2023).

## Chemically fueled dissipative assembly of complex molecular architectures

C. Scott Hartley and Dominik Konkolewicz, Department of Chemistry and Biochemistry, Miami University

**Keywords:** Nonequilibrium, carbodiimides, polymer networks, self-assembly, systems chemistry

### Research Scope

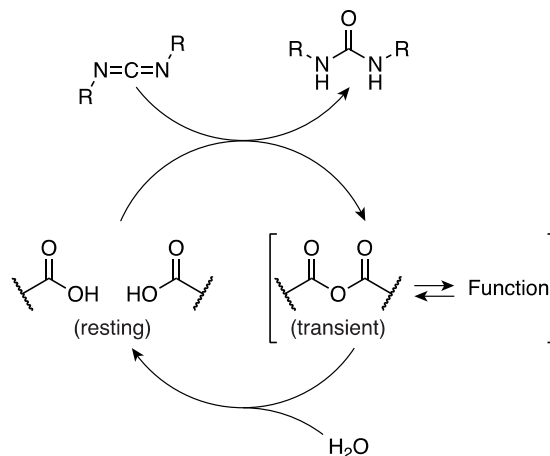
Biochemical systems often operate out of equilibrium by coupling functional behavior to spontaneous chemical reactions. This is best exemplified by ATP, which is used in many functional systems (e.g., muscle contraction). Using chemical “fuels” to drive systems out of equilibrium therefore has substantial potential for the creation of active materials with responsive, time-dependent behavior. Only recently has this concept been applied to nonbiological systems, however.

The conceptually simplest tool in the design of nonequilibrium chemical systems is the formation of a transient bond.<sup>1</sup> Many such reactions have been developed, including ester formation–hydrolysis, the decomposition of acids, and redox reactions. One of the most generally useful is the hydration of carbodiimides, most commonly coupled to the formation of carboxylic anhydrides as shown in Scheme 1. When carried out in aqueous solution, the anhydrides have lifetimes on the order of minutes to hours. This strategy was concurrently developed by Boekhoven and our group in 2017,<sup>2,3</sup> and has since been used in systems ranging from supramolecular assembly to the operation of molecular motors.

The overall goal of this project is to develop materials that exhibit time-dependent properties driven by carbodiimide hydration. We currently have three aims: (1) controlling the rate of carbodiimide activation, (2) exploiting transient polymerization, and (3) assembling transient three-dimensional molecular architectures.

### Recent Progress

**Controlling carbodiimide reactivity.** At its core, this project is about controlling the rates of reactions interacting in a reaction network. The minimal components of this network are obviously the anhydride formation (“activation”) and decomposition (“deactivation”) steps (Scheme 1). Controlling the rate of anhydride hydrolysis, through, for example, substituent effects or phase behavior, is reasonably well understood. However, little work has been done on



**Scheme 1.** Treatment of aqueous carboxylic acids with carbodiimides gives transient anhydrides.

controlling the rate of anhydride formation. Almost all studies simply use the water-soluble carbodiimide EDC with little consideration of the activation rate.

We had originally planned to address this issue through the synthesis of alternative water-soluble carbodiimides, but we serendipitously discovered an alternate solution to the problem. EDC is not a “true” carbodiimide; it undergoes ring–chain tautomerization in solution,<sup>4</sup> which limits its reactivity. We discovered that an alternative quaternized version of EDC, “mEDC”, undergoes rapid, reversible adduct formation with pyridine derivatives, as shown in Figure 1. This chemistry appears to be orthogonal to the rest of the reaction network (Scheme 1), and thus the adduct should serve as a reservoir of carbodiimide, effectively allowing the rate of carbodiimide delivery to be controlled. The method should be substantially more convenient to use than methods relying on the synthesis of additional carbodiimides, as all of the reagents are commercially available.

**Transient polymerization.** We had previously shown that aqueous carboxylic-acid-functionalized polymers could be transiently crosslinked by carbodiimides, giving transient hydrogels.<sup>5</sup> We have since investigated structure–property relationships in this system, looking at how polymer chain length, polymer composition, fuel concentration, and temperature affect mechanical properties and lifetimes in these systems.

We then applied this chemistry to new types of materials. While chemically driven sol → gel → sol transitions are of significant fundamental interest, for many practical applications weak gel → reinforced gel → weak gel transitions would arguably be more useful. Accordingly, we have investigated the effects of transient crosslinking in polymer network hydrogels with existing permanent crosslinks. Adding EDC to a suitable acid-functionalized network leads to a temporary strengthening of the gel, yielding increases in  $G'$  of up to an order of magnitude, as shown in Figure 2. Importantly, new applications of these materials are possible, since they remain rheological solids throughout the experiments. For example, separate pieces of the hydrogel can be reversibly adhered following treatment with EDC, with the time of adhesion determined by the EDC concentration. It is also possible to pattern temporary changes in mechanical properties in hydrogel films by spraying EDC solutions through a mask.

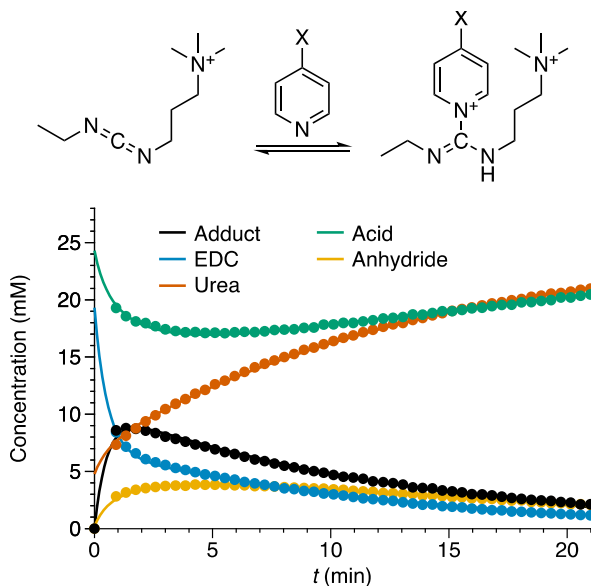


**Figure 1.** Formation of mEDC–pyridine adduct during a representative dimerization of a carboxylic acid.

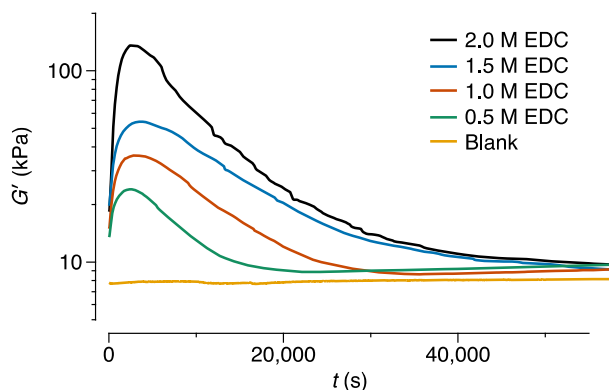


**Figure 2.**  $G'$  of a permanently crosslinked carboxylic-acid-containing hydrogel after treatment with EDC.

We have also explored the effect of polymer network architecture on changes in transient properties. Different starting semi-interpenetrated polymer networks (SIPNs) were prepared with different distributions of carboxylic acid groups, such that treatment with EDC would yield anhydride-linked single networks (SNs) or interpenetrated networks (IPNs). Network architecture has a substantial effect on the transient properties. Comparing materials with similar densities of carboxylic acids, transient IPN gels exhibited substantially lower peak  $G'$ , but a roughly fourfold increase in fracture energy (resistance to fracture), as shown in Figure 3.

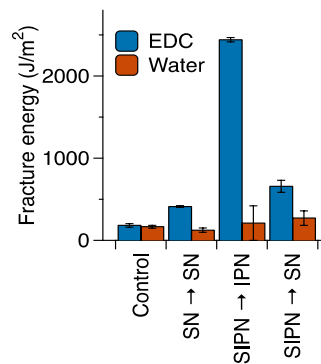


**Figure 3.** Effect of network architecture on fracture energy for materials with similar transient crosslink densities.

Inspired by the importance of transient polymers in biochemistry (e.g., actin filaments), we have recently developed a system that undergoes transient polymerization. Simple dicarboxylic acid monomers, shown in Figure 4, yield polymers on treatment with EDC. The properties (length, dispersity) and lifetimes are dictated by the amount of fuel used. Polymerization exhibits some unexpected behavior; for example, adding more EDC increases polymer length and dispersity early in the process, as expected, but lowers overall yield through increased formation of macrocycles. Because these are covalent polymers, the kinetics of growth and decomposition can be easily controlled, in contrast to the examples of transient supramolecular polymers that have been reported. For example, isomeric monomers with the alkoxy linkers para to the acids give polymers with much longer lifetimes.

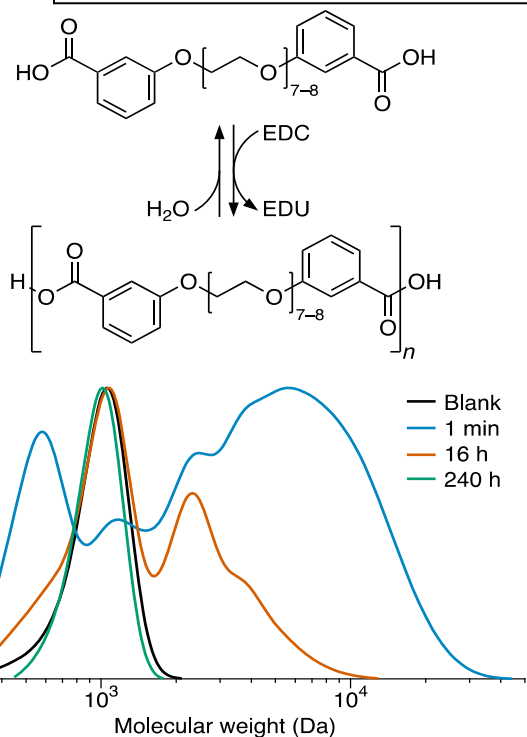


**Figure 4.** Transient polymerization of a diacid precursor.

**Transient assembly.** We have demonstrated a series of transient crown-ether-based cage compounds that can act as supramolecular hosts, shown in Chart 1. The formation and destruction of these cages is sensitive to the presence of alkali metal cation guests. Both positive and negative templation effects are observed for the smaller cages, and the larger cage binds  $\text{Na}^+$  in both its open and closed states.

## Future Plans

**Controlling carbodiimide reactivity.** We are currently optimizing the use of pyridine additives to control the rates of anhydride formation (and decomposition) in carbodiimide-driven reaction networks.

**Transient polymerization.** For the transient polymer networks, we are currently working to combine transient crosslinking with permanent but dynamic crosslinks in order to explore fuel-assisted self-healing behavior. As such, we have prepared polymers functionalized with both acids (for transient crosslinking) and terpyridine units (for dynamic crosslinking via coordination to metals). For the transient polymer chains, we plan to explore kinetically controlled self-sorting through the combination of monomers designed for both fast and slow anhydride hydrolysis.

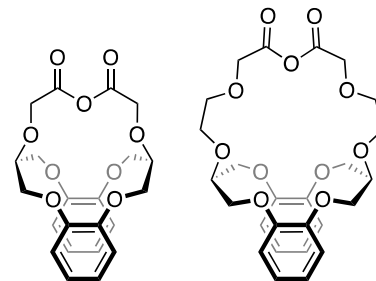


**Chart 1.** Transient crown-ether-based cages.

**Transient assembly.** We are currently focusing on two areas. We have prepared key intermediates for the synthesis of chemically controlled foldamers, taking advantage of our work on diphenic acids that undergo substantial changes in twist on treatment with carbodiimides. We are also developing model systems to study kinetic control mechanisms in the self-assembly of molecular cages.

## References

1. L. S. Kariyawasam, M. M. Hossain, and C. S. Hartley, *The Transient Covalent Bond in Abiotic Nonequilibrium Systems*, *Angew. Chem., Int. Ed.* **60**, 12648–12658 (2021).
2. M. Tena-Solsona, B. Rieß, R. K. Grötsch, F. C. Löhner, C. Wanzke, B. Käsdorf, A. R. Bausch, P. Müller-Buschbaum, O. Lieleg, and J. Boekhoven, *Non-Equilibrium Dissipative Supramolecular Materials with a Tunable Lifetime*, *Nat. Commun.* **8**, 15895 (2017).
3. L. S. Kariyawasam and C. S. Hartley, *Dissipative Assembly of Aqueous Carboxylic Acid Anhydrides Fueled by Carbodiimides*, *J. Am. Chem. Soc.* **139**, 11949–11955 (2017).
4. I. T. Ibrahim and A. Williams, *Reaction of the Water-Soluble Reagent N-Ethyl-N'-(3-dimethylaminopropyl)carbodiimide with Nucleophiles: Participation of the Tautomeric Cyclic Ammonioamidate as a Kinetically Important Intermediate*, *J. Am. Chem. Soc.* **100**, 7420–7421 (1978).
5. B. Zhang, I. M. Jayalath, J. Ke, J. L. Sparks, C. S. Hartley, and D. Konkolewicz, *Chemically Fueled Covalent Crosslinking of Polymer Materials*, *Chem. Commun.* **55**, 2086–2089 (2019).

## Publications

1. I. M. Jayalath, M. M. Gerken, G. Mantel, and C. S. Hartley, *Substituent Effects on Transient, Carbodiimide-Induced Geometry Changes in Diphenic Acids*, *J. Org. Chem.* **86**, 12024–12033 (2021).
2. O. J. Dodo, L. Petit, C. W. H. Rajawasam, C. S. Hartley, and D. Konkolewicz, *Tailoring Lifetimes and Properties of Carbodiimide-Fueled Covalently Cross-Linked Polymer Networks*, *Macromolecules* **54**, 9860–9867 (2021).
3. M. M. Hossain, I. M. Jayalath, R. Baral, and C. S. Hartley, *Carbodiimide-Induced Formation of Transient Polyether Cages*, *ChemSystemsChem* **4**, e202200016 (2022).
4. C. W. H. Rajawasam, C. Tran, M. Weeks, K. S. McCoy, R. Ross-Shannon, O. J. Dodo, J. L. Sparks, and C. S. Hartley, and D. Konkolewicz, *Chemically Fueled Reinforcement of Polymer Hydrogels*, *J. Am. Chem. Soc.* **145**, 5553–5560 (2023).

## **Activity-Enhanced Self-Assembly of Colloidal-Based Materials**

**Daphne Klotsa, University of North Carolina at Chapel Hill**

**David Pine, New York University**

**John Brady, California Institute of Technology**

**Keywords:** Active matter, colloids, self-assembly, defects, annealing

### **Research Scope**

The emerging field of *active matter*, has given us the ability to intentionally drive and dynamically manipulate individual particles in synthetic systems. Chemically-coated colloids and nanoparticles can self-propel or ‘swim’ in a directed way via a chemical fuel source and/or light activation. Doping of a material with active particles can speed up the assembly process by overcoming kinetic barriers, can increase the “effective local temperature” causing a rearrangement and annealing of defects, and can drive the system to completely new structures and pathways inaccessible through equilibrium processes. Our research program, which includes expertise in theory, simulation and experiment. is targeting three different classes of colloidal crystals made from passive Brownian colloidal particles and doped with active particles enhancing the self-assembly. Specifically, we are pursuing the following thrusts: assemble (i) FCC crystals using hard spherical colloids, (ii) FCC crystals and other cubic structures using DNA-coated colloids and (iii) clathrates and diamond. In this talk, we will present our recent results focusing on thrusts (i) and (ii).

### **Recent Progress**

#### Experiments

##### Active Matter: Light-activated Hematite particles

We are using light-activated particles to anneal different kinds of colloidal crystals. We synthesized active particles, consisting of a 900 nm hematite cube partially encapsulated on a 2  $\mu\text{m}$  TPM (3-methacryloxypropyl trimethoxysilane) spherical body. These active particles were studied under various conditions to control swimming speed. The conditions explored include H<sub>2</sub>O<sub>2</sub> concentration, pH (Bis-Tris is added to enhance hematite activity), and light intensity. Videos of the real-time movement of active particles are recorded under an optical microscope and evaluated according to their speed by tracking software (Trackpy). Active particles show a broad range of speeds under identical conditions. Thus, we are examining different methods of preparing active-particle as well optimizing the aqueous solvent in order to prepare particles with consistent high activity.

##### Passive Matter: Polystyrenes (PS) with modified surface

We designed and successfully prepared the cell to confine both passive and active particles using soft PDMS lithography. A hexagonal pattern mold is deposited on a glass substrate using SU-8 photoresist and UV exposure. The walls of the pattern are 5  $\mu\text{m}$  high, which is sufficient to confine the passive polystyrene particles that sediment within the hexagonal patterned walls (Figure 1). We use Python image-analysis software to detect the individual particles and identify the grains

and grain boundaries from optical microscope images. We then monitor the evolution of the grains to see how they anneal into a single crystal under the motion of the light-activated particles (Figure 2).

Our initial design was to use colloidal particles coated with DNA in order to induce crystallization. However, we have found that the DNA is denatured by hydrogen radicals that are produced by H<sub>2</sub>O<sub>2</sub> decomposition. Moreover, the PBS buffer required to stabilize the DNA significantly lowers the speed of the active particles. Therefore, we explored the possibility of using the depletion interaction to bind the particles together rather than using DNA. One concern in making this change is whether we could make the kind of patchy interactions that are needed to self-assemble the diamond lattice. Fortunately, we were able to find a way to make patchy colloids that have the desired attractive interaction only on the patches. Importantly, we find that the depletion interaction is still working even with the H<sub>2</sub>O<sub>2</sub> fuel in the solution. Thus, we feel that we have identified a good system for our studies of activity-induced annealing and crystallization. The immediate goal is to optimize the system for the maximal light-induced activity.

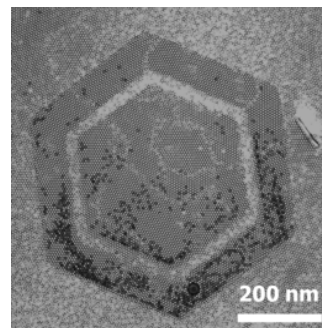


**Figure 1:** Hexagonal cell filled with a monolayer of sedimented Polystyrene spheres.

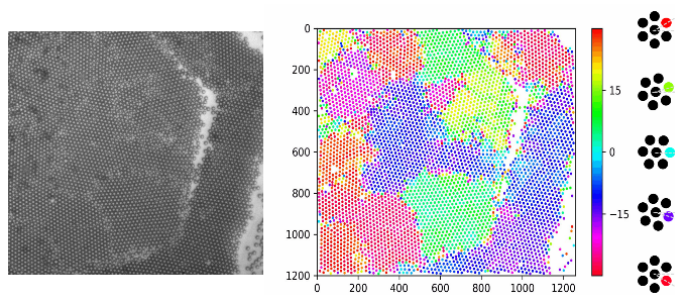


**Figure 2:** Microscope image showing the crystal domains (left) and grain detected image (right).

In terms of simulations, we characterized the annealing process, the structure and dynamics of each system by various measures. We characterized our simulation results using  $R_6$ , a measure estimated from the correlation function of the local orientational order  $g_6(r)$ , used in Ramananarivo et al. Nature Comms. 2019. A typical coarsening process for the Mie potential is shown in Figure 3. Based on these simulations, we observed a non-monotonic trend of crystallization as a function of the activity parameters, revealing the existence of an optimal swim force and doping fraction for each given packing density. At very high activity, the active particles first promote the crystallization, but after some time they disrupt the large crystal just formed, as shown in Figure 3. Using hard (Weeks-Chandler-Andersen) and Lennard Jones potentials, we see the same behavior further suggesting that the existence of optimal activity parameters and non-monotonicity is a robust feature independent of the specific potential.

We have also calculated the virial pressure, which reflects the stress relaxation as a function of time. The pressure is high when there is a lot of stress in the system, in our case stress comes from defects, and as the stress relaxes the pressure should drop. By doing this for many different parameters, we again recover non-monotonic behavior: there is an optimum activity and fraction

of active particles that enhance the self-assembly of the underlying passive crystal, beyond which the active particles disrupt the crystal rather than helping it.

We are discussing ways to understand and characterize the types of defects and the defect dynamics in our systems.

### Future Plans

Experiments:

- i) the immediate goal is to optimize the system for the maximal light-induced activity
- ii) perform the experiments and start measurements using depletion interaction
- iii) perform experiments of target classes of crystals identified in original goals

Simulations:

- i) continue exploration of parameter space and refine characterization tools
- ii) characterize and analyze defects and mechanisms for defect healing
- iii) start building the 3D simulation implementing knowledge from everything done so far

Theory:

- i) further quantify the dynamics of the defects
- ii) modify the point force model to account for the crystalline anisotropy
- iii) compare the simpler case of one embedded ABP interacting with one dislocation defect
- iv) use all the above to build up the theoretical model

### References

1. S. Ramanarivo, E. Ducrot and J. Palacci, *Activity-controlled annealing of colloidal monolayers*, Nature Comms. **10**, 3380 (2019).

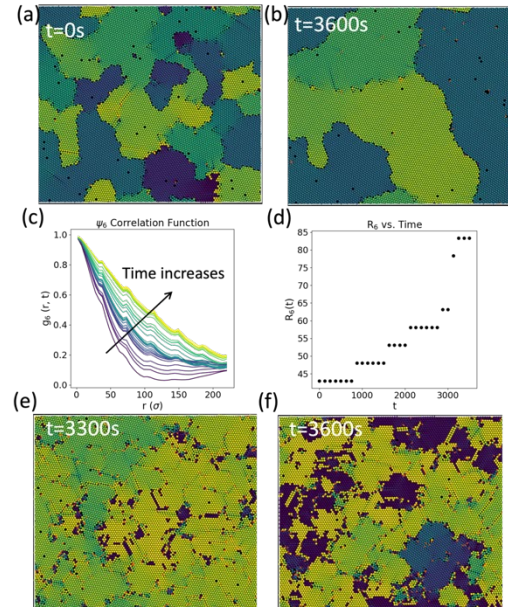


**Figure 3:** (a)-(b) Snapshots for the activity-induced coarsening process. The system shown of passive particles (5  $\mu\text{m}$  diameter) interact with each other through the attractive Mie potential at packing density of 0.85. Active particles are smaller (2  $\mu\text{m}$  diameter) shown in red. The colors of passive particles show the local orientation of crystalline order. Vacancies are visible as black dots. (c) Change in the correlation function  $g_6(r)$  with time. (d) Change in the typical crystallite domain size  $R_6$  with time. (e) At very high activity=200, the coarsening domain size reaches a maximum around  $t=3300s$ , but (f) the too high activity then disrupts the crystalline domains.

# Transport and Molecular Discrimination in Biomimetic Artificial Water Channels for Lanthanide Separations

Manish Kumar, The University of Texas at Austin.

**Keywords:** Membrane, lanthanides, supramolecular channel, rare earth elements, pillar[5]arene.

## Research Scope

Rare earth elements (REEs), encompassing seventeen metallic elements including fifteen lanthanides along with scandium and yttrium, are indispensable for modern industries and high-tech devices.<sup>1</sup> They play a vital role in renewable energy systems, energy-efficient infrastructure materials including in batteries for electric cars, energy-efficient lighting, display panels, and magnets for wind turbines,<sup>2</sup> medical imaging,<sup>3</sup> petroleum refining,<sup>4</sup> fertilizers,<sup>5</sup> and defense applications.<sup>6</sup> The extensive use of REEs in day-to-day life, combined with their unstable supply chains, has led to a rapidly increasing demand for these critical elements. Demand for some of these elements is estimated to grow by more than 2600% by 2035.<sup>7</sup> Five REEs (Y, Nd, Eu, Tb, and Dy) have been highlighted by the U.S. Department of Energy and the European Commission as at risk for supply disruption and criticality because of their frequent use in low-carbon and green energy technologies, such as wind turbines, electric vehicles, and LEDs.<sup>8,9</sup> However, the domestic production of these critical elements has declined significantly, while their extraction from natural ores is expensive, energy-intensive, and environmentally harmful.<sup>10</sup> Furthermore, efficient separation technologies for recovering REEs from electronic waste are currently lacking, posing challenges to the recycling process.<sup>11</sup> Size-based separation is ineffective due to the nearly identical sizes of lanthanides. To address these challenges, we proposed an affinity-based biomimetic separation technique that utilizes specific ligands attached to transmembrane channels for lanthanides. In this study, we have developed supramolecular channels (**Figure 1**) based on a pillar[5]arene scaffold with appended diphenyl phosphine oxide ligands (DPP) and these channels demonstrate remarkable selectivity for lanthanides over commonly found monovalent metal ions ( $\geq 18$ ) during electrochemically driven (voltage clamp) transport measurements. These channels exhibit promising selectivity towards medium lanthanides, such as Europium ions, showing a 20-fold preference over heavy lanthanides ( $\text{Yb}^{3+}$ ) and a 41-fold preference over light lanthanides ( $\text{La}^{3+}$ ), while effectively excluding all measured monovalent and divalent ions, including protons. The exceptional selectivity of these channels is attributed to their highly hydrophobic side chains and DPP functional groups, which enable the dehydration of medium lanthanides. Additionally, the oxygen atoms positioned above the central ring of the channel acts as a selectivity filter. Overall, this novel class of channels presents excellent potential as building blocks for sustainable lanthanide separation membranes.

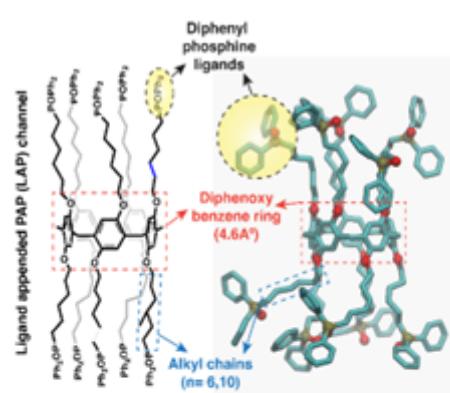


**Figure 1** The biomimetic artificial channel proposed combines lanthanide selective filter with selective nanoconfined transport was seen in selective ion channels such as KcsA by decorating DPP ligands at the channel entrance created around the pillar[5]arene central ring.

## Recent Progress

Our overall objective is to discover and design artificial ion channels that could interact and selectively transport metal ions of interest, and then incorporate them into polymeric membranes that are manufacturable, scalable, robust, and selective (**Figure 2**). We have been successful in synthesizing pillar[5]arene-based channels appended with DPP ligands, referred to as LAP5 channels. Ion transport activity and ion-ion selectivity was then measured across the lipid bilayer as a model system. In order to quantify the ion-ion selectivity of these channels, we used patch clamp ion current measurements to determine selectivity under applied potential gradients (**Figure 3**). In this setup, we painted planar lipid bilayer membranes containing multiple channels that separate two chambers with appropriate metal chloride solution to evaluate the electrochemically driven transport of various ions across these channels (**Figure 3A**). In general, under applied potentials, the measured currents for  $K^+$ ,  $La^{3+}$ , and  $Yb^{3+}$  ions were close to their background levels (**Figure 3B**), indicating limited transport through the channels. However, noticeable currents were observed for  $Eu^{3+}$  ions (**Figure 3B-C**). The selectivity of LAP5n6 for  $Eu^{3+}$  over  $La^{3+}$  was determined to be 41.4, indicating a preference for the middle lanthanides over the light lanthanides (**Figure 2C**). Similarly, the selectivity of  $Eu^{3+}$  over  $Yb^{3+}$  was found to be 21.4, also suggesting a preference for the mid lanthanides over the heavy lanthanides. These channels also showed high selectivity for  $Eu^{3+}$  ions over alkali metal ions with a  $Eu^{3+}/K^+$  selectivity of  $\sim 18$ . These selectivity values represent much higher than those observed for single stage solvent extraction ( $< 3.0$ ) and are the first values reported for a custom designed lanthanide channel.

## Future Plans

Our mission is divided into two primary components: fundamental transport studies and membrane development.

**Transport study:** Our proposed transport studies will be conducted to deepen our understanding of principles that

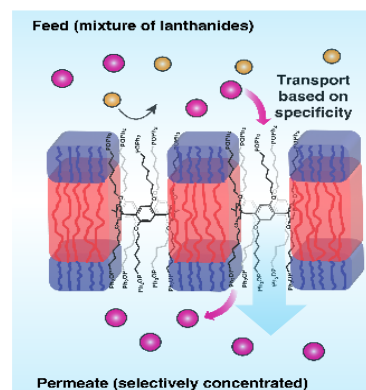


**Figure 2.** Schematic of continuous solvent-free lanthanide separation by selective transport

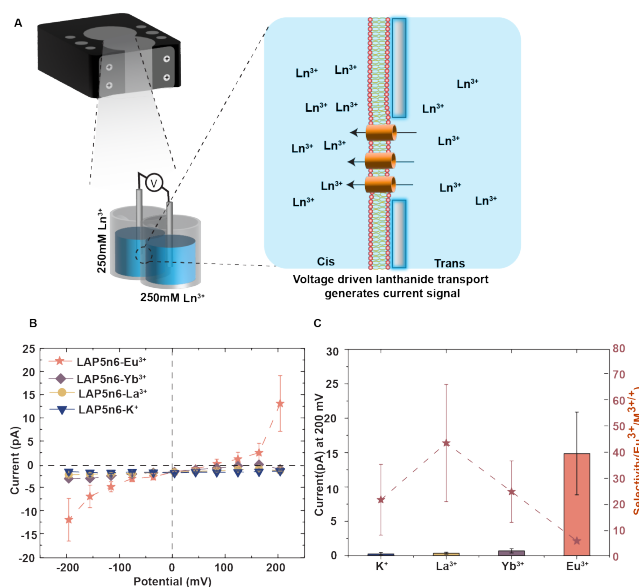


**Figure 3: Patch clamp measurements performed on LAP5 channels embedded in painted lipid bilayers.** A. Schematic representation of patch clamp apparatus used for conducting measurements B Voltage sweeps conducted with various ions provide confirmation of the selectivity of the LAP5n6 channel C. Summarized ion/ion selectivity values show high  $Eu^{3+}/La^{3+}$ ,  $Eu^{3+}/Yb^{3+}$  and  $Eu^{3+}/K^+$  selectivity

helps us to design and develop a class of artificial ion channels that has the required selectivity. In the upcoming year, our primary focus will be on the development of more robust and rigid architectures for highly selective artificial ion channels. An example of this would involve the design and synthesis of peptide-appended pillar[n]arene channels that mimic the recognition site found in the Lanmodulin protein's binding pocket. This approach aims to enhance the activity of the channels and provide the ability to finely tune their selectivity according to our desired specifications. The more rigid architecture would help to preserve the channel's selectivity when incorporated into the polymeric membrane.

**Membrane development:** Our ultimate goal is to develop a continuous and efficient separation process that is energetically efficient and environmentally friendly (**Figure 2**). Therefore, in the upcoming years, our focus would remain to fabricate highly stable, robust, and selective polymeric membranes for separating critical metal ions. Therefore, the developed ion-selective channels will be first incorporated into the polymeric membrane followed by crosslinking and additional sealing methods to stitch the micro-defects, similar to our previously published protocol.<sup>12</sup> A poly(isoprene)-poly(ethylene oxide)-poly(isoprene) triblock copolymer system will be used to fabricate the lamellar polymeric membranes. The membrane will be installed in a diffusion cell. The ion transport will be measured either by applying a potential and measuring the current or through a concentration gradient where ICP-OES will be employed to quantify the ion-ion selectivity.

## References

1. Cheisson, T.; Schelter, E. J. Rare earth elements: Mendeleev's bane, modern marvels. *Science* **2019**, *363* (6426), 489-493.
2. Bomgardner, M. M. The struggle to mine rare earths. *CHEMICAL & ENGINEERING NEWS* **2015**, *93* (30), 36-39.
3. Bottrill, M.; Kwok, L.; Long, N. J. Lanthanides in magnetic resonance imaging. *Chemical Society Reviews* **2006**, *35* (6), 557-571.
4. Vogt, E. T.; Weckhuysen, B. M. Fluid catalytic cracking: recent developments on the grand old lady of zeolite catalysis. *Chemical Society Reviews* **2015**, *44* (20), 7342-7370.
5. Skovran, E.; Martinez-Gomez, N. C. Just add lanthanides. *Science* **2015**, *348* (6237), 862-863.
6. Humphries, M. *Rare earth elements: the global supply chain*; Diane Publishing, 2010.
7. Alonso, E.; Sherman, A. M.; Wallington, T. J.; Everson, M. P.; Field, F. R.; Roth, R.; Kirchain, R. E. Evaluating Rare Earth Element Availability: A Case with Revolutionary Demand from Clean Technologies. *Environmental Science & Technology* **2012**, *46* (6), 3406-3414. DOI: 10.1021/es203518d.
8. Joint Research, C.; Institute for Energy and, T.; Tercero, E.; Bryson, R.; Chapman, A.; Tzimas, E.; Moss, R.; Ostertag, K.; Thompson, P.; Morley, N.; et al. *Critical metals in the path towards the decarbonisation of the EU energy sector : assessing rare metals as supply-chain bottlenecks in low-carbon energy technologies*; Publications Office, 2014. DOI: doi/10.2790/46338.
9. Chu, S. *Critical materials strategy*; DIANE publishing, 2011.

10. Navarro, J.; Zhao, F. Life-cycle assessment of the production of rare-earth elements for energy applications: a review. *Frontiers in Energy Research* **2014**, *2*, 45.
11. Tansel, B. From electronic consumer products to e-wastes: Global outlook, waste quantities, recycling challenges. *Environment international* **2017**, *98*, 35-45.
12. Lang, C.; Ye, D.; Song, W.; Yao, C.; Tu, Y.-m.; Capparelli, C.; LaNasa, J. A.; Hickner, M. A.; Gomez, E. W.; Gomez, E. D.; et al. Biomimetic Separation of Transport and Matrix Functions in Lamellar Block Copolymer Channel-Based Membranes. *ACS Nano* **2019**, *13* (7), 8292-8302. DOI: 10.1021/acsnano.9b03659.

## Publications

The following two manuscripts are under preparation/submitted

1. Harekrushna Behera, Tyler J Duncan, Laxmicharan Samineni, Hyeonji Oh, Chenhao Yao, Venkat Ganesan, Manish Kumar\* “*Bioinspired Super Selective Lithium Membrane Channels*” *Manuscript is submitted*
2. Harekrushna Behera, Tyler J Duncan, Laxmicharan Samineni, Hyeonji Oh, Venkat Ganesan and Manish Kumar “*Voltage-gated lanthanide selective supramolecular membrane channels*” *Manuscript is under preparation*

## Conferences

1. **Harekrushna Behera**, Tyler J Duncan, Laxmicharan Samineni, Hyeonji Oh, Venkat Ganesan and Manish Kumar. “*Biomimetic Supramolecular Channels for Sustainable Extraction of Rare Earth Elements*” Oral presentation at North American Membrane Society 2023, Tuscaloosa, Alabama.
2. **Tyler J Duncan**, Harekrushna Behera, Laxmicharan Samineni, Manish Kumar, Venkat Ganesan “*Ln (III) Selectivity in Biomimetic Ligand-appended Channels*” Oral presentation at American Physical Society Meeting 2023, Las Vegas, Nevada.

## Understanding functional dynamics on the nanoscale through an integrated experimental–computational framework

Erik Luijten, Northwestern University

Qian Chen, University of Illinois at Urbana-Champaign

### Program Scope

In this project, Luijten and Chen aim to establish a closely integrated experimental–computational program of work aimed at understanding and emulating the nanoscopic functional dynamics of living systems in synthetic materials. Our central hypothesis is that nanoparticles (NPs) with properly designed directional interactions will afford fine control over their equilibrium assembly, motility driven by chemical fuels or external fields, and ultimately non-equilibrium aggregation into functional materials. Our primary goals are to understand the working mechanisms of patchy machines on the nanoscale and to generate collective, spatiotemporal patterns from them as a new form of active materials, which exhibit form and function that change as needed. Specifically, cyclic spatiotemporal patterns underly most systems that perform useful work or transduce energy, yet their realization in man-made materials that are reconfigurable on the nanoscale is extremely limited. The ability of such patchy nanomachines to undergo dynamic cooperative transitions in morphology will provide radically new opportunities for controlling processes such as mass and energy transport. These materials differ from the vast majority of synthetic static materials that typically exist in only a single form, with limited function throughout their performance lifespan.

### Recent Progress

During this reporting cycle, we have made major breakthroughs in the following directions: (i) synthesis of a library of patchy NPs through an ion-mask method and through machine-learning (ML)-aided high-throughput morphology classification; (ii) in in-situ imaging, we have achieved large-scale imaging of the growth modes of NP-based superlattice assemblies, have extended the imaging from model metallic NPs to patchy NPs—in particular their formation and relaxation dynamics—and have demonstrated chemical-fuel driven motility and field-driven assembly under induced ion flow; (iii) development of advanced computational algorithms that permit the understanding of charge regulation (CR) effects and the implementation of hydrodynamic flow effects in large-scale simulations of self-propelled NP “swimmers”; (iv) application of these simulation methodologies to improve predictive capabilities for the aggregation of isotropic and anisotropic NPs and gain mechanistic insight into pathways observed via liquid-phase TEM. Progress in all these areas has advanced the frontiers of experimental and theoretical understanding of functional dynamics at the nanoscale, as we describe in detail below.

#### 1. Patchy NPs with charged polymer patches: high-yield synthesis and unsupervised ML-based analysis

We have utilized the variation of surface facets and local curvature in shape-anisotropic NPs and developed a general “ion-masking” strategy to achieve regioselective ion adsorption on the NP surface. As shown in Fig. 1, halide ions (e.g., I<sup>-</sup>) selectively adsorb onto specific surface locations of gold NP surfaces as confirmed through high-resolution element mapping by energy-dispersive X-ray spectroscopy (EDX). In this masking strategy, ligand patches only bind to the regions of NPs not covered by the halide ions. Moreover, the lateral attraction of ligands, when enhanced due to  $\pi$ – $\pi$  stacking or if the ligands are polymeric, enables a high degree of control, as it causes the

volumetric expansion of ligand domains to follow an island formation model. We have established a scaling theory and Monte Carlo (MC) simulation model to predict how NP shape and ligand–ligand interactions lead to a rich selection of patch size, shape, pattern, and interactions. More recently, we have demonstrated a symmetry-breaking effect as we increased polymer–polymer attraction, either by lowering the temperature (thus increasing the  $\chi$  parameter) or by increasing the molecular weight of the polymers, to create single-patched triangular prisms. Strong polymer attraction causes initially stochastically adsorbed polymers on one tip to continue recruiting more polymers to the same location, thereby augmenting the patch size even when the chemical or physical properties of all three tips are identical.

The yield of patchy NPs synthesized by this method is universally high (>80%), with controlled patch size, shape, placement, and number based on NP shapes, including octahedra, cubes, tetrahedra, bipyramids, and rhombic dodecahedra (Fig. 1b–f). One hallmark of this strategy is that we can achieve NP self-assembly over an extended area outside the TEM chamber, a first-time demonstration for patchy NPs. Chen and Luitjen developed an unsupervised ML workflow and a mathematical fingerprint function to identify the inorganic NP core and polymer patch of product NPs in TEM images containing multiple, possibly even superimposed, NPs, and to quantify complex patch patterns. This method enables batch processing of the TEM images of synthesized patchy NPs, which is highly useful for understanding synthesis–morphology relationships and automating the classification—essential in view of the high-dimensional space spanned by the synthetic parameters and shape attributes of patchy NPs.

## 2. Experimental–computational collaboration on understanding the self-assembly pathways of anisotropic NPs into large superlattices by liquid-phase TEM

We have made major technological advancements in controlling and containing large numbers (>1,000) of NPs in a liquid-phase TEM chamber, making it possible to capture the post-nucleation growth modes of superlattices in 3D. Based on this new experimental observation, we established a unified framework for understanding crystal growth modes across four orders of magnitude in length scale, from atomic (relevant for thin-film epitaxy in metallurgy and the semiconductor industry) to micron-sized constituents (relevant to photonics and colloidal physics). The newly

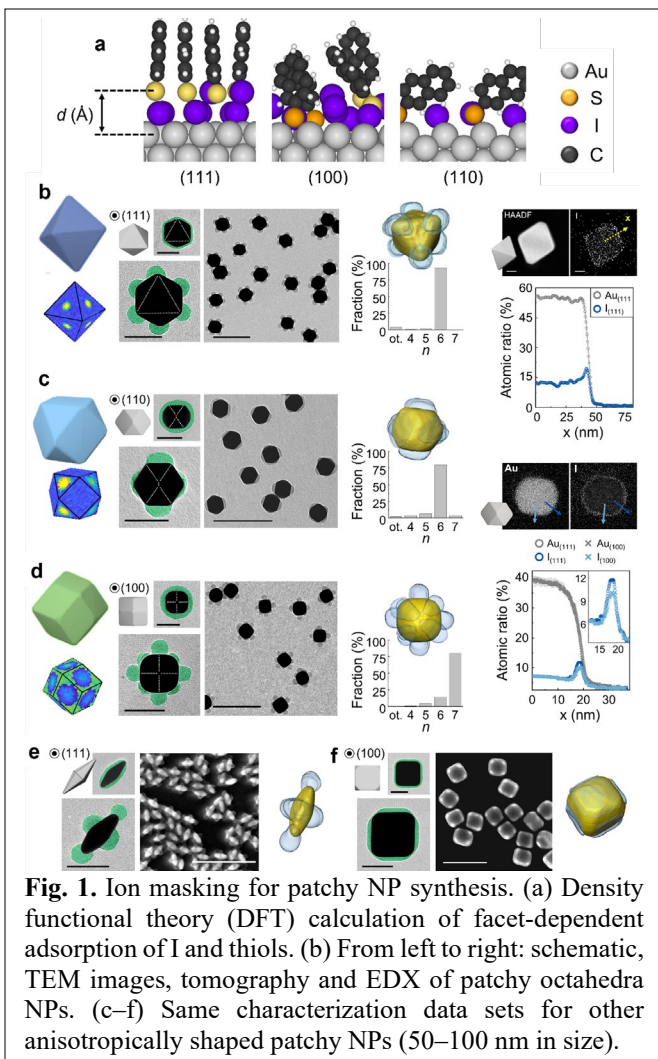


**Fig. 1.** Ion masking for patchy NP synthesis. (a) Density functional theory (DFT) calculation of facet-dependent adsorption of I and thiols. (b) From left to right: schematic, TEM images, tomography and EDX of patchy octahedra NPs. (c–f) Same characterization data sets for other anisotropically shaped patchy NPs (50–100 nm in size).

gained capability to image growth in 3D has allowed us to develop a comprehensive analytical theoretical framework that describes crystallization processes via two dimensionless parameters, capturing the role of particle size and energy barriers in a manner that makes it universally applicable. Specifically, we studied a diversity of NPs around 50 nm in size (gold nanocubes, concave nanocubes, and nanospheres), where the NP shape served as an important handle to independently control the energy barriers associated with intralayer and interlayer diffusion. We observed and quantified four distinct growth modes by resolving both the lateral and perpendicular growth of crystal layers, a first-time achievement. We observed both the layer-by-layer growth typical of atomic crystallization and the rough growth prevalent in colloidal systems at the respective extremes of inter-NP interactions and resulting diffusion barriers. Complementing the TEM imaging with molecular dynamics (MD) simulations to determine these barriers as well as kinetic MC (KMC) simulations of large-scale crystallization across parameter space, we arrived at our surprising central finding, namely that the lateral and perpendicular growth behavior can be controlled independently, resulting in *two mixed modes* that until now had only been sporadically observed and not within a coherent framework (Fig. 2a–d). In addition, our simulations, which cover a wide range of intrinsic diffusion rates, flux, and free-energy barriers determined by particle shape and interaction strength (Fig. 2a,b), successfully predicted the growth behaviors, crystal morphology, and bulk defect density for building blocks of various sizes and shapes.

### 3. Liquid-phase TEM observations of motion and assembly driven by chemical fuel and electric fields

We also advanced beyond the current experiments of NP self-assembly in equilibrium and started new liquid-phase TEM experiments to study two model systems of driven NP dynamics under the supply of external energy. We obtained the first TEM videos of catalytically active Pt NPs with asymmetric tadpole shapes that exhibit superdiffusive motion upon fueling with  $\text{NaBH}_4$ . A high correlation between the tadpole orientation and motion direction was observed following the local chemical concentration gradient originating from the catalytically activated decomposition of  $\text{NaBH}_4$  (Fig. 2e,f). We also realized the first TEM videos of rapidly evolving patterns of gold NPs driven by electro-osmotic flows under an electric field. We found that bulk diffusion of NPs inside the assemblies is comparable to their surface diffusion. In preparation for the proposed work, we established experimental protocols and obtained important data for directly imaging the driven dynamics of NPs, which—unlike extensively studied micron-sized colloidal and biological systems—has been uncharted. Both chemical and field-driven propulsion were applied *in situ*,

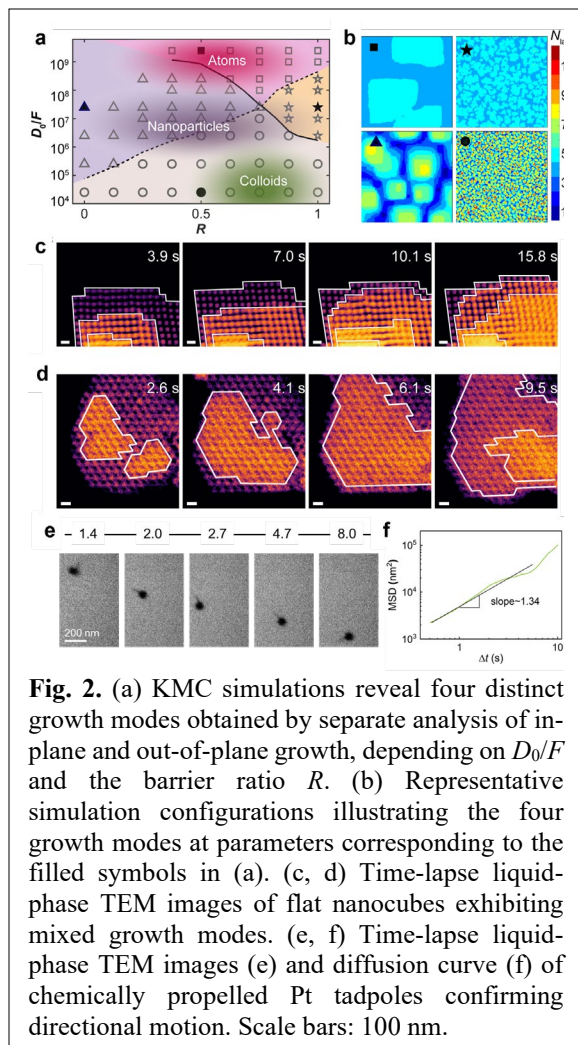


**Fig. 2.** (a) KMC simulations reveal four distinct growth modes obtained by separate analysis of in-plane and out-of-plane growth, depending on  $D_0/F$  and the barrier ratio  $R$ . (b) Representative simulation configurations illustrating the four growth modes at parameters corresponding to the filled symbols in (a). (c, d) Time-lapse liquid-phase TEM images of flat nanocubes exhibiting mixed growth modes. (e, f) Time-lapse liquid-phase TEM images (e) and diffusion curve (f) of chemically propelled Pt tadpoles confirming directional motion. Scale bars: 100 nm.

using chemical flow channels and micropatterned electrodes, respectively, within the liquid-phase TEM chamber.

#### 4. Autonomous learning and predictive modeling of NP pattern formation and assembly

Part of our work supported by the current DOE-BES grant consists of ML-supported classification of structures and phases. Such structures are often characterized by a specific order parameter, but recent advances in ML have demonstrated its capability to identify different phases without prior knowledge of the order parameter. Specifically, Luijten developed an approach based upon spectral learning. We demonstrated that this makes it possible to autonomously distinguish different phases by determining characteristic wave modes and utilizing their intensities as effective order parameters. We have illustrated the capabilities of this method for crystalline as well as nonequilibrium materials. Compared to real-space methods, it offers high training efficiency, direct physical interpretability, and applicability to experimental data.

In a separate development, we examined how dielectric mismatch in binary mixtures of NPs can be used as a control parameter to bias their self-assembly. Interestingly, we discovered that dielectric many-body effects can impart effective directionality to isotropic building blocks, which permits robust self-assembly of binary mixtures of oppositely charged NPs into anisotropic superstructures. This mechanism offers a potential avenue to designing materials with controllable structural properties. Conceptually interesting is the observation that repulsive dielectric mismatch, where NPs have a lower permittivity than the medium in which they are embedded, leads to an effective attraction that becomes *stronger* with increasing coordination number, while attractive dielectric mismatch, such as observed for metallic NPs and, more generally, for NPs suspended in low-permittivity solvents, *decreases* in attractive strength with increasing coordination number.

#### **Future Plans**

We will build on the efforts described here and synthesize patchy NPs with designed surface charge patterns that subsequently will be steered by external energy inputs. The procedures to guide particles into predetermined arrangements will rely on real-time feedback mechanisms, utilizing a workflow in which the effect of changing external fields is observed and adjusted “on the fly.” Beyond mere feedback, we will utilize predictive capabilities that are achieved by modeling diffusional dynamics, dielectric polarization effects, charge regulation (i.e., dynamic response of surface ionization of nanoparticles), and hydrodynamic flow fields. The procedures and insights thus developed will ultimately be used to realize scaled-up assemblies of engineered moiré patterns and 3D functional materials composed of patchy NPs through new pathways.

## Publications acknowledging this grant

1. B. Luo, Z. Wang, T. Curk, G. Watson, C. Liu, A. Kim, Z. Ou, E. Luijten\*, and Q. Chen\* Unravelling Crystal Growth of Nanoparticles. *Nature Nanotechnol.* **18**, 589 (2023).
2. Z. Lyu, L. Yao, W. Chen, F. C. Kalutantirige, and Q. Chen Electron Microscopy Studies of Soft Nanomaterials. *Chem. Rev.* **123**, 4051 (2023).
3. A. Kim, T. Vo, H. An, P. Banerjee, L. Yao, S. Zhou, C. Kim, D. J. Milliron, S. C. Glotzer, Q. Chen Symmetry-Breaking in Patch Formation on Triangular Gold Nanoparticles by Asymmetric Polymer Grafting. *Nat. Commun.* **13**, 6774 (2022).
4. Z. Wang, C. Liu, and Q. Chen In-Situ Imaging of Nucleation and Growth of Superlattices from Nanoscale Colloidal Nanoparticles. *J. Cryst. Growth* **601**, 126955 (2022).
5. L. Yao, H. An, S. Zhou, A. Kim, E. Luijten, and Q. Chen Seeking Regularity from Irregularity: Unveiling the Synthesis-Nanomorphology Relationships of Heterogeneous Nanomaterials Using Unsupervised Machine Learning. *Nanoscale* **14**, 16479 (2022).
6. A. Kim, C. Liu, E. Luijten, and Q. Chen Formation and Surface Melting of Nanoparticle Superlattices in a Solution. *Microsc. Microanal.* **27**, 1244 (2021).
7. G. R. Burks, L. Yao, F. C. Kalutantirige, K. J. Gray, E. Bello, S. Rajagopalan, S. B. Bialik, J. E. Barrick, M. Alleyne, Q. Chen, C. M. Schroeder Electron Tomography and Machine Learning for Understanding the Highly Ordered Structure of Leafhopper Brochosomes. *Biomacromolecules* **24**, 190 (2023).
8. T. Curk and E. Luijten\* Phase Separation and Ripening in a Viscoelastic Gel. *Proc. Nat. Acad. Sci.* (2023) [in press].

## **Memories and training in matter using inspiration from biology**

**Sidney R. Nagel, The University of Chicago**

**Keywords:** Training, Learning, Aging, Disorder, Degrees-of-freedom

### **Research Scope**

Memory arises in the biology and is obvious to all of us in our ability to recollect events from our past life going back to those occurring in our childhood. However, memory – the ability to encode, access, and erase signatures of past history – is of much broader utility. Many biological processes require the storage of information for later use and this storage occurs in many different ways in many different parts of an organism. To give only a few examples, one has long-term memory (*e.g.*, of our parents), muscle memory of how to perform a task properly (*e.g.*, in sports or music), short-term storage (*e.g.*, numbers in a calculation or an address or phone number), scars (reminding of previous mishaps) and calluses (that allow the body to grow accustomed to new activities). The list goes on.

What may not be so obvious is that non-biological materials also store memories and these memories are reminiscent of those in the biological realm including those just mentioned. Thus, memory formation is of broad intellectual relevance and sits at the interdisciplinary crossroads of physics, biology, chemistry, and computer science. Moreover, once the system has completely relaxed to thermal equilibrium, it is no longer able to recall aspects of its evolution. Likewise, if the system is completely ordered there is no place for the memory to reside. Thus, the storage of a memory requires some degree of disorder. Thus, memory formation is a feature that is specifically relevant to systems that have not yet completely relaxed to their equilibrium state or have not yet settled into too much uniformity. Therefore, many forms of memory are intrinsically tied to far-from-equilibrium behavior and to transient response to a perturbation.

This general behavior arises in diverse contexts in condensed-matter physics and materials, including phase change memory, shape memory, echoes, memory effects in glasses, return-point memory in disordered magnets, as well as related contexts in computer science. Yet, as opposed to the situation in biology, there is currently no common categorization and description of the memory behavior that appears to be prevalent throughout condensed-matter systems. Our focus is on memories that appear in physical (as distinct from biological) matter. The hope is that this will be a guide toward developing the unifying conceptual underpinnings for a broad understanding of memory effects that appear in materials.

### **Recent Progress**

Jammed packings of soft spheres subjected to repeated cycles of shear, cyclically crumpled sheets of paper, and interacting spins in an oscillating magnetic field all form memories of how they were trained. Memory in such systems hinges on the ability to learn a pathway between metastable states in the energy landscape. It has been compared to the memory seen in a collection of bistable elements, called hysterons, that flip between states when an external field is varied above or below

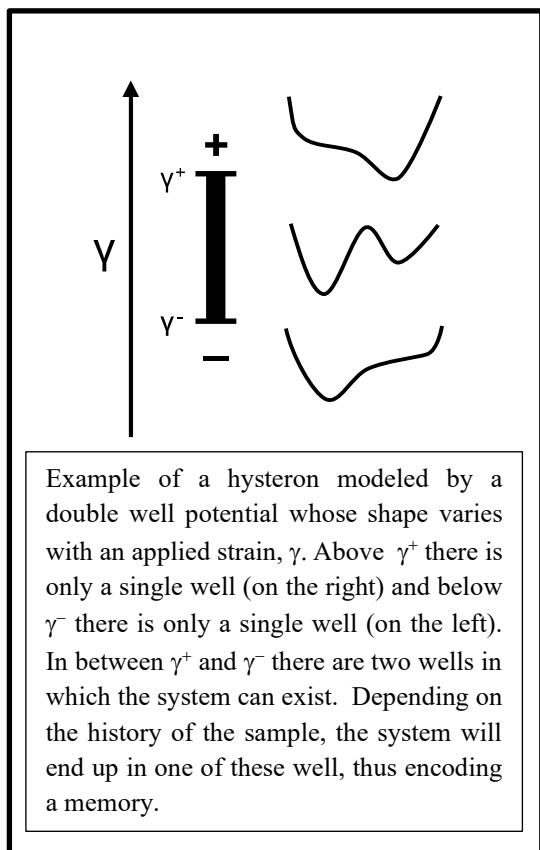
a critical value. A model of a hysteron is shown in the figure on the right. Although an enormous simplification, ensembles of independent hysterons capture surprisingly well some features of the memory formation seen in complex systems.

While simple models that treat clusters of rearranging particles as isolated two-state systems offer insight into this memory formation, they fail to account for the long training times and multiperiod orbits observed in simulated sheared packings. We have shown (1) that adding interactions between rearranging clusters overcomes these deficiencies. In addition, interactions allow simultaneous encoding of multiple memories, which would not have been possible otherwise. These memories are different in an essential way from those found in other systems, such as multiple transient memories observed in sheared suspensions, and contain information about the strength of the interactions.

Hysterons are typically treated quasistatically. We have generalized (2) hysterons to explore the effect of dynamics in a simple spring system with tunable bistability to study how the system chooses a minimum. Changing the timescale of the forcing allows the system to transition between a situation where its fate is determined by following the local energy minimum to one where it is trapped in a shallow well determined by the path taken through configuration space. Oscillatory forcing can lead to transients lasting many cycles, a behavior not possible for a single quasistatic hysteron.

Considered as materials, biological systems are striking in their ability to perform many individually demanding tasks in contexts that can often change over time. This success can be attributed to “metaproperties” such as modularity, robustness, plasticity for learning, and multifunctionality. In particular, we have been studying evolution in time-varying environments that naturally leads to adaptable biological systems that can easily switch functionalities (3). Advances in the synthesis of environmentally responsive materials therefore open up the possibility of creating a wide range of synthetic materials which can also be trained for adaptability. By periodically switching targets in a given design algorithm, we can teach a material to perform incompatible functionalities with minimal changes in design parameters. We have exhibited this learning strategy for adaptability in elastic networks that are designed to switch deformation modes with minimal bond changes.

Systems with disorder often have a complex and rugged energy landscape whose minima are determined by the system’s degrees of freedom and constraints. Finding low-lying states in such a system is a daunting challenge that lies at the heart of many constraint satisfaction statistical physics problems, ranging from machine learning to population ecology. More difficult is finding



rare minima in such systems that have specific desired properties or functions such as enhanced stability against external perturbations. Finding a framework for designing a desired function into a complex system in a flexible and reliable manner is an important goal that could lead to a paradigm shift in material processing. The introduction of transient degrees of freedom into a system can lead to novel material design and training protocols that guide a system into a desired metastable state. In this approach (4), some degrees of freedom, which were not initially included in the system dynamics, are first introduced and subsequently removed from the energy minimization process once the desired state is reached. Using this conceptual framework, we have created stable jammed packings that exist in exceptionally deep energy minima. It is important to emphasize that this added stability persists in the thermodynamic limit. The inclusion of particle radii as transient degrees of freedom leads to deeper and much more stable minima than does the inclusion of particle stiffnesses. This is because particle radii couple to the jamming transition, whereas stiffnesses do not. Thus, different choices for the added degrees of freedom can lead to very different training outcomes.

Disordered solids have microscopic elements that can deform plastically in response to stresses on them. We have shown that by driving the system periodically, this plasticity can be exploited to train in desired elastic properties, both in the global moduli and in local “allosteric” interactions. These allosteric interactions are inspired by the allostery found in proteins. Periodic driving can couple an applied “source” strain to a “target” strain over a path in the energy landscape. This coupling allows control of the system’s response, even at large strains well into the nonlinear regime, where it can be difficult to achieve control simply by design.

Disordered mechanical systems can deform along a network of pathways that branch and recombine at special configurations called bifurcation points. Multiple pathways are accessible from these bifurcation points; consequently, computer-aided design algorithms have been sought to achieve a specific structure of pathways at bifurcations by rationally designing the geometry and material properties of these systems. We have explored an alternative physical training framework in which the topology of folding pathways in a disordered sheet is changed in a desired manner due to changes in crease stiffnesses induced by prior folding. We study the quality and robustness of such training for different “learning rules,” that is, different quantitative ways in which local strain changes the local folding stiffness. We have experimentally demonstrated these ideas using sheets with epoxy-filled creases whose stiffnesses change due to folding before the epoxy sets. Our work shows how specific forms of plasticity in materials enable them to learn nonlinear behaviors through their prior deformation history in a robust manner.

## **Future Plans**

This project relies on previous works about how to design or train bio-inspired functionality into disordered matter. These have raised a number of fundamental questions that this project will address. The complexity of molecular structure has not yet been reproduced in the models used for learning or training in function. Studies of training have been performed for matter that has no internal stresses and which is at zero temperature. We must confront the question of whether pre-stress, temperature, long-range interactions, or angle-bending forces can be accommodated into the training and learning protocols that have been proposed so far and whether those protocols can be augmented to accommodate these features of living matter. This would make it possible to use analogous training of purely physical systems. However, the concept of training assumes that the

material is capable of storing a memory of its history so that it is able to retain the information and use it in its future behavior.

1) *Disordered matter is intrinsically different from crystalline material:* A crystal is formed by the repetition of a unit cell while glasses have no such order. Many biological systems capable of function, including proteins and neural networks, lie somewhere in between these extremes.

2) *Possible advantages of disorder:* The glass, or disordered solid, can exist in many possible stable configurations that may have different collective properties. Thus it is relatively easy to coax a glass into one state, with more desirable properties, rather than another. The glass is a reasonable starting point for understanding and designing new biomimetic materials.

3) *New principles of disordered matter:* There are new principles that govern the properties of glasses that would not be found in their crystalline counterparts. The systematic implementation of those principles forms the basis of this project.

4) *Tuning by double gradient descent:* We have used these principles to alter a material's structure to create unusual properties. By considering these alterations of structure as degrees of freedom, we view our training protocols as a generalization of minimization procedures. This requires the minimization of two cost functions via double gradient descent.

5) *Limitations:* While often successful, double gradient descent has limitations: (1) As system size increases, the computation time needed to obtain the ground states becomes enormous. (2) The ability to alter the individual bonds becomes difficult as the physical size decreases.

6) *Teaching with boundary conditions:* We train the material by applying a target-strain response in addition to an applied source strain. For any desired functionality that is a strain response to an applied strain, *we can express the learned state in terms of boundary conditions.*

7) *Directed aging:* Disordered materials, because they have many nearby metastable ground states, age over time as the system seeks to find lower and lower values of the free energy. If the aging occurs while the material is under a predetermined stress it is possible to use the aging to our advantage. Directed aging targets those bonds that are under the most strain since strained bonds will typically age more rapidly.

8) *Coupled learning:* Directed aging does not always succeed on the computer. The advantage of coupled learning over directed aging is that, if it can be implemented, it is far more reliable since it truly minimizes the learning cost function. As a result, coupled learning systems can learn more complex tasks than directed aging systems.

## References

1. Chloe W. Lindeman, Sidney R. Nagel, *Multiple memory formation in glassy landscapes*, Science Advances **7**, eabg7133 (2021). DOI: 10.1126/sciadv.abg7133
2. Chloe W. Lindeman, Varda F. Hagh, Chi Ian Ip, Sidney R. Nagel, *Competition between energy and dynamics in memory formation*, Phys. Rev. Lett. **130**, 197201 (2023). DOI: 10.1103/PhysRevLett.130.197201
3. Martin J. Falk, Jiayi Wu, Ayanna Matthews, Vedant Sachdeva, Nidhi Pashine, Margaret Gardel, Sidney R. Nagel, Arvind Murugan, *Learning to learn by using non-equilibrium training protocols for adaptable materials*, PNAS **120**, e2219558120 (2023). DOI: 10.1073/pnas.2219558120
4. Varda F. Hagh, Sidney R. Nagel, Andrea J. Liu, M. Lisa Manning, Eric I. Corwin, *Transient learning degrees of freedom for introducing function in materials*, PNAS **119** (19) e2117622119 (2022). DOI: <https://doi.org/10.1073/pnas.2117622119>
5. Chukwunonso Arinze, Menachem Stern, S. R. Nagel, Arvind Murugan, *Learning to self-fold at a bifurcation*, Phys. Rev. E **107**, 025001 (2023). DOI: 10.1103/PhysRevE.107.025001

## Publications

1. Daniel Hexner, Andrea J. Liu, Sidney R. Nagel, *Periodic training of creeping solids*, PNAS **117**, 31690 - 31695 (2020). DOI: <https://doi.org/10.1073/pnas.1922847117>
2. Nidhi Pashine, *Local rules for fabricating allosteric networks*, Phys. Rev. Materials **5**, 065607 (2021). DOI: 10.1103/PhysRevMaterials.5.065607
3. Chloe W. Lindeman, Sidney R. Nagel, *Multiple memory formation in glassy landscapes*, Science Advances **7**, eabg7133 (2021). DOI: 10.1126/sciadv.abg7133
4. Varda F. Hagh, Sidney R. Nagel, Andrea J. Liu, M. Lisa Manning, Eric I. Corwin, *Transient learning degrees of freedom for introducing function in materials*, PNAS **119** (19) e2117622119 (2022). DOI: <https://doi.org/10.1073/pnas.2117622119>
5. Chloe W. Lindeman, Varda F. Hagh, Chi Ian Ip, Sidney R. Nagel, *Competition between energy and dynamics in memory formation*, Phys. Rev. Lett. **130**, 197201 (2023). DOI: 10.1103/PhysRevLett.130.197201
6. Chukwunonso Arinze, Menachem Stern, S. R. Nagel, Arvind Murugan, *Learning to self-fold at a bifurcation*, Phys. Rev. E **107**, 025001 (2023). DOI: 10.1103/PhysRevE.107.025001
7. Martin J. Falk, Jiayi Wu, Ayanna Matthews, Vedant Sachdeva, Nidhi Pashine, Margaret Gardel, Sidney R. Nagel, Arvind Murugan, *Learning to learn by using non-equilibrium training protocols for adaptable materials*, PNAS **120**, e2219558120 (2023). DOI: 10.1073/pnas.2219558120
8. Chloe W. Lindeman, Sidney R. Nagel, *State-and-rate friction in contact-line dynamics*, Phys. Rev. Fluids Accepted (2023). arXiv:2212.11759

## Electrostatic Driven Self-Assembly Design of Functional Nanostructures

**PI: Monica Olvera de la Cruz, Northwestern University; co-PI: Michael J. Bedzyk, Northwestern University**

**Keywords:** chiral mesostructures, amphiphilic molecules, bacterial microcompartments, diffusionphoresis, nanostructures

### Research Scope

Biological structures have impressive functionalities that require the organization of heterogeneous molecules into mesoscale structures with precise compositions and architectures. We aim to understand the basic principle that govern such a robust biological assembly and discover the way to actuate these structures to exploit their functions. By assembling heterogeneous molecules, one can mimic the organization and function of specific biomolecular assemblies, such as microtubular structures and bacterial microcompartments. We design and characterize the organization of heterogeneous molecules with polar, non-polar, and charged groups, including proteins and amphiphiles, into specific nanostructures with broken symmetries to explore their functionalities.

The specific aims of this proposal are:

**Aim 1:** To design, synthesize, and characterize chiral mesostructures using chiral amphiphilic molecules that will undergo structural transitions in response to changes in the solution, including salt concentration and pH value.

**Aim 2:** To develop models to determine the factors that control the shape of multicomponent assemblies of heterogeneous molecules that mimic bacterial microcompartments to design microcompartments with specific shapes and surface composition heterogeneities as a function of the properties of the interactions and the concentrations of the different components.

**Aim 3:** To actuate mesoscale assemblies that mimic biological structures by thermophoresis when chiral, and by diffusionphoresis (including ionic diffusionphoresis) when catalytic.

### Recent Progress

**To address AIM 1,** we designed a simple homologous series of amphiphiles C<sub>n</sub>-K, where an ionizable, chiral amino acid lysine (K) is covalently linked to alkyl tails of varied lengths (n = 12, 14 or 16). This design allowed control over the repulsive intermolecular electrostatic interactions: the solution pH controlled the ionization of the lysine headgroups (a high pH corresponds to a lower average molecular charge), and salt concentration (C) controlled the range of interactions ( $\lambda_D \propto C^{-1/2}$ ). The strength of the attractive van der Waals interactions, which are essential for inducing assembly, was tuned by varying the amphiphile tail length.

In-situ characterization, via atomic force microscopy (AFM), cryo-transmission electron microscopy (cryo-TEM) and small- and wide- angle X-ray scattering (SAXS/WAXS), revealed a rich polymorphism: spherical micelles, planar, helical and helicoidal scroll membranes were observed [1]. From the perspective of chiral shapes, helical bilayer ribbons were observed regardless of molecular tail length when the average molecular charge was reduced by increasing pH. By contrast, high aspect ratio bilayer ribbons formed at low pH transformed to sheets and then rolled into helicoidal scrolls (cochleates) when salt concentration was increased (**Fig. 1**). A theoretical model that considered electrostatic and interfacial energies showed that the equilibrium planar membrane morphology depends sensitively on the range of electrostatic interactions. High aspect ratio membranes and planar sheets ( $L/W = 1$ ) are expected for long-ranged (low salt conditions) and short-ranged (high salt conditions) electrostatic interactions, respectively. Consequently, helices are observed in the low salt conditions because for a helix with 1 turns the membrane aspect ratio should exceed a critical value ( $L/W \geq 2l$ ). By contrast, the highly charged  $L/W = 1$  membranes cannot form helices. Instead, they roll into scrolls, with interbilayer separation greater than the electrostatic screening length. Overall, the combined theoretical and experimental work shows how electrostatic interactions affect chiral shape selection.

The charge regulation of ionizable groups, in soft structures, is described through ionization/deionization equilibrium constants  $pK$ . Typically, these effective  $pK$  are distinct from the ionization/deionization equilibrium constants for isolated ionizable groups in dilute solutions. To tackle this problem, we combined X-ray scattering and nonlinear Poisson-Boltzmann theory to predict the degree of ionization in assemblies of amphiphilic molecules with ionizable groups. Specifically, we analyzed the self-assembly of a peptide amphiphile  $C_{16}$ -K<sub>2</sub>, which consists of two ionizable amino acids [Lysine (K)] coupled to a 16-carbon length alkyl tail. The derived assembly size and shape-dependent degree of ionization was used to back calculate theoretical titration curves, which closely matched the experimental data (**Fig. 2**) without need for any adjustable parameters. These values also agree with the degrees of ionization obtained via a combined Monte Carlo-Molecular dynamics simulation scheme [2]. Overall, this study combines nano-scale structural details and electrostatics to deduce charge regulation for amphiphilic assemblies.

**To address AIM 2**, we developed a mesoscale model to design bacterial microcompartment mimics of specific shapes and surface compositions. Based on our past work on bacterial microcompartment [3], we constructed a continuum three-component model where the components have different bending rigidities (hard, soft, softest) and a line tension between

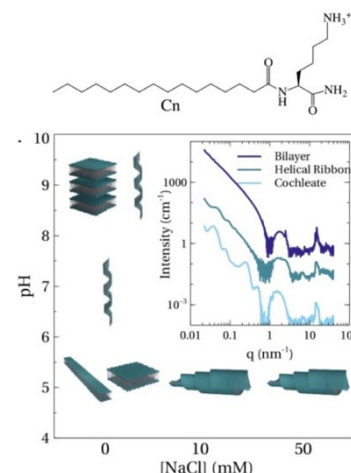


**Fig. 1**  $C_n$ -K molecular design (top) and experimentally determined structural phase diagram for  $C_{16}$ -K (bottom).

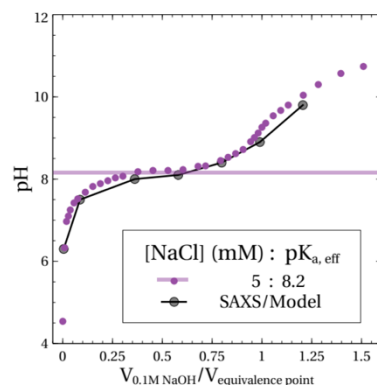


**Fig. 2** Comparison of experimental and theoretical titration curves for  $C_{16}$ -K<sub>2</sub>. The extended pH range encompasses regimes for spherical micelles ( $pH \leq 8.1$ ), cylindrical micelles ( $8.1 < pH < 8.9$ ) and planar membranes ( $pH \geq 8.9$ ) assemblies.

them. We showed complex pattern formation on the edges and vertices of irregular polyhedral morphologies. The soft component tends to prefer the vertices, while the softest component prefers the edges, creating many domains which can be optimized by controlling the ratio of their bending rigidities and the line tension strength. We find that this is due to the Gaussian rigidity, which is proportional to the negative of the bending rigidity. This means that the softest component is preferred for regions of high mean curvature and low gaussian curvature (edges) while the softest component is preferred for regions of high gaussian curvature (vertices). Future work should also include the effect of intrinsic curvature, which all-atom simulations of shell proteins suggest may exist even at continuum length scales.

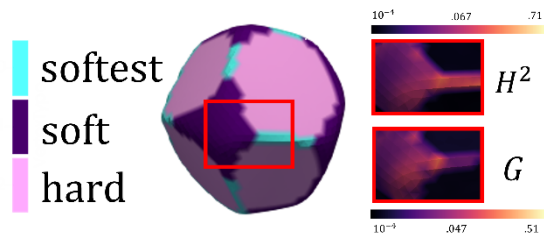


**Fig. 3.** Continuum elasticity model of a three-component shell showing composition domains with the computed mean ( $H$ ) and Gaussian ( $G$ ) curvatures.

**To address AIM 3,** we developed a theory to characterize chiral mesoscale structures such as those shown in chiral protein assemblies (**Fig. 1**). We established a thermally driven hydrodynamic description for the actuation and separation of mesoscale chiral structures in a fluid medium. Cross flow of a Newtonian liquid with a thermal gradient gives rise to chiral structure propulsion and separation according to their handedness (**Fig. 4**). In turn, the chiral suspension alters the liquid flow which thus acquires a transverse (chiral) velocity component. Since observation of the predicted effects requires a low degree of sophistication, our work provides an efficient and inexpensive approach to test and calibrate chiral particle propulsion and separation strategies. We showed that in the presence of a thermal gradient propulsion is possible even in the Stokes flow regime. Such propulsion of individual particles was studied in the past in the presence of external electromagnetic fields [4]. Single particle propulsion is also known to be possible in gradients of viscosity. Here we emphasize the “continuum” approach which implies averaging over the tumbling motion of the particles and applies at times much longer than the tumbling time.

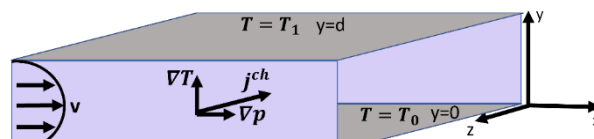


**Fig. 4.** Chiral current  $\mathbf{j}$  induced by crossed pressure and temperature gradients.

We also provided a theoretical framework to quantitatively determine the velocity of asymmetrically charged colloidal particles undergoing ionic self-diffusiophoresis. We found that asymmetry in surface charge offers an alternative mechanism to induce directed self-propulsion, even when the ionic flux on the particle’s surface is uniform [5]. Janus nanoparticles of sizes smaller than or comparable to the Debye length that are endowed with both surface charge and ionic flux asymmetries results in enhanced propulsion speeds of the order of  $\mu\text{m/s}$  or higher (**Fig.**

5). Our findings suggest a new avenue for the design of biomimetic microcompartments through specification of size and surface properties that optimize and regulate self-transport in ionic media.

## Future Plans

Molecular dynamics-Monte Carlo modeling of pH effects on bilayers of amphiphiles in different morphologies will be developed. We will also determine the adsorption of enzymes on the surface of cationic-anionic bilayers to design microcompartments capable of chemotaxis.

Thermal chiral propulsion is a general phenomenon that can be observed every time material parameters vary with temperature. Future plans include thermal propulsion in a Rayleigh-Benard cell where density varies with temperature.

Furthermore, we plan to extend our current work on ionic self-diffusiophoresis by incorporating the effects of rotation and multiple particle interactions. The addition of these key features into our model lends further insights on the optimal design of microcompartments to quantitatively enhance and control transport inside ionic media, particularly, at the level and scale of many-particle systems. Further plans also include studying chemotaxis of bacterial microcompartments with different sizes of active sites to enable effects to explore the interplay of diffusiophoretic and hydrodynamic effects.

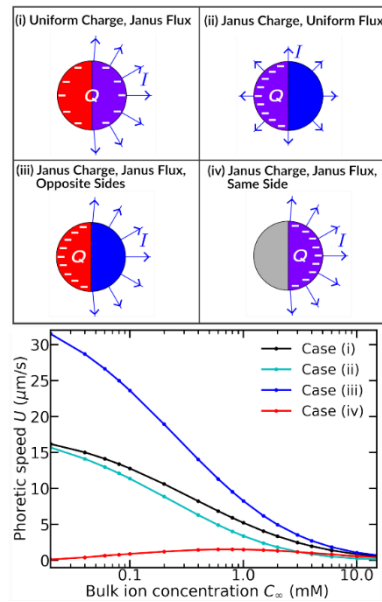


**Fig. 5.** Janus nanoparticles with four different configurations of surface charge and ionic flux, all with a net rate of ions release  $I$  and a net negative charge  $Q$  (top panel). The phoretic self-propulsion speeds  $U$  of the four cases as a function of bulk ion concentration  $C_\infty$  of 1:1 ionic

## References

1. J. M. McCourt, S. Kewalramani, C. Gao, E. W. Roth, S. Weigand, M. Olvera de la Cruz, and M. J. Bedzyk, *Electrostatic Control of Shape Selection and Nanoscale Structure in Chiral Molecular Assemblies*. ACS Central Sci. **8**, 1169-1181 (2022).
2. T. Curk and E. Luijten, *Charge regulation effects in nanoparticle self-assembly* Physical Review Letters **126** (13), 138003 (2021).
3. S. Li, D. A. Matoz-Fernandez, and M. Olvera de la Cruz, *Effect of mechanical properties on multicomponent shell patterning*, ACS Nano **15**, 14804–14812 (2021).
4. E. Kirkinis, A.V. Andreev and B. Spivak, *Electromagnetic propulsion and separation by chirality of nanoparticles in liquids*. Physical Review E **85**, 016321 (2012).
5. A. Shrestha & M. Olvera de la Cruz *Enhanced phoretic self-propulsion of active colloids through surface charge asymmetry* submitted to Phys. Rev. (2023); <https://arxiv.org/pdf/2305.01102v1.pdf>

## Publications

1. Y. Lin and M. Olvera de la Cruz, *Colloidal superionic conductors*, PNAS **120** (15), e2300257120 (2023).
2. J. McCourt, S. Kewalramani, C. Gao, E. W. Roth, S. Weigand, M. Olvera de la Cruz, and M. J. Bedzyk, *Electrostatic control of shape selection and nanoscale structure in chiral molecular assemblies*, ACS Central Science **8**, 1169-1181 (2022).
3. C. E. Mills, C. Waltmann, A. G. Archer, N. W. Kennedy, C. H. Abrahamson, A. D. Jackson, E. W. Roth, S. Shirman, M. C. Jewett, N. M. Mangan, M. Olvera de la Cruz, and D. Tullman-Ercek, *Vertex protein PduN tunes encapsulated pathway performance by dictating bacterial metabolosome morphology*, Nature Communications **13**, 3746 (2022).
4. Y. Li, N.W. Kennedy, S. Li, C.E. Mills, D. Tullman-Ercek, and M. Olvera de la Cruz, *Computational and experimental approaches to controlling bacterial microcompartment assembly*, ACS Central Science **7**, 658–670 (2021).
5. C. Waltmann, C. E. Mills, J. Wang, B. Qiao, J. M. Torkelson, D. Tullman-Ercek, and M. Olvera de la Cruz, *Functional enzyme-polymer complexes*, PNAS **19** (13), e2119509119 (2022).
6. S. Yoo, B. Qiao, T. Douglas, W. Bu, M. Olvera de la Cruz, and P. Dutta, *Specific ion effects in lanthanide-amphiphile structures at the air-water interface and their implications for selective separation*, ACS Applied Materials & Interfaces **14**, 7504-7512 (2022).
7. D. P. Erdosy, M. B. Wenny, J. Cho, C. DelRe, M. V. Walter, F. Jiménez-Ángeles, B. Qiao, R. Sanchez, Y. Peng, B. D. Polizzotti, M. Olvera de la Cruz, J. A. Mason, *Microporous Water with High Gas Solubilities*, Nature **608**, 712-718 (2022).
8. J. Wang, C. Waltmann, H. Kossio-Umana, M. Olvera de la Cruz and J. Torkelson, *Heterogeneous charged complexes of random copolymers for the segregation of organic molecules*, ACS Central Science **7**, 882-891 (2021).
9. S. Li, D. A. Matoz-Fernandez, and M. Olvera de la Cruz, *Effect of mechanical properties on multicomponent shell patterning*, ACS Nano **15**, 14804–14812 (2021).
10. S. Li, D. A. Matoz-Fernandez, A. Aggarwal, and M. Olvera de la Cruz, *Chemically controlled pattern formation in self-oscillating elastic shells*, PNAS **118** (10), e2025717118 (2021).

## **Biomolecules for non-biological things: Peptide ‘Bundlemers’ design for model colloidal particle creation and hierarchical solution assembly**

**Darrin J. Pochan, Materials Science and Engineering, University of Delaware**

**Christopher J. Kloxin, Materials Science and Engineering/Chemical and Biomolecular Engineering, University of Delaware**

**Jeffrey G. Saven, Department of Chemistry, University of Pennsylvania**

**Keywords:** peptides, self-assembly, nanoparticle, computational design

### **Research Scope**

A solution-assembled system comprising computationally designed coiled coil bundle motifs, also known as ‘bundlemers’, will be discussed as model colloidal particle systems as well as hierarchical polymer/material building blocks. The molecules and nanostructures are non-natural amino acid sequences and provide opportunities for controlled solution behavior and arbitrary nanostructure creation with peptides. With control of the display of the amino acid side chains (both natural and non-natural) throughout the peptide bundles, desired physical and covalent (through appropriate ‘click’ chemistry) interactions are designed to control interparticle interactions in solution, which involve both individual bundlemer particles as well as polymers of connected bundlemers. One-dimensional nanostructures are created that exhibit rigid rod character and form liquid crystal phases. The flexibility of the chains can be controlled by the organic linkers used to connect the bundlemers together. The individual bundlemer building blocks, as well as polymers made thereof, are also responsive to varying salt and pH, since computational design is used to design bundlemers with different net charge character to manipulate their interactions in solution. Patches of interaction can be designed on the surface of the particles to dictate their physical interaction in solution and to provide control of interparticle assembly (e.g., crystalline-like lattice vs. amorphous aggregation). Included in the discussion will be new peptide molecule design, hierarchical assembly pathway design, control of nanomaterials and fibers, liquid crystal formation, characterization of solution nanostructure (via electron microscopy, neutron and x-ray scattering), and rheological measurements.

### **Recent Progress**

Recent results involve bundlemer 1-D chains with defined lengths and with new organic linkers with which one can control longer polymer chain stiffness. In order to form monodisperse chains, we took advantage of computationally designed coiled coil designs for bundlemer formation. These are distinct from previously studied  $D_2$  symmetric (antiparallel) tetrahelical

bundles. One can have desired covalent ‘click’ chemical reactive groups on one end of the assembled bundlemer particle. Therefore, the bundlemer designs provide for anisotropic display of the functional groups. When two bundlemers are reacted together via a thiol-Michael click reaction, one bundlemer with cysteines as the N-terminal amino acid and the other bundlemer with a maleimide functionality placed at the N-terminus of the constituent peptides, they form bundlemer rods. Small-angle x-ray scattering clearly shows rigid cylinders in solution, which is precisely the nanostructure that would form from the click conjugation between the bundlemer building blocks. Preliminary studies of concentrated solutions show the formation of lyotropic liquid crystal phases with the monodisperse, short bundlemer rods. Another area of focus in chain formation is the creation of desired linker molecules for conjugation with bundlemer building blocks. The concept provides for polymer chain formation that will display a desired chain stiffness due to the designed flexibility of the organic linkers. The new linkers involve use of a copper-catalyzed azide alkyne click reaction (CuAAC) to link bundlemers with azides placed on the N-terminus of antiparallel bundlemer peptides and alkynes on the arms of two different organic linkers.

The other main area of discussion is the solution assembly of bundlemer building blocks into films and 2-D sheets. Recent results show

clearly how the bundlemers can be considered model colloidal nanoparticles. One example is the use of alloc side chains that contain a carbon-carbon double bond on the periphery of bundlemer building blocks to serve as a functional group to react with thiols in what is known as a thiol-ene click reaction. Cysteine thiols are included on either the same bundle as the allocs or on separate

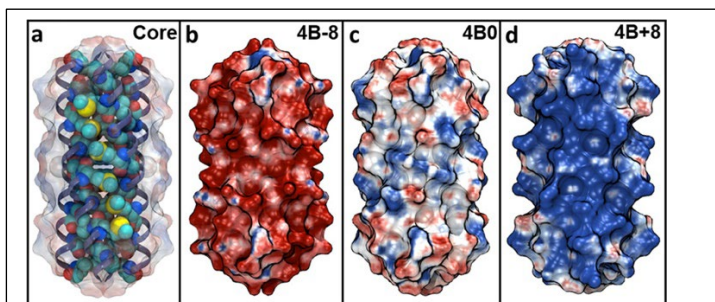


**Figure 1.** Renderings of model  $D_2$  symmetric homotetrameric helical bundles. (a) Conserved residues and the core structure of the bundle. Conserved hydrophobic residues rendered as space filling. Electrostatic potential surface of the  $4B0$  structure rendered as transparent. Tetrameric constructs are labeled  $4Bq$ , where  $q$  is charge of constituent peptide. Mutations were made to the remaining exterior residues to achieve putative charge states. (b–d) Electrostatic surface potential renderings of bundles comprising peptides  $4B-8$  (b),  $4B0$  (c), and  $4B+8$  (d). Electrostatic surfaces are colored red (negative) to blue (positive). (Adapted from Publication 3.)

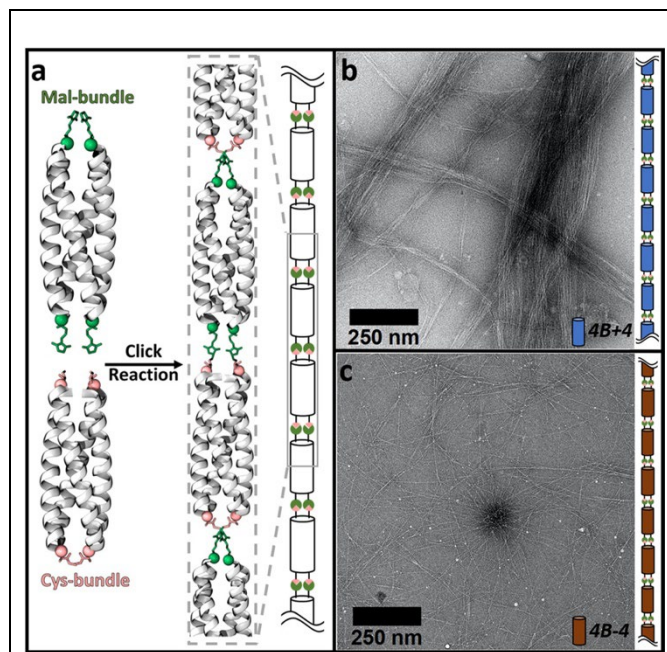


**Figure 2.** Polymers of functioned bundles. (a) Bundles linked by thiol-maleimide linkages. (b, c) TEM micrographs of cast-film and negatively stained polymeric assemblies of  $4B+4$  (b) and  $4B-4$  (c). (Adapted from Publication 3.)

bundles that can be mixed with alloc-functionalized bundles to produce covalently crosslinked films made exclusively from peptide bundles. The use of this thiol-ene click reaction is an example of the third click conjugation reaction used to link bundlemers together. In addition to forming crosslinked films, the hydrophobic alloc group incorporation causes the formation of self-assembled, crystalline-like interbundle lattices when casting films. A second example of solution assembly of 2-D sheets utilizes designs of peptides that form coiled coil bundlemers that have desired charge states. Specifically, mixtures between oppositely charged bundlemers are created to use electrostatic interactions to form nanostructure. Comparisons were made between mixtures of bundlemers with both positively and negatively charged amino acids within the individual bundlemers (what we call “mixed charge” bundlemers with a desired net charge) vs. mixtures using the bundlemer designs that only have one type of charged residue within their peptide primary sequence (what we call “single-charge bundlemers”). The desired display of charged groups was observed to have pronounced effects on the nanostructure formed via electrostatic complexation between oppositely charged bundlemer particles.

### **Future Plans**

Liquid crystal formation with new combinations of bundlemer designs will be a focus in the future with a particular focus on the possibility of forming monodisperse lengths of bundlemer chains. Also, through the study of new organic linkers, we will now have an additional orthogonal click reactions to use for chain and nanostructure formation as well as have different linkers to control the stiffness of polymer chains. Therefore, by combining linkers of different flexibilities and bundlemer building blocks with different charge states, we will be able to explore fundamental polyelectrolyte behavior as well as charged biopolymer solution behavior through scattering and real-space cryoTEM experiments. Liquid crystal formation dependence on chain stiffness due to linker type will also be determined.

An additional focus will be the extent to which we can control the assembly behavior by using new designs with display of desired sets of charged amino acids, different amino acid side chains (e.g., natural bases or acids vs non-natural ionic side chains), and different bundlemer symmetries (e.g., antiparallel coiled coils vs parallel). Furthermore, our ability to control the solution behavior of the bundlemers containing a single type of charged amino acid will be studied and compared to mixed-charge particles where we hypothesize greater dispersion and interparticle repulsion of the single-charge constructs vs the mixed-charge sequences, which have patches of charge that may facilitate to aggregation.

## Publications

1. S.S. Patkar, Y. Tang, A.M. Bisram, T. Zhang, J.G. Saven, D.J. Pochan, and K.L. Kiick, Genetic Fusion of Thermoresponsive Polypeptides with UCST-type Behavior Mediates 1D Assembly of Coiled-Coil Bundlers. *Angew. Chem. Int. Ed.*, 62, e202301331 (2023).
2. G.A. Taggart, A. Guliyeva, K. Kim, G.P.A. Yap, D.J. Pochan, T.H. Epps, and E.D. Bloch, Monitoring the Solution Persistence of Porous Coordination Cages with Diffusion NMR Spectroscopy and Cryogenic Transmission Electron Microscopy. *The Journal of Physical Chemistry C*, 127, 2379-2386 (2023).
3. R. Guo, N.J. Sinha, R. Misra, Y. Tang, M. Langenstein, K. Kim, J.A. Fagan, C.J. Kloxin, G. V. Jensen, D. J. Pochan, and J.G. Saven, Computational Design of Homotetrameric Peptide Bundle Variants Spanning a Wide Range of Charge States. *Biomacromolecules* 23, 2022, 1652-1661 (2022).
4. J.A. Villegas, N.J. Sinha, N. Teramoto, C.D. Von Bargen, D.J. Pochan, and J.G. Saven, Computational Design of Single-Peptide Nanocages with Nanoparticle Templating, *Molecules* 27, 1237 (2022).
5. N. J. Sinha, R. Guo, R. Misra, J. Fagan, A. Faraone, C.J. Kloxin, J.G. Saven, G.V. Jensen, and D.J. Pochan, Colloid-like Solution Behavior of Computationally Designed Coiled Coil Bundlers. *J Colloid Interf Sci* 606, 1974-1982 (2022).
6. K. Kim, C.J. Kloxin, J.G. Saven, and D.J. Pochan, Nanofibers Produced by Electrospinning of Ultrarigid Polymer Rods Made from Designed Peptide Bundlers. *ACS Appl Mater Inter* 13, 26339-26351 (2021).
7. N. J. Sinha, Y. Shi, Y. Tang, C.J. Kloxin, J. G. Saven, A. Faraone, G. V. Jensen, and D. J. Pochan, Intramolecular Structure and Dynamics in Computationally Designed Peptide-Based Polymers Displaying Tunable Chain Stiffness. *Phys Rev Mater* 5, 095601 (2021).
8. N. J. Sinha, C. J. Kloxin, J. G. Saven, G. V. Jensen, Z. Kelmane, and D. J. Pochan. Recombinant expression of computationally designed peptide-bundlers in *Escherichia coli*. *Journal of Biotechnology* 330, 57-60 (2021).

## **Self-organization of biomolecular motors and configurable substrates**

**Tyler D. Ross, Department of Computing and Mathematical Sciences; Paul W. K. Rothmund, Department of Bioengineering, Caltech**

**Keywords:** Active matter; Self-organization; DNA nanotechnology; Protein motors; Gliding assays

### **Research Scope**

The cell demonstrates that a combination of motors and filaments are capable of performing complex, micron-scale mechanical tasks such as cell division and propulsion. Further, the cell is able to redeploy its filaments and motors as it changes between different mechanical tasks. This capability to control and modulate self-organized structures is unmatched by engineered systems. It depends fundamentally on the modification of the physical properties of the filaments and their interactions with other molecules (Ref. 1). Yet we lack design principles of biomolecular self-organization as a function of the properties of the motor substrate (e.g. microtubule filaments). Development of such principles would be greatly enabled by an experimental system in which the properties of the motor substrate could be directly configured. Here, we begin to explore the design principles of configurable motor substrates by using engineered motor proteins (dyneins) (Ref. 2) that walk on DNA nanotubes. Unlike microtubules, DNA nanotube's geometric properties and motor interactions can be designed with nanometer precision. We first explore the properties of a configurable substrate in a DNA nanotube gliding assay, where nanotubes glide across a surface of motor proteins. We will use DNA strand displacement to stop/start gliding of DNA nanotubes as well as the polarity of the nanotube glide direction. Further, we will investigate the principles of spatially-localized motility switching by surface patterning DNA switching strands. Substrate-dependent self-organization will also be further explored in an aster assay, where crosslinked motors pull the ends of filaments together to form an aster structure. We will study how heterogeneous mixtures of nanotubes with different geometric (e.g. diameters) and interaction (e.g. binding site densities) properties influence the self-organization of a nanotube aster. Physical models of aster self-organization with heterogeneous nanotube populations will be developed and compared with experiments. Such models will then provide the basis for predicting assemblies with novel substrates, such as planar micron-scale geometries, which can then be tested with DNA origami. In turn, the design principles of self-organization with configurable substrates will provide a fundamental step toward the construction of dynamic structures that can eventually perform mechanical tasks on the micron scale.

## Recent Progress

We have developed DNA nanotube designs where gliding is modulated by strand displacement. As an initial proof of concept, we designed nanotubes that are only able to glide in the presence of a specific DNA strand. We achieve this by anchoring the DNA nanotubes to the surface of a coverslip with DNA strands (Fig.1a). Nanotubes are decorated with single-stranded DNA (ssDNA) handles and bound by a coverslip surface coated with motor proteins and ssDNA that are complementary to the nanotube's ssDNA handles. While the nanotube is anchored, the kicks from the motors are unable to move the nanotube. To initiate gliding, a third strand is introduced to displace the bonds between the nanotube and the surface ssDNA (Fig.1b).

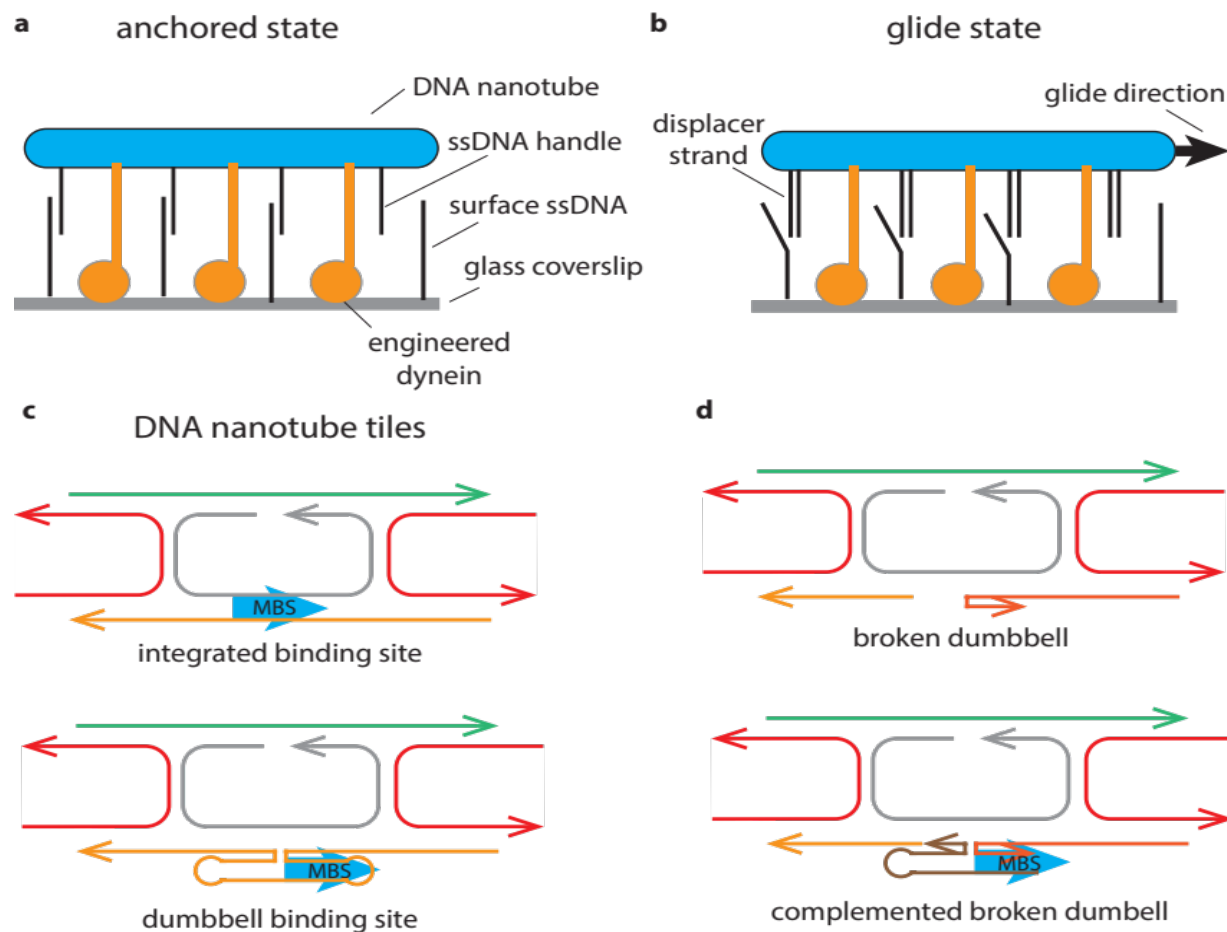


**Fig. 1** Designs of configurable DNA nanotube gliders. **a**, DNA nanotube anchored by surface strands. **b**, Bonds to surface strands are disrupted by the addition of a displacer, allowing the nanotube to glide. **c**, Schematic of nanotube tiles comparing integrated (from Ref. 2) and dumbbell designs for incorporating the motor binding site (MBS). **d**, Broken dumbbell design for toggling the MBS via strand hybridization.

Our success in using strand displacement to toggle gliding provided motivation for designing tubes where their gliding polarity could be toggled. As previously shown by Ibusuki et al., the polarity of the nanotube glide direction is determined by the orientation of the DNA sequence that the motor protein binds to. We find that these engineered motors only recognize the double stranded version of the binding sequence, which means that nanotube-motor interactions can be toggled by hybridizing/dehybridizing regions containing the motor binding sequence. We

first redesigned the DNA nanotube so that the motor binding site is no longer part of the integrated structure of the nanotube, but instead in a modular dumbbell that comes off of the nanotube (Fig.1c). We find that dumbbell nanotubes are found to glide as well as nanotubes with integrated binding sites. To make a motor binding sequence that can be toggled, we constructed a broken dumbbell design, where we effectively broke the single strand that forms the dumbbell into two strands (Fig.1d). The broken dumbbell design allows the DNA nanotube to still form independent of the presence of the dsDNA motor binding sequence. We are presently testing this design experimentally. In principle, the addition of a complementary strand will allow the broken dumbbell tubes to start gliding and a third invader strand will cause the tubes to fall off the coverslip surface. Our broken dumbbell design will be further adapted so that the nanotube glide polarity can be switched by the addition of different ssDNA strands.

### Future Plans

We have established the capability to reconfigure the DNA nanotube interactions with global addition of various ssDNA strands. Our next step is to spatially localize nanotube reconfiguration, which is fundamental for creating self-contained and eventually autonomous self-organizing systems. Spatially localized reconfiguration will be achieved by patterning the coverslip surface with DNA complexes. First, we will use both our surface anchoring and dumbbell designs to localize the release and capture of nanotubes (Fig.2a). Nanotubes will start out without any

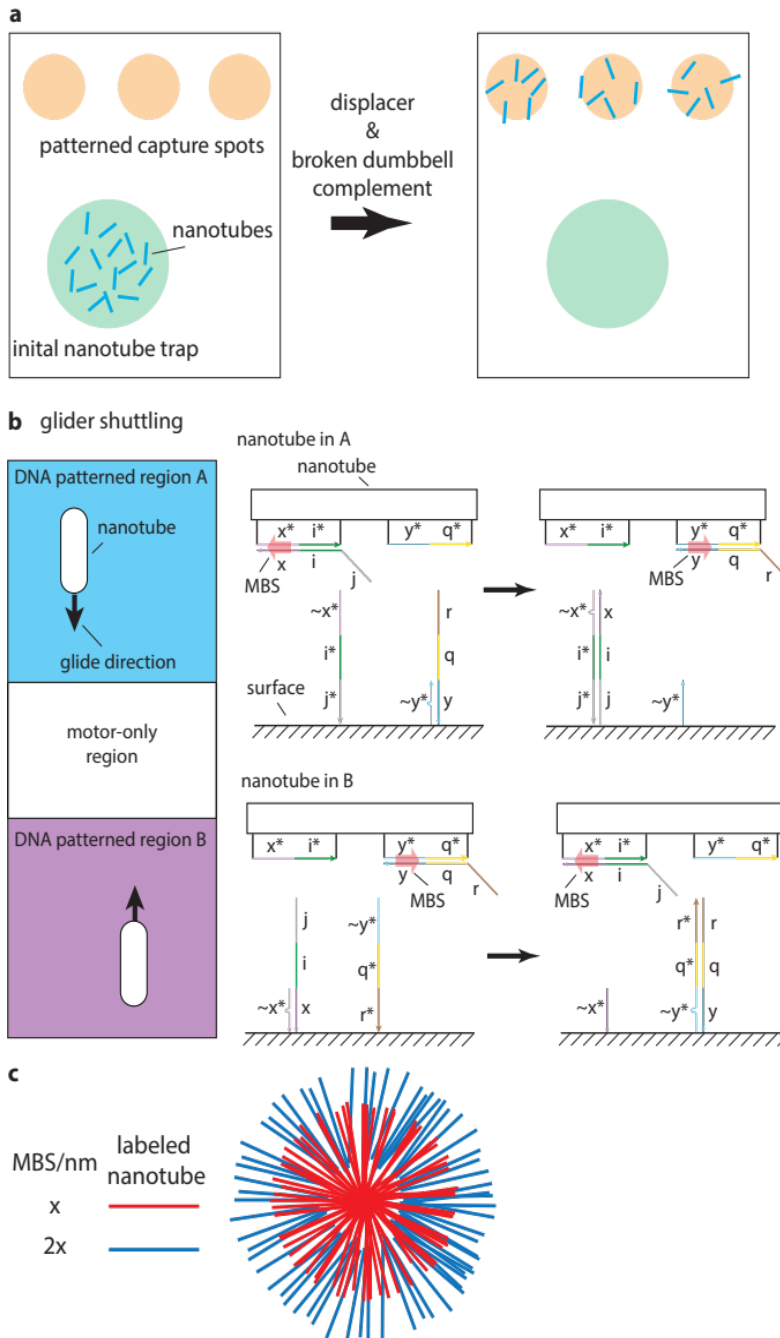


**Fig.2** Organization of configurable nanotubes. **a**, Overhead view of nanotube release and capture scheme. **b**, (left) Depiction of nanotubes shuttling between two patterned regions. (right) Strand displacement scheme for nanotube polarity switching. **c**, Organization of nanotubes with different motor binding site spacings into an aster via crosslinked motors.

hybridized motor binding sites, so their binding to the coverslip surface only depends on the presence of ssDNA. Upon the addition of both complements to broken dumbbells and surface strands, nanotubes will begin gliding until they are captured in a new patch of surface strands that contain an orthogonal sequence to the original anchoring strands. This provides a basic means for spatially reorganizing nanotube gliders.

For dynamic reorganization of gliding nanotubes, we will use the reconfiguration of nanotube gliding polarity as a means to make nanotubes shuttle between two regions (Fig.2b). Each patterned region will contain two DNA complexes: one complex will donate a strand to complete a broken dumbbell on the nanotube and the other complex will remove the broken dumbbell strand of the opposite polarity. The shuttling efficiency will be a function of both the gliding persistence length and the distance between the two patterned regions, which we can both model and experimentally test.

We also intend to move beyond the organization of gliding nanotubes and investigate the principles of self-organization of heterogeneous multi-nanotube structures in the form of an aster. As with engineered microtubule asters (Ref. 3), we will use crosslinked motor proteins to pull the ends of nanotubes together to form an aster. Nanotubes with different diameters and motor binding site spacings will have unique fluorescent labels. We will then be able to observe how different nanotube types are organized within the aster in addition to how they influence the overall aster structure (Fig.2c). Biophysical models will be tested experimentally and eventually used for prototyping. Specifically, we will use these models to explore how substrates with other geometries that are accessible through DNA origami may self-organize.

## References

1. C. Janke and M. M. Magiera, *The tubulin code and its role in controlling microtubule properties and functions*, Nature Reviews Molecular Cell Biology **21**, 307-326 (2020).
2. R. Ibusuki, T. Morishita, A. Furuta, S. Nakayama, M. Yoshio, H. Kojima, K. Oiwa, and K. Furuta, *Programmable molecular transport achieved by engineering protein motors to move on DNA nanotubes*, Science **375** 1159-1164 (2022).
3. F. J. Nédélec, T. Surrey, A. C. Maggs, and S. Leibler, *Self-organization of microtubules and motors*, Nature **389** 305-308 (1997)

## Publications

1. T. D. Ross, D. Osmanović, J. F. Brady, and P. W. K. Rothmund, *Ray optics for gliders*, ACS Nano **16**, 16191-16200 (2022).

## **Dissipation and control in nonequilibrium self-assembly**

**Grant M. Rotskoff**

**Keywords:** nonequilibrium control, dissipation, self-assembly, actin metamaterials

### **Research Scope**

An equilibrium interaction design framework requires modulating the nature of an interaction in a chemical or biomolecular component. Carrying out such a modification is not only highly nontrivial, but it also may disrupt the biological or chemical function of the constituent molecules. Biomolecular materials regulate structure not only with highly-specific interactions, but also by actively remodeling interactions and expending chemical energy. Indeed, energy dissipation is the distinguishing feature of living matter, and the expenditure of chemical energy is crucial to many biological assembly processes. In light of this fact, it is advantageous to view self-assembly of biomolecular materials as a dissipative, nonequilibrium process. Understanding a nonequilibrium assembly process requires understanding the dynamical trajectory by which the components assemble to determine the ultimate structure, not simply the thermodynamic ground state associated with a given potential energy.

A viewpoint focused on nonequilibrium dynamics affords new opportunities to control and design complex materials. Because assembly dynamics can be controlled by coupling the system to time-varying external fields, dissipative self-assembly raises the possibility of optimizing external protocols to target specific structures which may not be the thermodynamic free energy minimum structure as determined by energetic interactions among the material components. However, significant theoretical questions about dissipative self-assembly remain entirely unresolved. This scope of this project includes a focus on three questions concerning the controlling self-assembly: 1) How can we control active and dynamic materials to tune material properties? 2) How can we leverage multi-agent reinforcement learning techniques to exploit the natural multiscale structure of molecular self-assembly? 3) How do we efficiently explore chemical space to discover materials that will lead to assembled structures with designated physical properties?

Progress on these questions requires insight from nonequilibrium self-assembly, nonequilibrium control, and machine learning, and will substantively expand opportunities to design self-assembly.

### **Recent Progress**

We have made progress on the multifaceted research objectives outlined above in several different directions, developing new computational tools for large-scale atomistic simulation<sup>1</sup>, theoretical<sup>2</sup> and computational<sup>3</sup> tools for nonequilibrium control, and applying these tools to study controllable assembly of branched actin networks<sup>4</sup>.

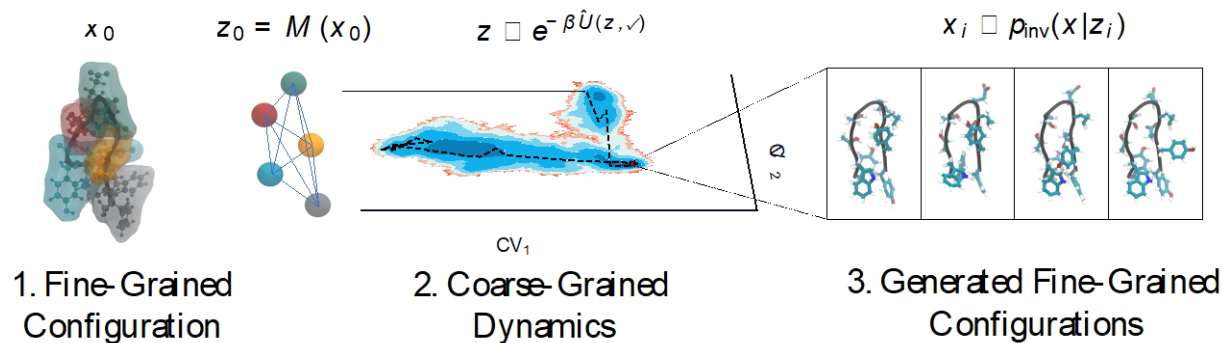


**Figure 1.** A new computational strategy for atomistic simulation that will give molecular insight into structures that arise from minimal models.

The new computational tools for atomistic simulation we developed can be viewed as an enhanced form of coarse-grained modeling, depicted in Fig. 1, which is a core computational tool in theoretical chemistry and biophysics. A judicious choice of a coarse-grained model can yield physical insight by isolating the essential degrees of freedom that dictate the thermodynamic properties of a complex, condensed-phase system. The reduced complexity of the model typically leads to lower computational costs and more efficient sampling compared to atomistic models. Designing “good” coarse-grained models, however, is an art. Generally, the mapping from fine-grained configurations to coarse-grained configurations itself is not optimized in any way; instead, the energy function associated with the mapped configurations is. In this work, we explore the consequences of optimizing the coarse-grained representation alongside its potential energy function. We use a graph machine learning framework to embed atomic configurations into a low dimensional space to produce efficient representations of the original molecular system. Because the representation we obtain is no longer directly interpretable as a real space representation of the atomic coordinates, we also introduce an inversion process and an associated thermodynamic consistency relation that allows us to rigorously sample fine-grained configurations conditioned on the coarse-grained sampling. We show that this technique is robust, recovering the first two moments of the distribution of several observables in proteins such as chignolin and alanine dipeptide.

Our efforts to expand both the theoretical and computational toolkit for nonequilibrium control led to a better understanding of objective functions for control problems: Controlling thermodynamic cycles to minimize the dissipated heat is a longstanding goal in thermodynamics, and more recently, a central challenge in stochastic thermodynamics for nanoscale systems. We introduced<sup>2</sup> a theoretical and computational framework for optimizing nonequilibrium control protocols that can transform a system between two distributions in a minimally dissipative fashion. These protocols optimally transport a system along paths through the space of probability distributions that minimize the dissipative cost of a transformation. Furthermore, we showed that the thermodynamic metric---determined via a linear response

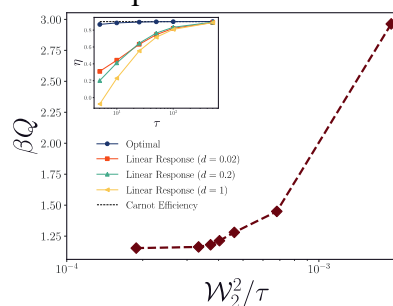


**Figure 2.** Optimizing nanoscale machines for low dissipation beyond linear response.

approach---can be directly derived from the same objective function that is optimized in the optimal transport problem, thus providing a unified perspective on thermodynamic geometries. We investigated this unified geometric framework in some model systems, shown in Fig. 2, and observe that our procedure for optimizing control protocols is robust beyond linear response.

The adaptive and surprising emergent properties of biological materials self-assembled in far-from-equilibrium environments serve as an inspiration for efforts to design nanomaterials and their properties. In particular, controlling the conditions of self-assembly can modulate material properties, but there is no systematic understanding of either how to parameterize this control or how controllable a given material can be. Here, we demonstrate that branched actin networks can be encoded with *metamaterial* properties by dynamically controlling the applied force under which they grow, and that the protocols can be selected using multi-task reinforcement learning. These actin networks have tunable responses over a large dynamic range depending on the chosen external protocol, providing a pathway to encoding “memory” within these structures, as shown in Fig. 3. Interestingly, we show that encoding memory requires dissipation and the rate of encoding is constrained by the flow of entropy---both physical and information theoretical. Taken together, these results emphasize the utility and necessity of nonequilibrium control for designing self-assembled nanostructures.

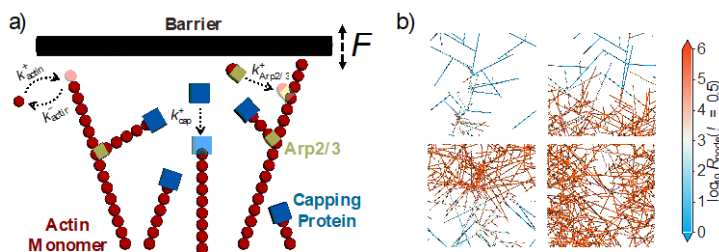


**Figure 3.** A minimal model of actin growth under load recapitulates experimental observations and demonstrates opportunities for nonequilibrium control.

Here, we demonstrate that branched actin networks can be encoded with *metamaterial* properties by dynamically controlling the applied force under which they grow, and that the protocols can be selected using multi-task reinforcement learning. These actin networks have tunable responses over a large dynamic range depending on the chosen external protocol, providing a pathway to encoding “memory” within these structures, as shown in Fig. 3. Interestingly, we show that encoding memory requires dissipation and the rate of encoding is constrained by the flow of entropy---both physical and information theoretical. Taken together, these results emphasize the utility and necessity of nonequilibrium control for designing self-assembled nanostructures.

## Future Plans

We plan to further characterize and investigate the limits of nonequilibrium control for self-assembly using both theoretical and computational approaches. Our overarching vision is to combine external, nonequilibrium control forces (e.g., time-dependent control of temperature, chemostats, electric fields) and de novo designed molecular components to guide the assembly dynamics towards materials with properties that may be inaccessible under conditions of thermodynamic equilibrium. Unlike the well-studied interaction design approach, in which a flexible---and not necessarily physically realizable---interaction is optimized to energetically stabilize the desired equilibrium structure, our strategy can directly impose the constraints of both the relevant chemistry and also the experimental limitations of external control.

We plan to continue to develop a theoretical framework to describe the extent and fundamental limits of controllability of chemical systems with fixed molecular components, ii) a computational approach for solving optimal control problems for the dynamical self-assembly of physics-based models of such systems, and iii) a semi-supervised machine learning framework to integrate experimental data into de novo design of molecular components within a target category of molecules.

We will also develop multi-agent reinforcement learning algorithms, which create opportunities to tune the external control protocol based on the stage of the assembly process, with agents acting locally and interactions developing larger length scale correlations, as our recent work has

emphasized. This approach has the potential to leverage precise local control of an assembly process to aid in the design of multiscale systems. We will develop multi-agent reinforcement learning algorithms that exploit correlations between agents to couple dynamics at multiple length-scales, enabling hierarchical self-assembly by controlling dynamics at different spatial and temporal resolutions. This effort will be carried out primarily in active matter systems.

## References

1. Chennakesavalu, S., Toomer, D. J. & Rotskoff, G. M. *Ensuring thermodynamic consistency with invertible coarse-graining*. J. Chem. Phys. **158**, 124126 (2023).
2. Chennakesavalu, S. & Rotskoff, G. M. *Unified, Geometric Framework for Nonequilibrium Protocol Optimization*. Phys. Rev. Lett. **130**, 107101 (2023).
3. Yan, J. & Rotskoff, G. M. *Physics-informed graph neural networks enhance scalability of variational nonequilibrium optimal control*. J. Chem. Phys. **157**, 074101 (2022).
4. Chennakesavalu, S., Manikandan, S. K., Hu, F. & Rotskoff, G. M. *Adaptive nonequilibrium design of actin-based metamaterials: fundamental and practical limits of control*. Submitted. <http://arxiv.org/abs/2306.10778> (2023).

## Publications

1. Chennakesavalu, S., Manikandan, S. K., Hu, F. & Rotskoff, G. M. *Adaptive nonequilibrium design of actin-based metamaterials: fundamental and practical limits of control*. Preprint at <http://arxiv.org/abs/2306.10778> (2023).
2. Chennakesavalu, S., Toomer, D. J. & Rotskoff, G. M. *Ensuring thermodynamic consistency with invertible coarse-graining*. J. Chem. Phys. **158**, 124126 (2023).
3. Chennakesavalu, S. & Rotskoff, G. M. *Unified, Geometric Framework for Nonequilibrium Protocol Optimization*. Phys. Rev. Lett. **130**, 107101 (2023).
4. Bowman, G. R. et al. *Remembering the Work of Phillip L. Geissler: A Coda to His Scientific Trajectory*. Annual Review of Physical Chemistry **74**, 1–27 (2023).

## Tension- and Curvature- Controlled Fluid-Solid Domain Patterning in Single Lamellae

Maria M. Santore and Gregory M. Grason  
Department of Polymer Science and Engineering  
University of Massachusetts, Amherst, MA 01003

**Keywords:** elasticity, assembly, two dimensional colloids, crystallization

### Research Scope

This program integrates theory and experiment to facilitate the discovery of dynamic patterning mechanisms in ultrathin materials such as elastic fluid-solid composite sheets that can reversibly assume dynamic contours having non-zero Gaussian curvature while reconfiguring their patterns. Patterns assembled from a common set of solid building blocks or ‘elements’ range from local structures to those spanning the system length scale. Examples include regular arrays and hexagonal lattices, or parallel stripes or interconnected networks, or complexity in the solid elements themselves. The latter can be engineered to include a variety of shapes from thin disks, hexagons, and diamonds to stars and elaborate flowers, and this shape may provide control over some aspects of the assembly process and resulting patterns. In this program, however, the interactions between the solid elements are often dominated by the elasticity of the fluid-solid sheets themselves. Therefore this program prioritizes an understanding of how elasticity and curvature produce shapes and assembled structures. An exciting and useful feature of these flexible composite sheets is their switchable nature, reconfiguring shapes and patterns on the timescales of seconds and minutes in response to mechanical stimuli. The elastic composite sheets can reconfigure when gently touched, or their mechanical response could be exploited to produce trapped patterns as part of the manufacture of patterned objects, accessing many properties from a one chemical composition.

This program exploits the 4nm-thick lamellae of giant unilamellar phospholipid vesicles containing fluid and solid membrane domains as a platform to establish mechanics of pattern formation in ultrathin sheet materials. These two-phase biomolecular membranes have 2D fluid regions with integrated 2D solids both with bending and stretching elasticity. The fluid regions flow freely via in-plane shear while the solid domains have large in-plane moduli that effectively eliminate shear deformation. Thus, solid shear elasticity underlies the geometrically nonlinear coupling between Gaussian curvature and in-plane strain of 2D sheets.

### Recent Progress

Overview. We present quantitative insights into the influence of elasticity on two aspects of pattern formation in composite sheets: 1) the morphologies of 2D solid crystals nucleating and growing within an elastic 2D fluid sheet and 2) an initial state space for multibody pattern formation in elastic composite fluid-solid sheets. In both cases theory and experiment target fundamental quantities such as the relative energies of the fluid and solid regions and of the whole system as a function of strain and shape, along with experimentally accessible quantities that relate

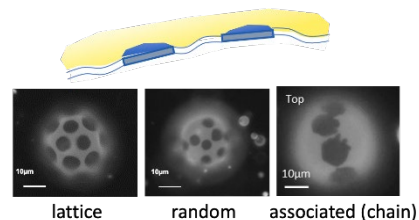


Figure 1. Schematic of 2D fluid-solid composite and examples of solid element configurations.

to membrane energies, or controllable engineering quantities that enable us to produce targeted patterns in bench scale quantities as opposed to one-at-a-time production.

Impact of elasticity on a 2D crystal growing in a membrane. Giant unilamellar vesicles were produced from a binary phospholipid mixture of 30 mol% DPPC (which forms molecularly-ordered crystalline lamella below its melting temperature) and 70% DOPC (which forms fluid lamellae). The addition of a tracer lipid rendered the fluid membrane domains fluorescent, enabling identification of solid domains, which were dark. Upon cooling from elevated temperatures near 50°C into the two phase region of the phase diagram in Figure 2A, solid domains nucleate and grow within the vesicle membranes. Figures 2B and 2C provide two series of images for separate vesicles on which different domain shapes grew with progressive cooling. The amount of solid within each vesicle generally adheres to that on the tie lines at progressively cooler temperatures, indicating the solid area follows the thermodynamic equilibrium of the phase diagram. However, an unusual feature of domain growth, in Figures 2B and C, is the preservation of domain shape with increasing domain size, either a compact hexagon or a six-petal flower. This growth morphology differs from dendritic growth since new protrusions do not progressively sprout at fluid-solid boundaries. More petaled or protruding shapes were found, as is the case in the examples of Figure 2 on larger vesicles compared with the more compact hexagonal shapes which were generally found on the smaller vesicles. This trend for vesicle or template size runs opposite to the predictions of Foppl von-Karman theory,<sup>1</sup> phase-field modeling,<sup>2</sup> and colloidal crystallization on spherical templates.<sup>3</sup>

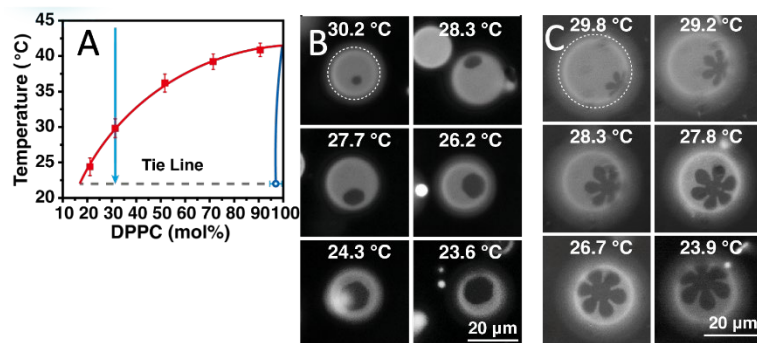


Figure 2. A. Phase diagram with cooling trajectory. B. and C. Examples of crystal growth, both for 30/70 DPPC/DOPC composition, and same solid fraction.

Insight into the mechanism for the growth of domains of different shapes is provided by *Surface Evolver* calculations revealing a continuum of shapes on vesicles with different degrees of inflation, in Figure 3A. Indeed, such a continuum was also found in for different vesicles in each cooling run in a single imaging chamber. Calculations reveal the mean and Gaussian curvatures of

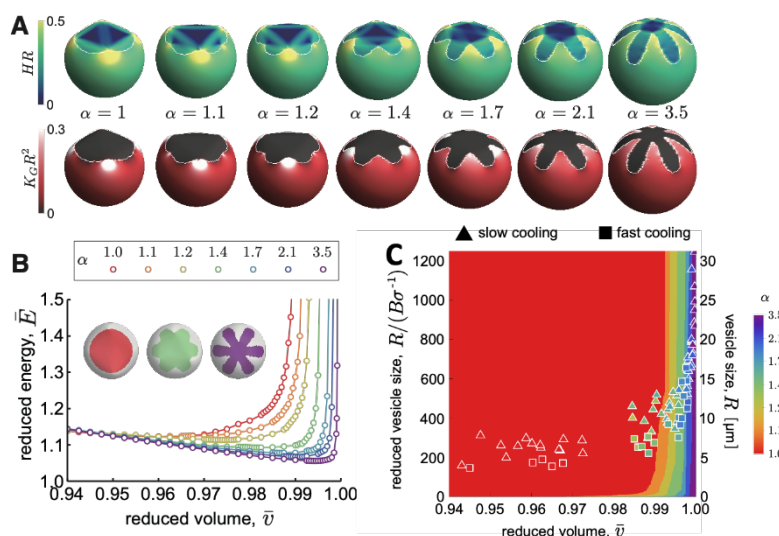


Figure 3. A. Surface Evolver calculations of vesicle shapes including fluid and solid domains, with coloring showing curvatures. B. Energy as a function of inflation for different shapes. C. State space of shapes including bending and line tension.

the solid domains and the total energy in Figure 3B, dominated by bending in the fluid and solid regions. Combining bending energy with a line tension at the fluid-solid edge, theory predicts compact domains on underinflated vesicles and flower shapes of increasing complexity on vesicles with greater inflations and membrane tensions, in the state space of Figure 3C, which superposes experimental data.

Tension-targeted processing for batch-scale production. We discovered that membrane tension in vesicles cooled from one temperature to another depends on a competition between cooling rate, which sets the rate of thermal membrane contraction (increasing tension), and water permeation across the membrane (reducing tension). The size dependence of water permeation, which occurs more effectively for smaller vesicles due to their greater surface to volume ratio, imparts a vesicle size dependence to the tensions of vesicles quenched into the two phase region for crystal growth. Greater tensions, also associated with greater degrees of inflation in Figure 3C, are found on larger vesicles. This further corresponds to greater protrusions and complexity of petal shapes in larger more inflated vesicles. As a result, in a single batch of vesicles controllably cooled into the two phase region, we systematically produce complex flower shapes on large vesicles and compact hexagons on small vesicles, in Figure 4.

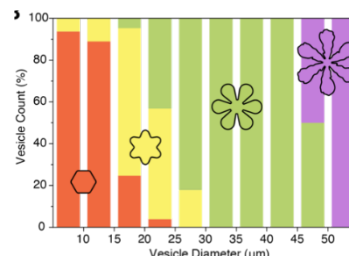


Figure 4. Distribution of crystal shapes as a function of vesicle size, for 500

Initial State space for vesicles containing 4-80 solid domain elements. A fascinating variety of domain patterns, including lattices and chains, is seen on vesicles containing many relatively monodisperse compact solid domains. Fixing the overall solid area fraction at 15%, we varied the domain-to-vesicle size ratio by varying the numbers of domains per vesicle via the nucleation density (via cooling rate). An additional parameter that was studied was the excess area,  $A_{XS}$ , defined in our recent paper<sup>4</sup> as the membrane area of a given vesicle to that of a sphere of equal volume.  $A_{XS}$  is determined from micropipette aspiration.

By eye in the examples of Figure 1, the domain patterns appear to be of 3 types: lattices, random arrangements, associated structures and networks. A Delaunay triangulation method connecting in-focus domains, and further analysis of the domain center-center distances from the Delaunay connectors reveals distinct coefficients of variation (COV) and Lindemann parameters for the three classes of domain patterns, substantiating our by-eye classification. The lattices wrap the entire vesicles and exhibit small COVs, corresponding to a high degree of order, while various chained patterns have large COVs. We further noted that the random patterns were quite dynamic and rearranged on a timescale of tens of seconds to minutes, while the lattices and associated structures were longer lived, on the order of

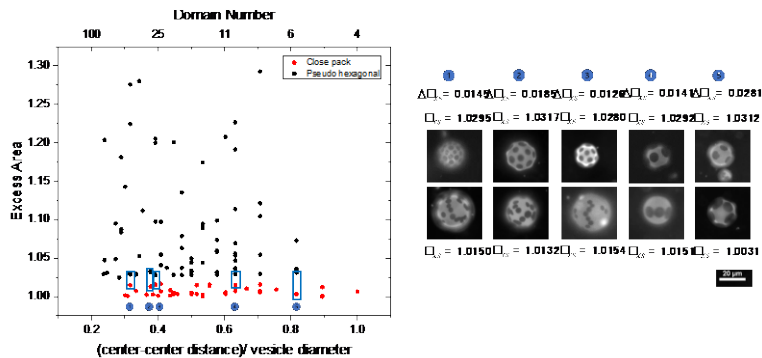


Figure 5. State space for lattice and associated chain configurations with sharp impact of excess area near possible phase transition.

minutes or much longer. Further consideration of lattice and chained structures revealed a state space in Figure 5 that argues the  $A_{XS}$ , related to the impact of bending energy in the fluid, is the single greatest variable influencing domain arrangement. The numbers of domains per vesicle and their size relative to the vesicle had minimal impact, even when the numbers of domains varied 1.5 orders of magnitude from 4 to 80. Moreover, there is a domain number-independent threshold in  $A_{XS}$  for lattice formation, with further  $A_{XS}$  not influencing the lattice arrangement, possibly signaling a melting transition.

## Future Plans

This program demonstrated a new mechanism for morphological control of bendy 2D crystal growth by elastic forces, and a curvature and size dependence of the crystal morphologies. 2D crystals can be produced at small batch scale, with targeted morphologies on vesicles of different sizes. Future work will explore the compositional dependence of crystal morphology, the impact of processing on the control of morphology, and the mechanical properties of individual single crystals. This program also developed a state space for 2D colloidal assembly in a thin fluid sheet, demonstrating how excess area, relating to bending forces, is the dominant variable and that extremely small changes produce dramatic morphological differences, reminiscent of a phase transition. The next phase of work will target dynamics of assembly and probing the origin of multibody interactions that do not arise in a straightforward way from pairwise interactions.

## References

1. S. Schneider, and G. Gompper, *Shapes of crystalline domains on spherical fluid vesicles*. Europhysics Letters **70**, 136-142 (2005).
2. C. Kohler, R. Backofen, and A. Voigt, *Stress Induced Branching of Growing Crystals on Curved Surfaces*. Phys Rev Lett **116**, (2016).
3. G. N. Meng, J. Paulose, D. R. Nelson, and V. N. Manoharan, *Elastic Instability of a Crystal Growing on a Curved Surface*. Science **343**, 634-637 (2014).
4. W. Y. Xin, H. Wu, G. M. Grason, and M. M. Santore, *Switchable positioning of plate-like inclusions in lipid membranes: Elastically mediated interactions of planar colloids in 2D fluids*. Science Advances **7**, eabf1943 (2021)

## Publications

1. W. Y. Xin, H. Wu, G. M. Grason, and M. M. Santore, *Switchable positioning of plate-like inclusions in lipid membranes: Elastically mediated interactions of planar colloids in 2D fluids*. Science Advances **7**, eabf1943 (2021)
2. H. Wan, G. Jeon, W. Xin, G.M. Grason and M. M. Santore, *Flowering of developable 2D crystal Shapes in closed, fluid membranes*, Nature Materials, submitted. Doi.org/10.48550/arXiv.2307.02606

## Synthesizing functionality in excitonic systems using DNA origami

Gabriela S. Schlau-Cohen (PI), Department of Chemistry  
Mark Bathe (co-PI), Department of Biological Engineering  
Adam P. Willard (co-PI), Department of Chemistry  
Massachusetts Institute of Technology

**Keywords:** DNA nanotechnology, light harvesting, excitons, solar energy conversion

### Research Scope

The overall goal of our research program is to establish a class of materials that enable programmable exciton dynamics. The functional breadth of electronic excited states, *i.e.*, excitons, is remarkably rich. For example, chlorophyll can function in multiple ways, performing nanoscale energy transfer, facilitating charge separation, and undergoing rapid non-radiative decay. Natural systems select amongst these functions via precise positioning of chlorophyll within protein scaffolds. This position-dependent functionality can be achieved using DNA origami architectures as scaffolds for molecular chromophores. The structural variety and geometric precision afforded by higher-order DNA origami architectures enable the development of synthetic excitonic systems with broad and tunable functionalities that mimic or potentially exceed those found in biology. DNA-based excitonic systems have been demonstrated previously, yet have employed a limited number of DNA structural motifs. These motifs have, in turn, limited control over chromophore positioning and interchromophoric coupling, and so studies have focused on exciton transport efficiency alone. Advances in the complexity and precision of these structures will enable the study of other fundamental functions in exciton dynamics, such as charge separation, singlet fission, and non-radiative decay.

### Recent Progress

*Geometric control over exciton dynamics for fluorescence imaging.* We constructed coupled DNA-chromophore assemblies for applications as fluorescent labels for biological and analytical imaging. By designing DNA structures with a strongly coupled molecular dimer and variable complementary strands (adding up to five additional bases), we were able to introduce geometric distortion (schematic in Figure 1A).<sup>1</sup> This yielded variation in both the coupling within excitonic states (Figure 1B) and the excited state lifetime

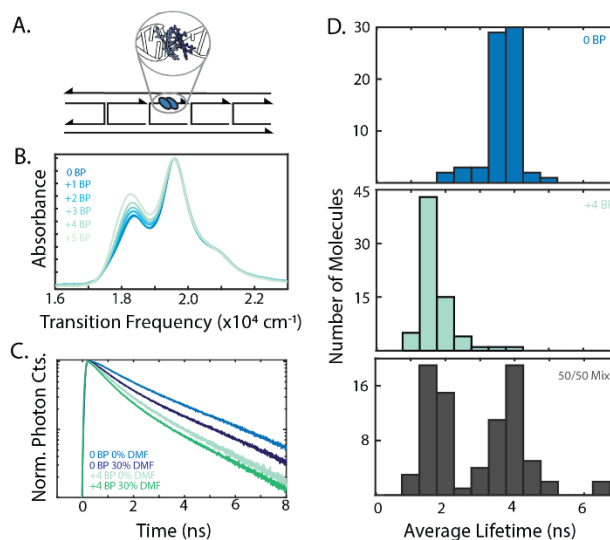


**Figure 1.** Tuning excitonic properties with geometric distortion. (A) Schematic of DNA-chromophore dimer. (B) Absorption profile of distorted dimer with the number of additional bases ranging from 0 to 5. (C) Emission lifetime of dimers with a distortion of 0 and 4 bases in an aqueous environment and with addition of 30% DMF. (D) Single molecule lifetime distributions of dimers with 0 and 4 base distortions and a 50/50 mixture of dimers, highlighting that the two species are distinguishable on the single molecule level.

(Figure 1C). Single-molecule measurements (Figure 1D) show that variation in excited state lifetime from differences in complementary strand is visible with limited heterogeneity on the single molecule level. This suggests these DNA scaffolded distorted dimers could be used as single molecule fluorescence lifetime imaging probes. The dimer excited state lifetimes are also sensitive to solvent polarity (Figure 3C with the addition of 30% non-polar solvent, DMF), highlighting the role these structures could play in imaging biological systems with an environmentally sensitive lifetime read-out.<sup>5</sup> This proof of principle study showed that engineered molecular dimers can be used as fluorescence lifetime imaging probes, and would be particularly useful in tracking DNA strand displacement reactions.

*Activating charge-transfer state formation in strongly-coupled dimers using DNA scaffolds.* Excitonic systems are typically regulated by long-range Coulombic coupling and short-range charge transfer coupling. Here, we leverage variable DNA-chromophore constructs to tailor the interplay between the types of couplings through the examination of a zwitterionic squaraine dye (Figure 2A). Steady-state measurements reveal the formation of strongly-coupled dimers possessing a charge transfer state (Figure 2B-C).<sup>2</sup> We further investigated this state via transient

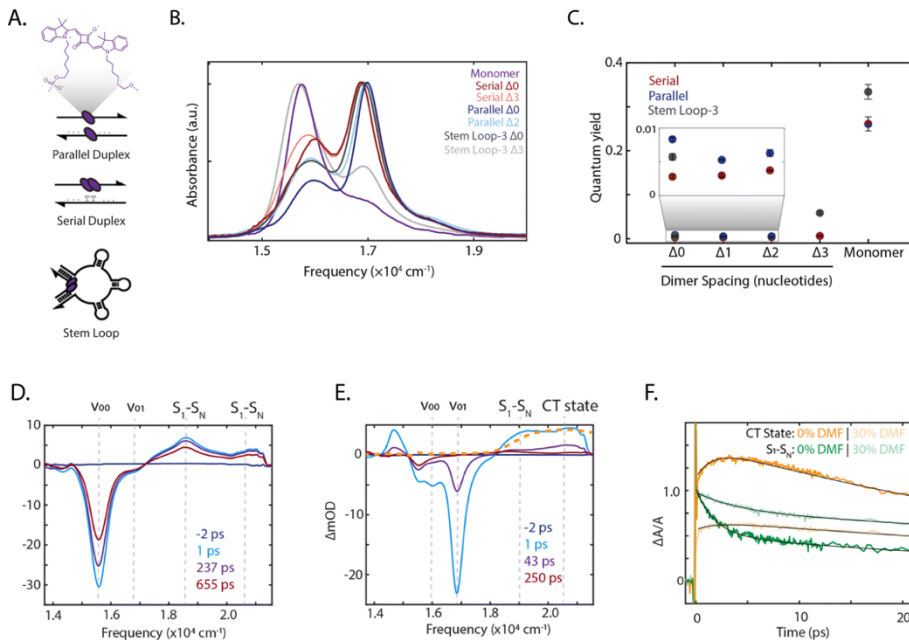


**Figure 2.** Exploring charge-transfer coupling in DNA-chromophore assemblies (A) Schematic of DNA-squaraine assembly. (B) Absorption spectra of squaraine monomers and dimer duplexes and stem loop constructs. (C) Quantum yield for DNA scaffolded monomers and dimers within serial and parallel duplexes and stem loop-3 constructs. Femtosecond transient absorption spectra for the stem loop-3 constructs (D) monomer and (E) dimer upon excitation centered at  $17,700 \text{ cm}^{-1}$ . (F) Transient absorption derived traces for the stem loop-3  $\square 0$  dimer construct.

absorption spectroscopy (Figure 2D-F). In comparison with the monomer, the strongly-coupled squaraine dimer exhibits symmetry-breaking charge transfer. Despite extensive previous studies, charge transfer had not been previously achieved in squaraine dimers. This work demonstrates that DNA scaffolds offer the potential to control the interplay of inter-molecular couplings, which allows the selection of distinct photochemical and photo-physical processes.<sup>5</sup>

*Excitonic state selection with DNA origami libraries.* The geometry of coupled chromophores dictates the nature of their coupling, and thus the emergence and propagation of excited electronic states. DNA-based systems had been limited to duplexes or DX-tiles, the building blocks of DNA origami. Here, we introduce six-helix bundles (6HB), a DNA origami scaffold, and leverage the additional geometric control offered by this more complex structure to program specific couplings in dimers of a prototypical molecular sensitizer, perylene diimide (PDI). We templated dimers to DNA scaffolds of varied structural complexity: duplexes and 6HBs (Figure 3A-C).<sup>3</sup> Transient absorption (TA) spectroscopy revealed that the structural complexity of the DNA scaffold can modulate the formation and dynamics of excitonic product states. TA spectra and kinetic traces illustrate that duplex scaffolds facilitate predominantly charge transfer coupling, while 6HBs can also generate excimer states (see Figure 3D-G). These findings suggest that DNA nanophotonic materials offer potential utility to steer emergent photophysics in designer photovoltaic and optoelectronic devices.

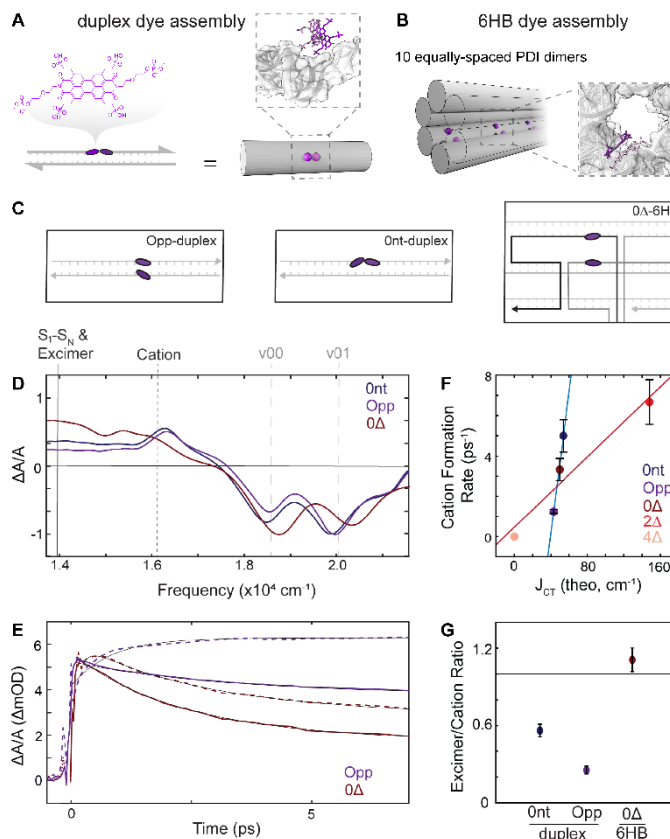


**Figure 3.** (A) Duplex and (B) 6HB dimers. (C) Diagrammatic illustration of strongly-coupling dimers in duplex and 6HB constructs. (D) TA spectrum collected at  $\Delta t=3$  ps of duplex dimers with 0 nucleotide spacing (0nt; blue) and opposite (opp; purple) configurations, as well as an opp-6HB dimer (0 $\Delta$ ; red). (E) Kinetic traces for PDI cation (dashed) and excimer (solid) in opp-duplex- and 0 $\Delta$  6HB-dimers. (F) Comparison of cation formation rate for duplex and 6HB assemblies with varied Coulombic coupling. (G) Excimer-cation sub-population ratios for duplex and 6HB assemblies.

*Investigating the role of complex-valued coupling for energy transfer.* Complex-valued electronic coupling presents an innovative approach to regulate coherent exciton transfer by incorporating a phase in electronic interaction. In highly symmetric molecules like porphyrins, circular polarization generates a current selecting one of two delocalized complex excitations based on light polarization. Coupling with a low-symmetry linear dye introduces a phase, resulting in imaginary coupling (see Figure 4A). We examined coupled dyes excited by circularly polarized light to create complex coupling interactions. Exciton flux control was demonstrated in three-dye

cycles (Figure 4B)<sup>4</sup> and constructed with circular dyes linked to distinct linear dye pathways.

Following theoretical guidelines, DNA-porphyrin assemblies were synthesized for molecular geometry control.

Additionally, we developed an instrument for chiral ultrafast transient absorption measurements in such systems.

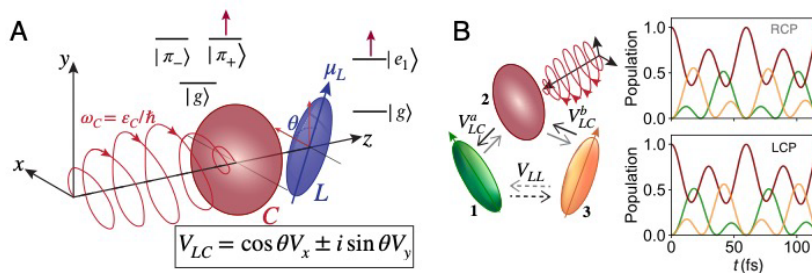


**Figure 4.** (A) Generation of complex-valued coupling through the interaction between a symmetric circular molecule and an asymmetric linear molecule. (B) Using light polarization to manipulate the direction of exciton flux in a three-dye cycle.

*Other projects.* Along with the efforts described, we have successfully produced several other DNA-based excitonic structure, including excimeric systems, light-harvesting systems with multiple strongly coupled chromophores, molecular photonic wires, and 2D systems with enhanced energy transport.

## Future Plans

Our ongoing and planned work is focused on both fundamental photophysics and photochemistry and higher-order structures for solar energy conversion, fluorescence assays, and computing. We are exploring the use of non-canonical nucleic acid structures to enhance coherent delocalization, many-body interactions to drive long-distance energy transport, and selecting the nature of the excitonic landscape. The development of such abilities will allow for the incorporation of new functionality into these nanoscale materials.

## References

1. S. M. Hart, X. Wang, J. Guo, M. Bathe, and G. S. Schlau-Cohen, *Tuning Optical Absorption and Emission Using Strongly Coupled Dimers in Programmable DNA Scaffolds*, *J. Phys. Chem. Lett.* **13**, 1863-1871 (2022).
2. S. M. Hart, J. L. Banal, M. A. Castellanos, L. Markova, Y. Vyborna, J. Gorman, R. Häner, A. P. Willard, M. Bathe, and G. S. Schlau-Cohen, *Activating Charge-Transfer State Formation in Strongly-Coupled Dimers Using DNA Scaffolds*, *Chem. Sci.* **13**, 13020-13031 (2022).
3. J. Gorman, S. M. Hart, T. John, M. A. Castellanos, J. L. Banal, M. N. Scott, A. P. Willard, G. S. Schlau-Cohen, and M. Bathe, *Probing the exciton dynamics of strongly-coupled chromophores using DNA origami libraries*, in preparation.
4. M. A. Castellanos, and A. P. Willard, *Imaginary Excitonic Coupling: Toward Directional Exciton Flux in Organic Semiconductors*, in preparation.
5. S. M. Hart, J. Gorman, M. Bathe, and G. S. Schlau-Cohen, *Engineering Exciton Dynamics with Synthetic DNA Scaffolds*, *Acc. Chem. Res.*, 159-166 (2023).

## Publications

1. S. M. Hart, X. Wang, J. Guo, M. Bathe, and G. S. Schlau-Cohen, *Tuning Optical Absorption and Emission Using Strongly Coupled Dimers in Programmable DNA Scaffolds*, *J. Phys. Chem. Lett.* **13**, 1863-1871 (2022).
2. S. M. Hart, J. L. Banal, M. A. Castellanos, L. Markova, Y. Vyborna, J. Gorman, R. Häner, A. P. Willard, M. Bathe, and G. S. Schlau-Cohen, *Activating Charge-Transfer State Formation in Strongly-Coupled Dimers Using DNA Scaffolds*, *Chem. Sci.* **13**, 13020-13031 (2022).
3. J. Gorman, S. M. Hart, T. John, M. A. Castellanos, J. L. Banal, M. N. Scott, A. P. Willard, G. S. Schlau-Cohen, and M. Bathe, *Probing the exciton dynamics of strongly-coupled chromophores using DNA origami libraries*, in preparation.
4. M. A. Castellanos, and A. P. Willard, *Imaginary Excitonic Coupling: Toward Directional Exciton Flux in Organic Semiconductors*, in preparation.
5. S. M. Hart, J. Gorman, M. Bathe, and G. S. Schlau-Cohen, *Engineering Exciton Dynamics with Synthetic DNA Scaffolds*, *Acc. Chem. Res.*, 159-166 (2023).
6. S. M. Hart, W. Chen, J. Banal, W. Bricker, A. Dodin, L. Markova, Y. Vyborna, A. P. Willard, R. Häner, M. Bathe, and G. S. Schlau-Cohen, *Engineering Couplings for Exciton Transport Using Synthetic DNA Scaffolds*, *Chem* **7**, 752-773 (2021).
7. W. Chen, J. Banal, S. M. Hart, A. Dodin, A. P. Willard, M. Bathe, and G. S. Schlau-Cohen, *Strongly-Coupled Excited State Enhances End-to-End Resonance Energy Transfer in DNA Scaffolded Molecular Photonic Wire*, in preparation.
8. M. Son, S. M. Hart, and G. S. Schlau-Cohen, *Investigating Carotenoid Photophysics in Photosynthesis with 2D Electronic Spectroscopy*, *Trends in Chemistry* (2021).
9. M. Castellanos, and A.P. Willard, *Designing Excitonic Circuits for the Deutsch-Jozsa Algorithm: Mitigating Fidelity Loss by Merging Gate Operations*, *Phys. Chem. Chem. Phys.* **23**, 15196-15208 (2021).

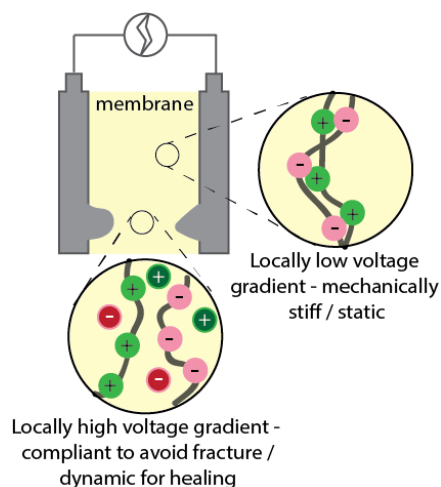
## Bio-inspired Polymer Membranes for Resilience of Electrochemical Energy Devices

Meredith N. Silberstein, Sibley School of Mechanical and Aerospace Engineering, Cornell University

**Keywords:** polyelectrolytes, electric field, electrophoresis, mechanical properties

### Research Scope

Like biological cell membranes, polymer membranes for electrochemical energy storage and conversion devices must control ion transport and be mechanically robust. Biological membranes are constantly assessing evolving “operating” conditions such as electric field and optimizing their function by dynamically adjusting their material state; the current generation of synthetic polymer membranes are static. Synthetic membrane performance and durability can be dramatically improved by imbuing the membrane with the ability to sense and adapt to the local electrochemical environment. One key enabler of biological self-regulation is ionic interactions. We are applying this biological concept to modulating ionic crosslinking within synthetic polymers.



The scope of this program is to discover the fundamental physical mechanisms for self-regulation of polymers and gels under electric fields by focusing on the following three aspects: (I) The influence of an external electric field on the strength of ionic bonds between polymer chains and how this interaction depends on concentration of ionic bonds, any solvent, free ions, polymer backbone rigidity, chemical details of the polymer; (II) How ionic bond strength and concentration among linear polymer chains influences polymer mechanical properties and self-healing for different polymer backbone rigidities and chain lengths; (III) Complete mechanical property dependence on electric fields by adding to I and II, key coupled aspects such as polymer reconfiguration guided by locally high electric field gradient. We are approaching this unexplored concept computationally, utilizing molecular dynamics (MD) simulations and constitutive modeling and validating our findings using synthesis, solution-based experiments, spectroscopy, and mechanical testing.

### Recent Progress

Over the past year we have finished up our study on the mechanical properties of a set of ionic copolymers that were previously found to have reasonable mechanical properties, pursued a controlled polymerization route to polymers we expected to have comparable properties, and focused on realizing electrophoresis inspired routes to modulating ionic polymer mechanical properties with electric fields.

The ionic copolymers we have been focusing are polyelectrolyte complex inspired. They consist of positively charged chains and negatively charged chains separately synthesized via free radical polymerization, chemically characterized, and then combined at a ratio to result in an overall neutral polymer, with mobile ions removed via dialysis. Control polymers were used that consist of only anionic or cationic chains, for which mobile ions must be present. Two neutral monomers were studied: ethyl acrylate (EA, low hydrophilicity) and 2-hydroxyethyl acrylate (HEA, high hydrophilicity). The charged monomer is [2-(acryloyloxy)ethyl]-trimethylammonium chloride (ATMAC) for the cationic copolymers and 3-sulfopropyl acrylate potassium (SPAP) for the anionic copolymers. Our experimental results showed that the ionic bonds between polymer chains in these elastomers substantially increase the stiffness, strength, and toughness (Figure 1) [1]. We infer from mechanical and spectroscopic data that the ionic bonds in the complex provide a resistance to interchain sliding that eventually yields, yet maintains strength through the bonds finding new pairs. This contribution is in conjunction with the entropic chain and entanglement contributions that are present in the control polymers as well. We formulated a continuum constitutive model in order to better understand the time dependence and cooperative nature of these underlying mechanisms [2]. The model was able to capture monotonic, cyclic, and stress-relaxation behavior of the polymer with different ratios of neutral-to-charged monomers, with only physically-based modifications of the material parameters. The model implies that most of the slow time dependent recovery is due to entanglement evolution. This highlights that for our work moving forward, we need to minimize entanglements if fast ionic responses to electric fields are needed. However, with a polyelectrolyte complex inspired material, this would also result in a more liquid like ionic-bond free reference material, which is a tradeoff that needs to be considered.

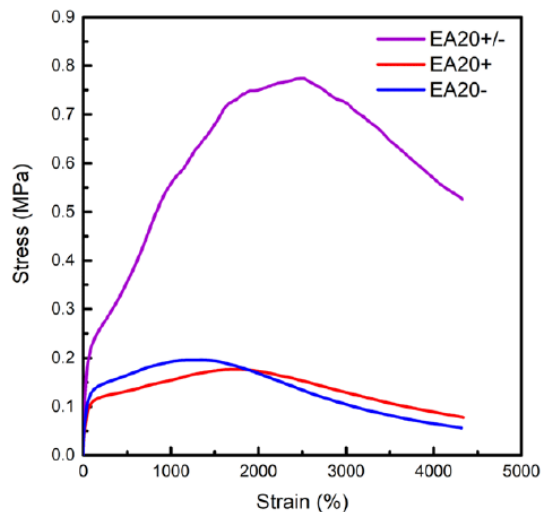


Figure 1. Stress-strain response of EA copolymer at a target neutral to ionic monomer ratio of 20:1. Comparison of the complex (+/-), cationic polymer only (-), and anionic polymer only (-).

To provide ourselves with more control over polymer composition moving forward, we have been working in collaboration with the Wiesner group to synthesize ionic copolymers of shorter and controlled chain length, using anionic polymerization. Here, we switched to an ethylene oxide (EO) neutral monomer and an allyl glycidyl ether (AGE) comonomer. This comonomer is converted to end in either a sulfonate (anionic) or an ammonium (cationic) group via a thiol-ene click reaction after the synthesized polymers chains have been chemically characterized. This approach, adapted from literature [3], greatly facilitates both charge matching of the anionic and cationic components in the complex (since the polymer chains for each are derived from the same batch of polymer) and chemical characterization (since it can be completed prior to ionic functionalization). To date, co-monomer ratios and molecular weights have deviated significantly from the target values. While we have used these polymers, as described below, we continue to work on improving this polymerization procedure.

In terms of electric field response, we have shifted our focus from our initial concept of a non-contact, static field-driven, direct chain separation, to current-drive (electrophoresis inspired) concepts. This shift was motivated by our year 2 molecular dynamics simulation results, that showed very large field strengths with no mobile ion contaminants, needed to achieve the initial concept. We are working with in all cases with anionic and cationic linear polymer chains interpenetrated (IPN) into a covalent neutral polymer network. We have synthesized both hydrogel and organogel versions. The hydrogels tend to be easier to tailor, but have the drawback of water splitting above 1.2V. There are two physical concepts under investigation in parallel, which we will refer to as “chain motion” and “ion motion”. Both require that the IPN makes a substantial contribution to the overall polymer mechanical response in the strongly interacting state.

In the first approach, “chain motion,” the concept is for the polymers themselves move to opposite ends of the host neutral matrix based on an applied electric current. This migration of the ionically charged polymer chains away from each other should result in a less stiff and more dynamic material, since the ionically crosslinked second network would effectively become a lubricating filler linear network. In these experiments, the gel is placed within a Tricine buffer solution to avoid pH effects, and an electric field is applied across the length via platinum electrodes. We conducted this experiment on an HEA covalent network polymerized around the EO-AGE-based polymer complex. The gel transitions from opaque to transparent over time as the field is applied, and not when the polymer is submerged in the buffer solution under no voltage. Subsequent characterization of each end of the polymer to prove that this transport occurred was inconclusive and is something we are still pursuing, as explained in the future plans section.

In the second approach, “ion motion,” the concept is for mobile ions to move in or out of the material, thereby interacting with the charges on the polymer chain and weakening the ionic bonding between oppositely charged chains. Here we place our adaptive material between two layers of just the neutral covalent network, to assemble a polymer stack that is three times the thickness of a single layer. The outer layers act as ion storing reservoirs. The initial polymer can be processed with either the middle or outer layers containing the mobile ions, depending on the desired property change. An electric field is then applied across the thickness via platinum electrodes, and not in solution. Controls consist of the material independently and the three layers stacked together but without an electric field applied. The stress-strain response of the active layer is tested independently, following removal from the stack, to help isolate changes to that layer. Here we have used an EA-based organogel as our covalent matrix. The active layer is interpenetrated with 20:1 neutral:charged EA copolymers and LiTFSI salt. Interestingly, and unexpectedly, the material with no electric field was found to be less stiff than the never stacked material. The material stacked and with electric field applied, was found to have a much larger spread in stiffness and strength than the other cases. It is unclear whether the unexpected stiffness trend is due to the details of the chemical composition, the low fraction of charged component, or the use of dimethylformamide (DMF) rather than water. From a solubility perspective for making the materials, we will need to change to a different solvent to utilize a greater ionic component.

## **Future Plans**

Over the final period of this grant, we will be pursuing both “chain motion” and “ion motion” approaches to electric field modulated stiffness and strength. Both have promising aspects, but neither is a guaranteed path to the targeted electric field dependence. For “chain

motion,” we will continue with the existing system, but improve our experimental methods to enable proof or disproof of the mechanisms underlying the macroscopically observed changes and to demonstrate mechanical property change. Key experimental improvements will be (1) utilizing a voltage applying system that can measure current, and (2) using a larger specimen. This larger specimen will enable us (1) to conduct spherical indentation mechanical characterization along the length of the polymer and (2) to have sufficient polymer after drying to characterize by FTIR. For “ion motion,” our primary approach will be to change the material system to an acrylamide-based hydrogel that we had synthesized and characterized earlier in the grant since we know the covalent gel plus IPN is stiffer and stronger than the covalent gel on its own. This choice comes at a tradeoff of needing to keep the applied voltage low to prevent water splitting, but gives much more design flexibility. Here too, we will improve our methods by measuring current during the electric field application. In addition to mechanical testing and controls as described above, we will conduct spectroscopy to analyze ion content and interchain bonding.

## References

1. Z. Wang, H. Cai, and M.N. Silberstein, *A Constitutive Model for Elastomers Tailored by Ionic Bonds and Entanglements*, *Mechanics of Materials* **179**, 104604 (2023).
2. H. Cai, Z. Wang, N.W. Utomo, Y. Vidavsky, and M.N. Silberstein, *Highly Stretchable Ionically Crosslinked Acrylate Elastomers Based on Polyelectrolyte Complexes*, *Soft Matter* **18**, 7679 (2022).
3. A. E. Neitzel, Y. N. Fang, B. Yu, A. M. Romyantsev, J. J. de Pablo and M. V. Tirrell, *Polyelectrolyte Complex Coacervation Across a Broad Range of Charge Densities*, *Macromolecules* **54**, 6878 (2021)

## Publications

1. Z. Wang, H. Cai, and M.N. Silberstein, *A Constitutive Model for Elastomers Tailored by Ionic Bonds and Entanglements*, *Mechanics of Materials* **179**, 104604 (2023).
2. H. Cai, Z. Wang, N.W. Utomo, Y. Vidavsky, and M.N. Silberstein, *Highly Stretchable Ionically Crosslinked Acrylate Elastomers Based on Polyelectrolyte Complexes*, *Soft Matter* **18**, 7679 (2022).

## **Biomimetic Strategies for Defect Annealing in Colloidal Crystallization**

**Michael J. Solomon and Sharon C. Glotzer, University of Michigan Ann Arbor**

**Keywords:** crystallization, annealing, confocal microscopy, Brownian dynamics simulation, colloids

### **Project Scope**

The purpose of this project is to generate fundamental understanding of mechanisms to correct and control for defects generated by self-assembly. By using colloids as a model system, we address the following scientific questions: (1) How may fields be applied to anneal colloidal crystal structures with orientational specificity? (2) How can angularly oscillating and rotating applied fields couple to rotational degrees of freedom of anisotropic colloids to impact crystal quality? and (3) How can active particles function as local agents that interact directly with defects to anneal them? Here we report the defect dynamics of self-assembled spherical colloids subjected to dipolar interactions and dielectrophoretic forces upon application of a rotating alternating current (AC) electric field. By combining oscillating AC fields and a static direct current (DC) electric field, we also switch discoidal colloids between parallel and perpendicular states in ways that generate a two-state optical response. Finally, we self-assemble thin films of colloids that yield structural color that is sensitively correlated with defect structures in the crystals and show that this relationship can be quantified in real time by confocal microscopy. In future work, mechanistic origins of the field effects, defect structures, and optical response will be elucidated by our approach of combining experiment and computational simulation. The biomimetic basis for this project is the interest in understanding how to recapitulate the reconfigurable structural color present in organisms such as cephalopods and by what means nature creates high quality crystal structures on conformal substrates and with anisotropic building blocks—environments and materials in which artificial methods of self-assembly are much less successful than nature.

### **Recent Progress**

We report our recent progress in: (1) applying rotating electric fields to understand how defects anneal in colloidal monolayers; (2) switching discoid colloids between parallel and perpendicular orientations to understand the dynamics of reconfiguration; (3) establishing the relationship between defect structures and the structural color response in thin films of colloidal crystals.

*Self-assembly and defect annealing in colloidal monolayers subjected to rotating electric fields.* In prior work, we have shown that switching applied fields with timing keyed to characteristic rates of melting can result in preferential rates of annealing [1]. The mechanism for the preferential annealing is the effect of the toggled field on the balance of defect creation and annihilation. The field applied in this prior work was an AC electric field directed along a specific axis. The AC field generated both dipolar interactions between the colloids and dielectrophoretic forces acting along the axis of field application. Switching this field configuration yielded annealing; the optimum was at about one-half the crystal's characteristic melting time. This approach to annealing works because the field cadence is coupled to the physics of melting; however, the approach lacks a connection to the underlying symmetry of the crystal. Might it not be possible to anneal large defect structures – like grain boundaries and dislocations – if the field application was cognizant of the crystal symmetry? To address this question, we have performed annealing

experiments in a device that allows application of fields with six-fold symmetry (Figure 1). Results show that under some conditions of field application, crystallite boundaries can be induced to propagate across the length of the specimen in ways that ultimately yield a single crystal structure. The dislocation dynamics can be captured by image analysis and the effect of field conditions understood; these conditions can also be recapitulated in simulation.

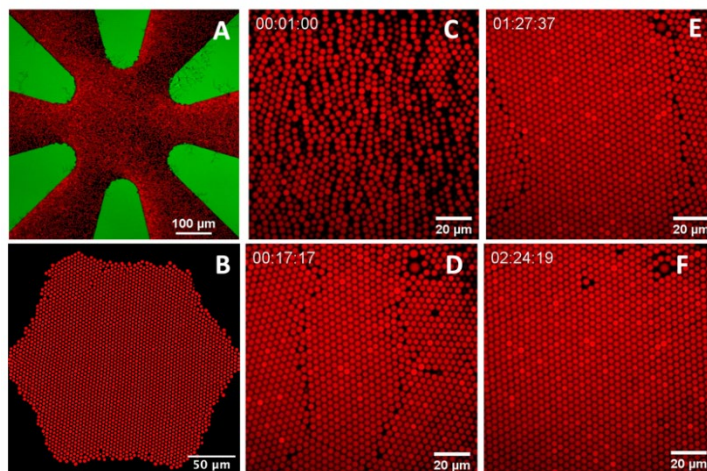


Figure 1. Six-electrode device to apply rotating AC electric fields that self-assemble colloidal monolayers. (A) Initial view of the colloids in the six-electrode device; the colloids (red) are micron-sized; the electrodes appear green. (B) At steady-state, a nearly defect free crystal is self-assembled through dipolar interactions and dielectrophoretic forces; (C-D) time series of images showing the particle-level annealing of defect structures in the colloidal monolayer.

*Switching the orientation of discoids in self-assembled monolayers by combined application of AC and DC electric fields.* In prior work, we studied the Bragg reflection structural color of crystals of  $\sim 200$  nm discoids produced by droplet evaporation [2]. Our recent work (data not shown) discovered that structural color by grating diffraction can be produced in self-assembled crystals of larger discoids and that the structure of these suspensions can be captured by confocal microscopy. Therefore, the effects of self-assembly, dynamically resolved at the single-particle level, on optical response can for the first time be studied. Anisotropic colloid shapes are interesting to study because their orientation can be controlled by the application of fields. Such orientational changes – because they occur at the single-particle level – are fast, and thus can yield strategies for rapid changes in crystal symmetry. We combine the application of DC and AC electric fields to rapidly switch the orientation of colloidal discoids (Figure 2). These transitions change optical properties of the crystals (data not shown). The results also show that the transition between discoid parallel and perpendicular orientation is incomplete. The mechanistic origin of this observation is under investigation, as is how the field properties affect this quality measure.

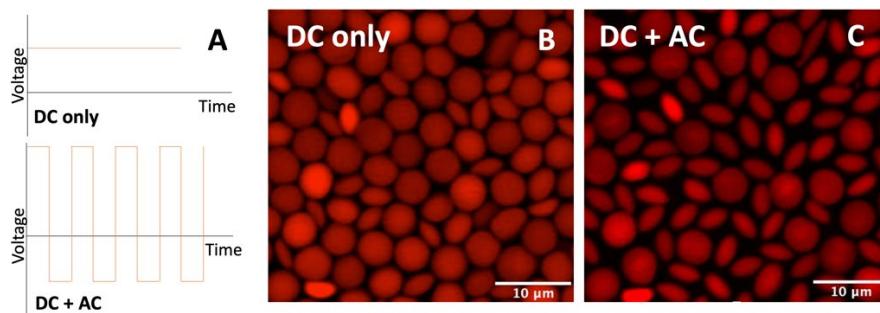


Figure 2. DC and AC electric fields are used to self-assemble crystals of discoloidal colloids that can switch their orientation between parallel and perpendicular configurations. The two field profiles used are shown in (A). Both fields are applied in a direction normal to the substrate. In the DC-only configuration (B), discoloidal colloids crystallize in orientations that are parallel to the substrate. When an AC electric field is additionally applied, many of the discoids flip to the perpendicular orientation (C).

*Relationship between defect structures and structural color response in thin films of self-assembled colloids.* Our earlier work established the role of defect type and abundance on the quality of Bragg reflected structural color from colloidal crystals self-assembled by evaporative deposition [1]. More recently, we reported that larger (micron-sized) colloids can also yield structural color when self-assembled into thin films and that this optical response can be modeled by scattering theory [2]. The mechanism for the optical response is grating diffraction. This discovery is important scientifically because the particles used to generate the optical response are in this case resolvable by optical microscopy. This opens the door to using confocal microscopy to quantify the individual positions and orientations of all the colloids and enable direct study of the relationship between microscopic properties of self-assembly (such as defect structures) and the macroscopic response generated by the self-assembled structure (such as structural color). As reported in Figure 3, we are exploiting the micron size of the colloids in crystals with the new ability of confocal microscopes to stitch multiple images together to yield very large images of colloidal crystals in which each particle's position and orientation can be resolved by image analysis. The results are being applied to identify local crystallinity, crystallite morphology, and grain boundary network connectivity. Statistical measures of these properties are being compared to the collective, structural color response to understand how defects impact the functional properties of self-assembled colloidal materials. We are also using computer simulation to generate mechanistic understanding of how the defect structures impact the measured collective properties.

## Future Plans

We plan to understand how to anneal crystals with spatial and orientational specificity. Life anneals crystal structures along preferred orientations, in ways that couple to rotational degrees of freedom in the system, and which can identify and resolve defects in local ways. As reported in Figures 1-3 and in references [4] and [5], we have tools to study defect structure and dynamics with spatial and orientational specificity and in real time, along with computational capabilities to simulate realistic models of our systems on spatial and temporal scales that align with experiment. Our next steps will explore this never-before-investigated parameter space, using both experiment and computer simulation, so as to generate new understanding of the mechanisms of the coupling between fields and defect structures in crystals.

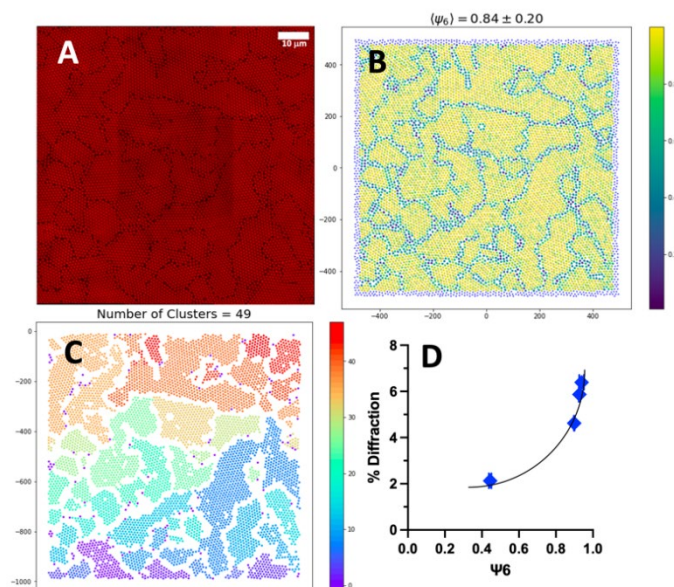


Figure 3. Thin films of spherical colloids are deposited using DC electric fields and the resulting crystal structures are imaged with confocal microscopy. (A) Nine images are stitched together to capture an ensemble of crystallites. (B) The average local order parameter,  $\psi_6$ , is applied to the results of image analysis to identify crystalline and non-crystalline particles. (C) Cluster analysis identifies the crystallite and grain boundary structure. (D) The results of the defect and order parameter analysis can be compared to collective properties of the crystal; here we compare the structural color diffraction intensity to  $\psi_6$ .

## References

1. Kao, P-K., B.J. VanSaders, S.C. Glotzer and M.J. Solomon, "Accelerated annealing of colloidal crystal monolayers by means of cyclically applied electric fields," *Scientific Reports* **11** 11042 (2021).
2. Liu, T., T. Liu, F. Gao, S.C. Glotzer, and M.J. Solomon, "Structural Color Spectral Response of Dense Structures of Discoidal Particles Generated by Evaporative Assembly," *J. Phys. Chem B* **126** 6 1315-1324 (2022).
3. Liu, T., B. VanSaders, S.C. Glotzer, and M.J. Solomon, "Effect of Defective Microstructure and Film Thickness on the Reflective Structural Color of Self-Assembled Colloidal Crystals," *ACS Applied Materials and Interfaces* **12** 8 9842-9850 (2020).
4. Liu, T. and M.J. Solomon, "Reconfigurable Grating Diffraction Structural Color in Self-Assembled Colloidal Crystals," *Small* (2023).
5. Saud, K.T. and M.J. Solomon, "Microdynamics of active particles in defect-rich colloidal crystals," *J. Colloid Interface Science.* **641** 950-960 (2023).
6. Ph.D. students Tianyu Liu, Syahidah Mohd Khairi, Chih-Mei Young, and Keara Saud performed research reported in this extended abstract.

## Publications supported by BES in the last two years

1. Liu, T. and M.J. Solomon, “Reconfigurable Grating Diffraction Structural Color in Self-Assembled Colloidal Crystals,” *Small* (2023). DOI: 10.1002/smll.202301871
2. Saud, K.T. and M.J. Solomon, “Microdynamics of active particles in defect-rich colloidal crystals,” *J. Colloid Interface Science*. **641** 950-960 (2023). PMID: 36989821; DOI: 10.1016/j.jcis.2023.03.025
3. Liu, T., T. Liu, F. Gao, S.C. Glotzer, and M.J. Solomon, “Structural Color Spectral Response of Dense Structures of Discoidal Particles Generated by Evaporative Assembly,” *J. Phys. Chem B* **126** 6 1315-1324 (2022). DOI: 10.1021/acs.jpcc.1c10015.
4. Liu, T., B. VanSaders, J.T. Keating, S.C. Glotzer, and M.J. Solomon, “Effect of Particles of Irregular Size on the Microstructure and Structural Color of Self-Assembled Colloidal Crystals,” *Langmuir* **37** 13300 – 13308 (2021). <https://doi.org/10.1021/acs.langmuir.1c01898>

# Far-from-equilibrium topological defects on active colloids in nematic liquid crystals for bio-inspired materials assembly

Kathleen J. Stebe, Chemical and Biomolecular Engineering, University of Pennsylvania

**Keywords:** active soft materials, directed assembly, emergent interactions, non-linear dynamics, topology

## Research Scope

We study active colloids in nematic liquid crystals (NLCs) that mimic biology’s ability to generate complex, adaptive, hierarchical structures via emergent interactions. We introduce ferromagnetic colloids with rotational motion controlled by external magnetic fields, designed to generate companion topological defects that dramatically reconfigure via elastoviscous effects. Topological defects on rotating colloids form far-from-equilibrium *topological flagella* that perform complex swim strokes that propel colloidal swimming, generating translation from rotation. Defect reconfiguration depends on the colloid’s genus, shape and rotation rate. In another example, non-equilibrium disclination lines will be studied as *topological filaments* that interact with topological swimmers, providing reconfigurable sites for assembly in the domain. We aim to develop fundamental understanding of these transient, far-from-equilibrium topological defects to exploit them as a new class of virtual functional structures that generate new modalities of motion and interaction.

Our prior work on defect dynamics focused on disks with hybrid anchoring (homeotropic tops and sides, degenerate planar bottoms)<sup>1</sup> and curved microrobots<sup>2</sup> designed to embed information in the domain (Fig. 1). In static experiments, the disk colloid has a metastable quadrupolar configuration featuring loops on either side of the disk pinned to its top and bottom edges, and two dipolar configurations featuring a single loop that pins on the disk’s top and bottom edges or pins only on the bottom edges. We rotate the disk colloids at different Ericksen number

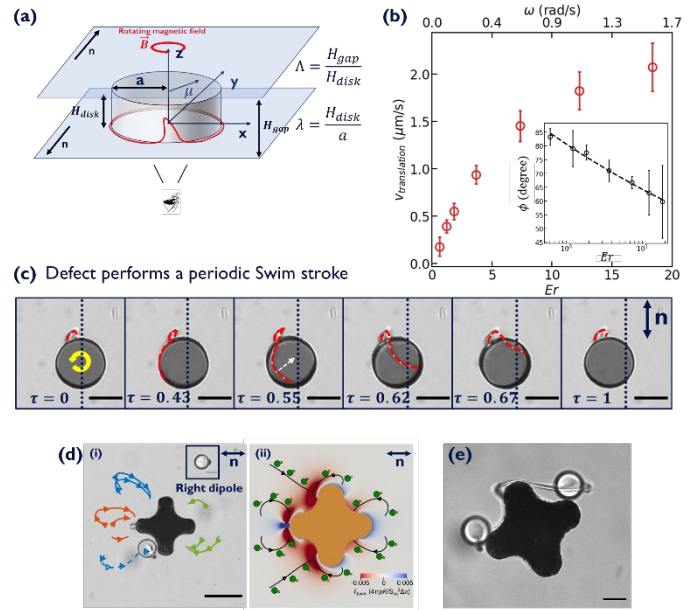


**Figure 1.** Prior work on far-from-equilibrium defects (a) Schematic of ferromagnetic disk (diameter  $2a = 75 \mu\text{m}$ , thickness  $H_{disk} \sim 30 \mu\text{m}$ ) between glass slides with gap  $H_{gap} = 50 \sim 55 \mu\text{m}$  filled with NLC. Confinement ratio  $\Lambda = \frac{H_{gap}}{H_{disk}} \sim 1.7$  and disk aspect ratio  $\lambda = \frac{H_{disk}}{a} \sim 0.9$ . The disk has hybrid anchoring; the cell surfaces have planar anchoring oriented in the y direction. A rotating magnetic field  $\vec{B}$  imposes an angular rotation  $\omega = \frac{2\pi}{T}$ . (b) Swimming velocity and direction depend on the rate of disk rotation. (c) Time-stamped images of the defect’s swim stroke under a rotating field.  $Er = 1.8$ , period  $T = 40\text{s}$ , where  $\tau = t/T$ . (d) Curved microrobot: Summary of the experimentally observed colloid trajectories (left) and corresponding numerical predictions (right) in the micro-robot fixed frame. (e) Cargo juggling and release by dynamic defect interaction. Scale bars =  $50 \mu\text{m}$ .

$Er = \frac{\eta\omega a^2}{K}$ , varying the ratio of viscous to nemato-elastic effects. In this expression  $\eta$  is the effective viscosity,  $\omega$  is the rotational frequency and  $K$  is the elastic constant of the NLC. At  $Er$  of roughly unity or below, the disk's dynamic disclination line pins to the disk's edge, extends, depins, and executes a swim stroke. At higher  $Er$ , the defect reconfigures and elongates significantly adjacent to the colloid. In our microrobotic studies, we use microrobot shape and anchoring energies to embed and reconfigure "information" in the NLC via their topological defects and nematic director field. This information generates interactions with passive colloidal building blocks, allowing directed assembly of colloidal cargo on the robot, and cargo expulsion using rotational dynamics.

## Recent Progress

We have altered the topology of the system by introducing genus-one (g1)-disks (Fig. 2); we fix the outer radius at  $a = 37.5 \mu\text{m}$ , and vary the pore to disk radius ratio  $\beta = \frac{b}{a}$  and offset ratio  $\eta = \frac{c}{a}$ , where  $\eta = 0$  indicates a centered pore and  $\eta = 0.13$  is the most eccentric case addressed thus far. The g1-disks defects perform a variety of swim strokes depending on the pore to disk ratio. For small pores,

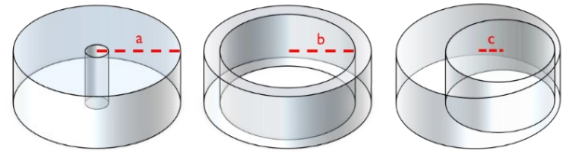


**Figure 2.** Geometry of genus 1 (g1)-disks with outer radius  $a$ , inner pore radius  $b$ , center offset  $c$ .

( $\beta = 0.27$ ), the g1-disk's companion defect has a stable dipolar configuration. Under rotation, the defect elongates along the disk's edge, releases, and sweeps across the face. During the sweeping event, the rough inner pore can periodically "catch" the defect (Fig.3) to form a keyhole configuration ( $\tau = 0.64 - 0.66$ ), providing the opportunity to study defect pinching. For g1-disks with larger pores ( $\beta = 0.53$ ), the companion defect has a metastable quadrupole state that transforms under perturbation to a dipole state sketched in Fig 3d. The disclination line is pinned on an edge of the g1-disk's pore, rises through the pore to pass over the g1-disk's top face, and protrudes adjacent to the disk along one of the poles aligned with the far field director. Under rotation,

edge elongation/depinning plays a role for moderate diameter pores ( $\beta = 0.53$ ) but is absent for g1-disks with larger pores ( $\beta = 0.733$ ). Rather, highly exposed disclination loops either pin on rough features, performing a pedaling

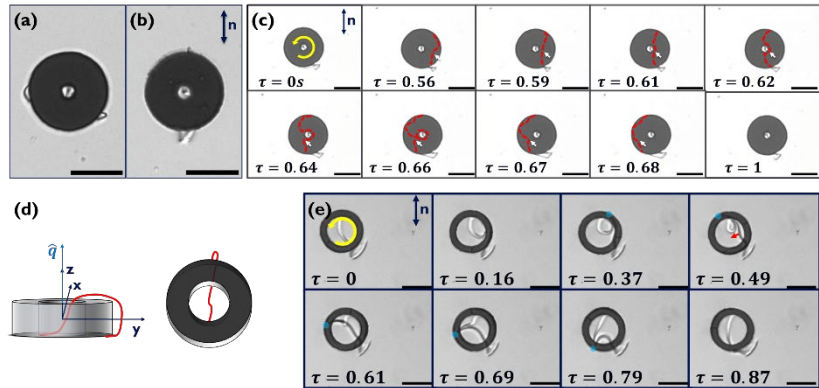


**Figure 3.** G1-disk colloid's companion defect configurations (a) metastable quadrupolar state; (b) dipole state. (c) Dimensionless time stamped images ( $\tau = \frac{t}{T}$ ) over one period  $T = 20\text{s}$ ;  $Er=3.7$  based on outer radius. At  $\tau = 0.56$ , the elongated defect begins sweeping over the g1-disk's surface, is caught on the inner pore at  $\tau = 0.64$ , and pinches off in a key-hole configuration from the pore at  $\tau = 0.66$ . (d) Schematic of the dipolar defect of g1-disks in the near  $y$ - $z$  plane (left) and near  $x$ - $y$  plane (right). (e) Time stamped images ( $\tau = \frac{t}{T}$ ) over one period  $T = 10\text{s}$  ( $Er=7.3$ ). The defect, pinned at a site indicated by a blue circle, moves in a cycling motion. Scale bars =  $50 \mu\text{m}$ .

motion under rotation, or rotate within the pore (loops swimming in loops). Translation velocities of all the disks studied have similar magnitude; the slowest objects have the weakest broken symmetries, and g1-disks with off-centered pores move rapidly.

## Future Plans

In the coming year, we will study:

*Rotationally induced swimming in NLC.* We will study the flow field, director field and elongated defects generated by spinning g0- and g1-disk colloids to understand rotationally induced swimming in NLC. The scallop theorem states that, at zero Reynolds number, disk rotation without broken symmetry cannot generate translation in an isotropic fluid. We hypothesize that the NLC is essential in generating broken symmetries under rotation; asymmetric rearrangement of nematogens owing to disk and defect motion can cause unequal stresses on either side of the disk. We will work to relate this concept to a thermodynamic cycle that generates net work to drive translation.

*Dynamic defect pinning, elongation and depinning* We will perform higher speed imaging of the defect dynamics and edge pinning made visible with fluorescent dye as a function of  $Er$  on rotated disks. We hypothesize that the colloid's undulated edge generates significant local bend and splay that attracts disclination lines which pin on these rough features via a stochastic, activated process. Pinning as an activated process would generate multiple static and dynamic configurations consistent with experiment and would be more significant in the low  $Er$  regime, for which slow convection would allow disclination lines to overcome kinetic barriers to trapping.

*Curved microrobot dynamics.* We will study defect hopping, an instability that differs from the defect pinning/depinning. We will characterize the trapping and release of passive colloidal cargo in far-from-equilibrium defects on rotated colloids as a function of swimmer and colloidal cargo geometry and surface features, including on rotating colloids with shapes that cannot align trivially with the far field director (Fig. 4).

*Pairs of active colloids.* We will study dimer swimming as a function of disks radius ratio, defect polarity, swimmer geometry, and initial configuration with respect to the far field director and rotation rate. Far-from-equilibrium defects on pairs of disks have several types of dynamic interaction, including disk co-migration without defect entanglement or dimerization, disk dimerization with defect merger, and defect entanglement.

*Generation of topological filaments* The director orientation of the NLC in the domain will be spatially designed within the domain, e.g. to seed topological defects to be used as topological filaments at well-defined locations (Fig. 5).<sup>3</sup> Ferromagnetic colloids will be used to manipulate these

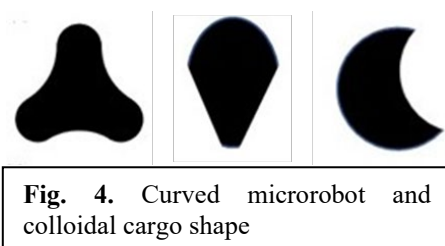


Fig. 4. Curved microrobot and colloidal cargo shape

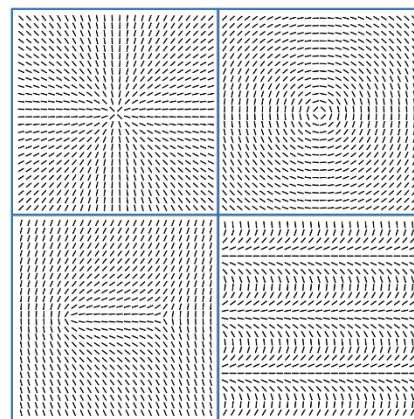


Fig. 5. Examples of patterned directors on cell boundaries to seed topological defects. Bars represent molecular orientation.

defects as a function of  $E_r$  to understand filament capture, extension, and release. We will develop these filaments as trapping sites for passive cargo and sites for passive colloidal cargo exchange with the rotated colloids. We will also study the most interesting aspects of the particles with different genus. For example, if the particles with higher genus yield shared or entangled defect structures with interesting thresholds and broken symmetries, we will study them in interaction with the patterned disclination lines.

*Nematic colloids in lyotropic liquid crystals* Finally, we intend to substitute the thermotropic liquid crystal (LC) medium with a lyotropic chromonic liquid crystal (LCLC). LCLCs offer the advantage of biocompatibility<sup>4</sup>, thereby presenting an opportunity to explore the interactions between our far-from-equilibrium structures and living organisms such as bacteria. Additionally, we aim to investigate the swimming behavior of the microrobots at the interface between the thermotropic LC and LCLC mediums. Swimming at the interface of two LC media presents a new avenue for exploration by combining the interfacial and elastic interactions, providing a new perspective to investigate a range of phenomena and potential applications<sup>5</sup>.

## References

1. Yao T, Kos Ž, Zhang QX, Luo Y, Steager EB, Ravnik M, and Stebe KJ. Topological defect-propelled swimming of nematic colloids. *Science Advances* (2022) 8: eabn8176. DOI: doi:10.1126/sciadv.abn8176
2. Yao T, Kos Ž, Zhang QX, Luo Y, Serra F, Steager EB, Ravnik M, and Stebe KJ. Nematic Colloidal Micro-Robots as Physically Intelligent Systems. *Advanced Functional Materials* (2022) 32: 2205546. DOI: <https://doi.org/10.1002/adfm.202205546>
3. Guo Y, Jiang M, Peng C, Sun K, Yaroshchuk O, Lavrentovich O, and Wei QH. High-Resolution and High-Throughput Plasmonic Photopatterning of Complex Molecular Orientations in Liquid Crystals. *Advanced Materials* (2016) 28: 2353-2358. DOI: 10.1002/adma.201506002
4. Peng C, Turiv T, Guo Y, Wei QH, and Lavrentovich OD. Command of active matter by topological defects and patterns. *Science* (2016) 354: 882-885. DOI: 10.1126/science.aah6936
5. Chisholm NG and Stebe KJ. Driven and active colloids at fluid interfaces. *Journal of Fluid Mechanics* (2021) 914: A29. DOI: 10.1017/jfm.2020.708

## Materials Exhibiting Biomimetic Carbon Fixation and Self Repair: Theory and Experiment

Michael S. Strano, Carbon P. Dubbs Professor of Chemical Engineering, Massachusetts Institute of Technology, Department of Chemical Engineering.

**Keywords:** carbon fixation, material repair, emergent behavior, active matter

### Research Scope

Recent work in our laboratory at MIT towards carbon fixing materials have expanded our analysis to methanotrophic systems that operate at ambient conditions. Methane is a critical fuel, chemical precursor, but also a potent greenhouse gas. Its production, transportation, and use result in its emission to the atmosphere, where it induces ~30 times more warming than CO<sub>2</sub> on a per-mass basis. Currently, there remains minimal understanding of efficient chemical methods for the conversion and or valorization of methane streams—specifically under the conditions in which they are emitted i.e. low partial pressures and ambient temperatures. These are also the conditions where we seek to generate materials that can capture, convert and utilize this carbon to generate active matter. To this end, we have created the first synthetic methanotrophic system which is capable of oxidizing methane at ambient temperatures and pressures into a growing polymer material. We also investigate the ability of commonly used transition metal-modified zeolite (ZSM-5) catalysts for the H<sub>2</sub>O<sub>2</sub>-mediated oxidation of methane in the liquid phase at ambient conditions—room temperature and one atmosphere of partial pressure. Current work is also incorporating such chemistry into larger systems and microscopic devices that exhibit unique, emergent properties of repair, temporal and spatial ordering, and dynamics that mimic aspects of living systems. In one recent discovery, spontaneous oscillations on the order of several hertz were generated with relatively simple particulate matter. Such low frequency oscillations are the drivers of many crucial processes in nature. Converting static energy inputs into slowly oscillating power is key to the autonomy of organisms across scales. However, the fabrication of slow micrometer-scale oscillators remains a major roadblock towards fully-autonomous microrobots. We have studied a collective of active microparticles at the air-liquid interface of a hydrogen peroxide drop to find that they demonstrate emergent behavior in the form of low-frequency oscillator from. To supplement components of microscale autonomous systems, we have also developed microscale battery by photolithographically patterning a microscale Zn/Pt/SU-8 system to generate the highest energy density at the picoliter (10<sup>-12</sup> L) scale. We have also numerically studied a concept of Smart Tracers that could record the local chemical concentrations, temperature or other conditions as they progress through reactors.

### Recent Progress

*Synthetic methanotrophic system to oxidize methane at ambient conditions into a growing polymer material:* We have created a synthetic methanotrophic system which is capable of oxidizing methane at ambient temperatures and pressures into a growing polymer material. Iron-modified ZSM-5 combined with the enzyme alcohol oxidase is capable of driving methane oxidation continually and catalytically towards formaldehyde. The alcohol oxidase performs methanol oxidation to formaldehyde to regenerate in tandem hydrogen peroxide to efficiently drive methane oxidation over the Fe-ZSM-5 catalyst. We observe the highest methane to formaldehyde selectivity to date for room temperature oxidation with hydrogen peroxide—

exceeding 80% under these conditions. We have shown that the generated formaldehyde can be incorporated into a growing polymer through reaction with urea to produce a urea-formaldehyde polymer with a material growth rate exceeding  $4.0 \text{ mg g}_{\text{cat}} \text{ hr}^{-1}$ , that of many cultured methanotrophic bacteria systems. This work presents a scalable, cost-effective, route for methane oxidation at ambient conditions to produce a high-value polymer material.

*Mathematical framework for methanotrophic material systems:* We have introduced the concept of methanotrophic material systems, capable of converting methane at ambient temperatures and pressures. We develop a mathematical framework used to evaluate these systems' ability to convert methane, using currently published activity data. As a case study, we model the ability of these systems to convert a characteristic stream of ventilation air methane (0.6% methane in air,  $1.7 \cdot 10^8 \text{ L hr}^{-1}$  equivalent to 100,000 standard cubic feet per minute). We show that when appropriately designed, such systems require coverage of less than 1,000 meters of mine tunnel length (equivalent to  $20,000 \text{ m}^2$  areal coverage) in order to reduce the methane emission from this stream by over 99%. Finally, we highlight formaldehyde as a reactive intermediate of methane oxidation which may itself be incorporated into these coating materials—allowing these systems to sequester the carbon from methane in a stable and solid form.

*Methane oxidation catalyst optimization at ambient conditions:* Methane is a critical fuel, chemical precursor, and potent greenhouse gas. Its production, transportation, and use result in its emission to the atmosphere, where it induces  $\sim 30$  times more warming than  $\text{CO}_2$  on a per-mass basis. The majority of anthropogenic emission of methane to the atmosphere is the result of many spatially distributed and dilute emission sources such as: leaks from natural gas infrastructure, ventilation air methane, landfill gas and raising of ruminant livestock. Currently, there remains minimal understanding of efficient chemical methods for the conversion and or valorization of these streams—specifically under the conditions in which they are emitted i.e. low partial pressures and ambient temperatures. To address this gap of understanding, in this work we investigate the ability of commonly used transition metal-modified zeolite (ZSM-5) catalysts for the  $\text{H}_2\text{O}_2$ -mediated oxidation of methane in the liquid phase at ambient conditions—room temperature and one atmosphere of partial pressure. We show that this catalytic system remains active and selective when converting methane even below its flammability limit, 5% in air. Further, we observe a consistent linear chemical mechanism relating methane conversion to product selectivity under the conditions employed. We find that methanol, directly produced from methane, is rapidly oxidized to formaldehyde, followed by conversion to formic acid, and then finally  $\text{CO}_2$ . Last, we report that the system remains active for methane oxidation down to below 5% in air, below its flammability limit.

*Emergent behavior in the form of low-frequency oscillator from a collective of active microparticles at the air-liquid interface of a hydrogen peroxide drop:* We have studied a low-frequency oscillator that emerges from a collective of active microparticles at the air-liquid interface of a hydrogen peroxide drop. Their interactions transduce ambient chemical energy into periodic mechanical motion and on-board electrical currents. Surprisingly, these oscillations persist at larger ensemble sizes only when a particle with modified reactivity is added to intentionally break permutation symmetry. We explain such emergent order through the discovery of a thermodynamic mechanism for asymmetry-induced order. The on-board power harvested from the stabilized oscillations enables the use of electronic components, which we demonstrate by cyclically and synchronously driving a micro-robotic arm.

*Micro-battery system for microscopic autonomous systems:* We have photolithographically patterned a microscale Zn/Pt/SU-8 system to generate the highest energy density micro-battery at the picoliter ( $10^{-12}$  L) scale. The device scavenges ambient or solution dissolved oxygen for a Zn oxidation reaction, achieving an energy density ranging from 760 to 1070 Wh L<sup>-1</sup> at scales below 100  $\mu$ m lateral and 2  $\mu$ m thickness in size. The parallel nature of photolithography processes allows 10,000 devices per wafer to be released into solution as colloids with energy stored onboard. Within a volume of only 2 pL each, these primary micro-batteries can deliver open circuit voltages of  $1.05 \pm 0.12$  V with total energies ranging from  $5.5 \pm 0.3$  to  $7.7 \pm 1.0$   $\mu$ J and a maximum power near 2.7 nW. We demonstrate that such systems can reliably power a micron-sized memristor circuit, providing access to non-volatile memory. We also cycle power to drive the reversible bending of microscale bimorph actuators at 0.05 Hz for mechanical functions of colloidal robots. Additional capabilities, such as powering two distinct nanosensor types and a clock circuit, are also achieved.

*Smart Tracer concept to study enclosed environments:* A widely utilized tool in reactor analysis is passive tracers that report the Residence Time Distribution (RTD), allowing estimation of the conversion and other properties of the system. Recently, advances in micro-robotics have introduced powered and functional entities with sizes comparable to some traditional tracers. This has motivated the concept of Smart Tracers that could record the local chemical concentrations, temperature or other conditions as they progress through reactors. We have analyzed the design constraints and advantages of Smart Tracers by simulating their operation in a laminar flow reactor model conducting chemical reactions of various orders. We note that far fewer particles are necessary to completely map even the most complex concentration gradients compared with their conventional counterparts. Design criteria explored in this work include sampling frequency, memory storage capacity, and ensemble number necessary to achieve a required accuracy to inform a reactor model. Cases of severe particle diffusion and sensor noise appear to bound the functional upper limit of such probes and require consideration for future design. The results of this study provide a starting framework for applying this new technology of micro-robotics to the broad and impactful set of problems classified as chemical reactor analysis.

## **Future Plans**

*Methanotrophic systems that operate at ambient conditions:* After creating synthetic methanotrophic system to oxidize methane at ambient conditions into a growing polymer material, we will interface the system with living systems in order to achieve enhanced performance and extend the application space of the system. This will include coupling with urea-producing bacteria such as *Delaya venusta* to supply urea to the growing methane-based polymer to allow for enhanced growth rates. The second route will comprise infiltration into plants for methane oxidation to be driven by hydrogen peroxide generated through natural plant signaling pathways.

The mathematical modeling informs us that current kinetics achieved with our synthetic methanotrophic system are able to remediate real methane emission streams in the environment. Next, we will couple our methanotrophic system to an inert support material in order to apply our methane oxidation chemistry as a coating for use in the ambient environment. Furthermore, the optimized methane oxidation catalyst for room temperature conversion will be incorporated into a combined synthetic methanotrophic system coupled with an enzyme alcohol oxidase in order to continually regenerate the H<sub>2</sub>O<sub>2</sub> needed to drive the reaction of methane. We believe this system will extend lifetime and enhance efficiency of the oxidation reaction.

*Systems and components that constitute active matter behavior:* We plan on extending our approach into studying larger collections of microparticles in search of general principles for the top-down design of active matter systems. This will involve understanding of system symmetries and the impact of environmental forcing to improve their task-capability. Furthermore, we will devise the experimental method that utilize emergent behaviors for harvesting energy from external sources, enabling the applications of this active matter system in carbon fixation and self-repair.

We plan to develop experimental designs to expand functionalities, including electrocatalysts and self-repair mechanisms, for micro-scale active matter systems that utilize the micro-battery energy source. Our subsequent goal is to integrate these micro-robotic components to emulate the behavior of microorganisms using a synthetic, inorganic system. For smart tracers, the computational framework demonstrates that smart active matter systems can provide the concentration mapping of their environment. We plan to enhance this framework for designing biomimetic synthetic micro-particles capable of self-repair, utilizing resources from their environment. Additionally, we will develop experimental procedures to substantiate the feasibility of this theoretical system.

## Publications

1. G. Zhang, J. F. Yang, S. Yang, A. M. Brooks, V. B. Koman, X. Gong, and M. S. Strano, *Colloidal State Machines as Smart Tracers for Chemical Reactor Analysis*, *Advanced Intelligent Systems*, **2023**, 2300130.
2. D. J. Lundberg, D. Parviz, H. Kim, M. Lebowitz, R. Lu, and M. S. Strano, *Universal Kinetic Mechanism Describing CO<sub>2</sub> Photoreductive Yield and Selectivity for Semiconducting Nanoparticle Photocatalysts*, *Journal of the American Chemical Society*, **2022**, 144, 30, 13623-13633.
3. J. F. Yang, T. A. Berrueta, A. M. Brooks, A. T. Liu, G. Zhang, D. Gonzalez-Medrano, S. Yang, V. B. Koman, P. Chvykov, L. N. LeMar, M. Z. Miskin, T. D. Murphey, and M. S. Strano. *Emergent microrobotic oscillators via asymmetry-induced order*, *Nature Communications*, **2022**, 13, 5374.
4. D. Parviz, D. J. Lundberg, S. Kwak, H. Kim, and M. S. Strano. *A mathematical analysis of carbon fixing materials that grow, reinforce, and self-heal from atmospheric carbon dioxide*, *Green Chemistry*, **2021**, 23, 5556-5570.
5. G. Zhang, J. Yang, D. Gonzalez-Medrano, M. Z. Miskin, S. Yang, V. B. Koman, Y. Zeng, S. X. Li, M. Kuehne, A. T. Liu, A. M. Brooks, and M. S. Strano. *High Energy Density Picoliter Zn-Air batteries for Colloidal Robots and State Machines*, **2023**, in review.
6. D. J. Lundberg, D. Parviz, and M. S. Strano, *Mathematical modeling of Methanotrophic Coating Materials to Mitigate Ambient Methane*, **2023**, in preparation.
7. D. J. Lundberg, C. Ritt, Y. Tu, D. Parviz, and M. S. Strano. *Optimizing Earth-Abundant Metal-Modified ZSM-5 Catalysts for High Efficiency Methane Oxidation with H<sub>2</sub>O<sub>2</sub> at Ambient Temperature and Pressure*, **2023**, in preparation.
8. D. J. Lundberg, C. Ritt, Y. Tu, D. Parviz, M. Quien, J. Kim, and M. S. Strano, *Methane Fixation at Ambient Temperature and Pressure Mediated by Enzyme-Coupled Fe-ZSM-5*, **2023**, in preparation.
9. H. Kim, D. J. Lundberg, D. Parviz, M. Chen, and M. S. Strano, *Tailoring CO<sub>2</sub> Photocatalytic Activity and Selectivity using Tunable Tungsten Oxide Materials*, **2023**, in preparation.
10. H. Kim, M. Chung, Y. Cho, J. Park, D. J. Lundberg, G. He, D. Parviz, J. Kong, H. J. Kulik, K. Manthiram, and M. S. Strano, *Defect Control of Monolayer Boron Nitride on Copper (hBNO/Cu) for High CO<sub>2</sub> Reduction Selectivity toward Methane*, **2023**, in preparation.

## Supramolecular Dynamics in Self-Assembling Materials

Samuel I. Stupp, Department of Materials Science & Engineering, Department of Chemistry, Department of Biomedical Engineering, Department of Medicine, and Simpson Querrey Institute, Northwestern University

**Keywords:** Donor-Acceptor, Ferroelectricity, Peptides, Supramolecular Dynamics

### Research Scope

The broad objective of this research program is to acquire knowledge on supramolecular dynamics, a poorly understood phenomenon utilized by biological systems that would greatly impact our ability to design scalable, functional materials with spatial and temporal control. In our DOE *Biomolecular Materials* program, we previously discovered several surprising phenomena while probing structure and dynamics in supramolecular materials containing peptides and DNA fragments. These observations have provided key insight into the design of biomolecular and synthetic materials that achieve their properties and functions through supramolecular dynamics. The molecular design is primarily based on peptides and electronically active molecules and target functions include ferroelectricity, catalytic activity, and dynamic reversibility of mechanical properties, among others. We seek to use self-assembly strategies with dynamic components at the supramolecular level to control and develop new properties in the resulting bulk materials.

### Recent Progress

*Metallurgical Alloy Approach to Two-Dimensional Supramolecular Materials.* In our previous DOE-funded research, we investigated the supramolecular assembly pathways for a class of amphiphilic molecules derived from perylene monoimide chromophores.<sup>1-4</sup> We recently investigated the ternary mixing behavior of PMI-based chromophore amphiphiles (CAs) that differ

in their 9-position substituents (proton, 3-pentylamino, and methoxy groups) (see **Figure 1**).<sup>5</sup> By comparing the UV-Vis spectra, X-ray scattering patterns, and TEM and CLSM images, we discovered a rich crystalline phase behavior that resembles alloying in metals (**Figure 1A**). For example, the addition of 20 mol % or less of 3-pentylamino-functionalized PMI-CA to the unfunctionalized PMI-CA led to fluorescence emission geometry changes from face-emitting to edge-emitting supramolecular polymers (**Figure 1B, C**), while the addition of methoxy-functionalized PMI-CA to the unfunctionalized PMI-CA increased the aspect ratio of the supramolecular assemblies (**Figure**

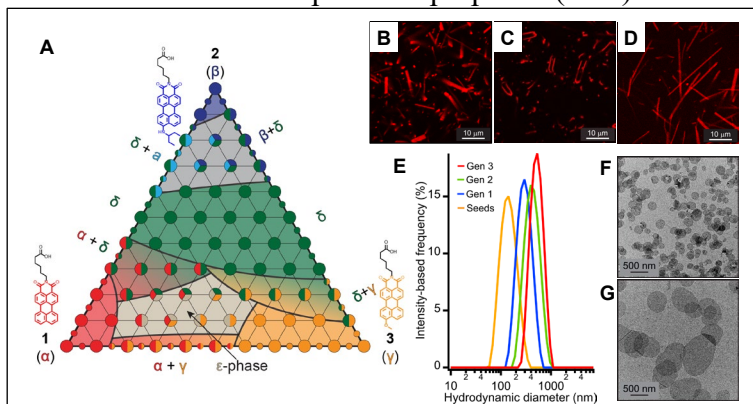
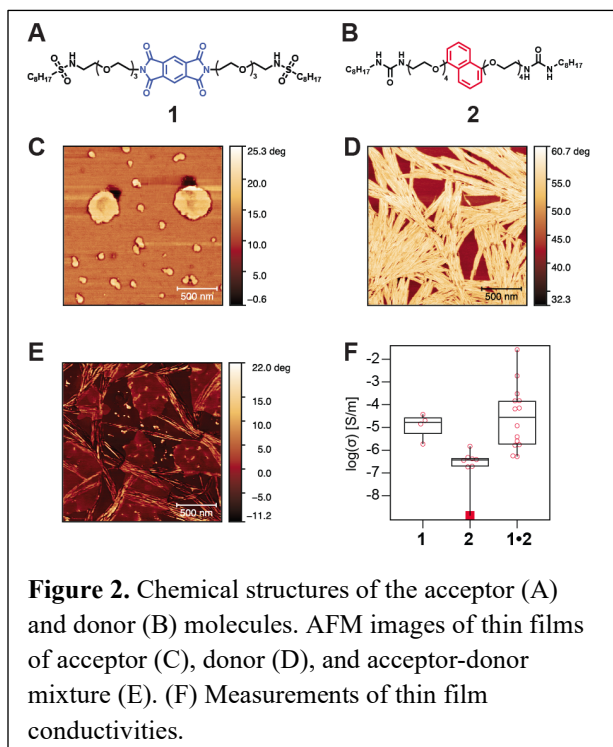


**Figure 1.** Ternary phase behavior of PMI-based chromophore amphiphiles. (A) Ternary phase diagram of the PMI-CAs **1-3** mixtures in saline solution. Colors indicate the dominant crystalline phase for the given composition. (B-D) CLSM images of pure **1** (B), 5% **2** / 95% **1** (C), and 10% **3** / 90% **1** (D) assemblies. (E) Dynamic light scattering-based size distribution for sequential living supramolecular polymerization of the nanodiscs. (F-G) Stained transmission electron microscopy (TEM) images of the nanodiscs before (F) and after three cycles of (G) seeded growth.

**1B, D).** We also discovered a new crystalline phase in 1:1 mixtures of 3-pentylamino-functionalized PMI-CA with unfunctionalized or methoxy-functionalized molecules, analogous to intermetallic compounds in alloys. Further investigation into their formation mechanism using variable temperature *in situ* methods revealed that this crystalline phase forms from mixtures of pure crystalline assemblies of the two components through the molecular exchange in solution with an activation energy of  $146 \pm 9$  kJ/mol, which is large enough to fully suppress secondary nucleation below 40 °C. This lack of secondary nucleation allowed us to perform seeded growth experiments by adding the mixtures of pure crystalline assemblies of the two components to pre-formed small crystals and obtain near-monodisperse disc-like objects (**Figure 1E-G**).

*Charge transfer complexation in supramolecular assemblies for improved conductivity in thin films.* We have also investigated the interplay between hydrogen bonding and charge transfer (CT) in supramolecular assemblies of electroactive small molecules. In this study, a sulfonamide-functionalized pyromellitic diimide electron acceptor molecule (**Figure 2A, C**) was co-assembled with a urea-functionalized 1,5-dialkoxynaphthalene electron donor molecule (**Figure 2B, D**). These functional groups were chosen for their propensity to selectively form heterodimers in solution via CT interactions and hydrogen bonding between the sulfonamide and urea groups. Indeed, absorbance, emission, and nuclear magnetic resonance spectroscopies indicated a 1:1 association between donor and acceptor molecules in solution. However, atomic force microscopy (AFM) (**Figure 2E**) and grazing incidence X-ray scattering (GIXS) revealed phase separation of the donors and acceptors when the mixed solutions were cast as thin films. Further analysis by absorbance and ultraviolet photoelectron spectroscopies revealed residual CT interactions in these films, which indicated that small amounts of donors were doped into assemblies of acceptors and vice versa. This doping effect significantly improved the electrical conductivity and ambipolar field-effect charge mobilities of the mixed thin films relative to films of the donor or acceptor alone (**Figure 2F**). Films prepared with donors and acceptors without the sulfonamide and urea groups had three orders of magnitude lower electrical conductivity. We concluded that the conductivity of the films cast from the mixture arose from both residual CT interactions and long-range ordering via hydrogen bonding. By elucidating the influence of these non-covalent interactions on electronic properties, this study could aid the development of organic electronics from supramolecular assemblies.

*Peptide Supramolecular Polymers with Ferroelectric Functionality.* Poly(vinylidene fluoride) (PVDF) is the leading organic ferroelectric material and has generated great interest for applications in electronics and electromechanical devices. Obtaining the electroactive polymorph requires mechanical drawing of the polymer or random copolymerization with additional monomers. However, these processes do not lead to precise control of nanoscale ferroelectric structure and



consequent properties. We recently developed VDF oligomers conjugated to peptides that self-assemble into nanoscale ferroelectric filaments in water (**Figure 3**). Specifically, we found that VDF<sub>6</sub>-VVEE assembled into narrow ribbons, whereas VDF<sub>6</sub>-VEVE formed wide ribbons. In these systems, the  $\beta$ -sheet secondary structure programs pure VDF oligomers to select the highly coveted conformation present in the ferroelectric polymorph of PVDF. Variations in the peptide sequence can also yield “relaxor” phases in which small ferroelectric domains generate strong electromechanical actuation. This biomolecular approach could potentially generate sustainable, water-processable ferroelectric structures for sensing, memory, and energy transduction.

In another example, we have also discovered a system in which carboxylic acid or peptide solubilizing groups are covalently linked to dyads of electron-donating naphthalenes and electron-accepting naphthalene diimide or pyromellitic diimide. In water, these molecules self-assemble into crystalline nanoscale ribbons. Selected area electron diffraction revealed the participation of the chiral peptide headgroup in the crystal structure and distortion to the underlying crystalline lattice. The resulting crystalline nanostructure is second harmonic active with induced chirality in the peptide amphiphiles and is ferroelectric at room temperature. We suggest that this method can be applied to various charge transfer systems to create new water-processable ferroelectric materials.

*Supramolecular polymerization pathways of peptide amphiphiles.* In collaboration with the research group of Prof. E. W. Meijer (Eindhoven University), we have used circular dichroism (CD) spectroscopy and hydrogen/deuterium exchange mass spectroscopy (HDX-MS) to investigate pH-induced changes in the supramolecular polymerization of peptide amphiphile molecules.

To avoid spurious contributions to the CD signal from linear dichroism and birefringence, we used palmitoyl-VVVAACKK-CONH<sub>2</sub> (C<sub>16</sub>V<sub>3</sub>A<sub>3</sub>K<sub>3</sub>), which shares the same  $\beta$ -sheet motif but has the opposite charges and was previously shown to produce easily interpreted CD data (Figure 4A). When we titrate with NaOH to high pH values (i.e., when the electrostatic repulsion among PA headgroups is small), the CD spectra indicate that the structure of the PA assemblies changes from random coil to  $\beta$ -sheet (Figure 4B). Importantly, the rate of pH titration affects the structural transition, where slow titration leads to near thermodynamic equilibrium condition, which is consistent with our earlier findings that temperature-induced supramolecular polymerization is strongly dependent on the cooling rate. By

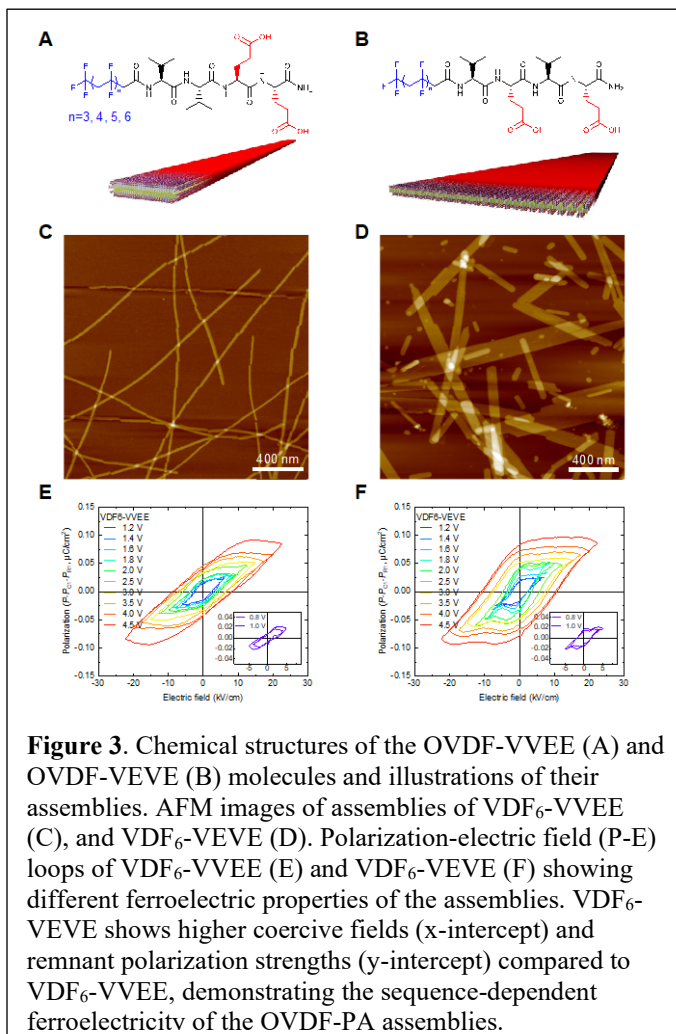
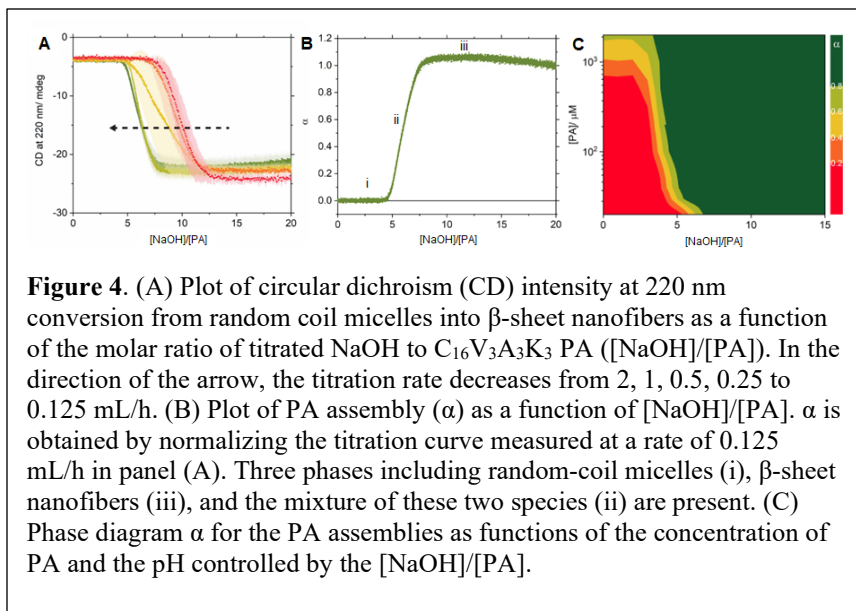


**Figure 3.** Chemical structures of the OVDF-VVEE (A) and OVDF-VEVE (B) molecules and illustrations of their assemblies. AFM images of assemblies of VDF<sub>6</sub>-VVEE (C), and VDF<sub>6</sub>-VEVE (D). Polarization-electric field (P-E) loops of VDF<sub>6</sub>-VVEE (E) and VDF<sub>6</sub>-VEVE (F) showing different ferroelectric properties of the assemblies. VDF<sub>6</sub>-VEVE shows higher coercive fields (x-intercept) and remnant polarization strengths (y-intercept) compared to VDF<sub>6</sub>-VVEE, demonstrating the sequence-dependent ferroelectricity of the OVDF-PA assemblies.

normalizing the CD spectra of these *in-situ* experiments, we can extract a quantitative degree of assembly ( $\alpha$ ). Our results suggest three distinct phases of PA assembly displaying a random coil signature (ii), a  $\beta$ -sheet signal (iv), or a mixture of these two species (iii) depending on the pH (Figure 4B). Combining the *in-situ* titration experiment with other experimental methods, such as static light scattering, small angle X-ray scattering, and TEM, as well



as computational modeling, we are now constructing a comprehensive phase diagram of PA assemblies as a function of PA concentration and added acid, base, and salt (schematically illustrated in Figure 4C). This type of phase diagram can be used as a fingerprint of PA assembly under different conditions allowing us to better measure exchange dynamics in these systems. For example, PA assemblies formed under different pH conditions display distinctly different local amide proton exchange dynamics in the HDX-MS experiments. The faster exchange dynamics of PA assemblies formed at higher pH can be attributed to the higher fraction of random coil micelles. Furthermore, the CD titration experiments provide the rate of addition as a kinetic handle, allowing us to investigate the rate-dependent morphological and compositional changes away from steady-state exchange dynamics.

## Future Plans

Inspired by the liquid–liquid phase separation observed in biological systems, in which changes in depletion conditions like external macromolecular concentration is a highly effective functional tool that does not require thermal changes. Our ongoing work seeks to explore the parameter space that leads to controlled superstructure formation from supramolecular assemblies using macromolecular crowding and attractive polar forces among the assemblies. We also propose to explore potential functions of these systems such as the enhancement of enzymatic reactions and investigate if polar assemblies can create superstructures with the potential for amplified ferroelectric behavior.

## References

1. A. S. Weingarten, R. V. Kazantsev, L. C. Palmer, M. McClendon, A. R. Koltonow, A. P. S. Samuel, D. J. Kiebal, M. R. Wasielewski, S. I. Stupp, *Self-Assembling Hydrogel Scaffolds for Photocatalytic Hydrogen Production*, *Nature Chemistry* **6**, 964-970 (2014).
2. R. V. Kazantsev, A. J. Dannenhoffer, T. Aytun, B. Harutyunyan, D. J. Fairfield, M. J. Bedzyk, S. I. Stupp, *Molecular Control of Internal Crystallization and Photocatalytic Function in Supramolecular Nanostructures*, *Chem* **4**, 1596 (2018).

3. A. J. Dannenhoffer, H. Sai, H. B. Harutyunyan, A. Narayanan, N. E. Powers-Riggs, A. N. Edelbrock, J. V. Passarelli, S. J. Weigand, M. R. Wasielewski, M. J. Bedzyk, L. C. Palmer, S. I. Stupp, *Growth of Extra-Large Chromophore Supramolecular Polymers for Enhanced Hydrogen Production*, Nano Letters, **21**, 3745 (2021).
4. H. Sai, G. C. Lau, A. J. Dannenhoffer, S. M. Chin, L. Đorđević, S. I. Stupp, *Imaging Supramolecular Morphogenesis with Confocal Laser Scanning Microscopy at Elevated Temperatures*, Nano Letters **20**, 4234 (2020).
5. A. J. Dannenhoffer, H. Sai, E. P. Bruckner, L. Đorđević, A. Narayanan, Y. Yang, X. Ma, L. C. Palmer, S. I. Stupp, *Metallurgical Alloy Approach to Two-Dimensional Supramolecular Materials*, Chem **9**, 170 (2023).

## Publications

1. R. Qiu, I. R. Sasselli, Z. Álvarez, H. Sai, W. Ji, L. C. Palmer, S. I. Stupp, *Supramolecular Copolymers of Peptides and Lipidated Peptides and their Therapeutic Potential*, Journal of the American Chemical Society **144**, 5532 (2022).
2. I. R. Sasselli, Z. Syrgiannis, N. Sather, L. C. Palmer, S. I. Stupp, *Modelling Interactions Within and Between Peptide Amphiphile Supramolecular Filaments*, Journal of Physical Chemistry B **126**, 650 (2022).
3. A. J. Dannenhoffer, H. Sai, H. B. Harutyunyan, A. Narayanan, N. E. Powers-Riggs, A. N. Edelbrock, J. V. Passarelli, S. J. Weigand, M. R. Wasielewski, M. J. Bedzyk, L. C. Palmer, S. I. Stupp, *Growth of Extra-Large Chromophore Supramolecular Polymers for Enhanced Hydrogen Production*, Nano Letters **21**, 3745 (2021).
4. A. J. Dannenhoffer, H. Sai, E. P. Bruckner, L. Đorđević, A. Narayanan, Y. Yang, X. Ma, L. C. Palmer, S. I. Stupp, *Metallurgical Alloy Approach to Two-Dimensional Supramolecular Materials*, Chem **9** 170 (2023).
5. J. Kolberg-Edelbrock, T. J. Cotey, S. Y. Ma, L. M. Kapsalis, D. M. Bondoc, S. R. Lee, H. Sai, C. S. Smith, F. Chen, A. N. Kolberg-Edelbrock, M. E. Strong, S. I. Stupp, *Biomimetic Extracellular Scaffolds by Microfluidic Superstructuring of Nanofibers*, ACS Biomaterials Science and Engineering **9**, 1251 (2023).

## Protein Self-Assembly by Rational Chemical Design

Akif Tezcan, University of California, San Diego

**Keywords:** Protein-Based Materials, Dynamic/Stimuli-Responsive/Self-Healing Systems, Weaving/Interlocking Topologies, Protein-Polymer Interface

### Research Scope

Our research aims to develop design strategies to control protein self-assembly and to construct protein-based materials with emergent properties. To circumvent the challenge of designing extensive non-covalent interfaces for controlling protein self-assembly, we have endeavored to develop a chemical bonding toolkit (metal coordination, disulfide linkages, computationally prescribed non-covalent bonds, DNA hybridization, host-guest interactions, etc.) to mediate protein-protein interactions. The initial focus of our DOE-funded program was to establish design strategies for obtaining desired structures such as discrete (*i.e.*, finite) or 0-, 1-, 2- and 3D (*i.e.*, extended) protein assemblies with crystalline order. While we still pursue such methodology development, our efforts now also focus on designing functional, dynamic, and reconfigurable protein architectures, constructing composite protein-inorganic-organic materials with new functional/physical properties, and developing an experimental/ computational/theoretical framework to obtain structure-property relationships in these materials. In this funding period, our particular goals have primarily been two-fold: (1) to construct hierarchical and spatially patterned crystalline protein materials integrated with polymer networks that are adaptive, stable, self-healing and capable of selectively taking up biological macromolecules toward fabricating multifunctional biomaterials, and (2) to design 2- and 3D protein arrays with interlocking/woven topologies, which—like their macroscopic counterparts—are proposed to have superior mechanical properties.

### Recent Progress

While we made progress on several different fronts (*e.g.*, functional/dynamic 2D protein frameworks, ATP-driven/dissipative protein assemblies), we will focus here on adaptive 3D protein crystals and topologically interlocked/woven protein assemblies.

**B.1. Exploiting the adaptiveness of Polymer-Integrated Protein Crystals (PIX) for selective uptake/release of biomacromolecular cargo (Publication 3):** The superior mechanical properties of many biomaterials are derived from the hierarchical integration of protein-based scaffolds with inorganic and organic components. Such hierarchical assembly not only leads to emergent properties that arise from combining multiple components (*e.g.*, flexibility/responsiveness, simultaneous strength and toughness, self-healing) but also augments the individual properties (*e.g.*, catalysis, stability) of the components themselves. With these advantages in mind, we recently developed a new class of protein-based materials, termed polymer-integrated protein crystals (PIX), using the cage-like, 24meric protein human heavy chain ferritin (HuHF) as a building block (Zhang et al., *Nature*, 557, 86, 2018). We exploited the mesoporosity of the HuHF crystals to thoroughly infuse them with acrylate/acrylamide, which were then polymerized *in crystallo* to form a hydrogel network that intimately bonded to underlying HuHF lattice through non-covalent interactions. The resulting HuHF-PIX possessed several unprecedented properties such as volumetric expansion by >500% while retaining crystalline periodicity, reversible

contraction back to their original state to fully regain atomic-level periodicity, highly efficient self-healing behavior, and isotropic or anisotropic motion, (Han et al., *JACS*, 142, 19402, 2020).

Given that HuHF-PIX can undergo large changes in unit cell dimensions without losing crystallinity (unlike typical 3D crystals), we envisioned that they could be used as a platform to reversibly encapsulate a variety of

macromolecular guests (**Fig. 1a**). Starting with polyacrylate-co-acrylamide as the polymer matrix and cytochrome c (cyt c) and lysozyme as guest cargoes, we discovered that the charge of the cargo has significant effects on ferritin-PIX uptake/expansion/contraction properties. Specifically, when single crystals of HuHF-PIX were placed in a solution containing cyt c or lysozyme (pH 6.0) the PIX did not expand owing to the positive charges of cyt c and lysozyme, allowing them to act as counterions to the negatively charged PIX matrix and keep the PIX contracted (**Fig. 1b**). This electrostatic complementarity also allowed cyt c and lysozyme molecules to rapidly perfuse the ferritin-PIX and be taken up with yields up to 45% w/w (**Fig. 1c**). To further test the effect of electrostatic charge on uptake, we repeated the encapsulation study with green fluorescent protein (GFP), which has similar dimensions to lysozyme, but exhibits a much lower positive charge at pH 6 and cannot keep PIX from expanding. As a result, GFP could only be trapped in PIX using a protocol in which GFP is left to penetrate into expanding PIX, which are then contracted with NaCl/CaCl<sub>2</sub> to entrap the GFP in PIX. This approach could be repeated with larger guest proteins such as glucose oxidase (GOx, 128 kDa) and horseradish peroxidase (HRP, 45 kDa). Overall, our results indicate that electrostatic guest-PIX interactions dominate guest uptake and PIX dynamics and that the expansion-contraction method is an effective approach to entrap macromolecules larger than the lattice pores. We also demonstrated that HuHF-PIX is a pH-responsive platform for macromolecular uptake and release, whereby protein cargo encapsulated at neutral pH could be rapidly released upon lowering the pH to  $\leq 5$  (where the HuHF-PIX is positively charged) with robust recyclability. Guest proteins encapsulated within HuHF-PIX were catalytically active and protected from proteolytic digestion, thus paving the way to the construction of robust multi-protein/enzyme platforms.

### **B.2. Spatial patterning of 3D protein crystals for constructing multi-functional materials**

**(Publication 8):** Although the primary utility of protein crystals has historically been in crystallographic structure determination, they are now also being recognized as functional, porous solid-state materials. With proper modifications (*e.g.*, chemical crosslinking, modification with organic, inorganic or biological functionalities), as we have demonstrated in the case of PIX, protein crystals can be rendered highly stable to denaturation even in organic solvents and tailored with new or improved physical, chemical and functional properties. A prominent strategy to

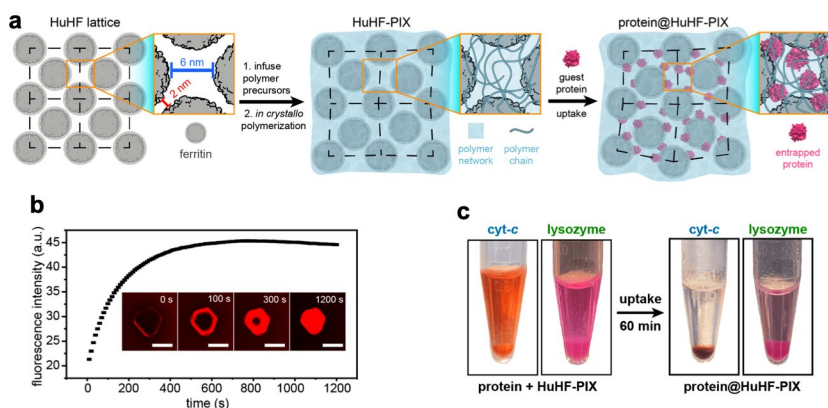


**Figure 1.** (a) Schematic illustration for the uptake of guest proteins in HuHF-PIX. (b) Time-dependent uptake of rhodamine-labeled lysozyme by a single HuHF-PIX crystal as monitored by confocal fluorescence microscopy. (c) Bulk-scale uptake of cyt c and lysozyme by HuHF-PIX.

enhance/enrich the functionalities of solid-state materials and nanoparticles involves their spatial patterning to create core-shell or anisotropic (Janus-type) architectures. Such composite materials often display cooperative functions and emergent properties (*e.g.*, selective separation, multi-step catalytic processes, new photophysical properties) which derive from the precise spatial organization of the individual components. Inspired by such examples, we envisioned that the utility of protein crystals as functional materials may also be augmented through their tunable spatial organization (**Fig. 2a**).

To probe this possibility, we took advantage of the metal-inducible

(and thus kinetically controllable) nature of HuHF assembly into face centered cubic (fcc) crystals. First, we demonstrated the facile formation of core-shell HuHF crystals in which pre-formed wild-type HuHF crystals were incubated in a solution of a cysteine-modified variant of HuHF ( $^{C157}$ HuHF) in the presence of  $Ca^{2+}$  to enable further crystal growth. To confirm the formation of distinct protein layers,  $HuHF@^{C157}HuHF$  crystals were treated with fluorescein-5-maleimide, a Cys-specific fluorophore. Confocal fluorescence imaging of the resulting crystals showed fluorescence only in the peripheral shell formed by the  $^{C157}$ HuHF molecules (**Fig. 2b**). When the duration of the epitaxial growth in  $^{C157}$ HuHF solution was varied from 1 to 24 h, we observed a corresponding increase in the width of the fluorescent shell. The order of core-shell assembly could be reversed to produce a fluorescent  $^{C157}$ HuHF core and a non-fluorescent wt-HuHF shell or the epitaxial growth could be carried out over multiple steps to obtain lamellar core-shell crystals with alternating fluorescent/non-fluorescent layers (**Fig. 2c**). Exploiting the fact that HuHF molecules can be used to encapsulate inorganic nanoparticles, we then demonstrated the formation of core-shell systems with the shells consisting of Pt-nanoparticle-loaded HuHF molecules. The resulting  $HuHF@^{Pt}HuHF$  crystals were capable of efficient catalase- and peroxidase-like catalysis. To the best of our knowledge, the  $\Delta CHuHF/C157HuHF$  crystals represent the first core-shell protein crystals assembled from chemically distinct building blocks.

We found that  $HuHF@^{C157}HuHF$  core-shell systems could be readily processed into PIX to render them adaptive to take up enzymes as guests. This allowed us to construct multi-enzyme systems whereby one enzyme such as GOx or catalase could be attached to the  $^{C157}$ HuHF via Cys-specific maleimide linker, whereas a complementary enzyme such as HRP could be taken up into the core of the crystals (**Fig. 2d**). These multi-enzyme systems were capable of cooperative/competing catalytic reactions within the confined, yet selectively porous framework of the HuHF crystals, analogous to cell-like systems. In the course of our studies on core-shell HuHF crystals, we also found that the morphologies of HuHF crystals can be modulated through their interactions with a solid substrate (in this case, the plastic crystallization plates), resulting in non-Wulff habits with high-energy surfaces. The differential crystal growth kinetics of the HuHF

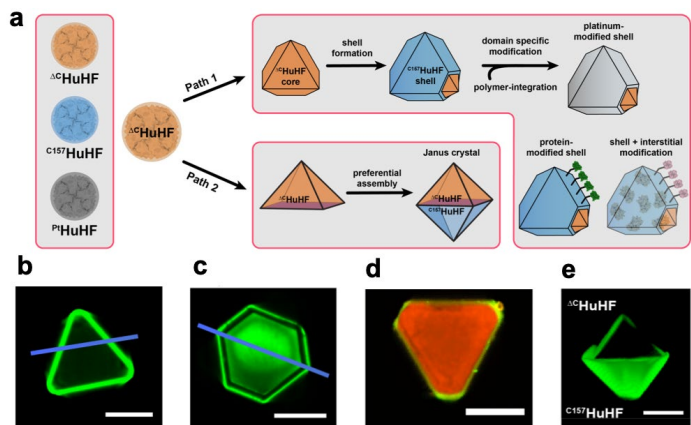


**Figure 2.** (a) Schematic illustration for the construction of spatially patterned HuHF crystals with chemically distinct domains. Confocal microscopy images for double- and triple-layered  $HuHF@^{C157}HuHF$  core-shell crystals (b and c),  $HuHF@^{C157}HuHF$  core-shell PIX modified with catalase on the shell (green) and rhodamine-labeled HRP (red) in the interior (d), and a Janus-type  $HuHF + ^{C157}HuHF$  crystal.

crystal facets were then exploited to create Janus-type architectures with an anisotropic arrangement of chemically distinct domains (**Fig. 2e**). These examples represent an important step toward using protein crystals as reaction vessels for complex multi-step reactions, and in general, broadening their utility as functional, solid-state materials.

***B.3. Designing protein building blocks for the bottom-up construction of 2- and 3D materials with woven/interlocked topologies (unpublished):*** Designing covalent and non-covalent interactions at protein interfaces has been a major focus in protein-based materials research that led to the development of discrete and extended protein assemblies. In these “conventional” protein assemblies, each protein is typically considered as a positionally rigid building block, chemically connected to its neighbors. However, one kind of bond that has been critically underexplored in protein assemblies is the mechanical bond. In mechanical bonds, one or more building blocks are mechanically interlocked, such that they can move freely within the topological limits set by their mechanically bonded partners, yet breaking of a covalent bond is necessary for their full dissociation (*e.g.*, catenanes, rotaxanes, weaves). Such woven protein materials—just like their macroscopic textile counterparts—are expected to have superior mechanical properties.

Using ApoCyt-RIDC1 (an engineered, heme-free variant of cytochrome *cb<sub>562</sub>*, a four-helix bundle protein) as building block, we explored different strategies to assemble protein weaves. In the presence of  $Zn^{2+}$ , ApoCyt-RIDC1 assembles into  $D_2$  symmetric tetramers composed of two pairs of interlacing V-shaped protein monomers, with each tetramer resembling the crossover points of a molecular weave (**Fig. 3**) We established conditions in which ApoCyt-RIDC1 crystallizes in an arrangement reminiscent of a chain-link weave. Next, we installed cysteine residues at strategic points at the vertex of the V-shaped dimer, as well as at its arms, providing the functional groups to connect the protein monomers to topologically interlocked, coherent threads. Crystallographic evidence confirmed the presence of a disulfide bond at one of the desired sites, and thiol-specific divalent linkers were explored to form the second required connection. As ApoCyt-RIDC1 is a  $Zn^{2+}$ -mediated tetramer, we speculated that removal of the metal ion could alter the crystal’s mechanical properties. Remarkably, chelation of the  $Zn^{2+}$  ions led to expanding protein crystals (**Fig. 3**), while non-crosslinked protein crystals readily dissolved. Furthermore, the expansion was reversible in response to the presence of osmolytes in the solution. Further characterization of this protein material by TEM, AFM, and SAXS is currently underway. These promising preliminary results indicate how topology engineering can transform a brittle protein crystal into a strong, stable, and stimuli-responsive biomaterial.

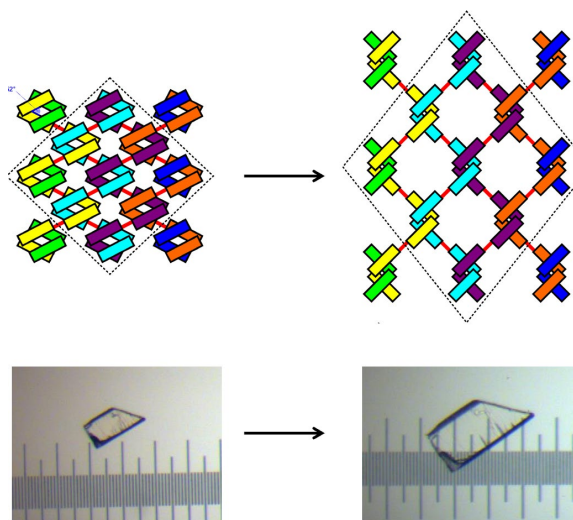


**Figure 3. (top)** Schematic illustration for the expansion of a “woven” protein crystal with a chain-link pattern. **(bottom)** Light micrographs showing the expansion of a woven/crosslinked-ApoCyt-RIDC1 crystal upon removal of Zn ions and incubation in water.

### Future Plans

- (1) Extend the scope of PIX and spatial patterning beyond HuHF crystals,
- (2) generate multi-enzyme catalytic PIX systems

that allow operation in non-aqueous solutions or allow O<sub>2</sub>-sensitive enzymes to function under aerobic conditions, (3) use host-guest interactions to control protein/biomacromolecule uptake within PIX or to control protein-polymer interaction dynamics, (4) finish characterization of first-generation “woven” protein crystals and design triaxially woven protein assemblies.

## Publications

1. J. Zhu, N. Avakyan, A. Kakkis, A. M. Hoffnagle, K. Han, Y. Li, Z. Zhang, T. Choi, Y. Na, C-J. Yu and F. A. Tezcan\*, *Protein Assembly by Design*, Chem. Rev., **121**, 13701-13796 (2021).
2. J. Zhu, L. Samperisi, M. Kalaj, J. A. Chiong, J. B. Bailey, Z. Zhang, C-J. Yu, E. Sikma, X. Zou, S. M. Cohen, Z. Huang\*, F. A. Tezcan\*, *Metal-Hydrogen-Pi-Bonded Organic Frameworks*, Dalton Trans., **51**, 1927-1935 (2022).
3. K. Han, Y. Na, L. Zhang, F. A. Tezcan\*, *Dynamic, Polymer-Integrated Crystals for Efficient, Reversible Protein Encapsulation*, J. Am. Chem. Soc., **144**, 10139-10144 (2022).
4. L. Spiegelman, A. Bahn, E. T. Montañó, L. Zhang, G. L. Hura, K. Patras, A. Kumar, F. A. Tezcan, V. Nizet, S. Tsutakawa, P. Ghosh\*, *Strengthening of enterococcal biofilms by Esp*, PLoS Pathog. **18**, e1010829 (2022).
5. A. M. Hoffnagle, V. H. Eng, U. Markel, F. A. Tezcan\*, *Computationally Guided Redesign of a Heme-Free Cytochrome with Native-like Structure and Stability*, Biochemistry, **61**, 2063-2072 (2022).
6. Y. Suzuki, F. A. Tezcan, “Method for Fabricating Two-Dimensional Protein Crystals”, US Patent 11,286,277, Issued March 2022.
7. R. G. Alberstein, J. L. Prelesnik, E. Nakouzi, S. Zhang, J. J. De Yoreo, J. Pfaendtner, F. A. Tezcan, C. J. Mundy\*, *Discrete Orientations of Interfacial Waters Direct Crystallization of Mica-Binding Proteins*, J. Phys. Chem. Lett., **14**, 80–87 (2023).
8. K. Han, Z. Zhang, F. A. Tezcan\*, *Spatially Patterned, Porous Protein Crystals as Multifunctional Materials*, J. Am. Chem. Soc., *under review* (2023).

# Towards principles for bio-inspired and far-from-equilibrium adaptive, information storing materials.

Suriyanarayanan Vaikuntanathan, University of Chicago

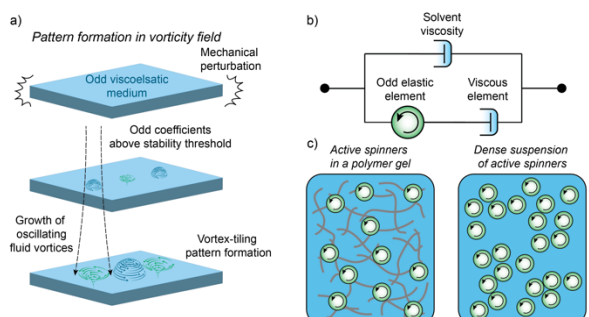
**Keywords:** non-equilibrium stat mech, actin, active nematic, associative memory

## Research Scope

Biological materials, such as those composed of actin and driven by molecular motors, routinely sense molecular cues and initiate microscopic reorganization events in response. Understanding how force-generating arrays of actin, molecular motors, and associated proteins can be tuned, built, and sustained can lead to the discovery of general design principles for the construction of non-equilibrium bioinspired materials with similar exotic adaptive properties. Progress in uncovering these principles is however impeded by the lack of general frameworks for non-equilibrium materials that predict or constrain (1) force response relations far from equilibrium, (2) requirements for ensuring precise spatio-temporal modulation of material properties under external time-dependent conditions, and (3) requirements for adaptive behavior. Indeed, addressing these questions has been posed as a grand challenge in non-equilibrium statistical mechanics. Our work develops and combines novel powerful non-equilibrium statistical mechanics frameworks to address such questions. Additionally, we combine these with machine learning techniques to unravel design principles for the construction of adaptive force-generating bioinspired materials.

## Recent Progress

In recent work we have made progress along multiple fronts, both towards advancing the state of the art in non-equilibrium statistical mechanics and combining such advances with AI inspired techniques.

- a) *A new route for templating pattern formation in bio-inspired non-equilibrium materials.* A striking feature of non-equilibrium systems is their tendency to undergo spatiotemporal pattern formation. Coherent structures such as convective, Turing patterns, and pulsatile contractions of active emerge spontaneously as the active driving in a system overcomes stabilizing dissipative forces. Pattern-forming instabilities are biologically important since, for example, they are utilized by growing organisms for morphogenesis. In many biological examples of soft active matter systems, patterns are driven by the interplay of an active contribution to the local stress, and a concentration field of chemical regulators. One can ask whether pattern formation in soft active matter systems can be reached through alternative routes which do not rely on active stresses and
- 
- The diagram consists of three parts: (a) shows a 3D schematic of an 'Odd viscoelastic medium' undergoing 'Pattern formation in vorticity field' under 'Mechanical perturbation'. It illustrates the 'Growth of oscillating fluid vortices' and 'Vortex-tiling pattern formation' as 'Odd coefficients above stability threshold'. (b) shows a 'three-element mechanical circuit' with 'Solvent viscosity', an 'Odd elastic element', and a 'Viscous element'. (c) shows two candidate systems: 'Active spinners in a polymer gel' and 'Dense suspension of active spinners'.
- (a) Schematic illustration of the pattern formation instability observed in odd viscoelastic fluids. (b) A three-element mechanical circuit, comprising a viscous solvent in parallel with an odd Maxwell element, represents a minimal model for an odd viscoelastic fluid. (c) Two candidate systems which may display odd viscoelastic phenomenology.

gradients of chemical regulators. In recent work we have discovered a new pattern formation mechanism in a viscoelastic fluid which can occur without either of these features, provided that the system displays *odd* non-equilibrium elastic responses to mechanical deformations. Using state of the art hydrodynamic simulations of a three-element active viscoelastic fluid using a recently developed extension of the hybrid lattice Boltzmann algorithm with analytical theory, we demonstrate that the interaction of passive viscosity and so called active odd elasticity allows for the emergence of an oscillating vortex array with a tunable characteristic wavelength and growth rate, a feature not observed in previous simplified models of odd viscoelasticity. We additionally show that the initial exponential growth of the vortices saturates if a shear-thickening non-linearity is included in the dynamics. Our results suggest that such dynamical signatures may be generic to broad classes of odd viscoelastic systems encompassing various microscopic dynamics. Further, these results can inform models of pattern formation in natural systems and guide engineering of odd dynamics in soft active matter.

- b) *Storing information in non-equilibrium materials*: Biological materials store information related to forces and conditions encountered by them. The underpinnings of such information storage and retrieval, particularly in non-equilibrium conditions, remain an open question. In recent work, we have shown how non-equilibrium activity can provide a new route to improving the information storage capacity of a material. Building on classical ideas developed in the context of explaining associative memory in biological systems, we theoretically elucidate how active materials can store and retrieve information more effectively (and with higher capacity) than their equilibrium counterparts. We anticipate that this work can have many implications for the design of bio-inspired materials that can robustly store and reliably retrieve information.
- c) *“Learning” to control active bio-inspired fluids*: Controlling the force generating properties of a soft material - akin to how biological control is achieved – is a long standing challenge in soft matter and non-equilibrium physics and chemistry. The field of active nematics, in which topological defects are introduced in a nematic material and driven by molecular motor or light activity, provides an excellent test bed to study how force generation in active materials can be controlled. Recent work in the field has proposed solutions to this problem using optimal control theory and AI/ML tools. However, the interpretability and experimental tractability of solutions discovered by such work can be limited due to their highly non-local nature. In ongoing (preliminary) work, we have started to address this problem using a physics inspired learning approach. Specifically, our work has uncovered how a poorly developed approximate model which takes very coarse-grained data as input can be coupled with a highly accurate blackbox simulator to discover close to optimal protocols for manipulating the dynamics of force generating defects in an active nematic system.

## Future Plans

In future work, we plan to combine some of the above mentioned non-equilibrium control and force generating ideas with Reinforcement learning and Graph Neural network approaches. The theoretical advances made in the information storing materials theme will also be developed further to explore how such materials can perform the equivalent of computation.

## References

1. C. Floyd, A. Dinner, and S. Vaikuntanathan. Pattern formation in odd viscoelastic fluids. (under review) *Physical Review Letters* (2023).
2. A. Behera, M. Rao, S. Sastry, S. Vaikuntanathan. Enhanced associative memory, classification, and learning with active dynamics, (under revision) *Physical Review X* (2023).

## Publications

1. Y. Qiu, M. Nguyen, G. Hockey, A. Dinner, S. Vaikuntanathan, *A Strong non-equilibrium bound for sorting of crosslinkers on growing biopolymers*. *PNAS* **118**, e2102881118 (2021).
2. A. Lamtyugina, Y. Qiu, E. Fodor, A. Dinner, S. Vaikuntanathan, *Thermodynamic control of activity patterns in cytoskeletal networks*. *PRL*, **129**, 128002 (2022).
3. G. Rassolov, L. Tociu, E. Fodor, S. Vaikuntanathan, *From predicting to learning dissipation from pair correlations of active liquids*. *JCP*, **157**, 054901 (2022).
4. L. Tociu, G. Rassolov, E. Fodor, S. Vaikuntanathan, *Mean field theory for the structure of strongly interacting active liquids*. *JCP*, **157**, 014902 (2022).

## Steering the Pathways of Hierarchical Self-assembly at Solid Surfaces

Tao Ye,<sup>1</sup> Yonggang Ke,<sup>2</sup> and Gaurav Arya<sup>3</sup>

<sup>1</sup> Chemistry & Biochemistry, University of California, Merced <sup>2</sup> Biomedical Engineering, Emory University and Georgia Institute of Technology <sup>3</sup> Mechanical Engineering and Materials Science, Duke University

**Keywords:** DNA origami, self-assembly, simulation, surface patterning

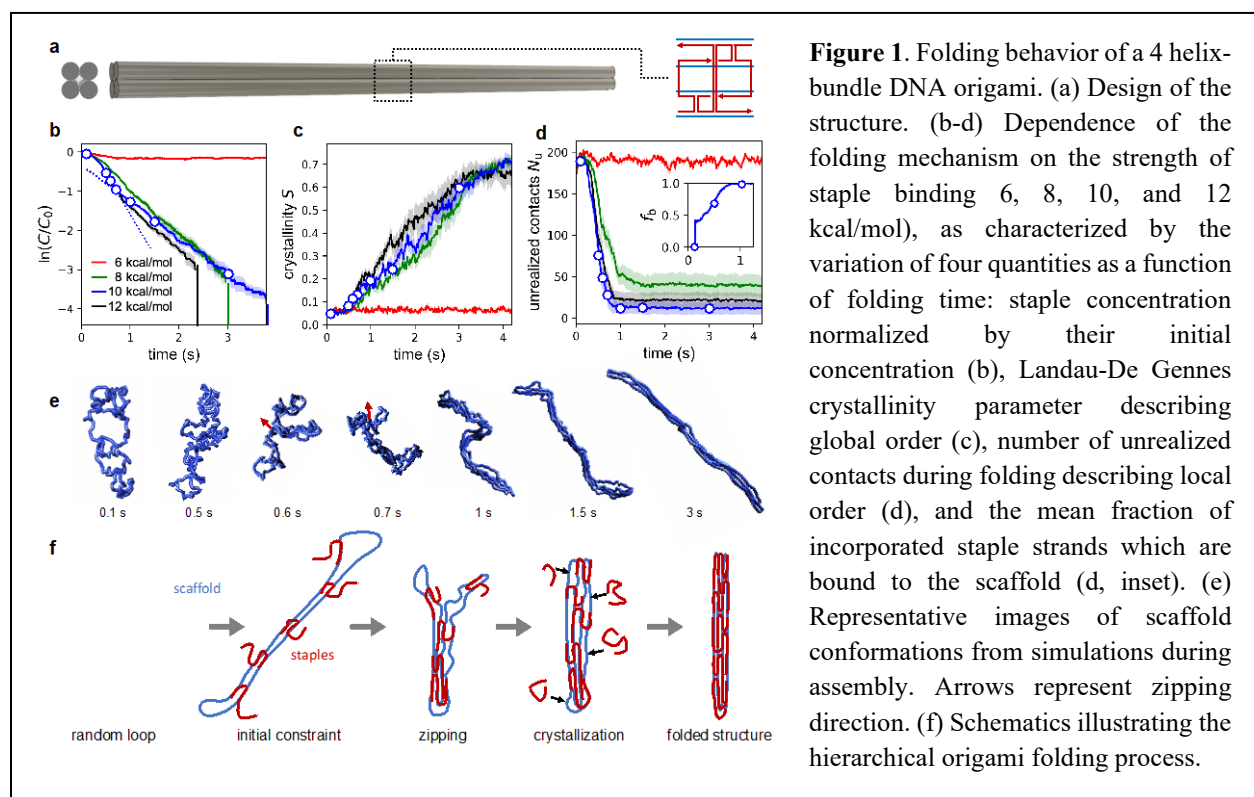
### Research Scope

This project seeks to systematically elucidate the roles of surface/interfacial interactions on self-assembly of biomolecular nanostructures and tailor these interactions to steer the self-assembly pathways of complex hierarchical structures. We will site-specifically nucleate the formation of surface-tethered DNA origami, prototypical designer biomolecular complexes on dynamic surfaces and then allow these mesoscale structures to connect to form superstructures. We hypothesize that our new approach to controlling the conformational degrees of freedom of these mesoscale components can help bypass many of the kinetic traps that make multicomponent self-assembly fundamentally difficult and facilitate rapid, defect-free self-assembly. By combining single molecule biophysical techniques and multi-scale simulation, we will develop a systematic understanding how the interactions of the solid surface influence self-assembly at three hierarchical levels: DNA origami folding itself, whose visualization will be facilitated by tethering, the interconnection of origamis, and creation of higher-order patterns of origamis. The knowledge will be applied to rationally regulate the interactions to steer the self-assembly pathways to form complex hierarchical structures.

### Recent Progress

*Mesosopic model of DNA origami folding.*

We currently lack the ability to compare the folding mechanism of DNA origamis confined to surfaces versus those in solution. To better understand this mechanism, we have developed a new mesoscopic model that captures key features of DNA origami (e.g., conformations and bending stiffness of single- and double-stranded DNA, hybridization thermodynamics, and the structural behavior of motifs like crossovers) at a low enough resolution of 8 nucleotides per bead enable dynamical simulations of origami folding at time scales of up to several seconds. Key to our model is the use of a “switchable” force field that recognizes when hybridization has occurred between two strands and applies the appropriate potentials. We simulated the folding of several different DNA origami structures and revealed for the first time how these structures evolve from their unfolded constituents to their target geometrical form. We found that many designs undergo a hierarchical folding process involving the zipping (collapse) of structural domains into a partially folded precursor structure followed by gradual crystallization into the final structure (Figure 1). This manifests as multiple kinetic phases of assembly where the first phase establishes local order and the second phase involves gradual crystallization of the precursor structure, explaining the



presence of two-phase kinetics observed in recent fluorescence experiments. Our approach allowed us to delineate the role of scaffold routing and staple design in controlling the folding pathway and kinetics, aspects that have until now remained elusive. We also demonstrated that the folding of low aspect ratio structures with significant interior geometry results in highly heterogeneous folding pathways and observed the formation of global topological defects in DNA origami in simulations, consistent with experiments showing lower yields for more complex or larger structures. *A manuscript based on this work is under review.*<sup>1</sup>

### *New surface chemistry for DNA origami placement*

Using nanolithography techniques to print hydrophilic nanopatterns onto an oxidized silicon or silica substrate, DNA origami placement (DOP) could place DNA origami structures onto these surface patterns with high occupancy and controlled orientation.<sup>2</sup> Here we are trying to address two challenges: first DOP remains inaccessible to many researchers due to the expensive and time-consuming processes for nanopattern production, most of which require cleanroom nanofabrication, such as electron beam lithography (EBL) or nanoimprinting. Second, it is not yet possible to form reliable interconnects between these surface-patterned DNA origami structures,<sup>1</sup> which are critically needed for a hierarchical architecture for nanoelectronic and nanophotonic circuits.

Here we demonstrate that nanopatterned self-assembled monolayers (SAMs) supported on gold could be a viable alternative to the commonly used Si wafer for DNA origami placement (Figure

2). Our new platform (1) allows for DNA origami placement with high precision and yield (Figure 2); (2) can be performed in a standard wet lab at significantly lower costs than what is possible with EBL; (3) allows for the exploration of a broad range of surface chemistries to understand and control the interactions with DNA origami and improve the precision and yield of DOP. Our study showed how buffer composition, size and shapes of surface patterns, surface chemistries for the background SAM can be tuned to control interactions between the patterned surface and the DNA origami and improve the yield and alignment. This new approach has potential to make DOP more accessible to a broad range of users. Our approach can also allow researchers to leverage the diverse surface functionalities and surface topography of SAMs to construct more complex DNA nanostructures.

*Surface-assisted deposition of DNA origami on solid surface.*

In addition to the proposed research methodologies, we actively research alternative strategies for controlled placement of DNA origami on solid surfaces. We recently investigated whether DNA origami nanostructures can form crystal-like patterns on mica surfaces. Our results showed DNA origami indeed formed closely packed two-dimensional assembly on mica surface, driven by the interaction between the surface and DNA origami. We also discovered that this surface-induced assembly behavior could be modulated by changing DNA origami

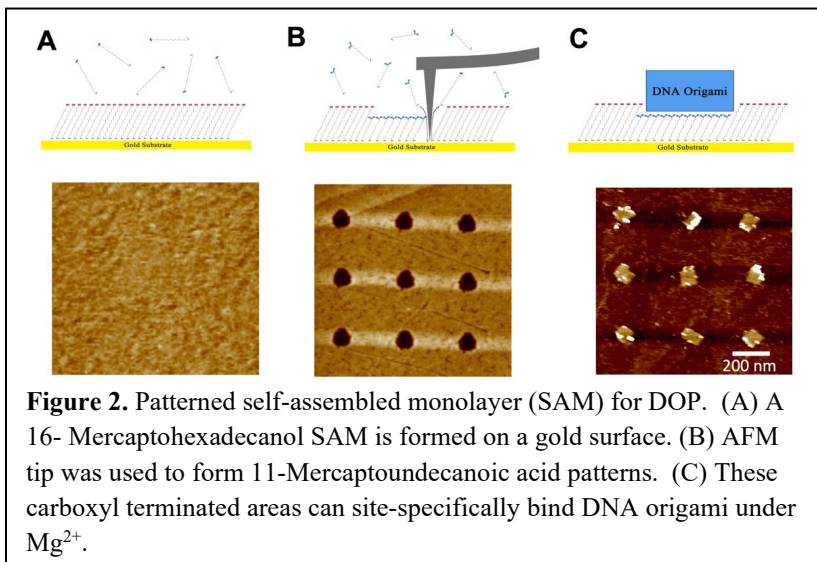


**Figure 2.** Patterned self-assembled monolayer (SAM) for DOP. (A) A 16- Mercaptohexadecanol SAM is formed on a gold surface. (B) AFM tip was used to form 11-Mercaptopundecanoic acid patterns. (C) These carboxyl terminated areas can site-specifically bind DNA origami under  $Mg^{2+}$ .

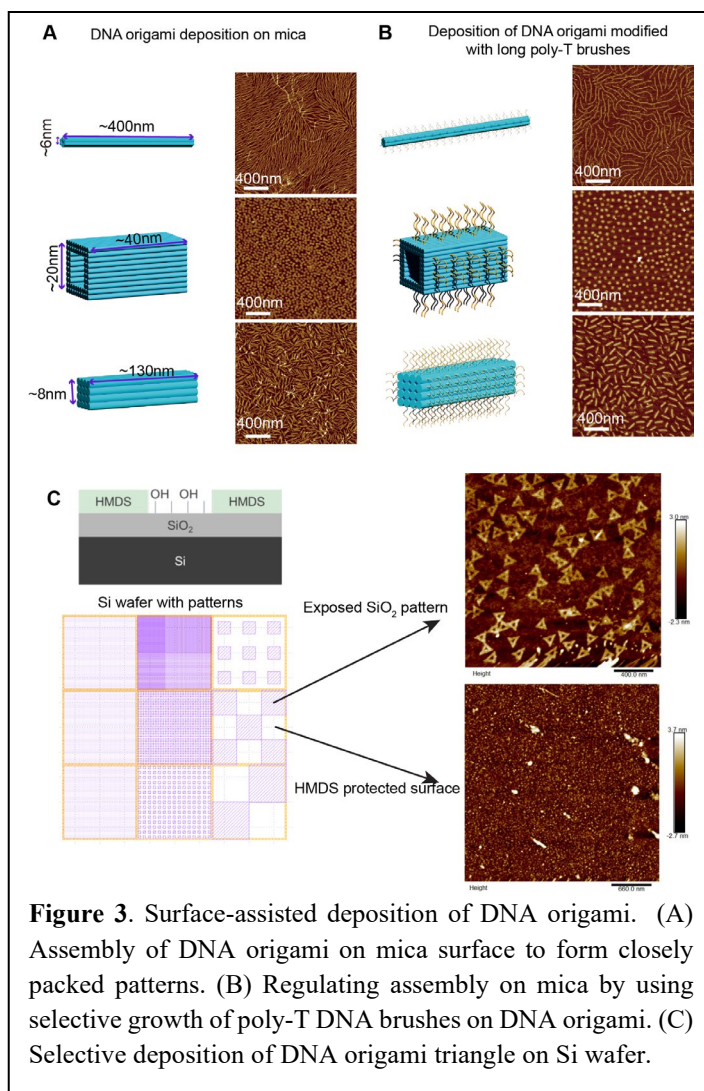
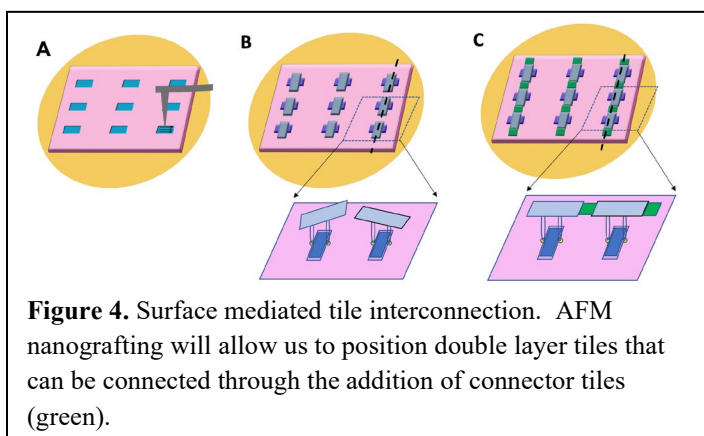


**Figure 3.** Surface-assisted deposition of DNA origami. (A) Assembly of DNA origami on mica surface to form closely packed patterns. (B) Regulating assembly on mica by using selective growth of poly-T DNA brushes on DNA origami. (C) Selective deposition of DNA origami triangle on Si wafer.

design and salt concentration (Figure 3A). Furthermore, using a method develop by us, we showed the patterns of DNA origami assembly could be programmably tuned by modification of DNA origami surface with poly-T DNA brushes (Figure 3B). *A manuscript for this work is currently under preparation for submission.* Separately, we are also working on selective deposition of DNA origami with the method depicted in Figure 3C. Our results clearly showed the DNA origami bind only to the unprotected surface of SiO<sub>2</sub>, which contains -OH groups, but not to the HMDS protected areas. We plan to continue research the surface-induced assembly and surface-selective assembly, and eventually combine these methods together for assembly of DNA origami on solid support with programmable control over their position and orientation.

## Future Plans

The successful placement of DNA origami on surfaces using our new surface chemistry positions us to study how double layer tiles can form interconnects on surfaces (Figure 4). The bottom layer will selectively bind to surface patterns. And the DNA origami tiles in the top layer, which are connected to the bottom layer through DNA tethers, will form interconnects through basepairing interactions. Our new approach places DNA origami components in close proximity to encourage the interconnect formation (Figure 4B). At the same time, the surface tethering offers these tiles sufficient conformational freedom to connect even if the bottom tiles deviate from the ideal position. On the computational side, we will finalize a new coarse-grained model of surface-tethered DNA origami tiles with stick-end base-pairing and blunt-end stacking interconnects that we have been parameterizing for the past year and use the model to understand the cooperative nature of tile binding and their higher-order self-assembly into surface-directed patterns.



## References

1. A. Gopinath, E. Miyazono, A. Faraon, and P. W. K. Rothemund, Engineering and mapping nanocavity emission via precision placement of DNA origami. *Nature*. 535:401 (2016).
2. M. DeLuca, T. Ye, M. Poirier, Y. Ke, C. Castro, and G. Arya, Mechanism of DNA origami folding elucidated by mesoscopic simulations (submitted)

## Publications

1. M. DeLuca, S. Sensale, P. A. Lin, and G. Arya, Prediction and Control in DNA Nanotechnology, *ACS Applied Bio Mater.* (2023). <https://doi.org/10.1021/acsabm.2c01045>
2. S. Sensale, P. Sharma, and G. Arya, Binding kinetics of harmonically confined random walkers, *Phys. Rev. E* **105**, 044136 (2022).
3. D. Wang, L. Yu, C. M. Huang, G. Arya, S. Chang, and Y. Ke, Programmable transformations of DNA origami made of small modular dynamic units, *J. Am. Chem. Soc.* **143**, 2256 (2021).
4. Y. Yang, Q. Lu, C. M. Huang, H. Qian, Y. Zhang, S. Deshpande, G. Arya, Y. Ke, and S. Zauscher, Programmable Site-Specific Functionalization of DNA Origami with Polynucleotide Brushes, *Angew. Chem. Int. Ed.* **60**, 23241 (2021).
5. C. Zhou, D. Yang, S. Sensale, P. Sharma, D. Wang, L. Yu, G. Arya, Y. Ke, and P. Wang, A bistable and reconfigurable molecular system with encodable bonds, *Sci. Adv.* **8**, eade3003 (2022).
6. Y. Zhang, D. Yang, P. Wang, and Y. Ke, Building Large DNA Bundles via Controlled Hierarchical Assembly of DNA Tubes, *ACS Nano* **17**, 10486-10495 (2023).
7. H. Su, J. M. Brockman, Y. Duan, N. Sen, H. Chhabra, A. Bazrafshan, A. T. Blanchard, T. Meyer, B. Andrews, J. P. K. Doye, Y. Ke, R. B. Dyer, and K. Salaita, Massively Parallelized Molecular Force Manipulation with On-Demand Thermal and Optical Control, *J Am Chem Soc* **143**, 19466-19473 (2021).
8. J. Shao, R. Breuer, M. Schmittl, and T. Ye, Potential-Dependent Adhesion Forces between dsDNA and Electroactive Surfaces. *Langmuir*, **38**(39), 11899-11908 (2022).
9. Q. Gu, E. A. Josephs, and T. Ye, Hybridization and self-assembly behaviors of surface-immobilized DNA in close proximity: A single-molecule perspective, *Aggregate*, **3**(4), e186 (2022).
10. P. Rahmani, M. Goodlad, Y. Zhang, Y. Li, and T. Ye, One-Step Ligand-Exchange Method to Produce Quantum Dot–DNA Conjugates for DNA-Directed Self-Assembly. *ACS Applied Materials & Interfaces*, **14**(42), 47359-47368 (2022).

*Author Index*

Abbott, Nicholas L.....	35	Kowalewski, Tomasz.....	46
Aronson, Igor.....	40	Kumar, Manish.....	124, 127
Arya, Gaurav.....	194	Kumar, Sanat K.....	95
Ashby, Paul.....	24	Lee, Daeyeon.....	112, 116
Baer, Marcel D.....	2, 19	Luijten, Erik.....	128
Baker, David.....	19, 44	Mallapragada, Surya.....	10
Balazs, Anna C.....	46	Marchetti, Christina.....	76
Bathe, Mark.....	159	Matyjaszewski, Krzysztof.....	46
Bayro, Marvin.....	6	Mundy, Chris.....	6
Bedzyk, Michael J.....	138	Nagel, Sidney R.....	133, 137
Brady, John.....	121	Nealey, Paul F.....	14
Bundschuh, Ralf.....	51	Nilsen-Hamilton, Marit.....	10
Castro, Carlos E.....	51	Norton, Michael M.....	99
Chaikin, Paul.....	60, 62	Noy, Aleksandr.....	19
Chaikin, Paul M.....	56, 60	Olvera de la Cruz, Monica.....	138
Chen, Chun-Long.....	6	Omar, Ahmad.....	24
Chen, Qian.....	128	Park, Jae S.....	99
Choi, Jong H.....	67	Pine, David.....	56, 121
Chun-Long Chen.....	19	Pochan, Darrin J.....	143
de Pablo, Juan J.....	14, 35	Poirier, Michael G.....	51
De Yoreo, James J.....	6, 19	Prozorov, Tanya.....	10
Delhommelle, Jerome.....	62	Ross, Tyler D.....	147
Dishari, Shudipto K.....	71	Rosso, Kevin.....	6
Dogic, Zvonimir.....	76, 108	Rothmund, Paul W. K.....	147
Emrick, Todd.....	80	Rotskoff, Grant M.....	151
Estroff, Lara A.....	85	Russell, Thomas P.....	24
Fraden, Seth.....	108	Sacanna, Stefano.....	62
Franco, Elisa.....	90	Santore, Maria M.....	155
Gang, Oleg.....	95	Saven, Jeffrey G.....	143
Glatz, Andreas.....	29	Schlau-Cohen, Gabriela S.....	159
Glotzer, Sharon C.....	168	Schulman, Rebecca.....	90
Good, Matthew C.....	112, 116	Sen, Ayusman.....	40
Grason, Gregory M.....	155	Sha, Ruoji.....	56
Grover, Piyush.....	99	Shaw, Wendy.....	6
Guan, Zhibin.....	104	Silberstein, Meredith N.....	164
Hagan, Michael F.....	108	Snezhko, Alexey.....	29
Hammer, Daniel A.....	112, 116	Sokolov, Andrey.....	29
Hartley, C. Scott.....	117	Solomon, Michael J.....	168
Helms, Brett.....	24	Stebe, Kathleen J.....	173
Hillier, Andrew.....	10	Strano, Michael S.....	177
Hong, Pengyu.....	108	Stupp, Samuel I.....	181
Ke, Yonggang.....	194	Tao, Jinhui.....	6
Klotsa, Daphne.....	121	Tezcan, Akif.....	186
Kloxin, Christopher J.....	143	Thallapally, Praveen.....	6
Konkolewicz, Dominik.....	117	Tirrell, Matthew V.....	14

Traveset, Alex .....	10	Wiesner, Ulrich .....	85
Vaikuntanathan, Suriyanarayanan .....	191	Willard, Adam P. ....	159
Vaknin, David .....	10	Winter, Jessica O. ....	51
van Burren, Anthony.....	19	Ye, Tao.....	194
Wang, Wenjie .....	10	Zettl, Alex .....	24
Weck, Marcus .....	56, 60		

## *Participant List*

<b>Name</b>	<b>Organization</b>
Abbott, Nicholas	Cornell University
Abdullah, Jobaer	Lawrence Livermore National Laboratory
Adhikari, Sabin	Columbia University
Adjasoo, Jonas	Iowa State University
Aggarwal, Aaveg	Northwestern University
Aizenberg, Joanna	Harvard University
Aizenberg, Michael	Harvard University
Amey, Christopher	Brandeis University
Aronson, Igor	Pennsylvania State University
Arya, Gaurav	Duke University
Ashby, Paul	Lawrence Berkeley National Laboratory
Baer, Marcel	Pacific Northwest National Laboratory
Baker, David	University of Washington
Balazs, Anna C.	University of Pittsburgh
Baskaran, Aparna	Brandeis University
Bathe, Mark	Massachusetts Institute of Technology
Batton, Clay	Stanford University
Bayro, Marvin	University of Puerto Rico
Behera, Harekrushna	University of Texas at Austin
Berezney, John	Brandeis University
Bernat, Victorien	Cornell University
Brady, John	California Institute of Technology
Brown, Kate	US Department of Energy, Office of Basic Energy Sciences
Bundschuh, Ralf	The Ohio State University
Cai, Hongyi	Cornell University
Castellanos, Maria	Massachusetts Institute of Technology
Castro, Carlos	The Ohio State University
Chaikin, Paul	New York University
Chakma, Progyateg	Pacific Northwest National Laboratory
Chen, Chun-Long	Pacific Northwest National Laboratory / University of Washington
Chen, Qian	University of Illinois at Urbana-Champaign
Chen, Wei	Argonne National Laboratory
Chennakesavalu, Shriram	Stanford University
Choi, Jong Hyun	Purdue University
de Pablo, Juan	University of Chicago
De Yoreo, Jim	Pacific Northwest National Laboratory
Delhommelle, Jerome	University of Massachusetts Lowell

Dishari, Shudipto	University of Nebraska–Lincoln
Dizani, Mahdi	University of California, Los Angeles
Dogic, Zvonimir	University of California, Santa Barbara
Duke, Daniel	Duke University
Emrick, Todd	University of Massachusetts Amherst
Estroff, Lara	Cornell University
Fang, Yan	University of Chicago / Argonne National Laboratory
Fecko, Chris	US Department of Energy, Office of Basic Energy Sciences
Ferron, Thomas	Lawrence Livermore National Laboratory
Fink, Zachary	Lawrence Berkeley National Laboratory
Fitzsimmons, Michael	US Department of Energy, Office of Basic Energy Sciences
Floyd, Carlos	University of Chicago
Fontanez, Kenneth	University of Puerto Rico, Río Piedras Campus
Franco, Elisa	University of California, Los Angeles
Frechette, Layne	Brandeis University
Gang, Oleg	Columbia University
Ghosh, Saptorshi	Brandeis University
Gimm, Aura	US Department of Energy, Office of Basic Energy Sciences
Glatz, Andreas	Argonne National Laboratory
Good, Matthew	University of Pennsylvania
Gorman, Jeffrey	Massachusetts Institute of Technology
Grason, Greg	University of Massachusetts Amherst
Grover, Piyush	University of Nebraska–Lincoln
Guan, Zhibin	University of California, Irvine
Gulati, Paarth	University of California, Santa Barbara
Hagan, Michael	Brandeis University
Hammer, Daniel	University of Pennsylvania
Han, Kenneth	University of California, San Diego
Hartley, Scott	Miami University
He, Hongrui	University of Chicago
Heble, Annie	Pacific Northwest National Laboratory
Hedderick, Konrad	Cornell University
Hong, Pengyu	Brandeis University
Hopkins, Amanda	University of Pennsylvania
Jergens, Elizabeth	The Ohio State University
Jiang, Yanqi	Johns Hopkins University
Juntunen, Nicholas	Stanford University
Ke, Yonggang	Emory University
Kerch, Helen	US Department of Energy, Office of Basic Energy Sciences

Kewalramani, Sumit	Northwestern University
Kirkinis, Eleftherios	Northwestern University
Klotsa, Daphne	University of North Carolina at Chapel Hill
Kolvin, Itamar	University of California, Santa Barbara
Konkolewicz, Dominik	Miami University
Kumar, Manish	University of Texas at Austin
Kumar, Sanat	Columbia University
Lee, Daeyeon	University of Pennsylvania
Lee, Jinhyun	University of North Carolina at Chapel Hill
Lee, Min Kyung	New York University
Ley Flores, Maria	University of Chicago
Li, Sherry	Stanford University
Li, Yichen	University of California, Merced
Li, Yuhao	Lawrence Livermore National Laboratory
Li, Yunrui	Brandeis University
Liang, Heyi	University of Chicago
Liu, Andrea	University of Pennsylvania
Liu, Chang	University of Illinois Urbana-Champaign
Lopez Flores, Leticia	Northwestern University
Lopez Rios, Hector Manuel	Northwestern University
Luijten, Erik	Northwestern University
Lyu, Zhiheng	University of Illinois Urbana-Champaign
Ma, Yingyu	Brandeis University
Madden, Ian	Northwestern University
Madhvacharyula, Anirudh	Purdue University
Majumder, Sagardip	University of Washington
Mallapragada, Surya	Ames National Laboratory
Manikandan, Sreekanth K.	Stanford University
Marchetti, M Cristina	University of California, Santa Barbara
Markel, Ulrich	University of California, San Diego
Markowitz, Michael	US Department of Energy, Office of Basic Energy Sciences
Mewes, Claudia	US Department of Energy, Office of Basic Energy Sciences
Minevich, Brian	Columbia University
Mitchell, Andy	Stanford University
Mondal, Manodeep	Brandeis University
Nagel, Sidney	University of Chicago
Naranjo Rubio, Angel Santiago	University of Nebraska–Lincoln
Nealey, Paul	Argonne National Laboratory / University of Chicago
Nishiyama, Katsu	Brandeis University

Noy, Aleksandr	Lawrence Livermore National Laboratory
O'Callaghan, Jessica	University of Pennsylvania
Olvera de la Cruz, Monica	Northwestern University
Omar, Ahmad	University of California, Berkeley
Osmanovic, Dino	University of California, Los Angeles
Pallock, Rumayel Hassan	University of Nebraska–Lincoln
Palmer, Liam	Northwestern University
Pechan, Mick	US Department of Energy, Office of Basic Energy Sciences
Pert, Emmit	Stanford University
Pine, David	New York University
Pochan, Darrin	University of Delaware
Prozorov, Tanya	Ames National Laboratory
Rajabi, Mojtaba	University of Pennsylvania
Redeker, Daniel	Columbia University
Roizen, Jennifer	US Department of Energy, Office of Basic Energy Sciences
Ross, Tyler	California Institute of Technology
Rothmund, Paul	California Institute of Technology
Rotskoff, Grant	Stanford University
Russell, Thomas	Lawrence Berkeley National Laboratory
Sacanna, Stefano	New York University
Saccuzzo, Emily	Pacific Northwest National Laboratory
Sai, Hiroaki	Northwestern University
Sanchez, Regina	Argonne National Laboratory
Santore, Maria	University of Massachusetts
Saven, Jeffery	University of Pennsylvania
Schlau-Cohen, Gabriela	Massachusetts Institute of Technology
Schmid, Sakshi	Pacific Northwest National Laboratory
Schulman, Rebecca	Johns Hopkins University
Schwartz, Andrew	US Department of Energy, Office of Basic Energy Sciences
Sharma, Pranav	Duke University
Sheth, Sejal	Cornell University
Shi, Chenyang	Pacific Northwest National Laboratory
Shrestha, Ahis	Northwestern University
Silberstein, Meredith	Cornell University
Snezhko, Alexey	Argonne National Laboratory
Snyder, Deborah	University of Massachusetts Amherst
Sokolov, Andrey	Argonne National Laboratory
Solomon, Michael	University of Michigan
Song, Zehao	Northwestern University

Sorrentino, Daniela	University of California, Los Angeles
Stebe, Kathleen	University of Pennsylvania
Steppan, Carla	University of Massachusetts Amherst
Strano, Michael	Massachusetts Institute of Technology
Stupp, Samuel	Northwestern University
Sushko, Peter	Pacific Northwest National Laboratory
Tait, William	Cornell University
Tezcan, Akif	University of California, San Diego
Tirrell, Matthew	Argonne National Laboratory
Tran, Phu	Brandeis University
Tran, Quang	Brandeis University
Trinh, Thi Kim Hoang	Pacific Northwest National Laboratory
Vaikuntanathan, Suriyanarayanan	University of Chicago
Waltmann, Curt	Northwestern University
Watson, Garrett	Northwestern University
Wiesner, Ulrich	Cornell University
Willard, Adam	Massachusetts Institute of Technology
Wilson, Lane	US Department of Energy, Office of Basic Energy Sciences
Winter, Jessica	The Ohio State University
Wu, Chunhui	Pacific Northwest National Laboratory
Wu, Xuefei	Lawrence Berkeley National Laboratory
Yang, Donglin	Duke University
Yang, Qizheng	University of Washington
Yang, Yang	Northwestern University
Yang, Zhefei	University of Massachusetts Amherst
Ye, Tao	University of California, Merced
Yu, Fei	Cornell University
Yu, Luke	Northwestern University
Zhang, Francis	University of Washington
Zhang, Mingyi	Pacific Northwest National Laboratory
Zhang, Qixing	University of Pennsylvania
Zhang, Wanting	Cornell University
Zhao, Liang	University of California, Santa Barbara
Zheng, Renyu	University of Washington
Zhou, Tingtao	California Institute of Technology
Zhou, Tingtao	California Institute of Technology
Zhou, Wenhao	University of Washington
Zhu, Shipei	Lawrence Berkeley National Laboratory